Electronic Supplementary Information (ESI)

The silica mineralisation properties of synthetic Silaffin-1A$_1$ (*syn*Sil-1A$_1$)

Fabian Daus,[a] Xiulan Xie[a] and Armin Geyer*[a]

[a] Department of Chemistry, Philipps-Universität Marburg, Hans-Meerwein-Straße 4, 35032 Marburg, Germany

*** Corresponding Author:** Armin Geyer (geyer@staff.uni-marburg.de)

Table of Contents

General information

All chemicals and solvents used for the synthesis of peptide building blocks or peptide synthesis were purchased from commercial sources and were not purified further, if not indicated. Unless otherwise noted, all reactions were executed under an argon atmosphere at ambient pressure.

For reaction control by analytical thin layer chromatography TLC plates coated with silica gel 60 F_{254} (*Merck KGaA*) were used, and detection was carried out by fluorescence quenching under UV light (λ= 254 nm) or by staining with ninhydrin solution followed by heating to 350 °C. Flash chromatography was performed on silica gel 60 (60 Å, 230-400 mesh) from *Macherey-Nagel*.

The purification of the peptides was achieved by semi-preparative reversed-phase HPLC with a *Thermo Scientific Dionex* UltiMate3000 including a MWD-3000 detector and *a Macherey-Nagel* VP Nucleodur C18 gravity column (125 x 21 mm, 5 µm, 100 Å) or ACE 5 SuperC18 (150 x 10 mm, 5 µm, 90 Å), using the eluents A: H_2O + 0.1% TFA and B: MeCN + 0.085% TFA. Analytical HPLC was performed on the same system using an *ACE* UltraCore 2.5 SuperC18, 150 x 2.1 µm. Afterwards, the peptides were lyophilized with a *Christ Alpha* 2–4LDplus.

The NMR spectra were recorded on *Bruker* AVII 600, AVIII 500 or AVIII HD 500 MHz spectrometers. Chemical shifts (δ) are given in ppm referring to the solvent signal. The coupling constants are ^3J couplings, unless otherwise indicated. All mass spectra were recorded on a *Finnigan* LTQ-FT spectrometer from *Fisher Thermo Scientific*.

All pH values were determined at room temperature using a SevenCompact pH meter S220 from *Mettler Toledo* unless otherwise noted.

UV-VIS measurements were determined at room temperature using a Multiskan™ GO microplate spectrophotometer from *Thermo Scientific*.

Safety statements

No unexpected or unusually high safety hazards were encountered in the reported work.

Caution! All reagents and solvents used have been used under standard operating procedures unless otherwise noted.

Caution! Extreme care should be taken both in the handling of the cryogen liquid nitrogen and its use in the Schlenk line trap to avoid the condensation of oxygen from air.

Experimental procedures

5-Hydroxy-6-trimethyl-L-lysyl-glycine building block for solid-phase peptide synthesis

Methyl-(2*S*)-2-((*tert*-butoxycarbonyl)amino)-3-hydroxypropanoate (Boc-Ser-OMe, S1)

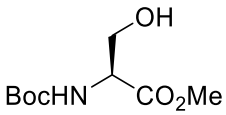

S1

The reaction was performed according to the literature.[1] Acetyl chloride (17.0 mL, 0.24 mol, 2.5 equiv.) was added dropwise at 0 °C to absolute methanol (150 mL). After complete addition, L-serine (10.0 g, 95.2 mmol; 1.0 equiv.) was added in one portion and the solution was heated to reflux for 2 h. The mixture was allowed to cool to room temperature before the solvent was removed *in vacuo* to give the methyl ester hydrochloride (14.7 g, 94.5 mmol, 99% yield) as a white solid, which was used without further purification in the next step.

The methyl ester hydrochloride (14.7 g, 94.5 mmol, 1.0 equiv.) was suspended in tetrahydrofuran (200 mL) and cooled to 0 °C. Triethylamine (28.8 mL, 0.21 mol, 2.2 equiv.) and a solution of di-*tert*-butyl dicarbonate (20.0 g, 91.7 mmol, 0.97 equiv.) dissolved in tetrahydrofuran were added dropwise and the resulting solution was stirred at room temperature for 16 h. The solvent was removed *in vacuo* and the residue was partitioned between Et_2O (200 mL) and saturated $NaHCO_3$ solution (200 mL). The layers were separated and the aqueous layer was extracted with Et_2O (200 mL x 2). The combined organic layer was washed with brine, dried over $MgSO_4$, filtered and concentrated *in vacuo* to afford Boc-Ser-OMe **S1** (20.1 g, 91.7 mmol, 97% yield) as colourless oil, which was used directly for the next step. R_f 0.37 (cyclohexane:EtOAc, 1:1, v/v); ^{1}H-NMR (300 MHz, DMSO-d_6, 300 K) δ = 6.92 (d, 1H, ^{3}J=8.0 Hz, α-NH), 4.88 (t, 1H, ^{3}J=6.1 Hz, β-OH), 4.06 (ddd, 1H, ^{3}J=8.1 Hz, ^{3}J=4.9 Hz, ^{3}J=4.9 Hz, α-CH), 3.68-3.56 (m, 2H, β-CH_2), 3.62 (s, 3H, OCH_3), 1.38 (s, 9H, Boc) ppm; ^{13}C-NMR (75 MHz, DMSO-d_6, 300 K) δ = 171.5, 155.3, 78.3, 61.3, 56.2, 51.7, 28.1 ppm; HRMS (ESI) calculated for [$C_9H_{17}NO_5Na^+$]: 242.0999, found: 242.0999.

Methyl-(2*R*)-2-((*tert*-butoxycarbonyl)amino)-3-iodopropanoate (S2)

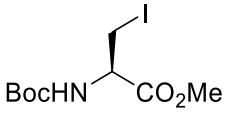

S2

In a *flame-dried* nitrogen round-bottom flask triphenylphosphine (15.6 g, 59.3 mmol, 1.3 equiv.) was dissolved in absolute tetrahydrofuran (200 mL), cooled to 0 °C and imidazole (4.35 g, 63.9 mmol, 1.4 equiv.) was added. Thereafter, solid iodine (15.1 g, 59.3 mmol, 1.3 equiv.) was added in three portions every 5 min at 0 °C. A solution of Boc-Ser-OMe **S1** (10.0 g, 45.6 mmol, 1.0 equiv.) in absolute

THF (50.0 mL) was added dropwise. The mixture was allowed to warm to room temperature and stirred for 2.5 h under exclusion of light. The resulting suspension was partitioned between Et_2O (200 mL) and 1 M HCl (100 mL). The layers were separated and the aqueous layer was extracted with Et_2O (100 ml x 3). The combined organic layer was washed with 1 M HCl (100 mL), 1 M $Na_2S_2O_3$ solution (200 mL), saturated $NaHCO_3$ solution (200 mL) and brine, dried over $MgSO_4$, filtered and concentrated *in vacuo*. The obtained crude material was purified by silica gel column chromatography (pentane:Et_2O, 9:1 v/v) to afford iodopropanoate **S2** (11.3 g, 34.3 mmol, 75% yield) as a pale yellow solid. R_f 0.29 (pentane:Et_2O, 9:1, v/v); ^{1}H-NMR (300 MHz, DMSO-d_6, 300 K) δ = 7.39 (d, 1H, ^{3}J=8.4 Hz, α-NH), 4.24 (ddd, 1H, ^{3}J=8.6 Hz, ^{3}J=8.6 Hz, ^{3}J=4.7 Hz, α-CH), 3.66 (s, 3H, OCH_3), 3.49 (dd, 1H, ^{3}J=4.7 Hz, ^{2}J=10.2 Hz, β-CH_2^T), 3.31 (dd, 1H, ^{3}J=9.2 Hz, ^{2}J=10.0 Hz, β-CH_2^H), 1.39 (s, 9H, Boc) ppm; ^{13}C-NMR (75 MHz, DMSO-d_6, 300 K) δ = 169.7, 155.0, 78.7, 55.3, 52.3, 28.1, 4.6 ppm; HRMS (ESI) calculated for [$C_9H_{16}INO_4Na^+$]: 352.0016, found: 352.0019.

Methyl-(2*S*)-2-((*tert*-butoxycarbonyl)amino)hex-5-enoate (Boc-Hag-OMe, S3)

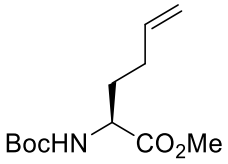

S3

The reaction was performed according to the literature.[1] Activated zinc dust (1.19 g, 18.2 mmol, 3.0 equiv.) was *flame-dried* in a nitrogen round-bottom flask under vacuum for 5 min, then the flask was purged with argon and cooled before the zinc dust was suspended in absolute DMF (10 mL). Thereafter, solid iodine (0.31 g, 1.22 mmol, 0.2 equiv.) was added in one portion and the mixture was stirred until it became colourless again. A solution of iodopropanoate **S2** (2.00 g, 6.08 mmol, 1.0 equiv.) in absolute DMF (50.0 mL) was added dropwise to the suspension, and the mixture was stirred at room temperature for 2 h until the zinc insertion was finished (TLC control). Stirring was stopped and the solid was allowed to settle. Copper(I) bromide (0.44 g, 3.04 mmol, 0.5 equiv.) was *flame-dried* in a nitrogen round-bottom flask under vacuum for 5 min, then the flask was purged with argon and cooled to room temperature before absolute DMF (10 mL) was added. Freshly distilled allyl chloride (0.74 mL, 9.12 mmol, 1.5 equiv.) was added dropwise and the resulting solution was cooled to −15°C. The supernatant of the organozinc reagent was carefully transferred dropwise into this solution using a syringe. After complete addition, the mixture was allowed to warm to room temperature and stirred for 16 h. The reaction solution was diluted with EtOAc (50 mL) and 0.5 M HCl (50 mL). The layers were separated and the aqueous layer was extracted with EtOAc (50 ml x 3). The combined organic layer was washed with 1 M $Na_2S_2O_3$ solution (50 mL), H_2O (50 mL) and brine, dried over $MgSO_4$, filtered and concentrated *in vacuo*. The obtained crude material was purified by silica gel column chromatography

(cyclohexane:EtOAc, 9:1, v/v) to afford Boc-Hag-OMe **S3** (1.20 g, 4.93 mmol, 82% yield) as a colourless oil. R_f 0.43 (cyclohexane:EtOAc, 5:1, v/v); ^{1}H-NMR (300 MHz, DMSO-d_6, 300 K) δ = 7.25 (d, 1H, ^{3}J=7.8 Hz, α-NH), 5.77 (dddd, 1H, ^{3}J=17.0 Hz, ^{3}J=10.3 Hz, ^{3}J=6.7 Hz, ^{3}J=6.7 Hz, δ-CH), 5.06-4.94 (m, 2H, ε-CH_2), 3.95 (ddd, 1H, ^{3}J=8.3 Hz, ^{3}J=8.3 Hz, ^{3}J=5.4 Hz, α-CH), 3.62 (s, 3H, OCH_3), 2.14-1.96 (m, 2H, γ-CH_2), 1.77-1.59 (m, 2H, β-CH_2), 1.38 (s, 9H, Boc) ppm; ^{13}C-NMR (75 MHz, DMSO-d_6, 300 K) δ = 173.1, 155.5, 137.4, 115.5, 78.1, 52.8, 51.6, 29.9, 29.5, 28.1 ppm; HRMS (ESI) calculated for [$C_{12}H_{21}NO_4Na^+$]: 266.1363, found: 266.1367.

Methyl-(2*S*)-2-((*tert*-butoxycarbonyl)amino)hex-5-enoic acid (Boc-Hag-OH, 1)

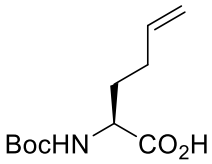

1

To a solution of Boc-Hag-OMe **S3** (1.20 g, 4.93 mmol, 1.0 equiv.) in tetrahydrofuran (6.0 mL) was added a 1 M LiOH solution (9.86 mL, 9.86 mmol, 2.0 equiv.) in water. The reaction mixture was stirred vigorously for 10 min at room temperature and then diluted with 0.5 M HCl (50 mL). The layers were separated and the aqueous layer was extracted with EtOAc (50 ml x 3). The combined organic layer was washed with brine, dried over $MgSO_4$, filtered and concentrated *in vacuo*. The obtained crude material was purified by silica gel column chromatography (cyclohexane:EtOAc, 5:1, v/v) to afford Boc-Hag-OH **1** (1.12 g, 4.88 mmol, 99% yield) as a colourless oil. R_f 0.06 (cyclohexane:EtOAc, 5:1, v/v); ^{1}H-NMR (300 MHz, DMSO-d_6, 300 K) δ = 12.43 (s, 1H, CO_2H), 7.08 (d, 1H, ^{3}J=8.1 Hz, α-NH), 5.78 (dddd, 1H, ^{3}J=17.0 Hz, ^{3}J=10.3 Hz, ^{3}J=6.7 Hz, ^{3}J=6.7 Hz, δ-CH), 5.06-4.93 (m, 2H, ε-CH_2), 3.86 (ddd, 1H, ^{3}J=8.7 Hz, ^{3}J=8.7 Hz, ^{3}J=4.8 Hz, α-CH), 2.15-1.95 (m, 2H, γ-CH_2), 1.80-1.54 (m, 2H, β-CH_2), 1.38 (s, 9H, Boc) ppm; ^{13}C-NMR (75 MHz, DMSO-d_6, 300 K) δ = 174.1, 155.5, 137.6, 115.4, 77.9, 52.8, 30.0, 29.6, 28.2 ppm; HRMS (ESI) calculated for [$C_{11}H_{19}NO_4Na^+$]: 252.1206, found: 252.1208.

***tert*-Butyl-(2*S*)-(2-((*tert*-butoxycarbonyl)amino)hex-5-enoyl)glycinate (Boc-Hag-Gly-O^{t}Bu, 2)**

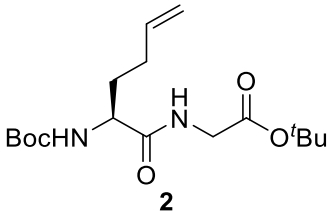

2

Boc-Hag-OH **1** (0.92 g, 4.03 mmol, 1.0 equiv.) and H_2N-Gly-O^{t}Bu · HCl (0.74 g, 4.43 mmol, 1.1 equiv.) were dissolved in a mixture of DCM/DMF (80 mL, 1:1). DIPEA (2.85 mL, 16.1 mmol, 4.0 equiv.), HOBt · H_2O (0.62 g, 4.03 mmol, 1.0 equiv.) and EDC · HCl (0.77 g, 4.03 mmol, 1.0 equiv.) were added

and the resulting solution was stirred at room temperature for 18 h. The reaction solution was diluted with EtOAc (100 mL), and the layers were separated. The organic layer was washed with 10% aqueous citric acid solution (100 mL x 3), H_2O (100 mL) and brine, dried over $MgSO_4$, filtered and concentrated *in vacuo*. The obtained crude material was purified by silica gel column chromatography (cyclohexane:EtOAc, 2:1, v/v) to afford Boc-Hag-Gly-O^{t}Bu **2** (1.23 g, 3.59 mmol, 89% yield) as a colourless solid. R_f 0.59 (cyclohexane:EtOAc, 1:1, v/v); ^{1}H-NMR (600 MHz, DMSO-d_6, 300 K) δ = 8.11 (t, 1H, ^{3}J=5.8 Hz, α-NH^{Gly}), 6.87 (d, 1H, ^{3}J=8.2 Hz, α-NH^{Hag}), 5.79 (dddd, 1H, ^{3}J=17.0 Hz, ^{3}J=10.3 Hz, ^{3}J=6.6 Hz, ^{3}J=6.6 Hz, δ-CH^{Hag}), 5.04-4.92 (m, 2H, ε-CH$_2^{Hag}$), 3.94 (ddd, 1H, ^{3}J=8.6 Hz, ^{3}J=8.6 Hz, ^{3}J=5.0 Hz, α-CH^{Hag}), 3.76 (dd, 1H, ^{2}J=17.6 Hz, ^{3}J=6.3 Hz, α-CH$_2^{Gly}$), 3.65 (dd, 1H, ^{2}J=17.5 Hz, ^{3}J=5.6 Hz, α-CH$_2^{Gly}$), 2.12-1.98 (m, 2H, γ-CH$_2^{Hag}$), 1.75-1.64 (m, 1H, β-CH$_2^{Hag}$), 1.62-1.53 (m, 1H, β-CH$_2^{Hag}$), 1.39 (s, 9H, Boc), 1.38 (s, 9H, CO$_2$^{t}Bu) ppm; ^{13}C-NMR (75 MHz, DMSO-d_6, 300 K) δ = 172.4, 168.8, 155.2, 137.9, 115.1, 80.5, 77.9, 53.6, 41.4, 31.2, 29.6, 28.2, 27.7 ppm; HRMS (ESI) calculated for [$C_{17}H_{30}N_2O_5Na^+$]: 365.2047, found: 365.2059.

tert-Butyl-((2*S*)-2-((_tert_-butoxycarbonyl)amino)-4-(oxiran-2-yl)butanoyl)glycinate (Boc-Enl-Gly-O^{t}Bu, 3)

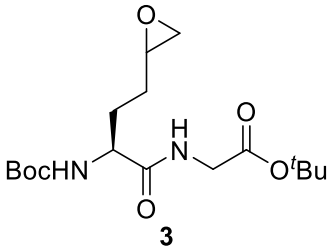

3

meta-Chloroperoxybenzoic acid (77w%, 1.23 g, 5.39 mmol, 1.5 equiv.) was added in portion at 0 °C to a solution of Boc-Hag-Gly-O^{t}Bu **2** (1.23 g, 3.59 mmol, 1.0 equiv.) in dichloromethane (25 mL), the solution was allowed to warm to room temperature and stirred for 16 h. The reaction mixture was diluted with 10% aqueous Na_2SO_3 solution (25 mL) and stirred vigorously for 1 h. The layers were separated and the organic layer was washed with 5% aqueous $NaHCO_3$ solution (25 mL) and brine, dried over $MgSO_4$, filtered and concentrated *in vacuo*. The obtained crude material was purified by silica gel column chromatography (cyclohexane:EtOAc, 1:1, v/v) to afford the side chain epoxy **3** (1.18 g, 3.30 mmol, 92% yield) as a colourless solid. R_f 0.28 (cyclohexane:EtOAc, 1:1, v/v); ^{1}H-NMR (600 MHz, DMSO-d_6, 300 K) δ = 8.19 (t, 1H, ^{3}J=6.0 Hz, α-NH^{Gly,4R}), 8.16 (t, 1H, ^{3}J=6.0 Hz, α-NH^{Gly,4S}), 6.93 (d, 1H, ^{3}J=7.8 Hz, α-NH^{Enl,4S}), 6.91 (d, 1H, ^{3}J=7.8 Hz, α-NH^{Enl,4R}), 4.01-3.91 (m, 1H, α-CH^{Enl}), 3.77 (dd, 1H, ^{3}J=17.2 Hz, ^{3}J=6.0 Hz, α-CH$_2^{Gly,4R}$), 3.76 (dd, 1H, ^{2}J=17.2 Hz, ^{3}J=6.0 Hz, α-CH$_2^{Gly,4S}$), 3.65 (dd, 1H, ^{2}J=17.4 Hz, ^{3}J=5.9 Hz, α-CH$_2^{Gly,4S}$), 3.64 (dd, 1H, ^{3}J=17.5 Hz, ^{3}J=6.0 Hz, α-CH$_2^{Gly,4R}$), 2.91-2.84 (m, 1H, δ-CH^{Enl}), 2.69-2.64 (m, 1H, ε-CH^{Enl}), 2.43 (dd, 1H, ^{3}J=5.3 Hz, ^{2}J=2.6 Hz, α-CH$_2^{Gly,4R}$), 2.40 (dd, 1H, ^{3}J=5.1 Hz, ^{2}J=2.6 Hz, α-CH$_2^{Gly,4S}$), 1.81-1.68 (m, 1H, β-CH$_2^{Enl}$), 1.65-1.55 (m, 1H, β-CH$_2^{Enl}$), 1.55-1.43 (m,

1H, γ-CH_2^{Enl}), 1.39 (s, 9H, Boc), 1.38 (s, 9H, $CO_2{}^tBu$) ppm; ^{13}C-NMR (125 MHz, DMSO-d_6, 300 K) δ = 172.2, 168.8, 155.2, 80.5, 78.0, 53.8, 53.5, 51.2, 51.0, 46.1, 41.4, 28.5, 28.2, 28.1, 27.7 ppm; HRMS (ESI) calculated for [$C_{17}H_{30}N_2O_6Na^+$]: 381.1996, found: 381.1998.

((2*S*)-2-Amino)-6-((trimethylammonium)trifluoroacetate)-5-hydroxyhexanoyl)glycine hydrotrifluoroacetate (H_2N-Hyl(Me)$_3$-Gly-OH · TFA, 4)

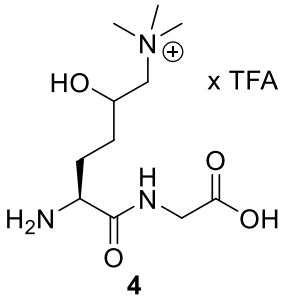

4

To a solution of Boc-Enl-Gly-O^{t}Bu·**3** (1.18 g, 3.30 mmol, 1.00 equiv.) in a mixture of MeCN/H_2O (7.5 mL, 2:1), a 45% aqueous NEt_3 solution (0.63 mL, 4.12 mmol, 1.25 equiv.) was added dropwise at 0 °C. The reaction mixture was allowed to warm to room temperature and stirred vigorously for 7 h. The solvent was removed *in vacuo* to give the δ-hydroxy-lysine as a white solid, which was used without further purification in the next step.

The crude Boc-Hyl(Me)$_3$-Gly-O^{t}Bu·(3.30 mmol, 1.00 equiv.) was suspended in dichloromethane (10 mL) and trifluoroacetic acid (5.08 mL, 7.52 mmol, 20.0 equiv.) was added at 0 °C. The resulting solution was stirred at room temperature for 2 h. The solvent was removed *in vacuo* and the crude material was several times treated with diethyl ether. The residue was lyophilized from a mixture of water/acetonitrile (10 mL, 1:1) to give H_2N-Hyl(Me)$_3$-Gly-OH · TFA **4** (1.60 g, 3.27 mmol, 99% yield) as a pale yellow foam. ^{1}H-NMR (600 MHz, DMSO-d_6, 300 K) δ = 12.72 (bs, 1H, CO_2H), 9.13 (t, 1H, ^{3}J=5.8 Hz, α-$NH^{Gly,5R}$), 9.08 (t, 1H, ^{3}J=6.0 Hz, α-$NH^{Gly,5S}$), 8.43 (d, 3H, ^{3}J=4.6 Hz, α-$NH_2{}^{Hyl,5S}$), 8.40 (d, 3H, ^{3}J=4.5 Hz, α-$NH_2{}^{Hyl,5R}$), 4.17-4.09 (m, 1H, δ-CH^{Hyl}), 4.00-3.90 (m, 1H, α-CH^{Hyl}), 3.90-3.85 (m, 1H, α-$CH_2{}^{Gly}$), 3.83-3.76 (m, 1H, α-$CH_2{}^{Gly}$), 3.39-3.24 (m, 2H, ε-$CH_2{}^{Hyl}$), 3.16 (s, 9H, $N^+(CH_3)_3{}^{Hyl}$), 1.95-1.81 (m, 2H, γ-$CH_2{}^{Hyl}$), 1.60-1.52 (m, 1H, β-$CH_2{}^{Hyl}$), 1.51-1.38 (m, 1H, β-$CH_2{}^{Hyl}$) ppm; HRMS (ESI) calculated for [$C_{11}H_{24}N_3O_4^+$]: 262.1761, found: 262.1757.

((2*S*)-2-((Fluorenylmethyloxycarbonyl)amino)-6-((trimethylammonium)trifluoroacetate)-5-hydroxyhexanoyl)glycine hydrotrifluoroacetate (Fmoc-Hyl(Me)$_3$-Gly-OH · TFA, 5)

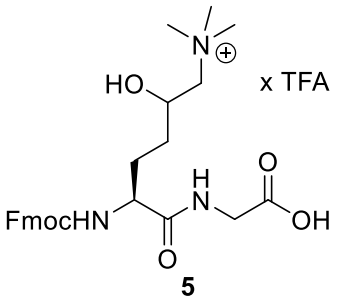

5

H_2N-Hyl(Me)$_3$-Gly-OH · TFA **4** (1.60 g, 3.27 mmol, 1.00 equiv.) was dissolved in water (15 mL) and the pH value was adjusted to 8 with a 10% aqueous Na_2CO_3solution. A solution of FmocOSu (1.32 g, 3.92 mmol, 1.20 equiv.) in 1,4-dioxane (7.5 mL) was added dropwise at 0 °C. The resulting suspension was allowed to warm to room temperature and stirred for 20 h. After the completion of the reaction, the mixture was gently acidified to pH 3 with 2 M HCl and the solvents was removed *in vacuo*. The crude material was purified by semi-preparative HPLC (*Thermo Scientific Dionex* UltiMate3000) using a C18 column (*Macherey-Nagel* VP Nucleodur C18, 125 x 21 mm, 5 µm, 100 Å) and a linear gradient of 10% to 50% of MeCN (containing 0.085% TFA) in H_2O (containing 0.10% TFA), in 30 min at a flow rate of 15 mL/min. Selected fractions were combined and lyophilized to obtain Fmoc-Hyl(Me)$_3$-Gly-OH · TFA **5** (1.47 g, 2.45 mmol, 75% yield) as a white hydroscopic solid. R_f 0.14 (MeOH:H_2O, 19:1, v/v); ^{1}H-NMR (600 MHz, DMSO-d_6, 300 K) δ = 12.59 (bs, 1H, CO_2H), 8.25 (t, 1H, ^{3}J=5.8 Hz, α-NH^{Gly,5R}), 8.20 (t, 1H, ^{3}J=5.8 Hz, α-NH^{Gly,5S}), 7.90 (d, 2H, ^{3}J=7.6 Hz, Fmoc^{Ar}), 7.74 (dd, 2H, ^{3}J=7.6 Hz, ^{3}J=10.6 Hz, Fmoc^{Ar}), 7.54 (dd, 1H, ^{3}J=8.3 Hz, ^{3}J=8.0 Hz, α-NH$^{Hyl,5R/S}$), 7.42 (t, 2H, ^{3}J=7.5 Hz, Fmoc^{Ar}), 7.33 (t, 2H, ^{3}J=7.4 Hz, Fmoc^{Ar}), 5.35 (dd, 1H, ^{3}J=5.1 Hz, ^{3}J=5.1 Hz, δ-OH$^{Hyl,5R/S}$), 4.33-4.19 (m, 3H, Fmoc^{Alip}), 4.10-3.98 (m, 2H, α-CH$^{Hyl,5R/S}$, δ-CH$^{Hyl,5R/S}$), 3.86-3.70 (m, 2H, α-CH$_2^{Gly}$), 3.31-3.19 (m, 2H, ε-CH$_2^{Hyl,5R/S}$), 3.10 (s, 9H, N$^+$(CH$_3$)$_3^{Hyl,5R/S}$), 1.88-1.54 (m, 2H, β-CH$_2^{Hyl,5R/S}$), 1.52-1.35 (m, 2H, γ-CH$_2^{Hyl,5R/S}$) ppm; ^{13}C-NMR (125 MHz, DMSO-d_6, 300 K) δ = 172.1, 171.2, 156.1, 156.0, 144.0, 143.8, 140.8, 127.7, 127.2, 125.4, 125.3, 120.2, 70.0, 69.9, 65.8, 64.8, 64.5, 54.4, 54.2, 53.4, 46.7, 40.7, 32.0, 27.8, 27.7 ppm; HRMS (ESI) calculated for [$C_{26}H_{34}N_3O_6^+$]: 484.2442, found: 484.2447.

v,v-Dimethyl-dipropyleneamino-lysine building blocks for SPPS

3-(*tert*-butyldimethylsilyloxy)propylamine (S4)

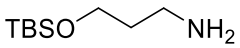

S4

The reaction was performed according to the literature.[2] In a *flame-dried* nitrogen round-bottom flask 1-amino-3-propanol (8.40 mL, 110 mmol, 1.0 equiv.) was dissolved in dry dichloromethane (200 mL) and cooled to 0 °C. NEt_3 (23.0 mL, 165 mmol, 1.5 equiv.) and TBDMSCl (18.2 g, 120 mmol, 1.1 equiv.) were added and the resulting suspension was stirred at room temperature for 18 h. The clear solution was washed with water (75 mL x 3) and brine, dried over $MgSO_4$, filtered, and concentrated *in vacuo*. The obtained crude oil was purified by distillation (bp 65-70 °C at 5 mbar) to afford 3-(*tert*-butyldimethylsilyloxy)propylamine **S4** (17.5 g, 92.4 mmol, 84% yield) as a colourless oil. R_f 0.20 ($CHCl_3$:MeOH, 9:1, v/v); ^{1}H-NMR (300 MHz, DMSO-d_6, 300 K) δ = 3.63 (t, 2H, ^{3}J=6.3 Hz, CH_2OTBS), 2.57 (t, 2H, ^{3}J=6.8 Hz, CH_2NH_2), 1.51 (qi, 2H, ^{3}J=6.5 Hz, CH_2), 1.26 (bs, 2H, NH_2), 0.86 (s, 9H, TBDMS), −0.02 (s, 6H, TBDMS) ppm; ^{13}C-NMR (75 MHz, DMSO-d_6, 300 K) δ = 60.6, 38.5, 36.4, 25.8, 17.9, −5.4 ppm; HRMS (ESI) calculated for [$C_9H_{23}NOSiH^+$]: 190.1622, found: 190.1622.

N-(3-(*tert*-butyldimethylsilyloxy)propyl)-2-nitrobenzenesulfonamide (S5)

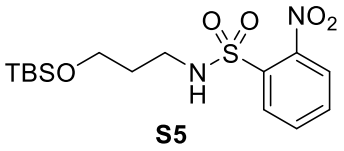

S5

3-(*tert*-butyldimethylsilyloxy)propylamine **S4** (11.3 g, 59.7 mmol, 1.0 equiv.) was dissolved in dichloromethane (55 mL), cooled to 0 °C and DIPEA (12.5 mL, 71.7 mmol, 1.2 equiv.) was added. A solution of 2-nitrobenzenesulfonyl chloride (15.9 g, 71.7 mmol, 1.2 equiv.) in dichloromethane (25 mL) was added dropwise. The resulting suspension was stirred at ambient temperature for 24 h. The solution was washed with 1.0 M HCl solution (250 mL x 2) and brine, dried over $MgSO_4$, filtered, and concentrated *in vacuo*. The obtained crude material was purified by silica gel column chromatography (DCM) to afford *N*-(3-(*tert*-butyldimethylsilyloxy)propyl)-2-nitrobenzenesulfonamide **S5** (14.7 g, 39.6 mmol, 66% yield) as a pale, yellow oil. R_f 0.44 (DCM); ^{1}H-NMR (300 MHz, DMSO-d_6, 300 K) δ = 8.05-7.91 (m, 3H, NH, Ns^{Ar}), 7.91-7.80 (m, 2H, Ns^{Ar}), 3.56 (t, 2H, ^{3}J=6.1 Hz, CH_2OTBS), 2.95 (dt, 2H, ^{3}J=6.7 Hz, ^{3}J=6.4 Hz, CH_2NHNs), 1.60 (qi, 2H, ^{3}J=6.6 Hz, CH_2), 0.81 (s, 9H, TBDMS), −0.02 (s, 6H, TBDMS) ppm; ^{13}C-NMR (75 MHz, DMSO-d_6, 300 K) δ = 147.8, 134.0, 132.5, 132.4, 129.4, 124.3, 59.7, 32.1, 25.8, 25.7, 17.8, −5.8 ppm; HRMS (ESI) calculated for [$C_{15}H_{26}N_2O_5SSiNa^+$]: 397.1224, found: 397.1227.

***N*-(3-(*tert*-butyldimethylsilyloxy)propyl)-*N*-(3-(dimethylamino)propyl)-2-nitrobenzenesulfonamide (S6)**

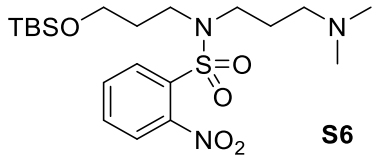

S6

In a *flame-dried* nitrogen round-bottom flask triphenylphosphine (10.6 g, 40.5 mmol, 1.5 equiv.) was dissolved in dry tetrahydrofuran (90 mL), cooled to 0 °C and diisopropyl azodicarboxylate (8.00 mL, 40.5 mmol, 1.5 equiv.) was added. The mixture was stirred at 0 °C until a precipitate was formed (15 min). To the betaine suspension was added a solution of silyl ether **S5** (10.1 g, 27.0 mmol, 1.0 equiv.) in dry THF (10.0 mL) and stirred at 0 °C for 20 min. Afterwards 3-dimethylamino-1-propanol (4.80 mL, 40.5 mmol, 1.5 equiv.) was added dropwise and the resulting mixture was warmed to room temperature and stirred for 18 h. The solvent was removed *in vacuo* and the crude material was purified by silica gel column chromatography ($CHCl_3$:MeOH; 9:1; v/v) to afford amino-silyl ether **S6** (10.2 g, 22.1 mmol, 82% yield) as an orange-yellowish oil. R_f 0.44 (DCM:MeOH, 9:1, v/v); ^{1}H-NMR (300 MHz, DMSO-d_6, 300 K) δ = 8.02-7.93 (m, 2H, Ns^{Ar}), 7.92-7.79 (m, 2H, Ns^{Ar}), 3.55 (t, 2H, ^{3}J=6.0 Hz, CH_2OTBS), 3.39-3.23 (m, 4H, $NNsCH_2$), 2.22 (t, 2H, ^{3}J=6.9 Hz, $CH_2N(CH_3)_2$), 2.11 (s, 6H, $N(CH_3)_2$), 1.73-1.56 (m, 4H, CH_2), 0.84 (s, 9H, TBDMS), 0.00 (s, 6H, TBDMS) ppm; ^{13}C-NMR (75 MHz, DMSO-d_6, 300 K) δ = 147.6, 134.4, 132.3, 131.8, 129.7, 124.2, 59.8, 55.8, 45.6, 44.7, 44.5, 31.4, 25.7, 25.6, 17.8, −5.5 ppm; HRMS (ESI) calculated for [$C_{20}H_{37}N_3O_5SSiH^+$]: 460.2296, found: 460.2291.

***N*-(3-(dimethylamino)propyl)-*N*-(3-hydroxypropyl)-2-nitrobenzenesulfonamide (6)**

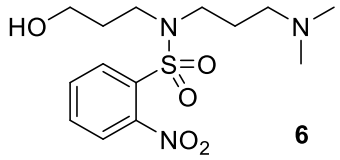

6

To a solution of amino-silyl ether **S6** (10.2 g, 22.1 mmol, 1.0 equiv.) in dry tetrahydrofuran (200 mL) was added 1.0 M tetrabutylammonium fluoride solution (24.3 mL, 24.3 mmol, 1.1 equiv.) in tetrahydrofuran. The mixture was vigorously stirred at room temperature for 2 h. The solvent was removed *in vacuo* and the crude material was purified by silica gel column chromatography ($CHCl_3$:MeOH; 8:2; v/v) to afford protected amino alcohol **6** (7.33 g, 21.2 mmol, 96% yield) as a-yellow oil. R_f 0.13 (DCM:MeOH, 9:1, v/v); ^{1}H-NMR (300 MHz, DMSO-d_6, 300 K) δ = 8.02-7.93 (m, 2H, Ns^{Ar}), 7.92-7.80 (m, 2H, Ns^{Ar}), 4.73 (bs, 1H, CH_2OH), 3.38 (d, 2H, ^{3}J=6.2 Hz, CH_2OH), 3.35-3.23 (m, 4H, $NNsCH_2$), 2.19 (t, 2H, ^{3}J=7.0 Hz, $CH_2N(CH_3)_2$), 2.09 (s, 6H, $N(CH_3)_2$), 1.64 (qi, 2H, ^{3}J=6.3 Hz, CH_2), 1.62 (qi, 2H, ^{3}J=6.7 Hz, CH_2) ppm; ^{13}C-NMR (75 MHz, DMSO-d_6, 300 K) δ = 147.6, 134.3, 132.4, 131.9, 129.6, 124.2, 58.0, 55.9, 45.7, 45.0, 44.9, 31.4, 25.8 ppm; HRMS (ESI) calculated for [$C_{14}H_{23}N_3O_5SH^+$]: 346.1431, found: 346.1438.

***tert*-Butyl-(2*S*)-2-[(*tert*-butoxycarbonyl)amino]-6-[(benzyloxycarbonyl)amino]hexanoate (Boc-Lys(Cbz)-O^{t}Bu, S7)**

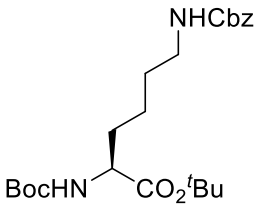

S7

H_2N-Lys(Cbz)-O^{t}Bu (5.00 g, 13.4 mmol, 1.00 equiv.) was suspended in dichloromethane (50 mL), cooled to 0 °C and DIPEA (4.56 mL, 26.8 mmol, 2.00 equiv.) was added. A solution of Boc_2O (3.66 g, 16.8 mmol, 1.25 equiv.) in dichloromethane (25 mL) was added dropwise at 0 °C. The resulting suspension was stirred at ambient temperature for 24 h. The alkaline mixture was washed with 0.5 M HCl solution (50 mL x 2) and brine, dried over $MgSO_4$, filtered and concentrated *in vacuo*. The obtained crude material was purified by silica gel column chromatography (cyclohexane:EtOAc, 4:1 → 2:1; v/v) to afford Boc-Lys(Cbz)-O^{t}Bu **S7** (5.34 g, 12.2 mmol, 91% yield) as a colourless oil. R_f 0.30 (cyclohexane:EtOAc, 1:1, v/v); ^{1}H-NMR (300 MHz, DMSO-d_6, 300 K) δ = 7.42 (m, 5H, Cbz^{Ar}), 7.22 (t, 1H, ^{3}J=5.6 Hz, ε-NH), 7.05 (d, 1H, ^{3}J=7.6 Hz, α-NH), 5.00 (s, 2H, Cbz^{Alip}), 3.80-3.62 (m, 1H, α-CH), 2.97 (dt, 2H, ^{3}J=6.1 Hz, ^{3}J=6.1 Hz, ε-CH_2), 1.68-1.49 (m, 2H, δ-CH_2), 1.44-1.22 (m, 4H, β-CH_2, γ-CH_2), 1.38 (s, 18H, Boc, O^{t}Bu) ppm; ^{13}C-NMR (75 MHz, DMSO-d_6, 300 K) δ = 171.9, 156.1, 155.5, 137.3, 128.3, 127.7, 80.1, 78.0, 65.1, 54.3, 39.9, 30.3, 28.9, 28.2, 27.6, 22.7 ppm; HRMS (ESI) calculated for [$C_{23}H_{36}N_2O_6Na^+$]: 459.2477, found: 459.2461.

***tert*-Butyl-(2*S*)-2-[(*tert*-butoxycarbonyl)amino]-6-amino-hexanoate hydrochloride (Boc-Lys-O^{t}Bu · HCl, S8)**

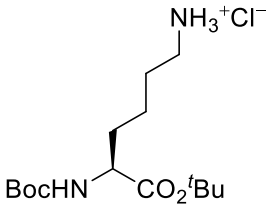

S8

Boc-Lys(Cbz)-O^{t}Bu **S7** (5.34 g, 12.2 mmol, 1.00 equiv.) was dissolved in ethanol (50 mL) and 1 M HCl solution (15.3 mL, 15.2 mmol, 1.25 equiv.) and palladium on charcoal (10 wt.%, 0.65 g, 0.61 mmol, 0.05 equiv.) were added. The resulting suspension was stirred under hydrogen atmosphere (10 bar) at ambient temperature for 22 h. The mixture was filtered through *Celite* and concentrated *in vacuo*. Titration with chloroform and drying under high vacuum afforded Boc-Lys-O^{t}Bu · HCl **S8** (3.92 g, 11.6 mmol, 95% yield) as a colourless hygroscopic solid. R_f 0.01 (cyclohexane:EtOAc, 1:1, v/v); ^{1}H-NMR (300 MHz, DMSO-d_6, 300 K) δ = 8.00 (s, 3H, ε-NH^{3+}), 7.09 (d, 1H, ^{3}J=7.6 Hz, α-NH), 3.73 (ddd, 1H, ^{3}J=7.9

Hz, ^{3}J=7.9 Hz, ^{3}J=5.6 Hz, α-CH), 2.73 (t, 2H, ^{3}J=7.1 Hz, ε-CH_2), 1.64-1.47 (m, 4H, δ-CH_2, β-CH_2), 1.44-1.28 (m, 2H, γ-CH_2), 1.38 (s, 18H, Boc, O^{t}Bu) ppm; ^{13}C-NMR (75 MHz, DMSO-d_6, 300 K) δ = 171.8, 156.6, 80.2, 78.0, 54.2, 38.3, 30.0, 28.2, 27.6, 22.5 ppm; HRMS (ESI) calculated for [$C_{15}H_{30}N_2O_4H^+$]: 303.2278, found: 303.2281.

tert-Butyl-(2*S*)-2-[(_tert_-butoxycarbonyl)amino]-6-[(2-nitrobenzenesulfonyl)amino]hexanoate (Boc-Lys(Ns)-O^{t}Bu, 7)

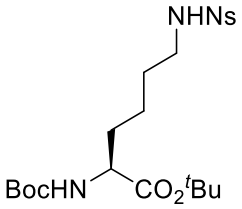

7

Boc-Lys-O^{t}Bu · HCl **S8** (3.92 g, 11.6 mmol, 1.00 equiv.) was suspended in dichloromethane (85 mL), cooled to 0 °C and DIPEA (5.04 mL, 28.9 mmol, 2.50 equiv.) was added. A solution of 2-Nitrobenzenesulfonyl chloride (2.82 g, 12.7 mmol, 1.10 equiv.) in dichloromethane (15 mL) was added dropwise at 0 °C. The resulting suspension was stirred at ambient temperature for 24 h. The solvent was removed *in vacuo* and the residue was dissolved in a mixture of H_2O/EtOAc (120 mL, 1:1, v/v). The layers were separated and the aqueous layer was extracted with EtOAc (60 mL x 2). The combined organic layer was washed with brine, dried over $MgSO_4$, filtered and concentrated *in vacuo*. The obtained crude material was purified by silica gel column chromatography (cyclohexane:EtOAc, 3:1; v/v) to afford Boc-Lys(Ns)-O^{t}Bu **7** (5.34 g, 12.2 mmol, 91% yield) as an orange-yellowish oil. R_f 0.48 (cyclohexane:EtOAc, 1:1, v/v); ^{1}H-NMR (300 MHz, DMSO-d_6, 300 K) δ = 8.04 (t, 1H, ^{3}J=5.7 Hz, ε-NH), 8.00-7.97 (m, 1H, Ns^{Ar}), 7.96-7.94 (m, 1H, Ns^{Ar}), 7.87-7.83 (m, 2H, Ns^{Ar}), 7.02 (d, 1H, ^{3}J=7.7 Hz, α-NH), 3.70 (ddd, 1H, ^{3}J=8.3 Hz, ^{3}J=8.3 Hz, ^{3}J=5.0 Hz, α-CH), 2.87 (dt, 2H, ^{3}J=6.8 Hz, ^{3}J=6.5 Hz ε-CH_2), 1.57-1.44 (m, 2H, β-CH_2), 1.44-1.32 (m, 2H, δ-CH_2), 1.38 (s, 18H, Boc, O^{t}Bu), 1.32-1.23 (m, 2H, γ-CH_2) ppm; ^{13}C-NMR (75 MHz, DMSO-d_6, 300 K) δ = 171.8, 155.5, 147.7, 133.9, 132.8, 132.5, 129.3, 124.3, 80.1, 78.0, 54.2, 42.4, 30.1, 28.7, 28.1, 27.6, 22.5 ppm; HRMS (ESI) calculated for [$C_{21}H_{33}N_3O_8SH^+$]: 488.2061, found: 488.2078.

***tert*-Butyl-(2*S*)-2-[(*tert*-butoxycarbonyl)amino]-6-{3-[(3-dimethylaminopropyl)-(2-nitrobenzene-sulfonyl)amino]propyl}-6-(2-nitrobenzenesulfonyl)amino]hexanoate (Boc-Kdp(Me)$_2$(Ns)$_2$-O^{t}Bu, 8)**

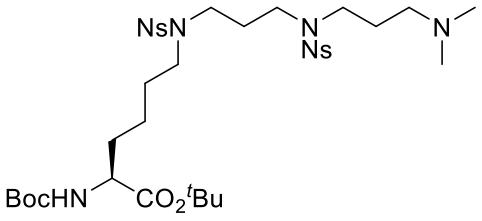

8

In a *flame-dried* nitrogen round-bottom flask triphenylphosphine (1.26 g, 4.79 mmol, 1.0 equiv.) was dissolved in dry tetrahydrofuran (25 mL), cooled to 0 °C and diisopropyl azodicarboxylate (0.97 mL, 4.79 mmol, 1.0 equiv.) was added. The mixture was stirred at 0 °C until a precipitate was formed (15 min). To the betaine suspension was added a 0.5 M solution of Boc-Lys(Ns)-O^{t}Bu **7** (10.0 mL, 5.04 mmol, 1.05 equiv.) in dry THF and stirred at 0 °C for 10 min. Afterwards a 0.5 M solution of aminoalcohol **6** (10.0 mL, 5.04 mmol, 1.05 equiv.) in dry THF was added and the resulting mixture was warmed to room temperature and stirred for 20 h. The solvent was removed *in vacuo* and the crude material was purified by silica gel column chromatography ($CHCl_3$:MeOH; 20:0 → 19:1; v/v) to afford Boc-Kdp(Me)$_2$(Ns)$_2$-O^{t}Bu **8** (2.08 g, 2.55 mmol, 51% yield) as a yellow oil. R_f 0.35 ($CHCl_3$:MeOH, 9:1, v/v); ^{1}H-NMR (300 MHz, DMSO-d_6, 300 K) δ = 8.00-7.93 (m, 4H, Ns^{Ar}), 7.92-7.79 (m, 4H, Ns^{Ar}), 7.06 (d, 1H, ^{3}J=7.7 Hz, α-NH), 3.72 (ddd, 1H, ^{3}J=8.3 Hz, ^{3}J=8.2 Hz, ^{3}J=5.2 Hz, α-CH), 3.29-3.13 (m, 8H, ε-CH_2, η-CH_2, ι-CH_2, λ-CH_2), 2.16 (t, 2H, ^{3}J=6.8 Hz, ν-CH_2), 2.08 (bs, 6H, N(CH_3)$_2$), 1.70 (qi, 2H, ^{3}J=7.3 Hz, μ-CH_2), 1.64-1.50 (m, 4H, β-CH_2, θ-CH_2), 1.48-1.31 (m, 2H, δ-CH_2), 1.38 (s, 18H, Boc, O^{t}Bu), 1.30-1.13 (m, 2H, γ-CH_2) ppm; ^{13}C-NMR (75 MHz, DMSO-d_6, 300 K) δ = 171.7, 155.5, 147.5, 134.5, 132.4, 132.3, 131.7, 131.6, 129.7, 129.6, 124.3 (2x), 80.1, 78.0, 55.8, 54.2, 47.3, 45.6, 44.8, 44.7, 30.2, 28.1, 27.6, 27.4, 26.9, 25.8, 22.6 ppm; HRMS (ESI) calculated for [$C_{35}H_{54}N_6O_{12}S_2H^+$]: 815.3314, found: 815.3314.

(2*S*)-2-Amino-6-{3-[(3-dimethylaminopropyl)-(2-nitrobenzenesulfonyl)amino]propyl}-6-(2-nitro-benzenesulfonyl)amino]hexanoic acid hydrotrifluoroacetat (H$_2$N-Kdp(Me)$_2$(Ns)$_2$-OH · TFA, 9)

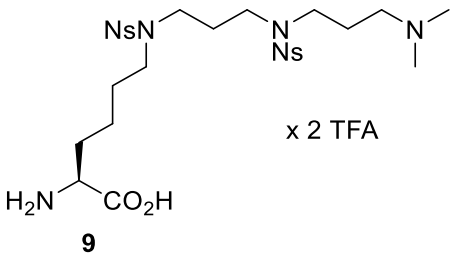

9

To a solution of Boc-Kdp(Me)$_2$(Ns)$_2$-O^{t}Bu **8** (2.08 g, 2.55 mmol, 1.0 equiv.) in dichloromethane (25 mL) was added triethylsilane (8.15 mL, 51.0 mmol, 20.0 equiv.) and trifluoroacetic acid (19.5 mL, 255 mmol, 100 equiv.) at 0 °C. The resulting solution was stirred at room temperature for 20 h. The solvent was removed *in vacuo* and the crude material was several times treated with diethyl ether.

The residue was lyophilized from a mixture of water/acetonitrile (50 mL, 1:1) to give H_2N-Kdp(Me)$_2$(Ns)$_2$-OH · TFA **9** (2.22 g, 2.50 mmol, 98% yield) as a pale yellow foam. ^{1}H-NMR (500 MHz, DMSO-d_6, 300 K) δ = 9.62 (bs, 1H, NH$^+$(CH$_3$)$_2$), 8.22 (bs, 3H, α-NH$_3^+$), 8.00-7.81 (m, 8H, Ns^{Ar}), 3.90-3.83 (bs, 1H, α-CH), 3.31 (t, 2H ^{3}J=7.2 Hz, λ-CH$_2$), 3.26 (t, 2H, ^{3}J=7.5 Hz, ι-CH$_2$), 3.23-3.15 (m, 4H, ε-CH$_2$, η-CH$_2$), 3.02 (t, 2H, ^{3}J=7.9 Hz, ν-CH$_2$), 2.77 (s, 6H, NH$^+$(CH$_3$)$_2$), 1.88 (qi, 2H ^{3}J=7.3 Hz, μ-CH$_2$), 1.80-1.65 (m, 4H, θ-CH$_2$, β-CH$_2$), 1.45 (qi, 2H, ^{3}J=7.5 Hz, δ-CH$_2$), 1.40-1.31 (m, 1H, γ-CH$_2$), 1.30-1.19 (m, 1H, γ-CH$_2$) ppm; ^{13}C-NMR (125 MHz, DMSO-d_6, 300 K) δ = 170.9, 147.5 (2x), 134.7, 134.6, 132.6, 132.5, 131.5, 131.3, 129.6, 129.5, 124.5, 124.4, 54.1, 51.8, 47.3, 45.0 (2x), 44.9, 42.2, 29.5, 27.6, 27.0, 23.2, 21.5 ppm; HRMS (ESI) calculated for [$C_{26}H_{38}N_6O_{10}S_2H^+$]: 659.2164, found: 659.2157.

(2*S*)-2-[(Fluorenylmethyloxycarbonyl)amino]-6-{3-[(3-dimethylaminopropyl)-(2-nitrobenzene-sulfonyl)amino]propyl}-6-(2-nitrobenzenesulfonyl)amino]hexanoic acid hydrotrifluoroacetate (Fmoc-Kdp(Me)$_2$(Ns)$_2$-OH · TFA, 10)

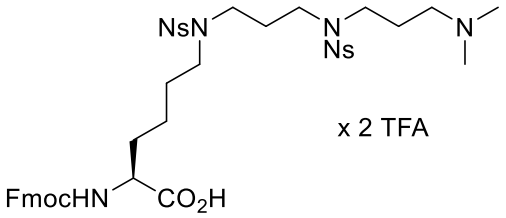

10

H_2N-Kdp(Me)$_2$(Ns)$_2$-OH · TFA **9** (2.22 g, 2.50 mmol, 1.0 equiv.) was suspended in dichloromethane (50 mL), cooled to 0 °C and DIPEA (1.70 mL, 10.0 mmol, 4.0 equiv.) was added. A solution of FmocOSu (1.01 g, 3.00 mmol, 1.2 equiv.) in dichloromethane (10 mL) was added at 0 °C. The resulting suspension was stirred at ambient temperature for 20 h. The solvent was removed *in vacuo* and the crude material was purified by silica gel column chromatography ($CHCl_3$:MeOH:TFA; 19:1:0.01; v/v) to afford Fmoc-Kdp(Me)$_2$(Ns)$_2$-OH · TFA **10** (2.01 g, 2.03 mmol, 81% yield) as a yellow oil. The product was converted to a colourless solid by purification using semi-preparative HPLC (*Thermo Scientific Dionex* UltiMate3000) using a C18 column (*Macherey-Nagel* VP Nucleodur C18, 125 x 21 mm, 5 µm, 100 Å) and a linear gradient of 30% to 90% of MeCN (containing 0.085% TFA) in H_2O (containing 0.10% TFA), in 30 min at a flow rate of 15 mL/min. Selected fractions were combined and lyophilized to obtain a white hydroscopic solid. R_f 0.32 ($CHCl_3$:MeOH:AcOH, 9:1:0.01, v/v/v); ^{1}H-NMR (500 MHz, DMSO-d_6, 300 K) δ = 12.56 (bs, 1H, CO_2H), 9.51 (bs, 1H, NH$^+$(CH$_3$)$_2$), 8.00-7.96 (m, 2H, Ns^{Ar}), 7.96-7.92 (m, 2H, Ns^{Ar}), 7.91-7.87 (m, 4H, Fmoc^{Ar}, Ns^{Ar}), 7.87-7.79 (m, 2H, Ns^{Ar}), 7.72 (dd, 2H, ^{3}J=7.4 Hz, ^{4}J=2.9 Hz, Fmoc^{Ar}), 7.58 (d, 1H, ^{3}J=8.1 Hz, α-NH), 7.41 (t, 2H, ^{3}J=7.4 Hz, Fmoc^{Ar}), 7.32 (t, 2H, ^{3}J=7.4 Hz, Fmoc^{Ar}), 4.29 (d, 2H, ^{3}J=7.3 Hz, Fmoc^{Alip}), 4.23 (t, 1H, ^{3}J=7.2 Hz, Fmoc^{Alip}), 3.88 (ddd, 1H, ^{3}J=9.0 Hz, ^{3}J=8.4 Hz, ^{3}J=4.8 Hz, α-CH), 3.32 (t, 2H, ^{3}J=7.2 Hz, λ-CH$_2$), 3.26 (t, 2H, ^{3}J=7.5 Hz, ι-CH$_2$), 3.22-3.14 (m, 4H, ε-CH$_2$, η-CH$_2$), 3.06-2.99 (m, 2H, ν-CH$_2$), 2.77 (s, 3H, NH$^+$(CH$_3$)$_2$), 2.76 (s, 3H, NH$^+$(CH$_3$)$_2$), 1.94-1.84 (m, 2H, μ-CH$_2$), 1.71 (qi, 2H,

^{3}J=7.3 Hz, θ-CH_2), 1.68-1.60 (m, 1H, β-CH_2^{ProS}), 1.60-1.51 (m, 1H, β-CH_2^{ProR}), 1.50-1.34 (m, 2H, δ-CH_2), 1.30-1.14 (m, 2H, γ-CH_2) ppm; ^{13}C-NMR (125 MHz, DMSO-d_6, 300 K) δ = 173.7, 156.0, 147.5, 143.7, 140.7, 134.7, 132.3, 131.4, 129.6, 129.3, 127.4, 126.9, 125.1, 124.3, 120.0, 65.4, 53.9, 53.5, 47.2, 46.5, 44.7 (2x), 44.5, 42.1, 30.1, 27.2, 26.8, 23.0, 22.4 ppm; HRMS (ESI) calculated for [$C_{41}H_{48}N_6O_{12}S_2H^+$]: 881.2844, found: 881.2885.

Dipeptide coupling with Fmoc Kdp(Me)$_2$(Ns)$_2$-OH · TFA

To determine the enantiomeric excess (*ee*) of the building block Fmoc-Kdp(Me)$_2$(Ns)$_2$-OH · TFA **10** we performed a dipeptide coupling with L-Ala-O^{t}Bu · HCl. The diastereomeric ratio was determined from the ^{1}H NMR integral ratio of the amide and α-protons. Assuming that no stereo information on L-Ala-O^{t}Bu was lost during the peptide coupling, the *ee* was determined directly from the *dr*.

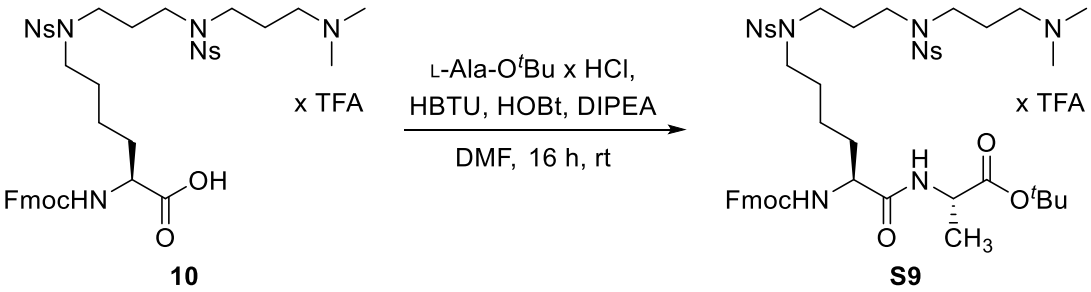

Fmoc-Kdp(Me)$_2$(Ns)$_2$-OH · TFA **10** (25.0 mg, 25.1 µmol, 1.0 equiv.) and H_2N-Ala-O^{t}Bu · HCl (5.02 mg, 27.6 µmol, 1.1 equiv.) were dissolved in DMF (250 µL) at room temperature. DIPEA (21.4 µL, 125 µmol, 5.0 equiv.), 0.25 M HBTU (110 µL, 27.6 µmol, 1.1 equiv.) in DMF and 0.5 M HOBt (55.3 µL, 27.6 µmol, 1.1 equiv.) in DMF were added and the resulting solution was stirred at room temperature for 18 h. The solvent was removed under reduced pressure and the obtained crude residue was purified by semi-preparative HPLC (*Thermo Scientific Dionex* UltiMate3000) using a C18 column (*Macherey-Nagel* VP Nucleodur C18, 125 x 21 mm, 5 µm, 100 Å) and a linear gradient of 30% to 90% of MeCN (containing 0.085% TFA) in H_2O (containing 0.10% TFA), in 60 min at a flow rate of 15 mL/min. Selected fractions were combined and lyophilized to obtain Fmoc-Kdp(Me)$_2$(Ns)$_2$-Ala-O^{t}Bu · TFA **S9** as a white solid, which was dissolved in DMSO-d_6 and *dr* was determined by NMR-spectroscopy. ^{1}H-NMR (600 MHz, DMSO-d_6, 300 K) δ = 9.39 (bs, 1H, $NH^+(CH_3)_2$), 8.17 (d, 1H, ^3J=6.9 Hz, α-NH^{Ala}), 8.00-7.79 (m, 10H, $Fmoc^{Ar}$, Ns^{Ar}), 7.72 (t, 2H, ^3J=6.8 Hz, $Fmoc^{Ar}$), 7.42 (d, 1H, ^3J=8.5 Hz, α-NH^{Kdp}), 7.41 (t, 2H, ^3J=7.4 Hz, $Fmoc^{Ar}$), 7.32 (t, 2H, ^3J=7.4 Hz, $Fmoc^{Ar}$), 4.30-4.17 (m, 3H, $Fmoc^{Alip}$), 4.10 (qd, 1H, ^3J=7.0 Hz, ^3J=7.1 Hz, α-CH^{Ala}), 3.96 (ddd, 1H, ^3J=8.8 Hz, ^3J=8.8 Hz, ^3J=4.8 Hz, α-CH^{Kdp}), 3.31 (t, 2H, ^3J=7.2 Hz, λ-CH_2), 3.26 (t, 2H, ^3J=7.5 Hz, η-CH_2), 3.24-3.12 (m, 4H, ε-CH_2, ι-CH_2), 3.05-2.98 (m, 2H, ν-CH_2), 2.77 (s, 3H, $NH^+(CH_3)_2$), 2.76 (s, 3H, $NH^+(CH_3)_2$), 1.92-1.84 (m, 2H, μ-CH_2), 1.71 (qi, 2H, ^3J=7.3 Hz, θ-CH_2), 1.64-1.55 (m, 1H, β-CH_2), 1.52-1.33 (m, 12H, β-CH_2, δ-CH_2, O^{t}Bu), 1.24 (d, 3H, ^3J=7.0 Hz, CH_3^{Ala}), 1.23-1.15 (m, 2H, γ-CH_2) ppm.

Serine building blocks for SPPS

O-(*tert*-Butyldimethylsilyl)-L-serine (H_2N-Ser(TBS)-OH, S10)

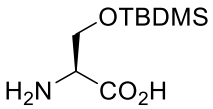

S10

L-Serine (2.63 g, 25.0 mmol, 1.0 equiv.) was suspended in dry DMF and cooled to 0 °C. Imidazole (3.41 g, 50.0 mmol, 2.0 equiv.) and TBDMSCl (4.15 g, 27.5 mmol, 1.1 equiv.) were added in one portion, the mixture was allowed to warm to rt and stirred for 18 h. DMF was removed by condensation and the remaining slurry was treated with 80 mL H_2O/pentane (1:1) and stirred for 4 h. The resulting colourless precipitate was filtered off, washed with cold pentane and dried under vacuum to give H_2N-Ser(TBS)-OH **S10** (3.88 g, 17.7 mmol, 71% yield). ^{1}H-NMR (300 MHz, CD_3OD, 300 K) δ = 4.06 (dd, 1H, ^{2}J=10.9 Hz, ^{3}J=3.8 Hz, β-CH_2) 3.99 (dd, 1H, ^{2}J=10.9 Hz, ^{3}J=6.1 Hz, β-CH_2), 3.61 (dd, 1H, ^{3}J=6.0 Hz, ^{3}J=3.8 Hz, α-CH), 0.93 (s, 9H, TBDMS), 0.13 (s, 6H, TBDMS) ppm; ^{13}C-NMR (75 MHz, CD_3OD, 300 K) δ = 171.7, 63.6, 58.0, 26.4, 19.3, −5.3, −5.4 ppm; HRMS (ESI) calculated for [$C_9H_{21}NO_3SiH^+$]: 220.1363, found: 220.1369.

N-(Fluorenylmethyloxycarbonyl)-*O*-(*tert*-butyldimethylsilyl)-L-serine (Fmoc-Ser(TBS)-OH, S11)

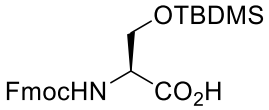

S11

H_2N-Ser(TBS)-OH **S10** (3.85 g, 17.6 mmol, 1.0 equiv.) was suspended in 5% aqueous solution of Na_2CO_3 (100 mL) and the pH value was adjusted to 8 with 2 M HCl. The mixture was cooled to 0 °C and a solution of FmocOSu (8.89 g, 26.4 mmol, 1.5 equiv.) in acetone (20 mL) was added dropwise. The resulting suspension was allowed to warm to rt and stirred for 18 h. The alkaline aqueous solution was washed with cyclohexane (200 mL) and then acidified to pH 3 with 2 M HCl and extracted with EtOAc (80 mL x 3). The combined organic layer was washed with brine, dried over $MgSO_4$, filtered and concentrated *in vacuo*. The obtained crude material was purified by silica gel column chromatography (cyclohexane:EtOAc:AcOH, 3:1:0.01; v/v/v) to afford Fmoc-Ser(TBS)-OH **S11** (5.88 g, 13.3 mmol, 71% yield) as a colourless solid. R_f 0.38 (CH:EE:AcOH, 3:1:0.01, v/v/v); ^{1}H-NMR (300 MHz, DMSO-d_6, 300 K) δ = 12.77 (s, 1H, CO_2H), 7.89 (d, 2H, ^{3}J=7.5 Hz, Fmoc^{Ar}), 7.73 (d, 2H, ^{3}J=7.2 Hz, Fmoc^{Ar}), 7.42 (t, 2H, ^{3}J=7.1 Hz, Fmoc^{Ar}), 7.42 (d, 1H, ^{3}J=8.3 Hz, α-NH), 7.32 (t, 2H, ^{3}J=7.4 Hz, Fmoc^{Ar}), 4.33-4.18 (m, 3H, Fmoc^{Alip}), 4.18-4.07 (m, 1H, α-CH), 3.90-3.77 (m, 2H, β-CH_2), 0.84 (s, 9H, TBDMS), 0.03 (s, 6H, TBDMS) ppm; ^{13}C-NMR (75 MHz, DMSO-d_6, 300 K) δ = 171.6, 155.9, 143.8, 143.7, 140.7, 127.6, 127.0, 125.2, 120.0, 65.8, 62.7, 56.1, 46.6, 25.7, 17.9, −5.5 ppm; HRMS (ESI) calculated for [$C_{24}H_{31}NO_5SiNa^+$]: 464.1864, found: 464.1862.

***N*-(*tert*-butoxycarbonyl)-*O*-(*tert*-butyldimethylsilyl)-L-serine (Boc-Ser(TBS)-OH, S12)**

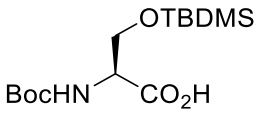

S12

H_2N-Ser(TBS)-OH **S10** (1.10 g, 5.00 mmol, 1.0 equiv.) was suspended in 5% aqueous solution of Na_2CO_3 (25 mL) and the pH value was adjusted to 8 with 2 M HCl. A solution of Boc_2O (1.31 g, 6.00 mmol, 1.2 equiv.) in acetone (50 mL) was added dropwise. The resulting suspension was stirred at rt for 18 h. The alkaline aqueous mixture was washed with cyclohexane (100 mL) and then acidified to pH 3 with 2 M HCl and extracted with EtOAc (100 mL x 3). The combined organic layer was washed with brine, dried over $MgSO_4$, filtered and concentrated *in vacuo*. The obtained crude material was purified by silica gel column chromatography (DCM:AcOH, 1:0.01; v/v) to afford Boc-Ser(TBS)-OH **S12** (1.15 g, 3.61 mmol, 72% yield) as a colourless oil. R_f 0.20 (DCM:AcOH, 1:0.01, v/v); ^{1}H-NMR (300 MHz, DMSO-d_6, 300 K) δ = 12.66 (s, 1H, CO_2H), 6.61 (d, 1H, ^{3}J=8.4 Hz, α-NH) 4.05 (dt, 1H, ^{3}J=8.5 Hz, ^{3}J=5.1 Hz, α-CH), 3.79 (d, 2H, ^{3}J=5.3 Hz, β-CH_2), 1.38 (s, 9H, Boc), 0.84 (s, 9H, TBDMS), 0.02 (s, 6H, TBDMS) ppm; ^{13}C-NMR (75 MHz, DMSO-d_6, 300 K) δ = 171.8, 155.1, 78.1, 62.8, 55.6, 28.1, 25.7, 17.9, −5.5 ppm; HRMS (ESI) calculated for [$C_{14}H_{29}NO_5SiNa^+$]: 342.1707, found: 342.1705.

LCPA mixtures for precipitation and DOSY experiments

LCPA H_3C-NH-[$(CH_2)_3$-N(CH_3)-]$_n$-H (S13, LCPA)

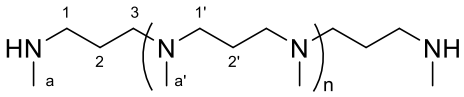

S13, LCPA

The reaction was performed according to the literature.[3] *N*,*N*-*Bis*[3-(methylamino)propyl]methylamine (4.60 mL, 26.5 mmol, 2.00 equiv.) was dissolved in anhydrous ethanol (1.0 mL) and a solution of 1,3-dibromopropane (1.35 g, 13.3 mmol, 1.00 equiv.) in anhydrous ethanol (4.45 mL) was added dropwise by a syringe pump (100 µL/min) at room temperature. After reaction work up according to the literature[3] the LCPAa mixture **S13a** (1.42 g, 2.37 mmol, 18% yield) was obtained as a yellow oil. The average chain length was calculated on 9 nitrogen from the integral ratio of terminal and internal protons of the methyl groups. The yield was determined for the average chain length of 9 nitrogen. ^{1}H-NMR (600 MHz, D_2O, 300 K) δ = 2.54 (t, 4H, ^{3}J=7.3 Hz, 1-CH_2), 2.41 (t, 4H, ^{3}J=8.1 Hz, 3-CH_2), 2.44-2.35 (m, 24, 1'-CH_2), 2.30 (s, 6H, a-CH_3), 2.20 (s, 21H, a'-CH_3), 1.69-1.61 (m, 16H, 2-,2'-CH_2) ppm; ^{13}C-NMR (75 MHz, D_2O, 300 K) δ = 54.6, 54.3, 48.7, 41.1, 34.5, 25.4, 22.9 ppm; HRMS (ESI) calculated for [$C_{33}H_{77}N_9H^+$]: 600.6375, found: 600.6380.

The reaction was repeated with a faster addition rate (25 µL/min) at room temperature. After reaction work up according to the literature[3] the LCPAb mixture **S13b** (1.25 g, 1.54 mmol, 12% yield) was obtained as a yellow oil. The average chain length was calculated on 12 nitrogen from the integral ratio of terminal and internal protons of the methyl groups. The yield was determined for the average chain length of 12 nitrogen. ^{1}H-NMR (600 MHz, D_2O, 300 K) δ = 2.57 (t, 4H, ^{3}J=7.3 Hz, 1-CH_2), 2.44 (t, 4H, ^{3}J=7.8 Hz, 3-CH_2), 2.40 (t, 36H, ^{3}J=7.8 Hz, 1'-CH_2), 2.34 (s, 6H, a-CH_3), 2.22 (s, 30H, a'-CH_3), 1.70-1.65 (m, 22H, 2-,2'-CH_2) ppm; ^{13}C-NMR (75 MHz, D_2O, 300 K) δ = 54.5, 54.3, 48.7, 41.0, 34.4, 25.3, 22.9 ppm; HRMS (ESI) calculated for [$C_{45}H_{104}N_{12}H^+$]: 813.8580, found: 813.8593.

Peptide synthesis

Activation of the 2-chlorotritylchloride resin

The partially hydrolysed 2-chlorotritylchloride resin (2-chlorotritylalcohol resin) was fully activated by chlorination. The resin was washed several times with DMF, dry DCM and dry toluene (5.00 mL/g resin) in a sintered glass funnel before it was transferred to a *flame-dried* nitrogen round-bottom flask equipped with a reflux condenser. Dry toluene (5.00 mL/g resin) and freshly distilled acetyl chloride (1.00 mL/g resin) was added. The resulting suspension was heated to 70 °C for 3 h. The resin was filtered, washed several times with dry toluene and dry DCM (10.0 mL/g resin) and dried under vacuum and used immediately.

Resin loading with standard Fmoc amino acids

2-Chlorotritylchloride resin (1.46 mmol/g, 200-400 *mesh*) was loaded by adding Fmoc-Lys(Boc)-OH (2.00 equiv.) and DIPEA (6.00 equiv.) in DCM (10 mL/g resin) and stirring at room temperature for 3 h. The resin was filtered, washed several times with DCM before it was treated with a mixture of DCM/MeOH/DIPEA (80:15:5) two times for 30 min. Finally, the resin was washed again several times with MeOH and DCM and dried under vacuum. The loading of the used resin was determined to be 0.60 mmol/g by UV-Vis spectroscopy at 289 nm and 300 nm after cleaving the Fmoc-protecting group with 20% piperidine in DMF for 20 min.

Resin loading with Fmoc-Kdp(Me)$_2$(Ns)$_2$-OH · TFA

Activated 2-chlorotritylchloride resin (1.46 mmol/g, 200-400 *mesh*) was loaded with Fmoc-Kdp(Me)$_2$(Ns)$_2$-OH · TFA **10** by adding the protected amino acid (0.50 equiv.) and DIPEA (1.50 equiv.) in DCM (20 mL/g resin) and stirring at room temperature for 3 h. The resin was filtered, washed several times with DCM before it was treated with a mixture of DCM/MeOH/DIPEA (80:15:5) three times for 30 min. Finally, the resin was washed again several times with MeOH and DCM and dried under vacuum. The loading of the used resin was determined to be 0.20 mmol/g by UV-Vis spectroscopy at 289 nm and 300 nm after cleaving the Fmoc-protecting group with 20% piperidine in DMF for 20 min.

Automated solid phase peptide synthesis

Peptides were synthesised on a microwave assisted *CEM Liberty Blue* peptide synthesizer. Fmoc-strategy was applied. The 2-chlorotritylchloride resin preloaded with Fmoc-Lys(Boc)-OH (scheduled quantity: 0.10 mmol, 1.00 equiv.) was swollen in DMF (20 mL/g resin) for 30 min at ambient temperature before it ran through the following cycles of Fmoc-deprotection and amino acid coupling.

- **Fmoc-deprotection:**

  T = 50 °C, $P_{microwave}$ = 30 W, t = 210 s with piperidine (20 w% in DMF, 3.00 mL/deprotection)

- **Amino acid coupling:**

  for amino acids except Fmoc-Arg(Pbf)-OH:

  T = 50 °C, $P_{microwave}$ = 30 W, t = 600 s with Fmoc-protected amino acid (0.2 M in DMF, 5.00 equiv., 2.5 mL/coupling), DIC (0.5 M in DMF, 5.00 equiv., 1.0 mL/coupling) and Oxyma (1.0 M in DMF, 5.00 equiv., 0.5 mL/coupling)

  for Fmoc-Arg(Pbf)-OH:

  1. T = 25 °C, $P_{microwave}$ = 0 W, t = 1500 s
  2. T = 50 °C, $P_{microwave}$ = 35 W, t = 660 s

  with Fmoc-protected amino acid (0.2 M in DMF, 5.00 equiv., 2.5 mL/coupling), DIC (0.5 M in DMF, 5.00 equiv., 1.0 mL/coupling) and Oxyma (1.0 M in DMF, 5.00 equiv., 0.5 mL/coupling).

Manual solid phase peptide synthesis

Peptides were synthesised using a special SCHLENK-frit for peptide synthesis. Fmoc-strategy was applied. The 2-chlorotritylchloride resin preloaded with Fmoc-Kdp$(Me)_2(Ns)_2$-OH · TFA **10** (scheduled quantity: 0.10 mmol, 1.00 equiv.) was swollen in DMF (20 mL/g resin) for 30 min at ambient temperature before it ran through the following cycles of Fmoc-deprotection and amino acid coupling.

- **Fmoc deprotection:**

  The Fmoc protecting group was removed by treatment of the pre-swollen resin with 25% piperidine in DMF (5.00 mL/0.1 mmol resin) at ambient temperature for 10 min. This procedure was performed three times. After completion, the solution was drained and the resin was washed several times with DMF, MeOH and DCM.

- **Standard amino acid coupling:**

  Fmoc-Xaa-OH (2.50 equiv.), HBTU (2.50 equiv.) and HOBt (2.50 equiv.) were dissolved in DMF (20.0 mL/mmol), added to the pre-swollen resin (1.00 equiv.) and DIPEA (5.00 equiv.) was added. The suspension was swirled with a flow of argon at ambient temperature for 60 min. After completion the solution was drained and the resin was washed several times with DMF,

MeOH and DCM. The completion of couplings was ascertained by KAISER-test [4], TNBS-test [5], acetaldehyde/chloranil-test [6] or NMR-test cleavage.

- **Fmoc-Ser(TBS)-OH and Boc-Ser(TBS)-OH coupling:**

  Fmoc-Ser(TBS)-OH **S10** (1.25 equiv.) or Boc-Ser(TBS)-OH **S11** (1.25 equiv.), HBTU (1.25 equiv.) and HOBt (1.25 equiv.) were dissolved in DMF (20.0 mL/mmol), added to the pre-swollen resin (1.00 equiv.) and DIPEA (2.50 equiv.) was added. The suspension was swirled with a flow of argon at ambient temperature for 30 min. Double coupling was used for this coupling step. After completion the solution was drained and the resin was washed several times with DMF, MeOH and DCM. The completion of couplings was ascertained by KAISER-test [4] or TNBS-test.

- **Fmoc-Lys(Me)$_2$-OH · HCl coupling:**

  Fmoc-Lys(Me)$_2$-OH · HCl (1.50 equiv.), HBTU (1.50 equiv.) and HOBt (1.50 equiv.) were dissolved in DMF (20.0 mL/mmol), added to the pre-swollen resin (1.00 equiv.) and DIPEA (4.00 equiv.) was added. The suspension was swirled with a flow of argon at ambient temperature for 45 min. Double coupling was used for this coupling step. After completion the solution was drained and the resin was washed several times with DMF, MeOH and DCM. The completion of couplings was ascertained by KAISER-test [4], TNBS-test [5], acetaldehyde/chloranil-test [6] or NMR-test cleavage.

- **Fmoc-Hyl(Me)$_3$-Gly-OH · TFA coupling:**

  Fmoc-Hyl(Me)$_3$-Gly-OH · TFA **5** (1.00 equiv.) was dissolved in DMF (15.0 mL/mmol) and DIPEA (2.50 equiv.), 0.25 M HATU (1.00 equiv.) in DMF and 0.5 M HOAt (1.00 equiv.) in DMF were added. After 5 min pre-activation the solution was transferred to the pre-swollen resin (1.00 equiv.). The suspension was treated at 55 °C and 200 rpm on the rotary evaporator for 60 min. Triple coupling was used for this coupling step. After completion the solution was drained and the resin was washed several times with DMF, MeOH and DCM. The completion of couplings was ascertained by KAISER-test [4], TNBS-test [5], acetaldehyde/chloranil-test [6] or NMR-test cleavage.

- **Fmoc-Kdp(Me)$_2$(Ns)$_2$-OH · TFA coupling:**

  Fmoc-Kdp(Me)$_2$(Ns)$_2$-OH · TFA **10** (1.50 equiv.), HBTU (1.50 equiv.) and HOBt (1.50 equiv.) were dissolved in DMF (20.0 mL/mmol), added to the pre-swollen resin (1.00 equiv.) and DIPEA (4.00 equiv.) was added. The suspension was swirled with a flow of argon at ambient temperature for 60 min. Double coupling was used for this coupling step. After completion the solution was drained and the resin was washed several times with DMF, MeOH and DCM. The completion of couplings was ascertained by KAISER-test [4], TNBS-test [5], acetaldehyde/chloranil-test [6] or NMR-test cleavage.

TBDMS deprotection on the solid phase

The TBDMS protecting group was removed by treatment of the pre-swollen resin (1.00 equiv.) with 1.0 M tetrabutylammonium fluoride (5.00 equiv./TBDMS group) in THF at ambient temperature for 30 min. This procedure was performed three times. After completion, the solution was drained and the resin was washed several times with DMF, MeOH and DCM.

Ns deprotection on the solid phase

2-Mercaptoethanol (10.0 eq/Ns-group) was dissolved in DMF (0.50 mL/Ns-group) and DBU (5.00 eq/Ns-group) was added. After 5 min pre-activation the thiolate solution was transferred to the pre-swollen resin (1.00 equiv.). The suspension was swirled with a flow of argon at ambient temperature for 30 min. This procedure was performed three times. After completion, the solution was drained and the resin was washed several times with DMF, MeOH and DCM.

Phosphorylation on the solid phase

The phosphorylation was carried out under an argon atmosphere with exclusion of moisture. Therefore, the peptide resin (0.05 mmol, 1.00 equiv.) with unprotected serine-hydroxyl groups was placed in a special reaction vessel. The following procedure describes the phosphorylation for peptides without free primary or secondary amines in the side chains. For peptides with free primary or secondary amine in the peptide resin, an additional amount (0.50 equiv./NH group.) of reagents and solvents was used for each free amine.

The resin was swollen in dry DMF (1.00 mL/OH group) at ambient temperature for 2 h before 1*H*-tetrazol (0.45 M in MeCN, 7.50 equiv./OH group) and dibenzyl *N,N*-diisopropylphosphoramidite (3.00 equiv./OH group) were added. The suspension was swirled with a flow of argon at ambient temperature for 3 h before the solution was drained and the resin was washed several times with dry DMF. Afterwards the organophosphite was oxidized by adding *tert*-butyl hydroperoxide (5.55 M in decane, 37.7 equiv./OH group,) in dry DMF (1.00 mL/OH group). The suspension was swirled with a flow of argon at room temperature for 1.5 h before the solution was drained and the resin was washed several times with DMF and DCM and dried *in vacuo*.

Simultaneous cleavage from the resin and of the side chain protecting groups

A cleavage cocktail of TFA/H_2O/TIPS (95:2.5:2.5, 5.0 mL/0.1 mmol) was added to the dry resin (1.00 equiv.). The suspension was swirled with a flow of argon for 3 to 6 h at room temperature before the solution was drained and the resin was washed several times with TFA. The acidic cleavage of the benzyl ester protecting groups from the phosphates requires an extended reaction time. However, a deprotection time of 6 h at ambient temperature was not exceeded to prevent hydrolysis of the peptides. The combined filtrate was concentrated under reduced pressure. Peptides were precipitated from cold diethyl ether (40 mL), washed three times with diethyl ether and lyophilized from H_2O/MeCN (80:20) mixture.

Purification

The peptides were purified by semi-preparative reversed-phase HPLC on a *Thermo Scientific Dionex* UltiMate3000 with an MWD-3000 detector. To avoid elution of the highly polar peptides in the void volume of the column, specially optimised conditions were used. An isocratic eluent mixture was used at the beginning for 10 min before switching to a slow gradient for 60 min with the following conditions.

Column: ACE 5 SuperC18 (150 x 10 mm, 5 µm, 90 Å)

Gradient: 0% MeCN + 0.085% TFA in H_2O + 0.1% TFA for 10 min, thereafter 0% → 30% MeCN + 0.085% TFA in H_2O + 0.1% TFA in 60 min with 7.50 mL/min at 28 °C and 215 nm, 230 nm, 254 nm and 270 nm.

0% MeCN + 0.085% TFA in H_2O + 0.1% TFA for 10 min, thereafter 0% → 50% MeCN + 0.085% TFA in H_2O + 0.1% TFA in 60 min with 7.50 mL/min at 28 °C and 215 nm, 230 nm, 254 nm and 270 nm.

Analytical HPLC

Analytical HPLC was performed on a *Thermo Scientific Dionex* UltiMate3000 with an MWD-3000 detector under the following conditions (if not indicated otherwise).

Column: *ACE* UltraCore 2.5 SuperC18, 150 x 2.1 µm

Gradient: 0% → 30% MeCN + 0.085% TFA in H_2O + 0.1% TFA in 10 min with 0.45 mL/min at 28 °C and 230 nm.

Synthesis of Ser-pSer-Lys-Lys-Ser-Gly-pSer-Tyr-Ser-Gly-pSer-Lys-Gly-Ser-Lys (p3-Sil01, S14)

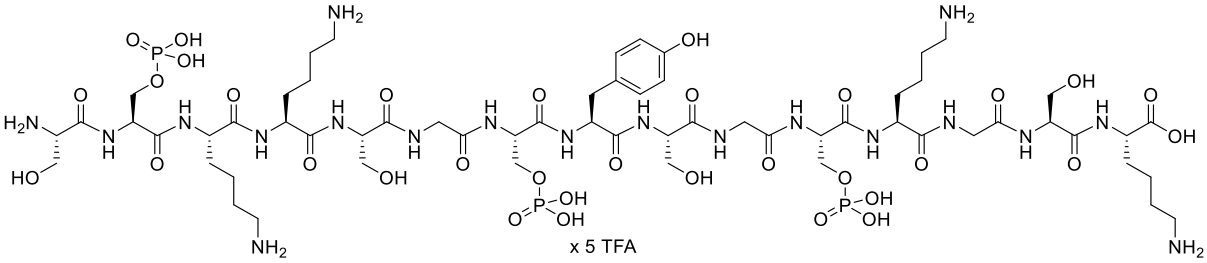

S14

The peptide **S14** was synthesised under standard coupling condition on a microwave assisted peptide synthesizer (*Liberty Blue*, CEM) on a 0.10 mmol scale with the conditions described above. The peptide was posttranslationally desilylated, subsequently phosphorylated and cleaved from the resin as described above. The crude peptide p3-Sil01 **S14** was obtained as a colourless solid (155 mg, 67.8 µmol 68% yield) and purified by semi-preparative HPLC.

LC-HRMS (ESI+, H_2O/MeCN) calculated for $[C_{60}H_{106}N_{19}O_{33}P_3H_2]^{2+}$: 857.8279, found: 857.8293.

HPLC t_R = 4.360 min, purity ≥ 85%, (0% → 30% MeCN + 0.085% TFA in H_2O + 0.1% TFA, 10 min, 28 °C, 0.45 mL/min, 230 nm, ACE Ultracore 2.5 SuperC18).

^{31}P-NMR (202 MHz, 300 K, H_2O/D_2O (9:1), pH 3.0), δ = 0.77 (s, 1P, $pSer^2$), 0.76 (s, 1P, $pSer^7$), 0.62 (s, 1P, $pSer^{11}$) ppm.

^{1}H-NMR (600 MHz, 300 K, H_2O/D_2O (9:1), pH 3.0), 1.79 mg in 500 µL.

Table S1: ^{1}H-NMR signal assignment for p3-Sil01 **S14** from TOCSY and HSQC spectrum (600 MHz, 300 K, H_2O/D_2O (9:1), pH 3.0). n.d. = not definable, - = not available.

amino acid	NH / ppm	Hα / ppm	Hβ / ppm	further / ppm		
Ser^1	n.d.	4.24	4.05			-
$pSer^2$	9.00	4.65	4.19, 4.14			-
Lys^3	8.36	4.34	1.81, 1.75	Hγ: 1.42	Hδ: 1.65	Hε: 2.99
				ε-NH_3^+: 7.50		
Lys^4	8.44	4.37	1.90, 1.81	Hγ: 1.43	Hδ: 1.66	Hε: 2.99
				ε-NH_3^+: 7.50		
Ser^5	8.41	4.47	3.92, 3.89			-
Gly^6	8.46	4.01	-			-
$pSer^7$	8.36	4.58	4.08			-
Tyr^8	8.29	4.62	3.03	$CH_{Ar}{}^o$: 7.14	$CH_{Ar}{}^m$: 6.83	

Ser[9]	8.26	4.43	3.85, 3.79			-
Gly[10]	7.71	3.97	-			-
pSer[11]	8.50	4.57	4.22, 4.11			-
Lys[12]	8.44	4.36	1.85, 1.75	Hγ: 1.43	Hδ: 1.66	Hε: 2.99
				ε-NH_3^+: 7.50		
Gly[13]	8.26	3.97	-			-
Ser[14]	8.14	4.46	3.87			-
Lys[15]	8.28	4.35	1.90, 1.78	Hγ: 1.43	Hδ: 1.67	Hε: 2.99
				ε-NH_3^+: 7.50		

Synthesis of pSer-pSer-Lys-Lys-pSer-Gly-pSer-Tyr-pSer-Gly-pSer-Lys-Gly-pSer-Lys (p7-Sil01, S15)

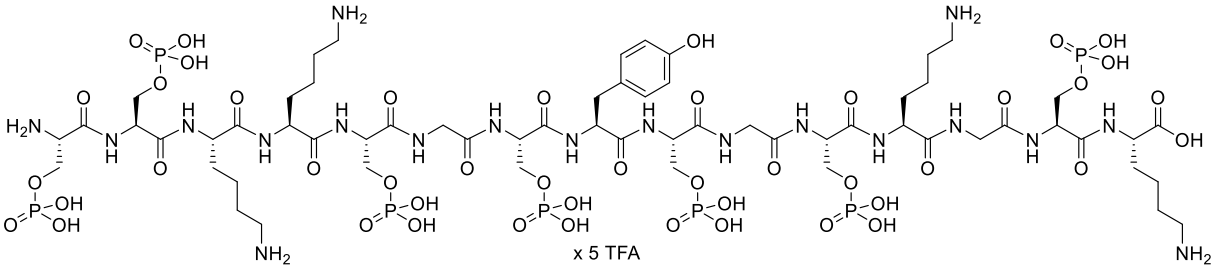

S15

The peptide **S15** was synthesised under standard coupling condition on a microwave assisted peptide synthesizer (*Liberty Blue*, CEM) on a 0.10 mmol scale with the conditions described above. The peptide was posttranslationally desilylated, subsequently phosphorylated and cleaved from the resin as described above. The crude peptide p7-Sil01 **S15** was obtained as a colourless solid (100 mg, 38.4 µmol 38% yield) and purified by semi-preparative HPLC.

LC-HRMS (ESI+, H_2O/MeCN) calculated for $[C_{60}H_{110}N_{19}O_{45}P_7H_2]^{2+}$: 1017.7606, found: 1017.7631.

HPLC t_R = 1.037 min, (1% → 30% MeCN + 0.085% TFA in H_2O + 0.1% TFA, 10 min, 28 °C, 0.45 mL/min, 230 nm, ACE Ultracore 2.5 SuperC18).

^{31}P-NMR (202 MHz, 300 K, H_2O/D_2O (9:1), pH 3.0), δ = 0.76 (s, 1P, pSer[2]), 0.75 (s, 1P, pSer[9]), 0.71 (s, 1P, pSer[7]), 0.69 (s, 1P, pSer[11]), 0.59 (s, 1P, pSer[14]), 0.58 (s, 1P, pSer[5]), 0.38 (s, 1P, pSer[1]) ppm.

^{1}H-NMR (600 MHz, 300 K, H_2O/D_2O (9:1), pH 3.0), 1.66 mg in 500 µL, purity ≥ 85%.

Table S2: ^{1}H-NMR signal assignment for p7-Sil01 **S15** from TOCSY and HSQC spectrum (600 MHz, 300 K, H_2O/D_2O (9:1), pH 3.0). n.d. = not definable, - = not available.

amino acid	NH / ppm	Hα / ppm	Hβ / ppm	further / ppm		
pSer[1]	n.d.	4.40	4.30			-
pSer[2]	9.03	4.67	4.14			-
Lys[3]	8.48	4.36	1.91, 1.80	Hγ: 1.43	Hδ: 1.66	Hε: 2.98
				ε-NH_3^+: 7.50		
Lys[4]	8.52	4.41	1.85, 1.78	Hγ: 1.43	Hδ: 1.66	Hε: 2.98
				ε-NH_3^+: 7.50		
pSer[5]	8.58	4.60	4.15			-
Gly[6]	8.43	4.01	-			-
pSer[7]	8.33	4.60	4.09			-
Tyr[8]	8.30	4.64	3.04	CH_{Ar}^{o}: 7.15	CH_{Ar}^{m}: 6.84	
pSer[9]	8.53	4.57	4.13			-
Gly[10]	7.68	4.00, 3.96	-			-
pSer[11]	8.52	4.55	4.10			-
Lys[12]	8.49	4.40	1.92, 1.79	Hγ: 1.44	Hδ: 1.67	Hε: 2.99
				ε-NH_3^+: 7.50		
Gly[13]	8.16	3.99	-			-
pSer[14]	8.50	4.55	4.11.			-
Lys[15]	8.28	4.42	1.92, 1.82	Hγ: 1.43	Hδ: 1.67	Hε: 2.99
				ε-NH_3^+: 7.50		

Synthesis of pSer-pSer-Kdp(NH)$_2$(Me)$_2$-Lys(Me)$_2$-pSer-Gly-pSer-Tyr-pSer-Gly-pSer-pHyl(Me)$_3$-Gly-pSer-Kdp(NH)$_2$(Me)$_2$ (*syn*Sil-1A$_1$, S16)

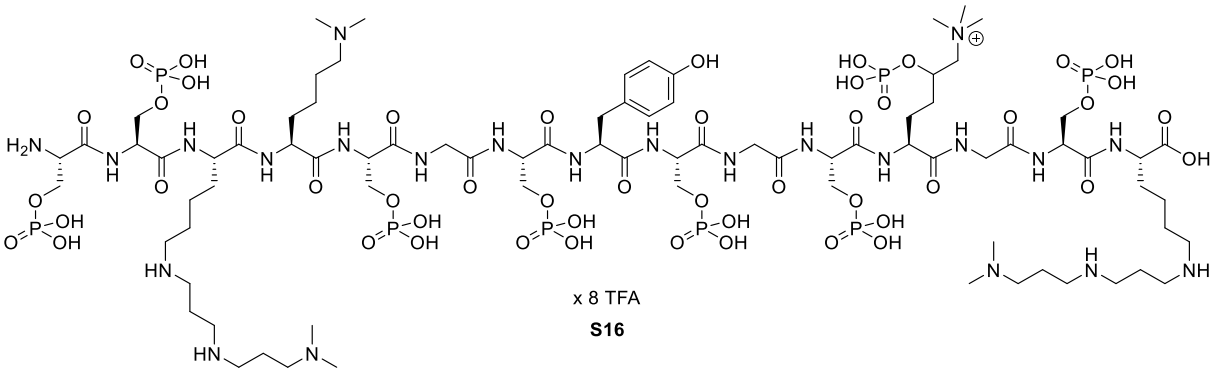

S16

The peptide **S16** was synthesised manually on a 0.05 mmol scale under the coupling conditions described above. The peptide was posttranslationally desilylated, subsequently phosphorylated and cleaved from the resin as described above. The crude peptide *syn*Sil-1A$_1$ **S16** was obtained as a colourless solid (81 mg, 38.4 µmol 38% yield) and purified by semi-preparative HPLC.

LC-HRMS (ESI+, H_2O/MeCN) calculated for $[C_{81}H_{158}N_{23}O_{49}P_8H]^{2+}$: 1242.9273, found: 1242.9344.

HPLC t_R = 3.623 min, purity ≥ 98%, (0% → 30% MeCN + 0.085% TFA in H_2O + 0.1% TFA, 10 min, 28 °C, 0.45 mL/min, 230 nm, ACE Ultracore 2.5 SuperC18).

^{31}P-NMR (202 MHz, 300 K, H_2O/D_2O (9:1), pH 3.0), δ = 0.76 (s, 1P, pSer^2), 0.72 - 0.63 (m, 4P, pSer^{5,7,9,11,}), 0.59 (s, 1P, pSer^{14}), 0.37 (s, 1P, pSer^1), −1.20 (s, 1P, pHyl(Me$_3$)^{12}) ppm.

^{1}H-NMR (600 MHz, 300 K, H_2O/D_2O (9:1), pH 3.0), 2.09 mg in 200 µL.

Table S3: ^{1}H-NMR signal assignment for *syn*Sil-1A$_1$ **S16** from TOCSY and HSQC spectrum (600 MHz, 300 K, H_2O/D_2O (9:1), pH 3.0). n.d. = not definable, - = not available.

amino acid	NH / ppm	Hα / ppm	Hβ / ppm	further / ppm		
pSer^1	n.b.	4.40	4.31			-
pSer^2	9.05	4.66	4.14			-
Kdp(Me)$_2$^{3}	8.40	4.38	1.83, 1.81	Hγ: 1.42	Hδ: 1.69	Hε: 3.04
				Hη: 3.15	Hθ: 2.11	Hι: 3.15
				Hλ: 3.14	Hμ: 2.15	Hν: 3.23
				ν-NMe$_2$: 2.90		
Lys(Me)$_2$^{4}	8.58	4.37	1.88, 1.79	Hγ: 1.43	Hδ: 1.71	Hε: 3.10
				ε-NMe$_2$: 2.84		ε-$^+$NHMe$_2$: 8.89
pSer^5	8.54	4.59	4.17			-

Gly[6]	8.43	4.02, 4.00	-			-
pSer[7]	8.32	4.60	4.09			-
Tyr[8]	8.30	4.63	3.06, 3.03	$CH_{Ar}{}^{o}$: 7.16	$CH_{Ar}{}^{m}$:6.85	
pSer[9]	8.55	4.59	4.15			-
Gly[10]	7.73	4.02, 3.98	-			-
pSer[11]	8.54	4.58	4.16			-
pHyl(Me)$_3$[12]	8.62	4.44	2.11, 2.07	Hγ: 1.92	Hδ: 4.74	Hε: 3.59, 3.43
		4.37	1.99, 1.98	Hγ: 1.83		Hε: 3.59, 3.45
				ε-$N^{+}Me_3$: 3.21		
Gly[13]	8.24	3.98	-			-
Ser[14]	8.54	4.54	4.24			-
Kdp(Me)$_2$[15]	8.16	4.41	1.92, 1.80	Hγ: 1.45	Hδ: 1.69	Hε: 3.03
				Hη: 3.15	Hθ: 2.11	Hι: 3.15
				Hλ: 3.14	Hμ: 2.15	Hν: 3.23
				ν-NMe_2: 2.90		

In vitro silica precipitation assays

In vitro silica precipitation assays were performed as described in the experimental section of the manuscript, according to the methods described by KRÖGER *et al.*[7] in 2002 and GEYER *at al.*[8] in 2020. All experiments were performed in a 50 mM sodium acetate buffer at the desired pH value, with pre-hydrolysed tetramethyl orthosilicate (TMOS) solution as a silicic acid source. The silica precipitation took place in a time frame of precisely 10 min and was stopped by the addition of 1.0 M HCl solution. The amount of precipitated silica was quantified photometrically by a modified β-silicomolybdate method.[9] For each datapoint, a double determination was performed. The respective mean values of the experimental data were plotted and are shown in Figures S2 and S3. Error bars are not shown in the figures because they are disproportionately large at low silica amounts.

pH Dependence of LCPA and peptides

The results of the pH dependent *in vitro* precipitation experiments, which were all performed at a concentration of 1.0 mM are shown in Figure S1 to Figure S3.

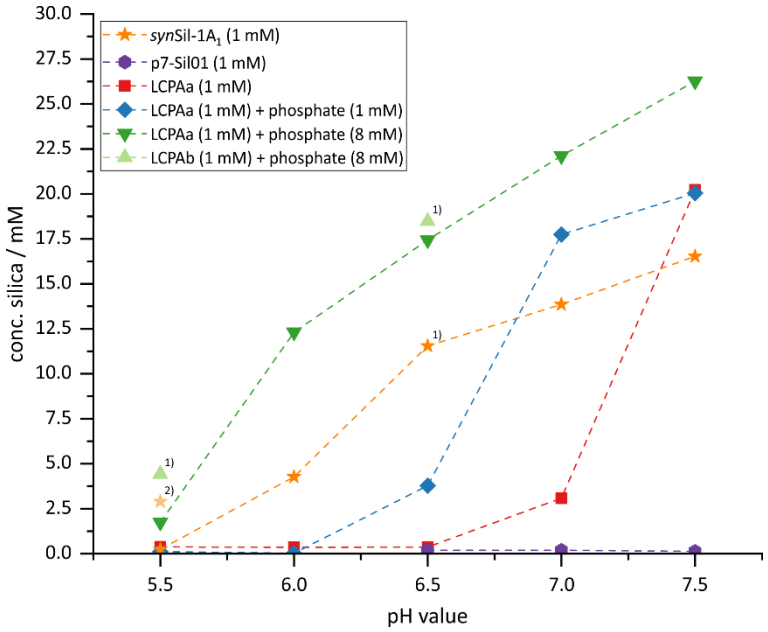

Figure S1: The pH dependence of LCPA- and peptide-induced silica precipitation in a 50 mM sodium acetate buffer. At each pH value, the concentration of the respective LCPA or peptide was 1.0 mM. The dotted lines show silica precipitation using *syn*Sil-1A$_1$ **S16** (orange), p7-Sil01 **S15** (purple) LCPAa **S13a** (red), LCPAa **S13a** in the presence of 1.0 mM phosphate (blue), LCPAa **S13a** in the presence of 8.0 mM phosphate (green) and LCPAb **S13b** in the presence of 8.0 mM phosphate (light-green).

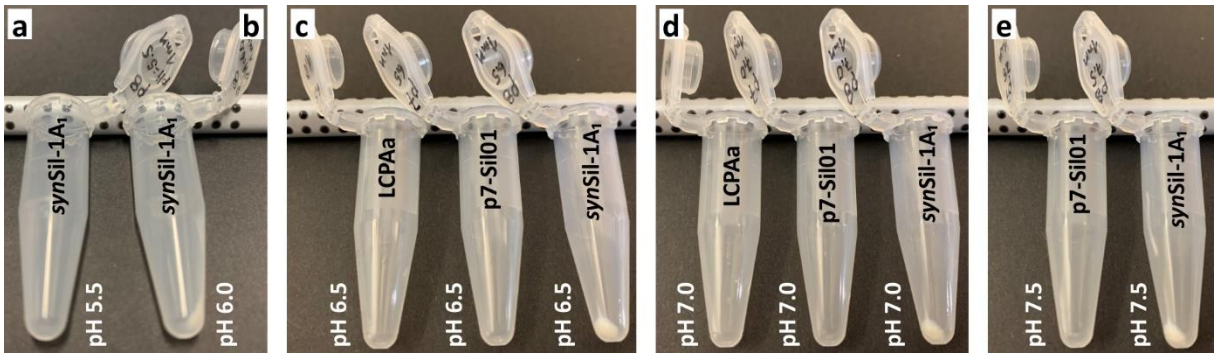

Figure S2: Amount of precipitated silica of LCPA- and peptide-induced precipitation in a 50 mM sodium acetate buffer at the indicated pH value, the concentration of the respective LCPA or peptide was 1.0 mM. Obtained silica at pH 5.5 (a), pH 6.0 (b), pH 6.5 (c), pH 7.0 (d) and pH 7.5 (e).

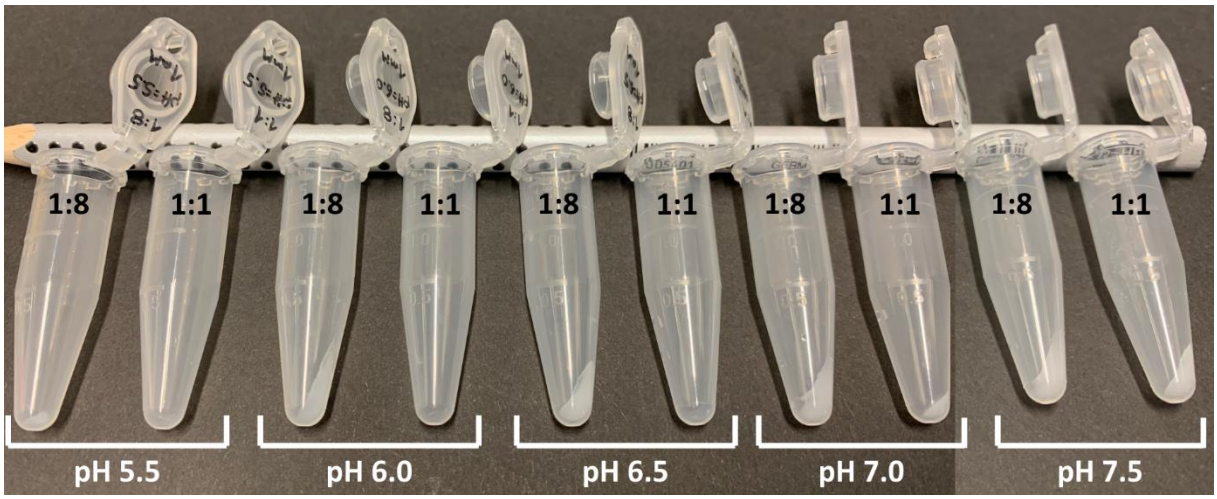

Figure S3: Amount of precipitated silica of LCPA-induced precipitation in a 50 mM sodium acetate buffer at the indicated pH value, the concentration of the LCPAa **S13a** was 1.0 mM and the indicated ratio phosphate left (8.0 mM) right (1.0 mM) was added.

Concentration dependence of LCPA and *syn*Sil-1A$_1$

The results of the concentration dependent *in vitro* silica precipitation experiments of *syn*Sil-1A$_1$ **S16** (orange) and LCPAb **S13b** in the of phosphate (light-green) in a 50 mM sodium acetate buffer at pH 6.5 are shown in Figure S4. Data points were fitted linear if no saturation effect was observed at higher concentrations of organic compounds. The results of the linear fits are shown in Figure S4 and the data of the calculated functions are summarized in Table S4.

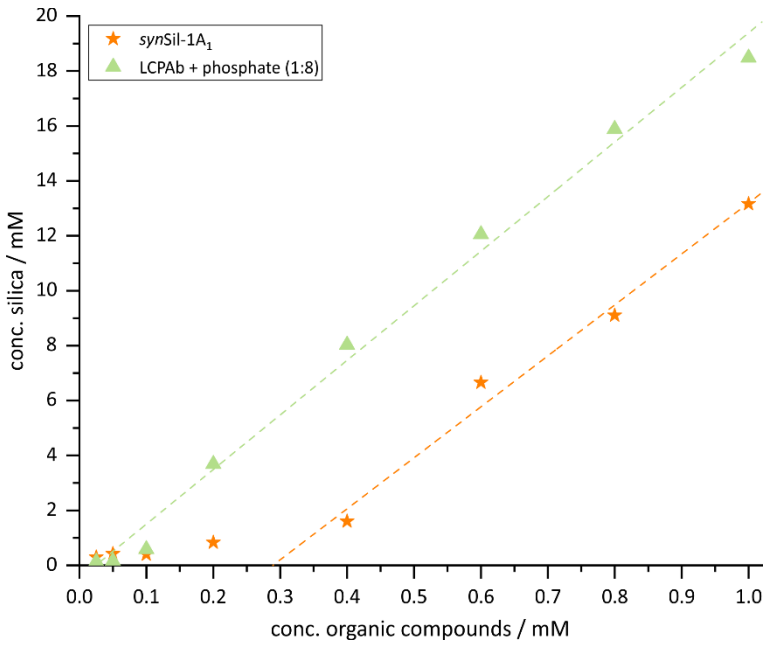

Figure S4: The concentration dependence of LCPA- and peptide-induced silica precipitation in a 50 mM sodium acetate buffer at pH 6.5. The dotted lines show the correlation between the amount of precipitated silica and the amount of *syn*Sil-1A$_1$ **S16** (orange) or LCPAb **S13b** in the presence of 8.0 mM phosphate (light-green).

Table S4: Data of the linear fit with the function $f(x) = a + bx$.

	a	b	R^2
*syn*Sil-1A$_1$ **S16**	−5.36	18.56	0.9755
LCPAb **S13b** + phosphate (1:8)	−0.48	19.88	0.9865

Concentration dependence of mixtures

In order to investigate the role of stereochemistry in silicification, we synthesised a mixture of four diastereomers (*rac*Sil-1A$_1$) using the racemic amino acid *rac*-Dde-Kdp(Me)$_2$(Ns)$_2$-OH · TFA at Lys^3 and Lys^{15}, which was synthetized according to the literature. [10] The results of the concentration dependent *in vitro* silica precipitation experiments of mixture between LCPA and peptide or phosphate in a 50 mM sodium acetate buffer at pH 5.5 are shown in Figure S5b and Figure S6. The dotted lines show silica precipitation using p7-Sil01 **S15** in the presence of LCPAa **S13a** (red), *syn*Sil-1A$_1$ **S16** in the presence of LCPAa **S13a** (blue), *rac*Sil-1A$_1$ in the presence of LCPAa **S13a** (purple), LCPAa **S13a** in the presence of phosphate (light-green) and LCPAb **S13b** in the presence of phosphate (green). Data points were fitted linear if no saturation effect was observed at higher concentrations of organic compounds. When a saturation effect was observed at higher concentrations, data points were fitted asymptotic. For the asymptotic fit the data points at which no silica precipitate was detected were excluded to determine

the threshold concentration. The result of the linear and asymptotic fits are shown in Figure S5b and the data of the calculated functions are summarized in Table S5.

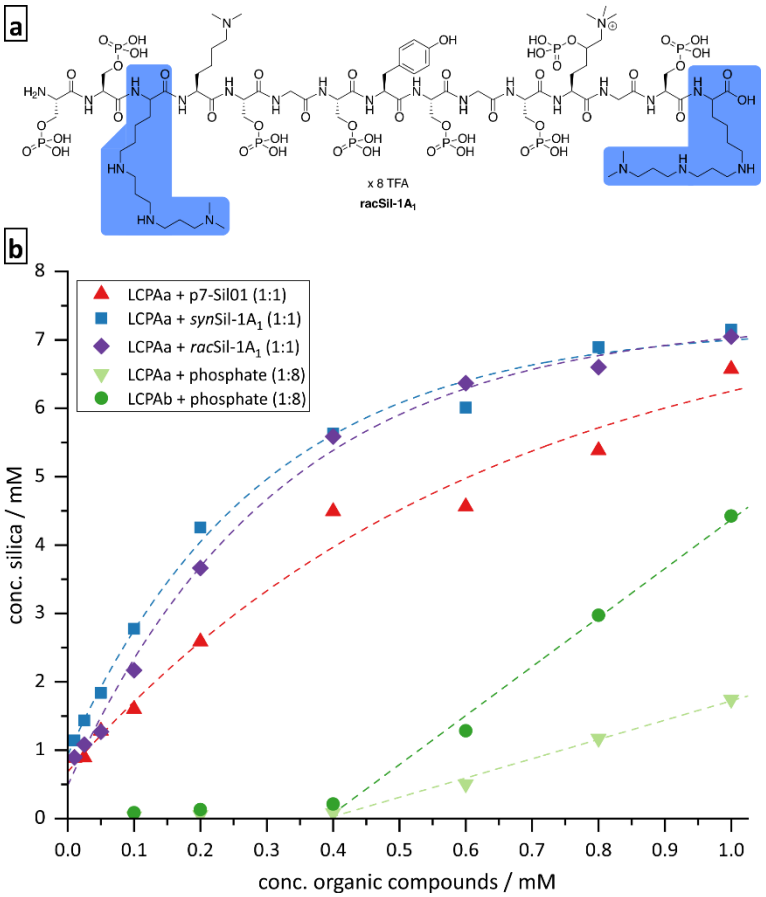

Figure S5: The chemical structure of *rac*Sil-1A$_1$ shown in a) with the racemic building blocks highlighted in blue. The concentration dependence of different mixtures of LCPA and peptides in a 50 mM sodium acetate buffer at pH 5.5 is shown in b). The dotted lines show the correlation between the amount of precipitated silica and the amount of p7-Sil01 **S15** in the presence of LCPAa **S13a** (red), *syn*Sil-1A$_1$ **S16** in the presence of LCPAa **S13a** (blue), *rac*Sil-1A$_1$ in the presence of LCPAa **S13a** (purple), LCPAa **S13a** in the presence of phosphate (light-green) and LCPAb **S13b** in the presence of phosphate (green).

Table S5: Data of the linear fit with the function $f(x) = a + bx$ and of the asymptotic fit with the function $f(x) = a - bc^x$.

	a	b	c	R^2
LCPAa **S13a** + p7-Sil01 **S15** (1:1)	7.69	7.01	0.206	0.9695
LCPAa **S13a** + *syn*Sil-1A$_1$ **S16** (1:1)	7.20	6.27	0.032	0.9908
LCPAa **S13a** + *rac*Sil-1A$_1$ (1:1)	7.32	6.83	0.013	0.9951
LCPAa **S13a** + phosphate (1:8)	−2.79	7.16	-	0.9894
LCPAb **S13b** + phosphate (1:8)	−1.10	2.82	-	0.9894

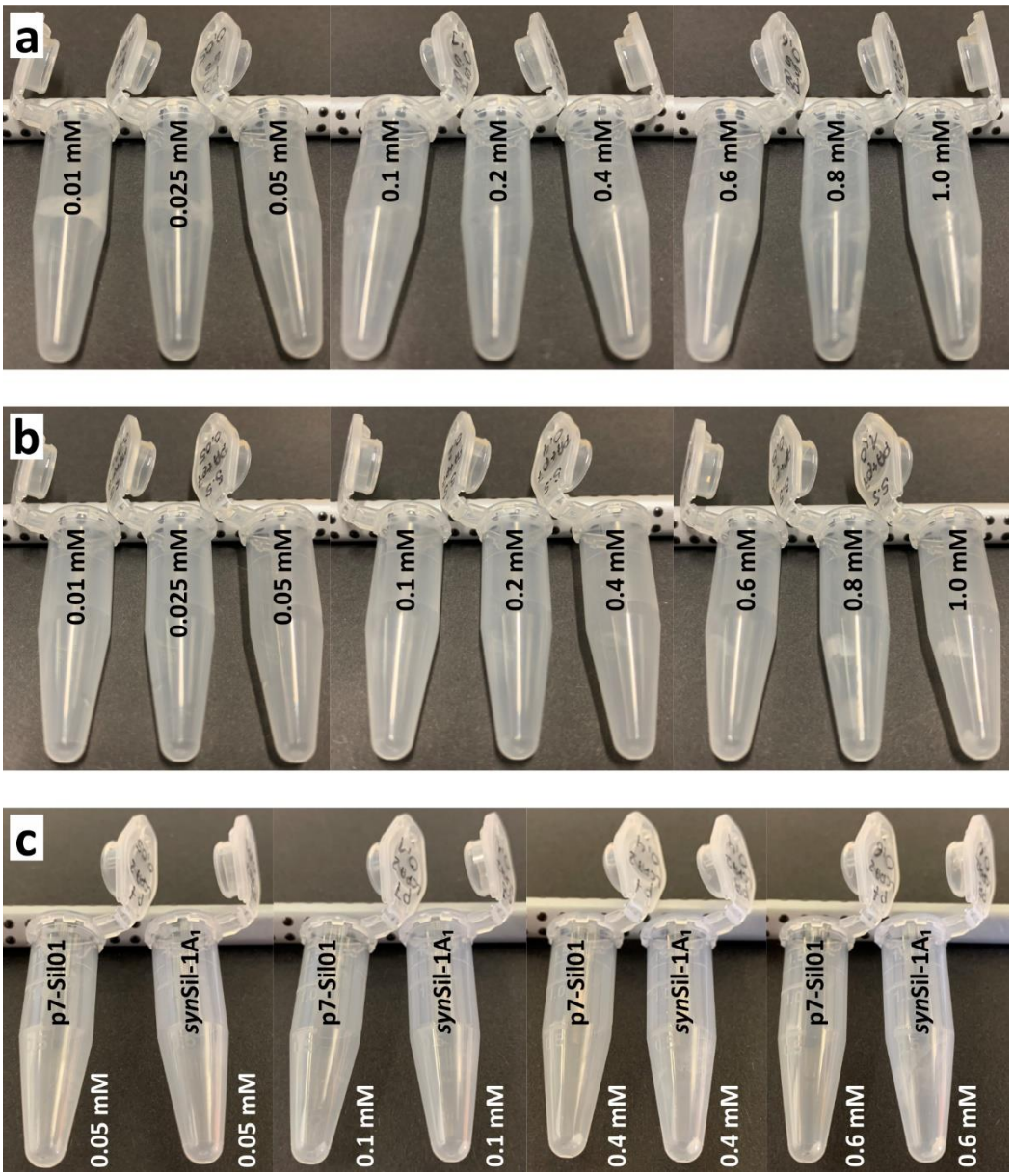

Figure S6: Amount of precipitated silica of a LCPA/peptide mixture- (1:1) in a 50 mM sodium acetate buffer at pH 5.5 and the indicated concentrations. Obtained silica amount of *syn*Sil-1A$_1$ **S16** in the presence of LCPAa **S13a** (a), p7-Sil01 **S15** in the presence of LCPAa **S13a** (b). Comparison of *syn*Sil-1A$_1$ **S16** in the presence of LCPAa **S13a** and p7-Sil01 **S15** in the presence of LCPAa **S13a** at selected concentrations is shown in c).

Hydrolysis stability of the serine phosphates

In order to be able to make a statement about the hydrolysis stability of serine phosphates, the stability of the tri-monophosphate p3-Sil01 **S14** against hydrolysis in aqueous systems at different pH values was investigated. We decided to use p3-Sil01 **S14** as a reference peptide, because here the β-methylene signals of serine and phosphorylated serine can be monitored simultaneously. The hydrolysis was analysed by ^{1}H-^{13}C HSQC and ^{1}H- NMR spectroscopy. The disappearance of the β-methylene signals of phosphoserine from 4.15-3.96 ppm identifies the hydrolysis. The stability was tested with p3-Sil01 **S14** (2.5 mg) in a mixture of H_2O/D_2O (9:1) at pH 7.0, 9.3 and 12.1 at room temperature. The pH values were adjusted with 2 M HCl and 2 M NaOH solutions. The results of hydrolysis stability of p3-Sil01 **S14** at pH 7.0 are shown in Figure S7.

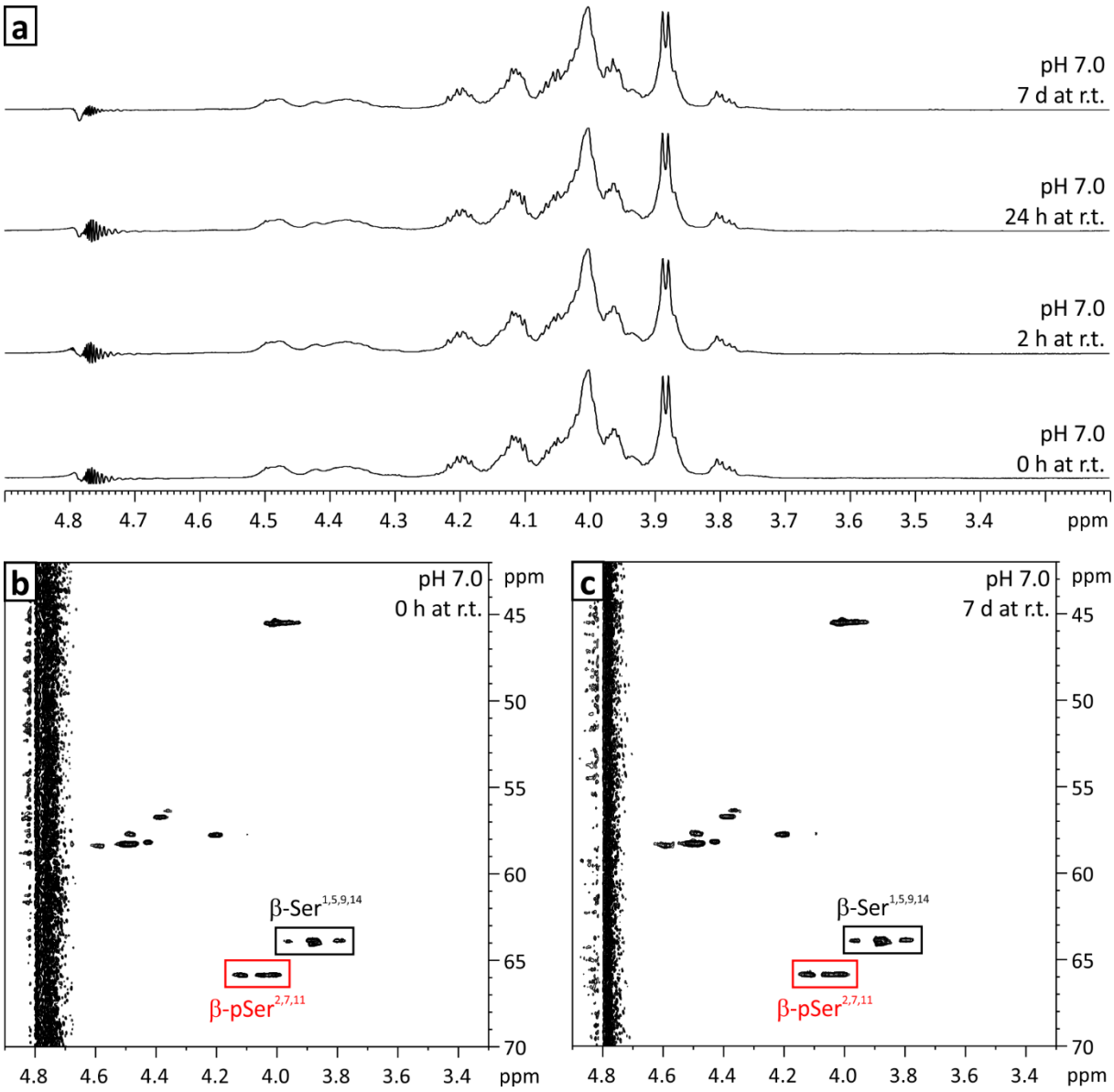

Figure S7: ^{1}H-NMR spectra (600 MHz, 300 K, H_2O/D_2O 9:1) of p3-Sil01 **S14** treated at pH 7.0 and room temperature for different times (a). ^{1}H-^{13}C HSQC spectra (600 MHz, 300 K, H_2O/D_2O 9:1) of

p3-Sil01 **S14** at pH 7.0 and room temperature at different times (b) t = 0 h and (c) t = 7 d. The black boxes highlight the signals from the β-methylene groups of the non-phosphorylated serines. Sufficiently separated are the β-methylene groups of the phosphorylated serines highlighted by red boxes. r.t. = room temperature.

There are no changes detectable in the ^{1}H and ^{1}H-^{13}C HSQC spectra of p3-Sil01 **S14** after one week at room temperature and pH 7.0. These results confirm that the serine phosphates of p3-Sil01 **S14** are stable to hydrolysis under these conditions. To localize the hydrolysis point of the serine phosphates of p3-Sil01 **S14**, the experiments were repeated under alkaline conditions (pH 9.3) at room temperature. The results are shown in Figure S8.

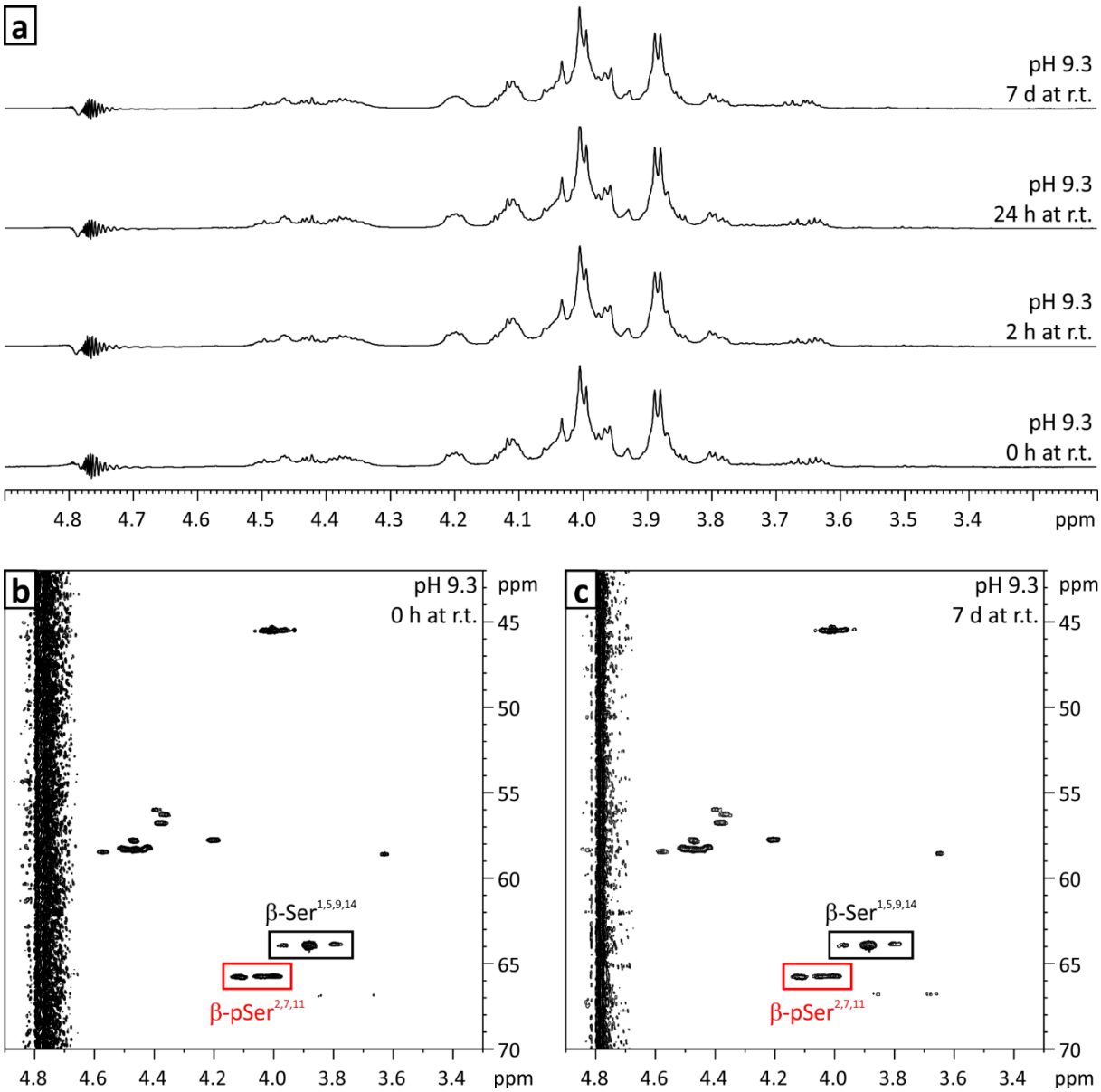

Figure S8: ^{1}H-NMR spectra (600 MHz, 300 K, H_2O/D_2O 9:1) of p3-Sil01 **S14** treated at pH 9.3 and room temperature for different times (a). ^{1}H-^{13}C HSQC spectra (600 MHz, 300 K, H_2O/D_2O 9:1) of

p3-Sil01 **S14** at pH 9.3 and room temperature at different times (b) t = 0 h and (c) t = 7 d. The black boxes highlight the signals from the β-methylene groups of the non-phosphorylated serines. Sufficiently separated are the β-methylene groups of the phosphorylated serines highlighted by red boxes. r.t. = room temperature.

Similarly, at pH 9.3 and room temperature, no changes can be observed in the ^{1}H and ^{1}H-^{13}C HSQC spectra of p3-Sil01 **S14** after one week. Under these conditions, the serine phosphates of p3-Sil01 **S14** are also stable against hydrolysis. To localize the hydrolysis point of the serine phosphates of p3-Sil01 **S14**, the experiments were repeated under strong alkaline conditions (pH 12.0) at room and higher temperatures (70 °C and 100 °C). The results are shown in Figure S9.

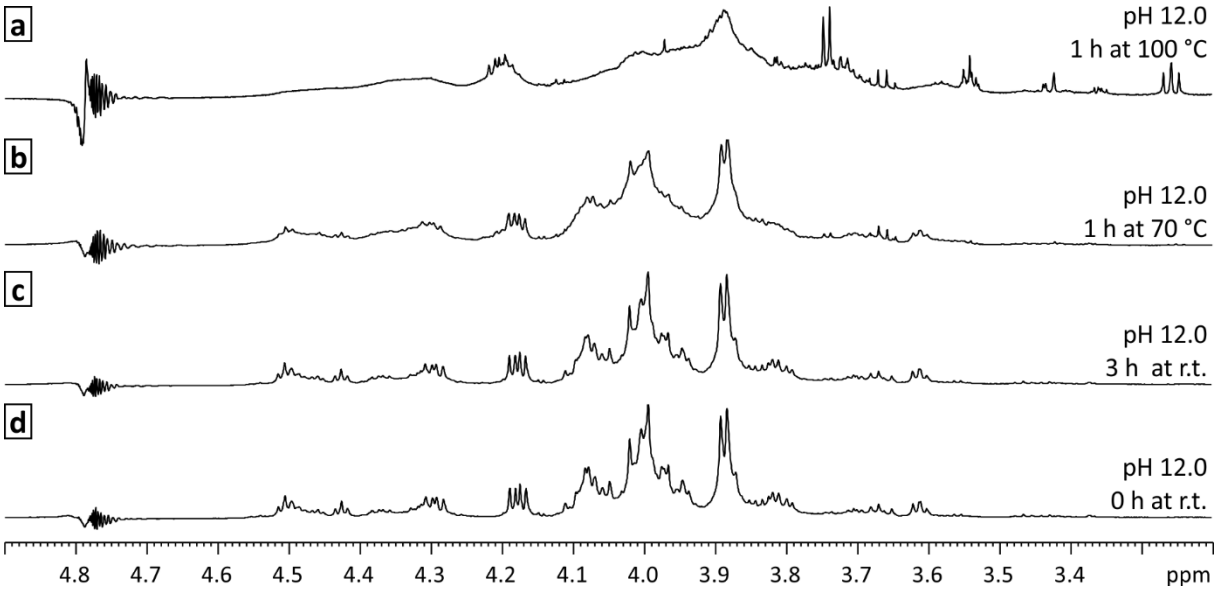

Figure S9: ^{1}H-NMR spectra (600 MHz, 300 K, H_2O/D_2O 9:1) of p3-Sil01 **S14** treated at pH 12.0 at room temperature for 0 h (d) and 3 h (c) and treated at 70 °C for 1 h (b) and at 100 °C for 1 h (a). r.t. = room temperature.

Similarly, at pH 12.0 and room temperature, no changes can be observed in the ^{1}H spectra of p3-Sil01 **S14** after 3 h. Under these conditions, the serine phosphates of p3-Sil01 **S14** are also stable against hydrolysis. After another hour at 70 °C, no hydrolysis can be observed either. Complete hydrolysis of the serine phosphates together with partial hydrolysis of the peptide sequence can be observed after p3-Sil01 **S14** was heated to 100 °C at pH 12.0 for 1 h. These results show that the serine phosphates are remarkably stable to hydrolysis under alkaline conditions at room temperature.

DOSY-Experiments

In a DOSY experiment, a pair of pulsed field gradients are implemented into a spin-echo with an echo delay. Due to changes in the molecules spatial position caused by their translational diffusion, incomplete refocusing of the signal occurs. Such incomplete refocusing results in an attenuation of the signal intensity, which can be correlated to the duration of the delay, the strength of the applied gradients, and the diffusion coefficient of the molecule, as described by the STEJSKEL-TANNER relation in equation (1):

$$I = I_0 \exp\left[-D\gamma^2\delta^2 g^2\left(\Delta - \frac{\delta}{3}\right)\right] \qquad (1)$$

I_0 is the signal intensity in the absence of an applied gradient, γ is the gyromagnetic ratio of the nucleus in concern, δ the duration of the gradient pulses, g the strength of the applied gradient, and Δ is the total delay where diffusion occurs. In a typical DOSY experiment, the signal attenuation is detected by varying the gradient strength g while holding the gradient duration δ and the diffusion delay Δ constant. By fitting the experimental data to a non-linear exponential decay using equation (1), the diffusion coefficient D can be extracted. The results are usually presented as a Stejskal-Tanner plot, a typical one being shown in Figure S10.

3-(Trimethylsilyl)propionic-2,2,3,3-d_4 acid sodium salt (TSP) was used as an internal standard to adjust the required concentrations and ratios of peptide to LCPA. The pH value was adjusted with NaOD and DCl in D_2O. All experiments were performed with a peptide concentration of 1 mM and the amount of LCPA was increased stepwise. Samples of the peptide were dissolved in either H_2O/D_2O (9:1) with manually adjusted pH of about 3.0, while peptide - LCPA complexes were dissolved in D_2O buffer and pH values adjusted. The pH values of the D_2O buffers were determined according to the literature of Artur KRĘŻEL *et al*.[11] using equation (2):

$$pH = 0.929pH^* + 0.41 \qquad (2)$$

The pH^* was directly read in the D_2O buffer solution using a H_2O calibrated pH meter. All DOSY spectra have been recorded on a Bruker AVII 600 MHz at 298 K. Temperature was calibrated with Bruker standard 4% methanol in methanol-d_4. DOSY experiments were performed using the stimulated echo method with bipolar gradient pulses and one spoil gradient.[12] The pulse sequence was stebpgp1s from Bruker pulse program library. The gradient shape used was smoothed square SMSQ10.100 and gradient length was 2 ms, which resulted in δ of 4 ms. The optimized diffusion delays (Δ) were between 50 and 100 ms. Diffusion attenuation was realized with 9 gradient increments. The DOSY 2D spectra

were recorded with 9 experiments and each with minimal 64 to maximal 1024 transients. Relaxation delays were 3 s.

DOSY assay of polyelectrolyte complex (PEC) formed from mixture of *syn*Sil-1A$_1$ **S16** and LCPAb **S13b**, with an equilibrium, as shown in Equation (3),

$$L + P \rightleftharpoons LP \qquad (3)$$

where *L* stands for the LCPA, *P* for the peptide and *LP* for PEC complex. A dissociation constant, K_d, is introduced to describe the strength of the peptide–LCPA interaction depending on the concentrations of the single equilibrium components, as shown in Equation (4):

$$K_d = \frac{[L][P]}{[LP]} \qquad (4)$$

In the limit of fast chemical exchange on the time scale of NMR measurements, a single set of resonance signals is observed. The measured spectra represent the average behaviour of LCPA in the free and bound states. Thus, the observed diffusion coefficient, D_o, is the weighted average one for the ligand in the free and bound states,

$$D_o = F_f D_f + F_b D_b \qquad (5)$$

$$F_f + F_b = 1 \qquad (6)$$

where F_f and F_b are fraction of the free and bound LCPA, respectively. The diffusion coefficient of the peptide in the mixture was used to approximate the diffusion coefficient of the bound state D_b. The diffusion coefficient of the LCPA in free state D_f was measured under the same experimental condition separately. Taking the total concentration of the peptide and LCPA P_{tot} and L_{tot}, respectively, as the additional known parameters, the dissociation K_d can be readily determined according to Equation (7), while faction of LCPAb **S13b** bound to *syn*Sil-1A$_1$ **S16** calculated from Equation (8).

$$K_d = P_{tot} \cdot \frac{D_o - D_b}{D_f - D_o} - L_{tot} \cdot \frac{D_o - D_b}{D_f - D_b} \qquad (7)$$

$$F_f = \frac{D_o - D_b}{D_f - D_b};\ F_b = \frac{D_f - D_o}{D_f - D_b} \qquad (8)$$

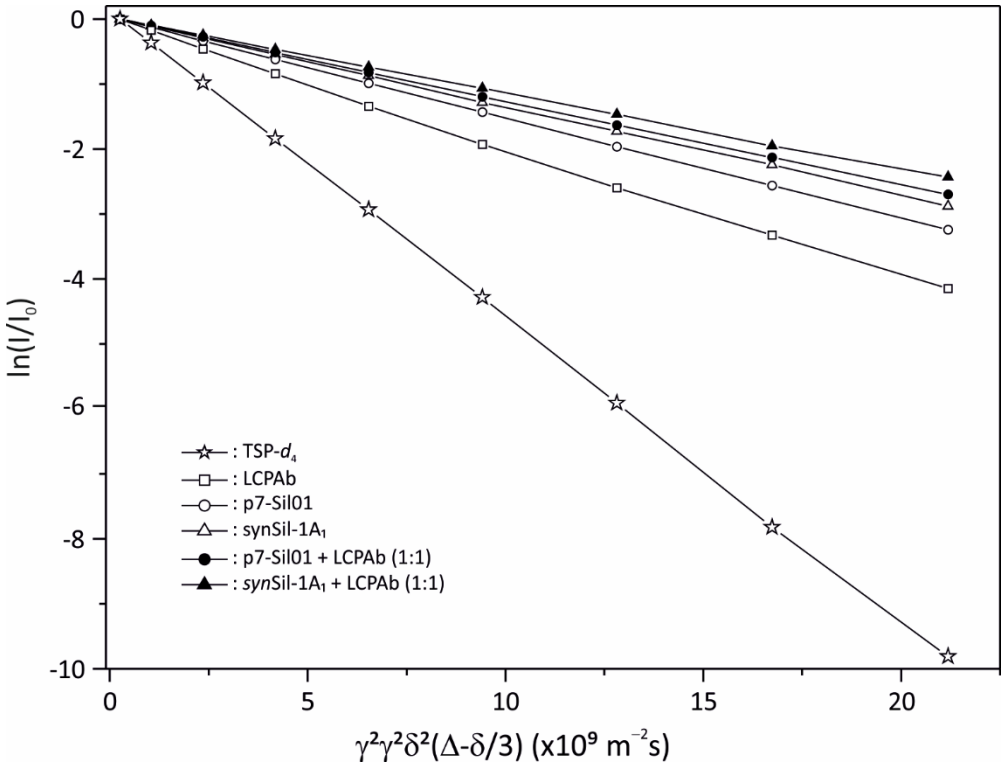

Figure S10: STEJSKAL-TANNER plots of the reference TSP-d_4, p7-Sil01 **S15**, *syn*Sil-1A$_1$ **S16**, and the respective complex with LCPAb **S13b**, all at concentration 1.0 mM in D_2O buffer at 298 K.

Coacervate droplet size

The diffusion data and the calculated droplet sizes based on the Stokes-Einstein equation are summarized in Table S6. The predicted size of one molecule of **S16** is 3.2 kÅ^3 and an individual LCPAb **S13b** without associated counterions is 1.3 kÅ^3 according to molmovdb.org.[13]

Table S6: DOSY analysis of *syn*Sil-1A$_1$ **S16** and LCPAb **S13b** in D_2O at 298 K with diffusion coefficients, PEC coacervate droplet size, and bound fractions of LCPAb.

Component	D_{exp} (10^{-10}·m^2/s)	r_H (Å)	Vol_{exp} (kÅ^3)	bound fraction
*syn*Sil-1A$_1$ **S16**	1.39	15.6	16.0	-
LCPAb **S13b**	2.13	10.1	4.3	-
*syn*Sil-1A$_1$ / LCPAb (1:1)	1.17 / 1.48	18.6 [a]	26.9 [a]	70% [b]
*syn*Sil-1A$_1$ / LCPAb (1:2.8)	1.08 / 1.81	20.0 [a]	33.5 [a]	30% [b]
*syn*Sil-1A$_1$ / LCPAb (1:6.4)	1.04 / 1.84	20.8 [a]	37.7 [a]	25% [b]

[a]) based on the diffusion coefficient of *syn*Sil-1A$_1$ **S16**, [b]) based on the diffusion coefficient of LCPAb **S13b**, -) not available.

^{31}P and ^{1}H-^{31}P HMBC experiments of phosphopeptides

The ^{31}P and ^{1}H-^{31}P HMBC spectra were measured on a Bruker AVIII 500 MHz installed with a Prodigy BBO at 298 K. The ^{31}P spectra were recorded both with and without decoupling on ^{1}H channel. For the ^{1}H-^{31}P HMBC experiments, pulse sequence with sensitivity enhancement was used.[14] Spectra were optimized for a long-range coupling constant of 7 Hz, with adiabatic decoupling on ^{31}P during acquisition. Gradients in smooth square shape were used, with ratio g1 : g2 = 49 : 20 % of the maximal gradient strength 65.7 G/cm for coherence selection. Spectral widths of 10 and 5 ppm were applied to ^{1}H and ^{31}P dimension, respectively. The 2D complex data were recorded with 128 to 256 increments, whereby 64 to 180 scans and a relaxation delay of 2 s was used for each increment. The measurement time was from 9 to 12 h. The ^{31}P chemical shift was referenced to 85% H_3PO_4 enclosed in a coaxial tube for the p7-Sil01 **S15**, sample and externally for the rests.

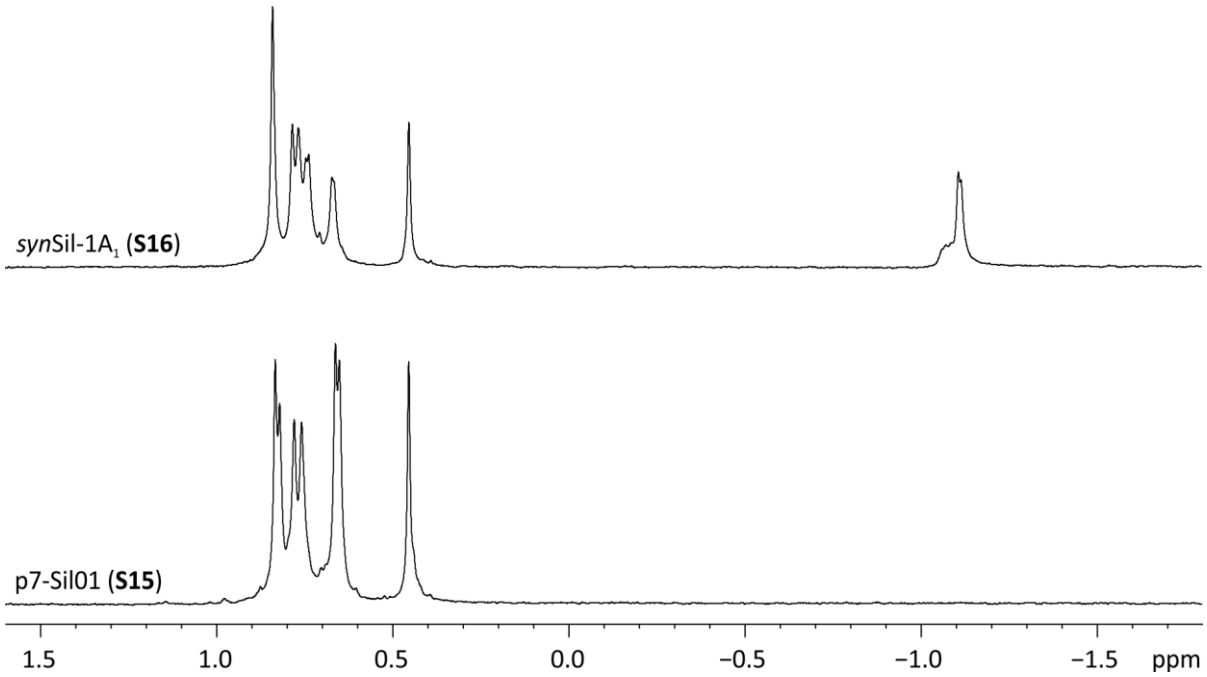

Figure S11: ^{31}P NMR spectra of p7-Sil01 **S15** (bottom) and *syn*Sil-1A$_1$ **S16** (top) 1.0 mM in H_2O/D_2O (9:1) at pH 3.02, with ^{1}H-decoupling (202.5 MHz, 300 K). ^{31}P chemical shift was referenced to 85% H_3PO_4 enclosed in a coaxial tube for the p7-Sil01 **S15**, sample and externally for the rests. The ^{31}P NMR phospho-choline resonance signal of *syn*Sil-1A$_1$ **S16** observed at −1.20 ppm nearly 2 ppm highfield shifted of the serine phosphates. The seven serine phosphates of both compounds show a very similar pattern and are largely in agreement with the significantly broader serine phosphates of the microheterogeneous isolated *nat*Sil-1A$_1$ described by KRÖGER *et al*. in 2002.[7]

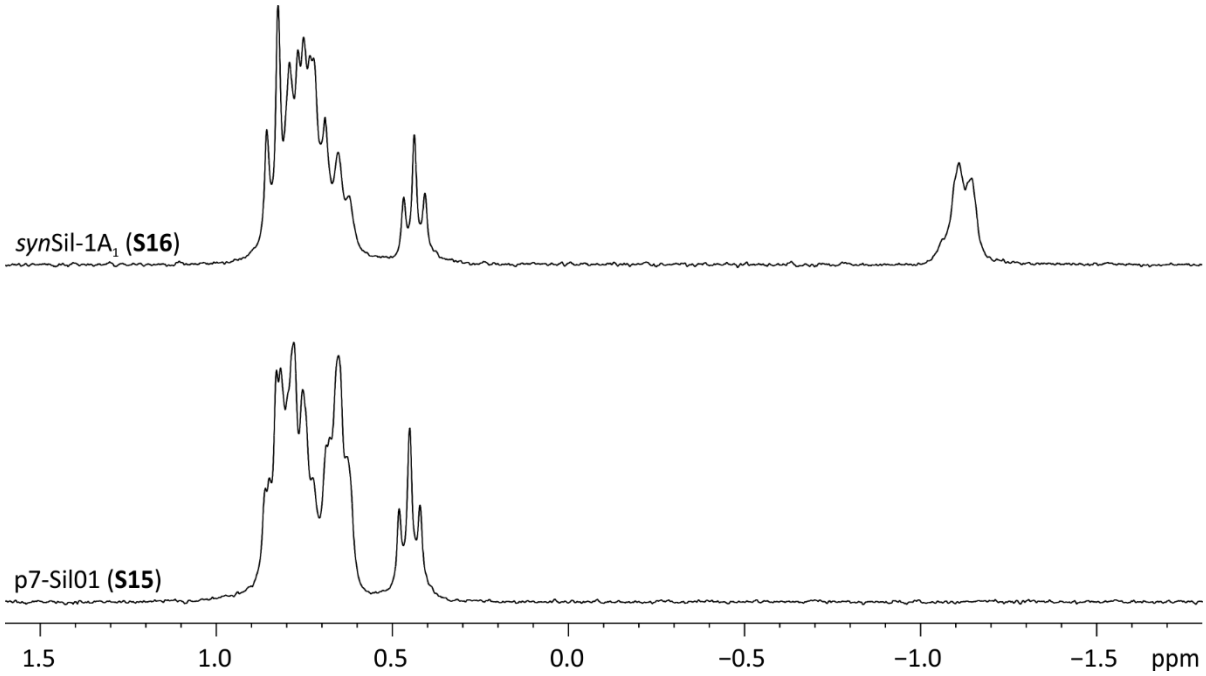

Figure S12: ^{31}P NMR spectra of p7-Sil01 **S15** (bottom) and *syn*Sil-1A$_1$ **S16** (top) 1.0 mM in H_2O/D_2O (9:1) at pH 3.02, without ^{1}H-decoupling (202.5 MHz, 300 K).

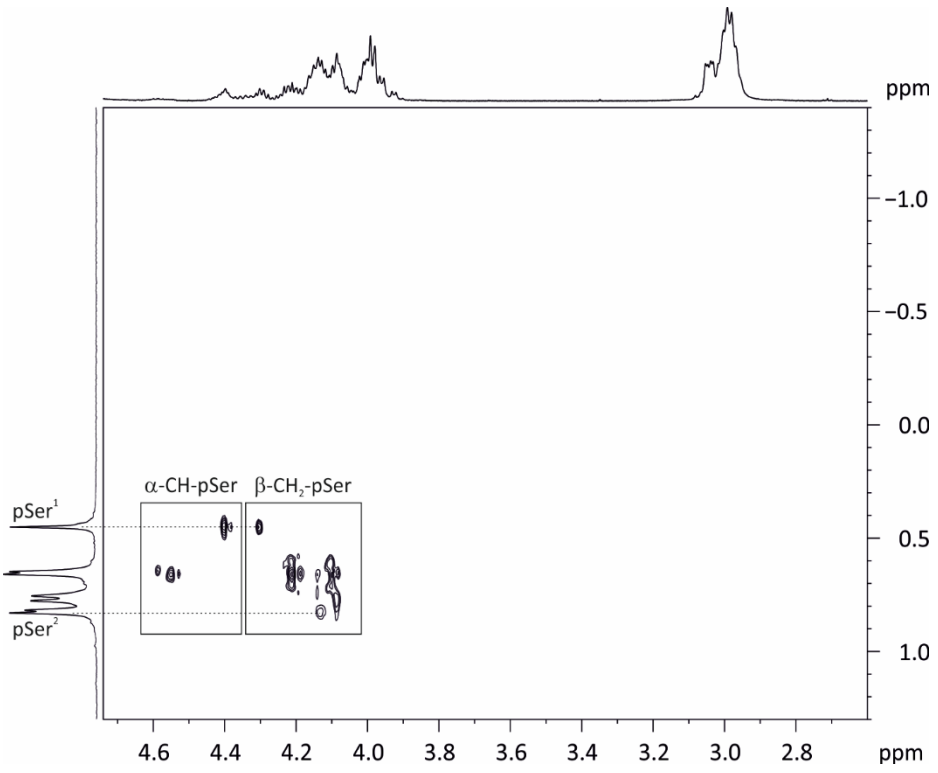

Figure S13: ^{1}H-^{31}P HMBC spectrum of 1 mM p7-Sil01 **S15** in H_2O/D_2O (9:1) at pH 3.02 (500 MHz, 300 K).

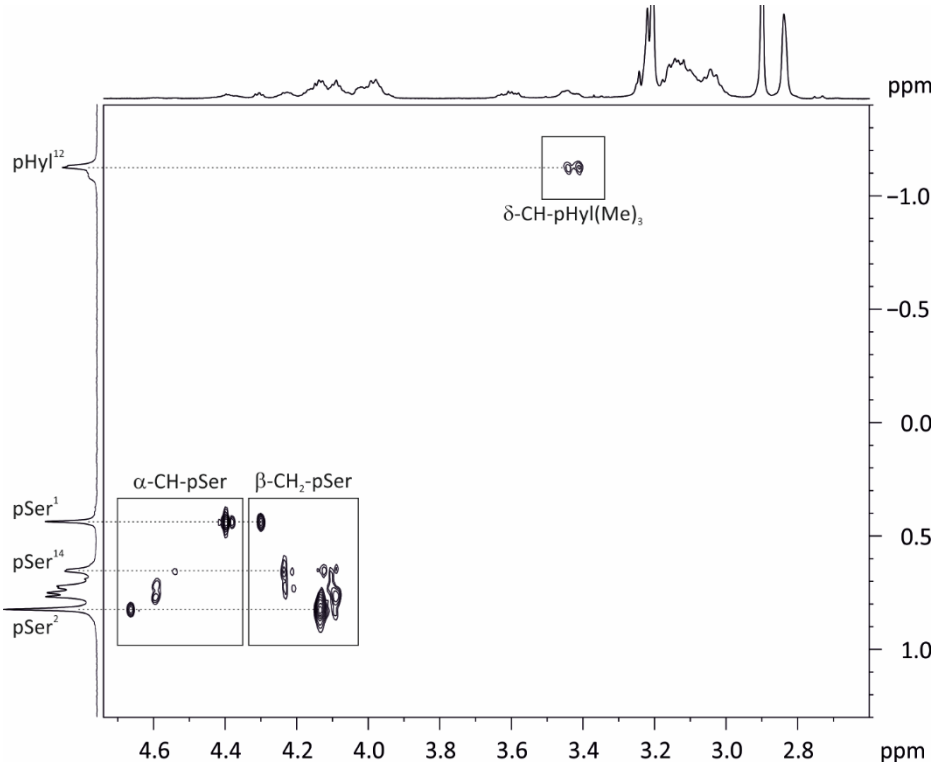

Figure S14: ^{1}H-^{31}P HMBC spectrum of 1 mM *syn*Sil-1A$_1$ **S16** in H_2O/D_2O (9:1) at pH 3.02 (500 MHz, 300 K).

Analytical data

Methyl-(2*S*)-2-((*tert*-butoxycarbonyl)amino)-3-hydroxypropanoate (Boc-Ser-OMe, S1)

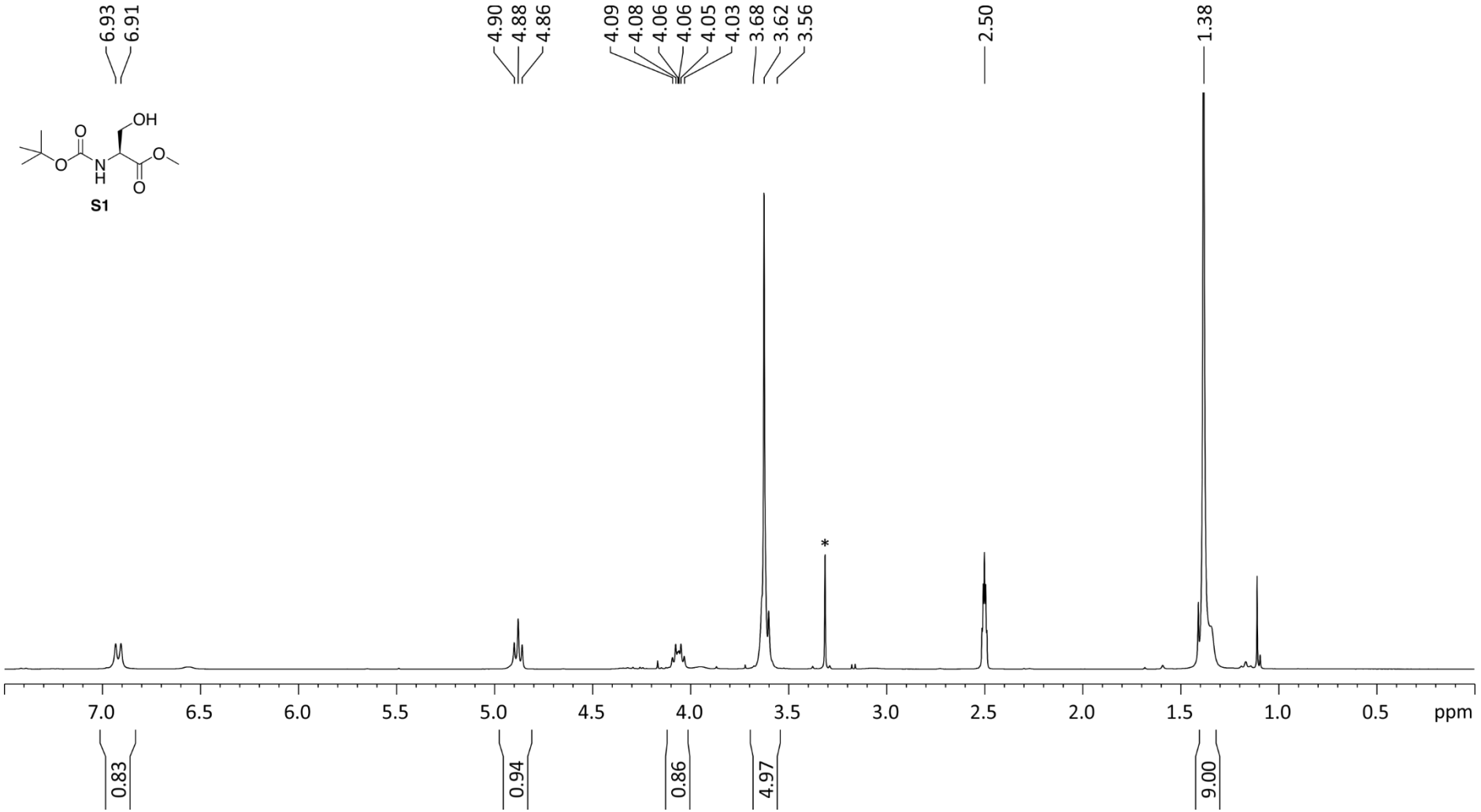

Figure S15: ^{1}H-NMR spectrum of Boc-Ser-OMe **S1** (300 MHz, 300 K, DMSO-d_6). * Signal of H_2O.

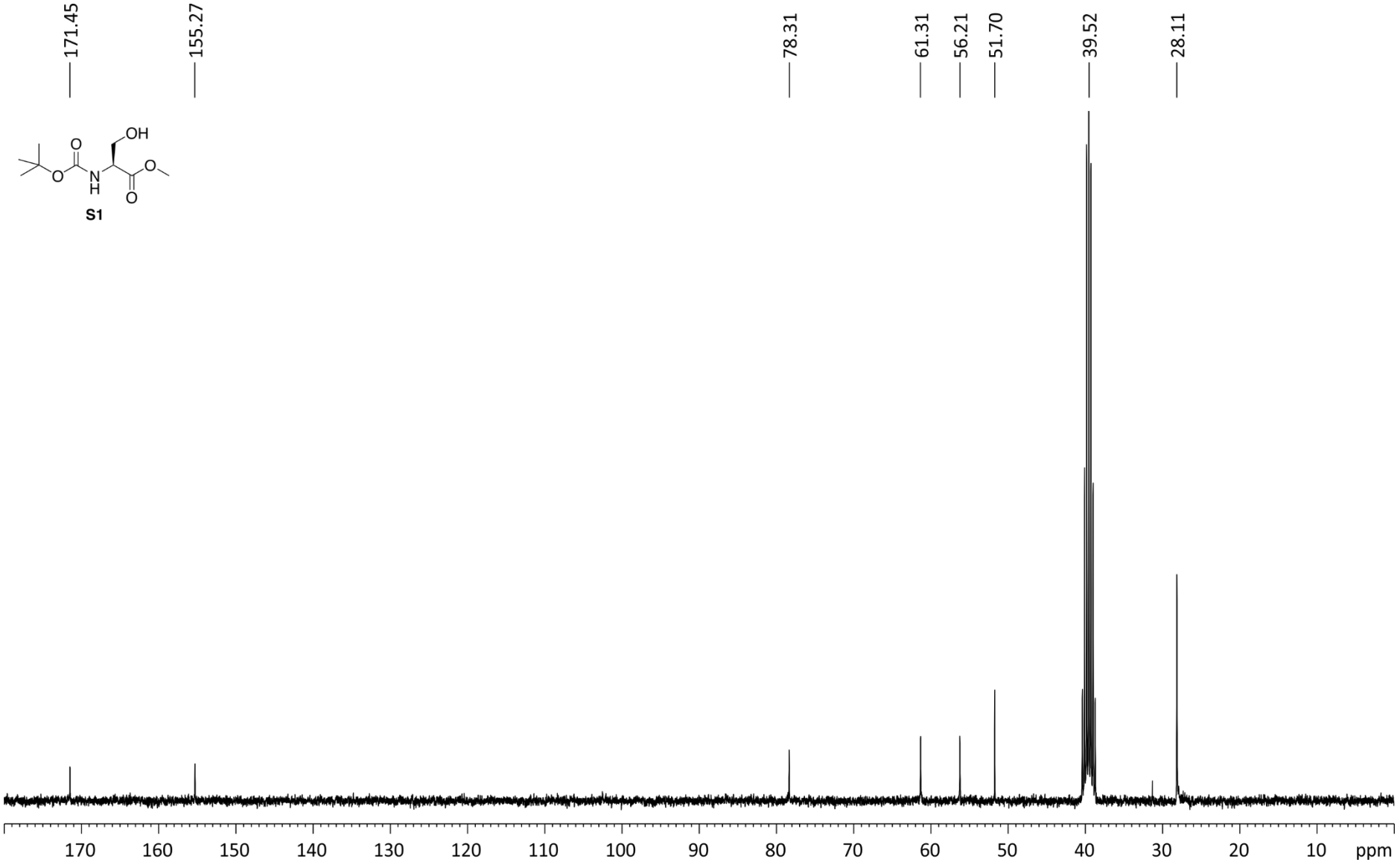

Figure S16: ^{13}C-NMR spectrum of Boc-Ser-OMe **S1** (75 MHz, 300 K, DMSO-d_6).

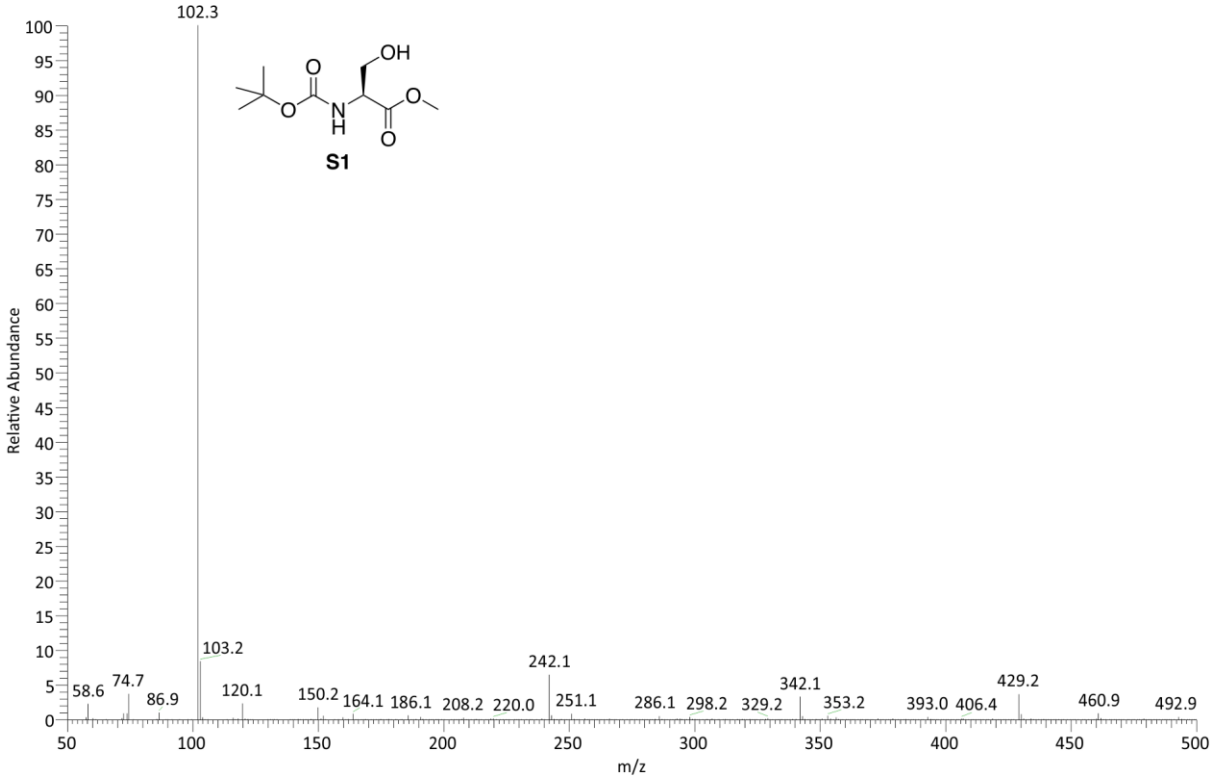

Figure S17: ESI+ mass spectrum with charge pattern m/z of Boc-Ser-OMe **S1**.

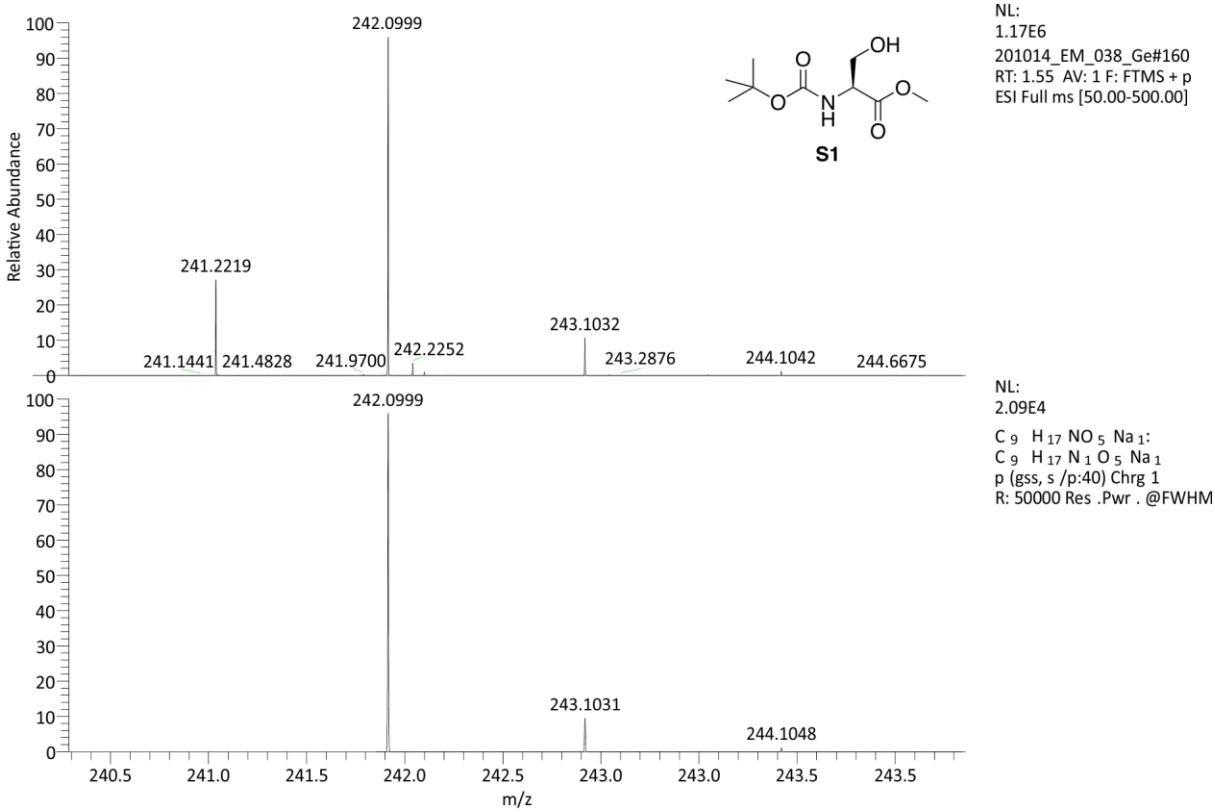

Figure S18: High resolution mass spectrum with isotope pattern of Boc-Ser-OMe **S1**.

Methyl-(2*R*)-2-((*tert*-butoxycarbonyl)amino)-3-iodopropanoate (S2)

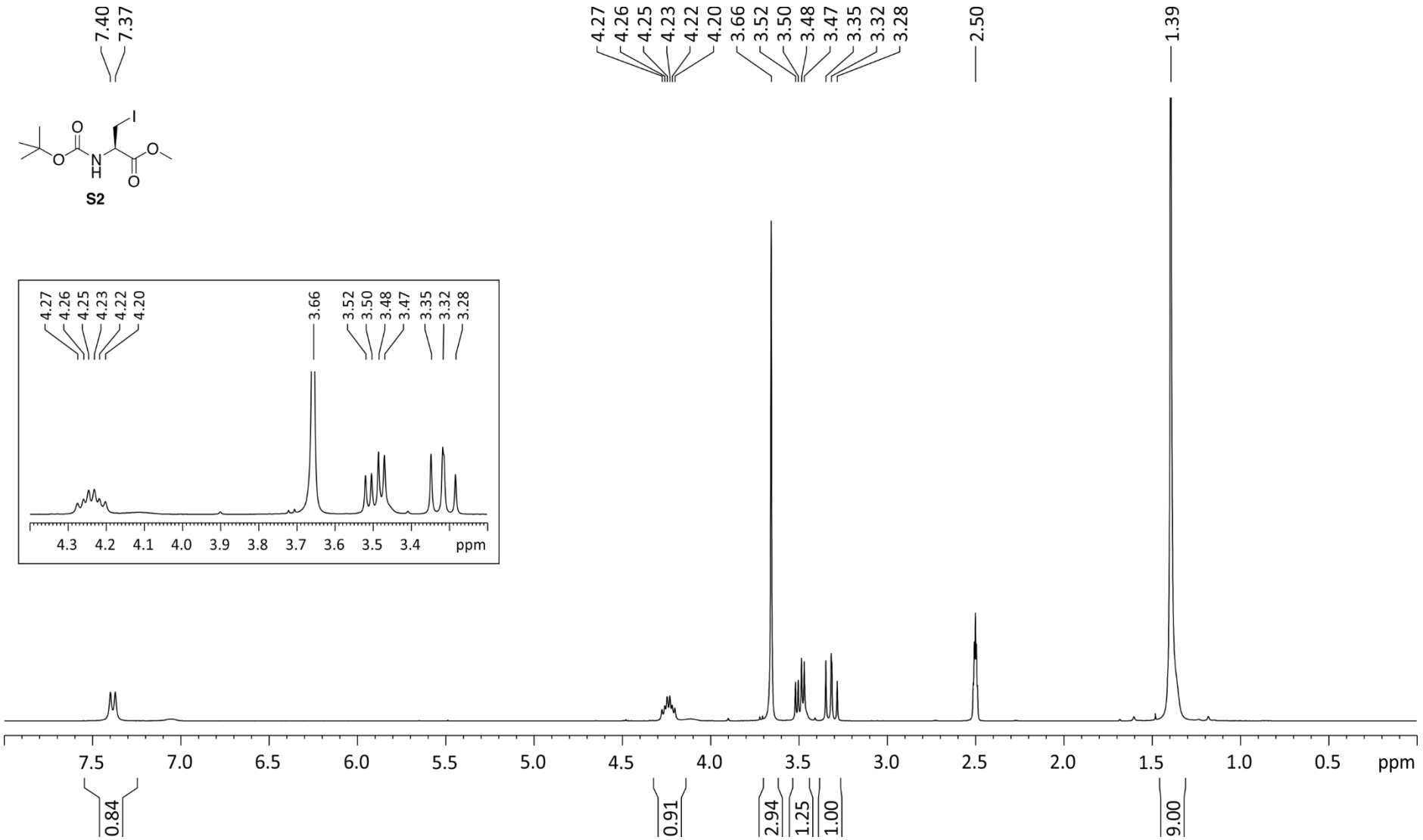

Figure S19: ^{1}H-NMR spectrum of iodopropanoate **S2** (300 MHz, 300 K, DMSO-d_6).

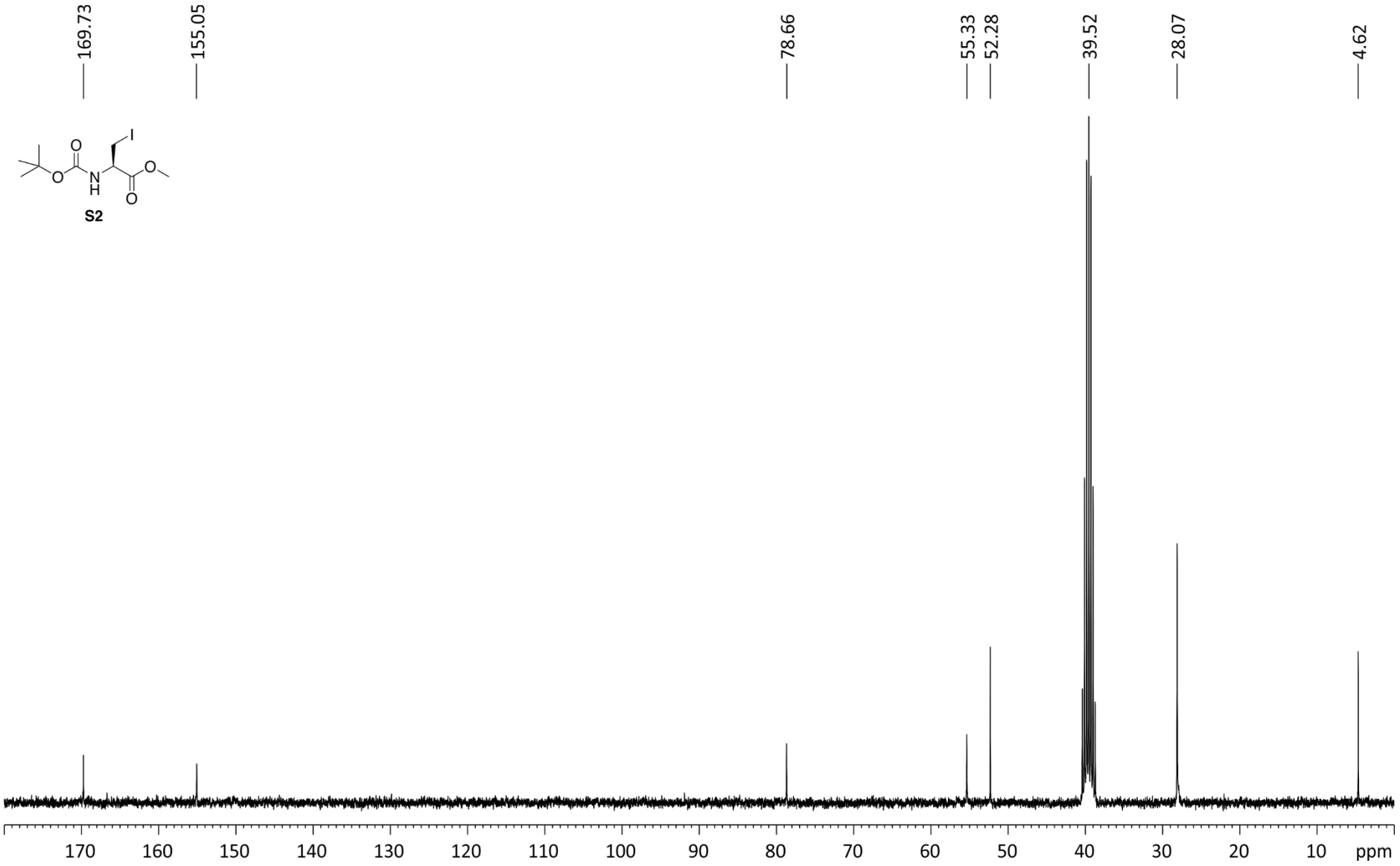

Figure S20: ^{13}C-NMR spectrum of iodopropanoate **S2** (75 MHz, 300 K, DMSO-d_6).

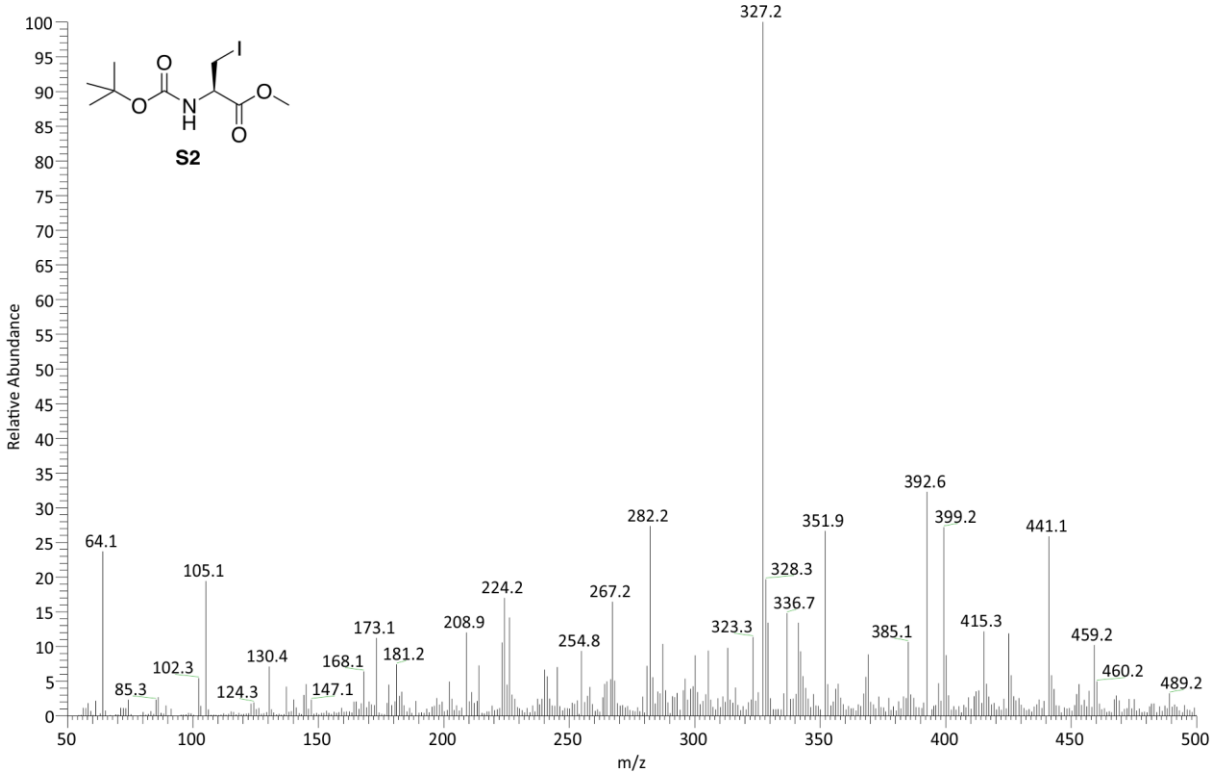

Figure S21: ESI+ mass spectrum with charge pattern m/z of iodopropanoate **S2**.

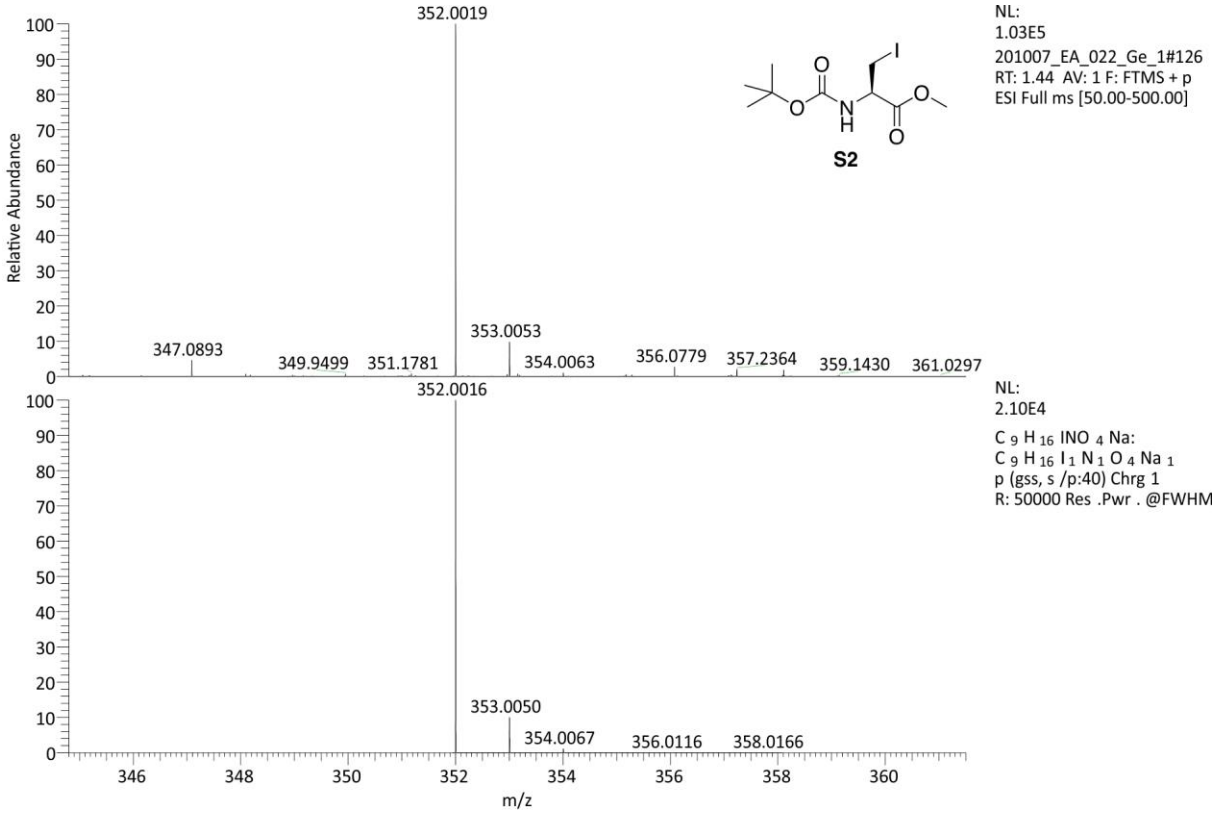

Figure S22: High resolution mass spectrum with isotope pattern of iodopropanoate **S2**.

Methyl-(2*S*)-2-((*tert*-butoxycarbonyl)amino)hex-5-enoate (Boc-Hag-OMe, S3)

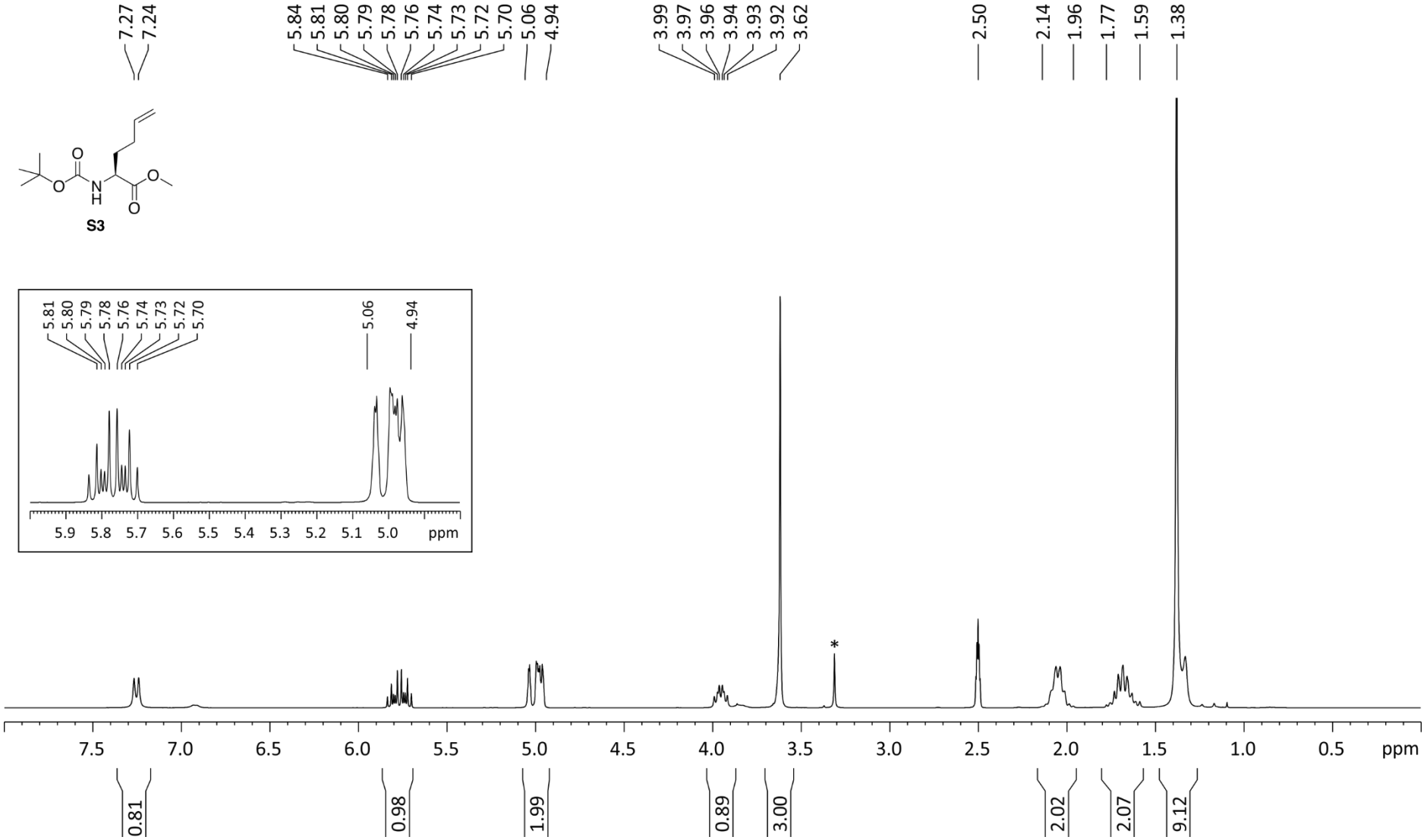

Figure S23: ^{1}H-NMR spectrum of Boc-Hag-OMe **S3** (300 MHz, 300 K, DMSO-d_6). * Signal of H_2O.

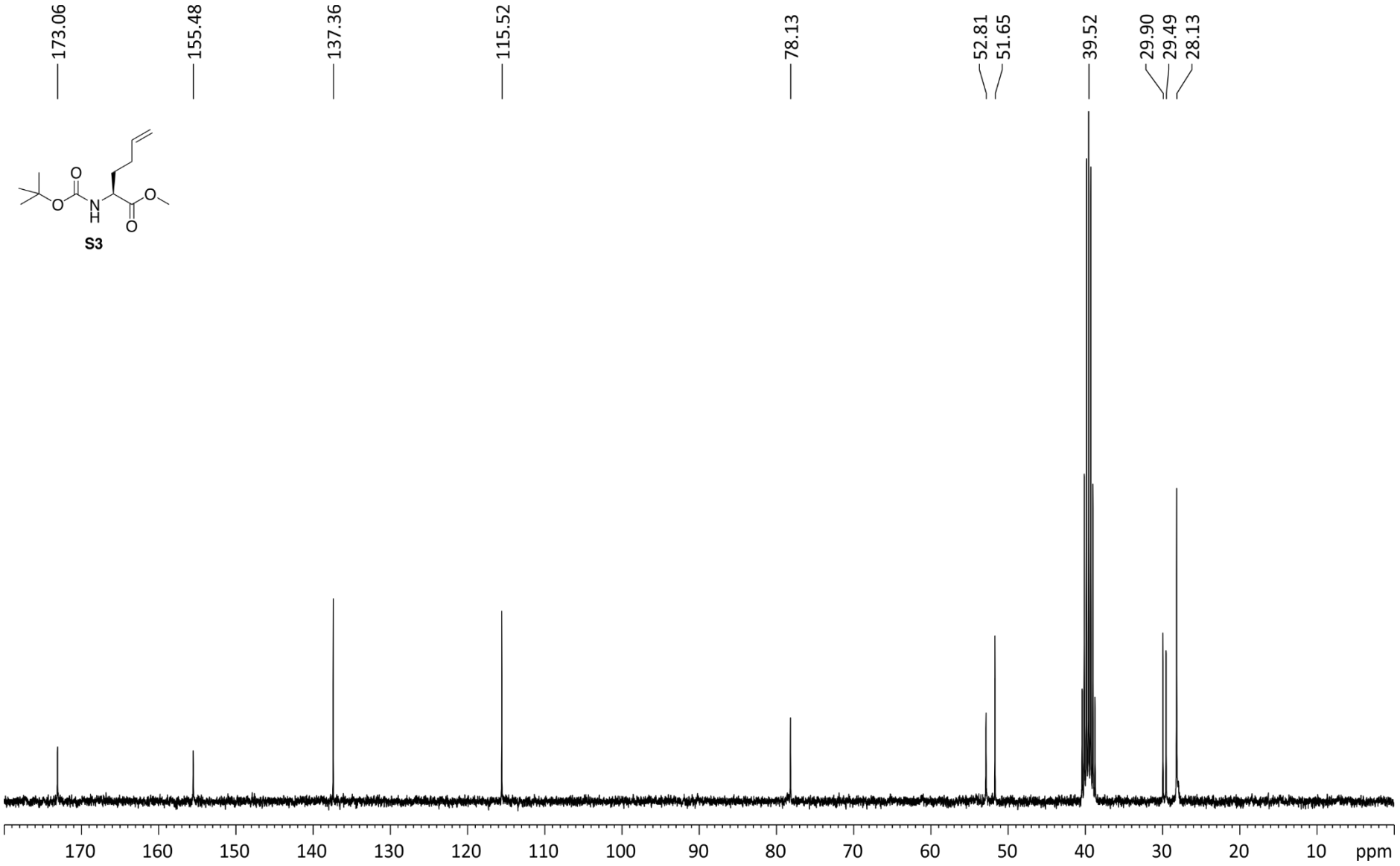

Figure S24: ^{13}C-NMR spectrum of Boc-Hag-OMe **S3** (75 MHz, 300 K, DMSO-d_6).

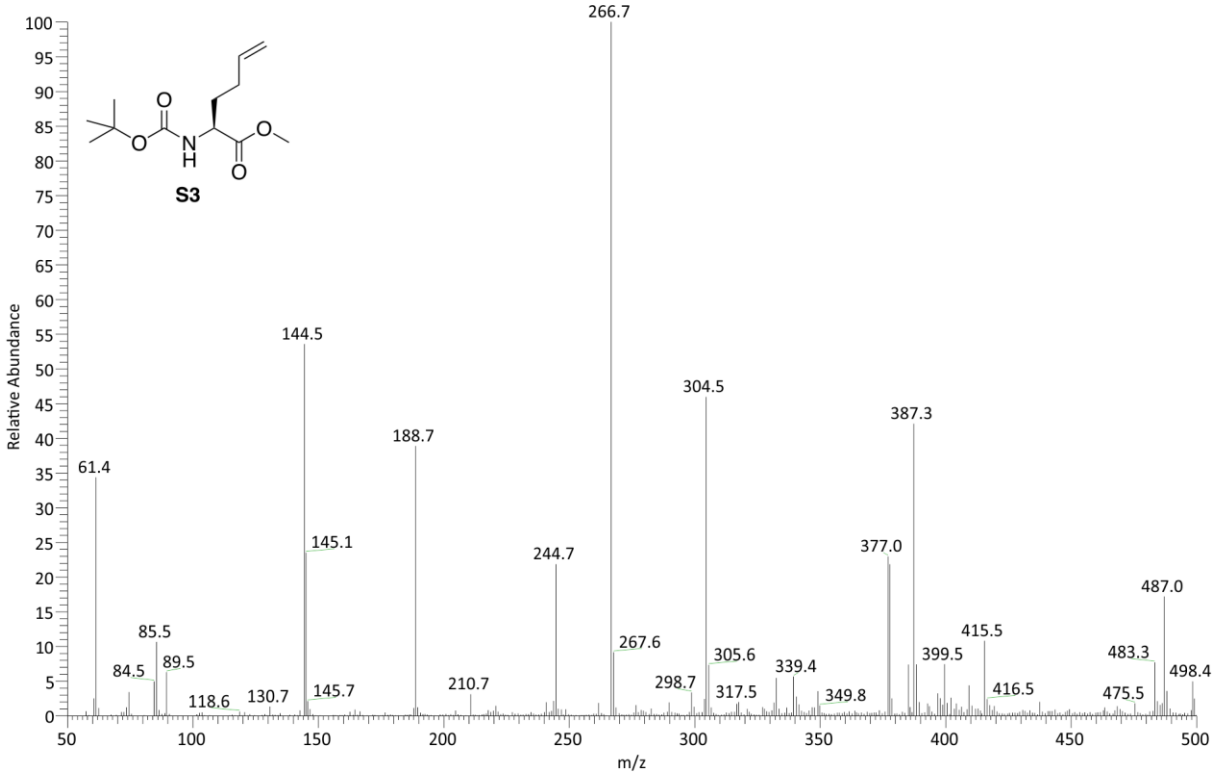

Figure S25: ESI+ mass spectrum with charge pattern m/z of Boc-Hag-OMe **S3**.

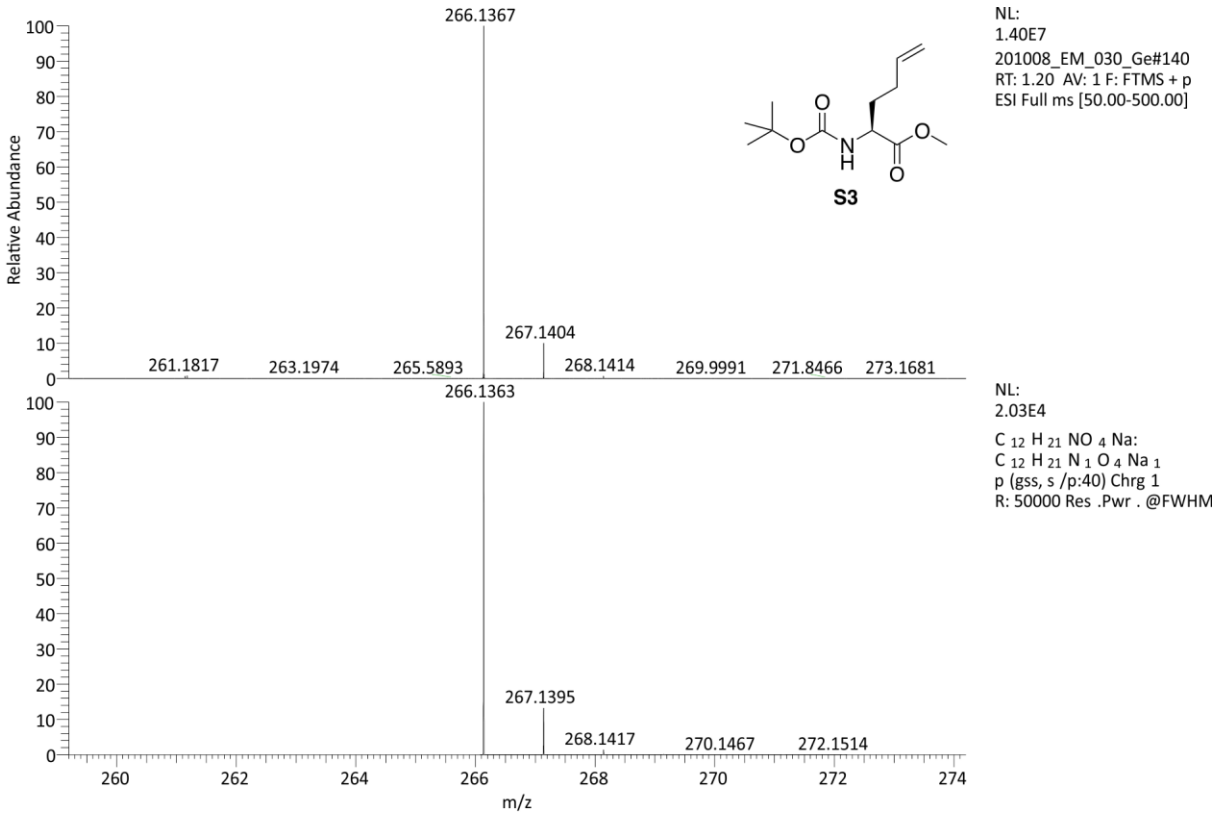

Figure S26: High resolution mass spectrum with isotope pattern of Boc-Hag-OMe **S3**.

Methyl-(2*S*)-2-((*tert*-butoxycarbonyl)amino)hex-5-enoic acid (Boc-Hag-OH, 1)

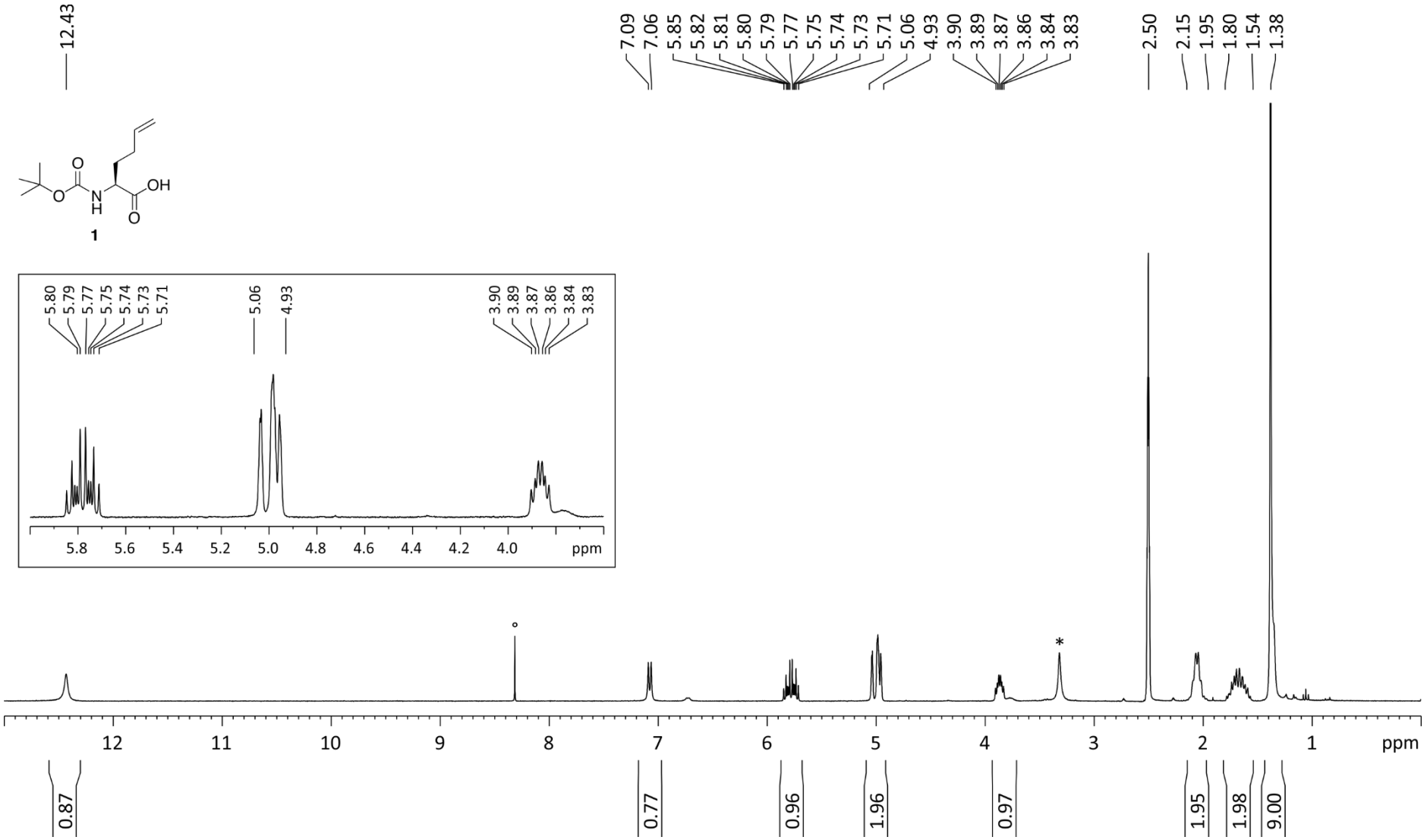

Figure S27: ^{1}H-NMR spectrum of Boc-Hag-OH **1** (300 MHz, 300 K, DMSO-d_6). * Signal of H_2O. ° Signal of $CHCl_3$.

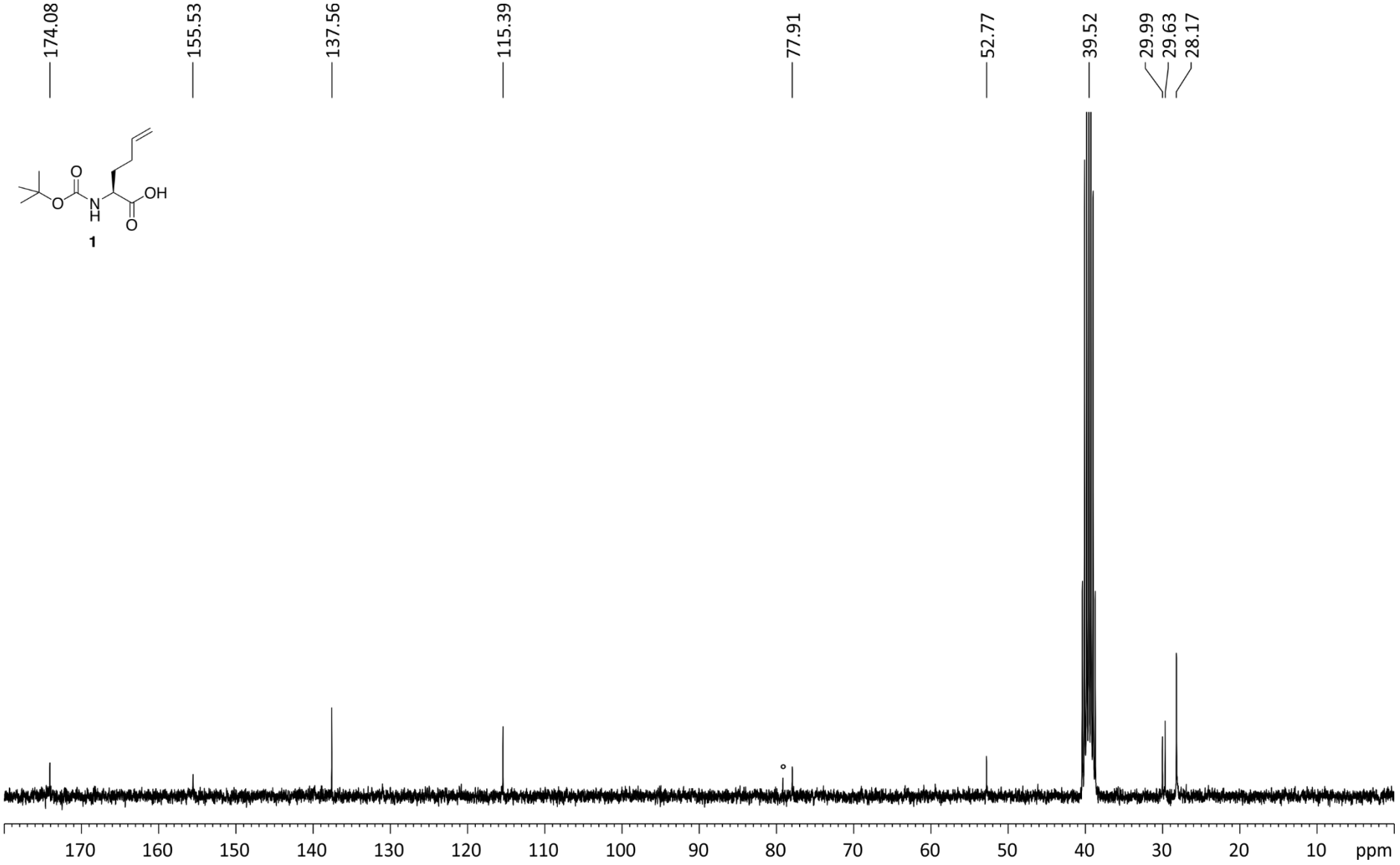

Figure S28: ^{13}C-NMR spectrum of Boc-Hag-OH **1** (75 MHz, 300 K, DMSO-d_6). ° Signal of $CHCl_3$.

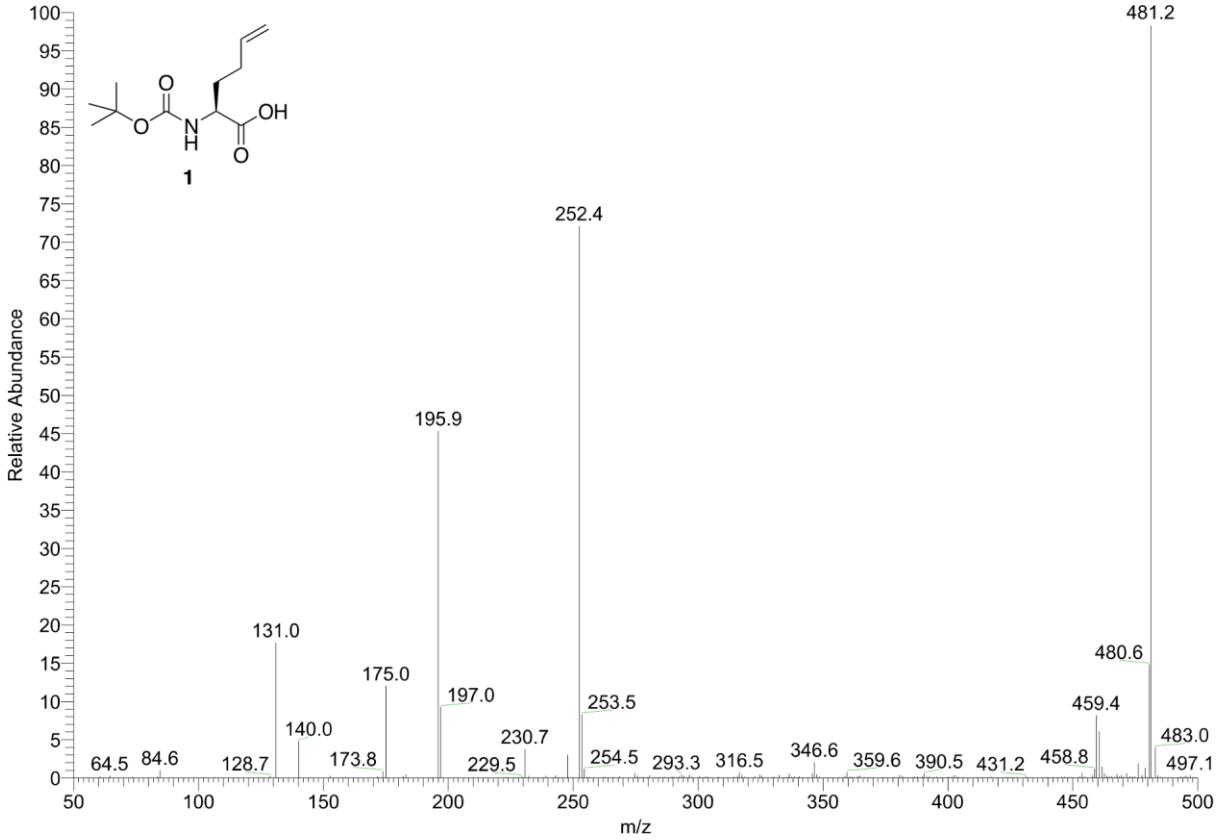

Figure S29: ESI+ mass spectrum with charge pattern m/z of Boc-Hag-OH **1**.

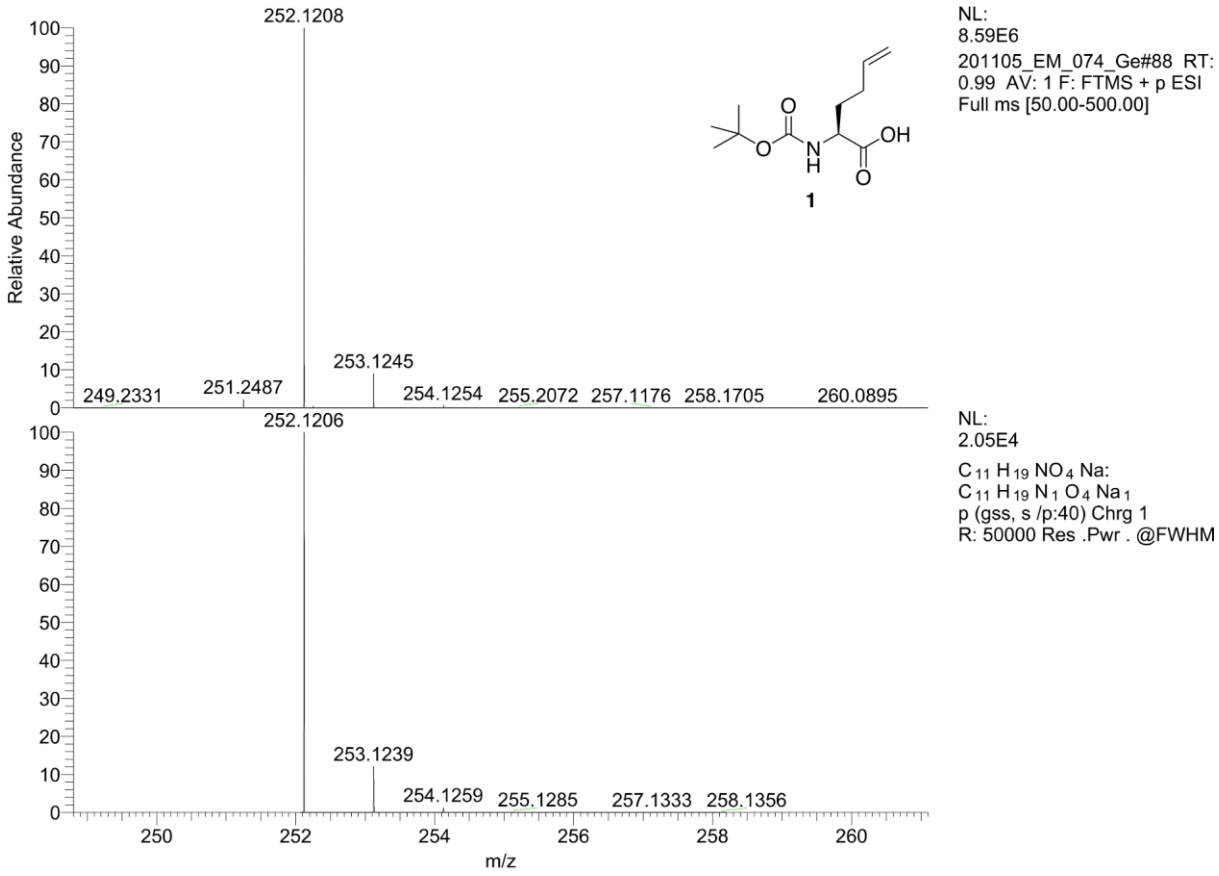

Figure S30: High resolution mass spectrum with isotope pattern of Boc-Hag-OH **1**.

***tert*-Butyl-(2*S*)-(2-((*tert*-butoxycarbonyl)amino)hex-5-enoyl)glycinate (Boc-Hag-Gly-O^{t}Bu, 2)**

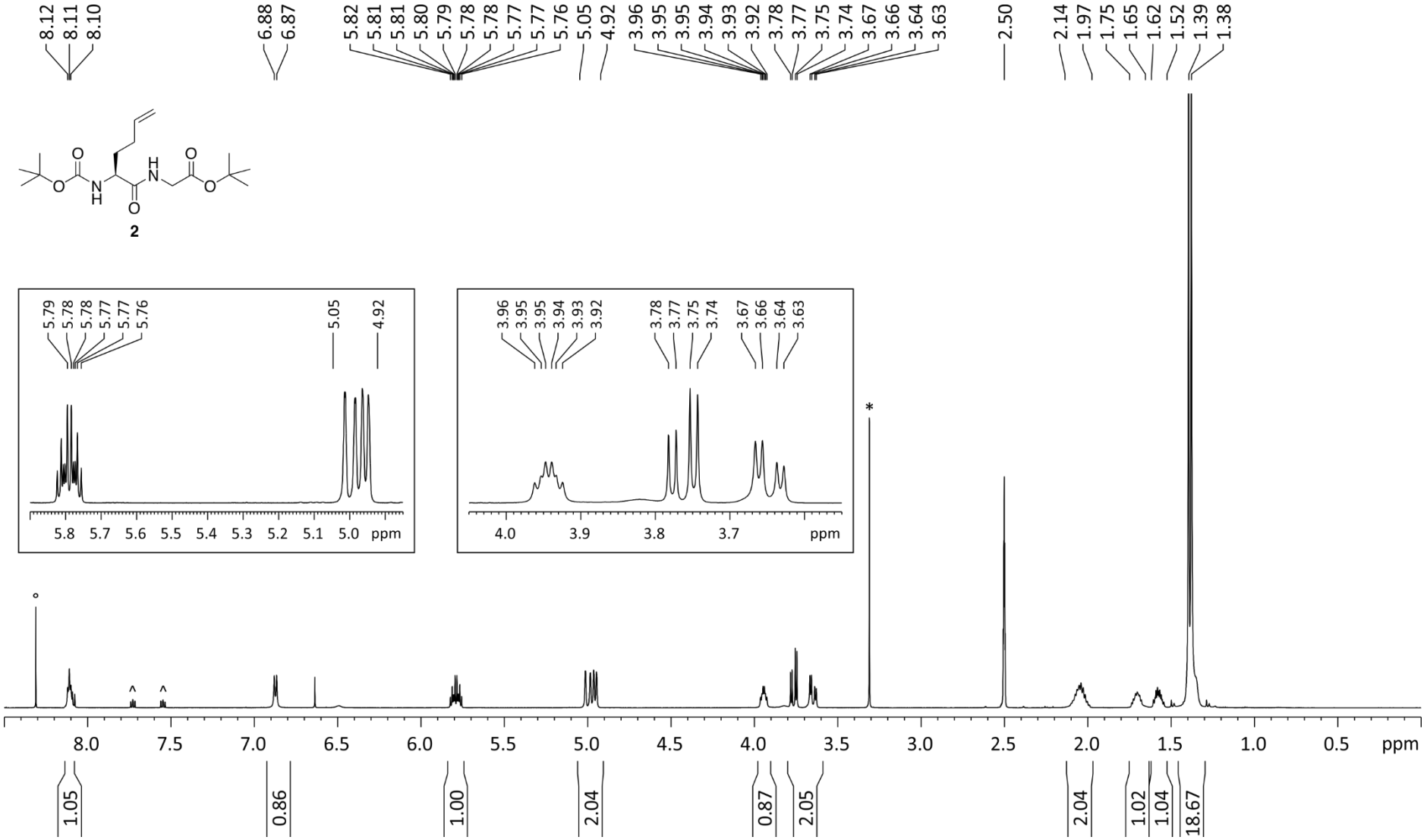

Figure S31: ^{1}H-NMR spectrum of Boc-Hag-Gly-O^{t}Bu **2** (600 MHz, 300 K, DMSO-d_6). * Signal of H_2O. ° Signal of $CHCl_3$. ^ Signals of HOBt.

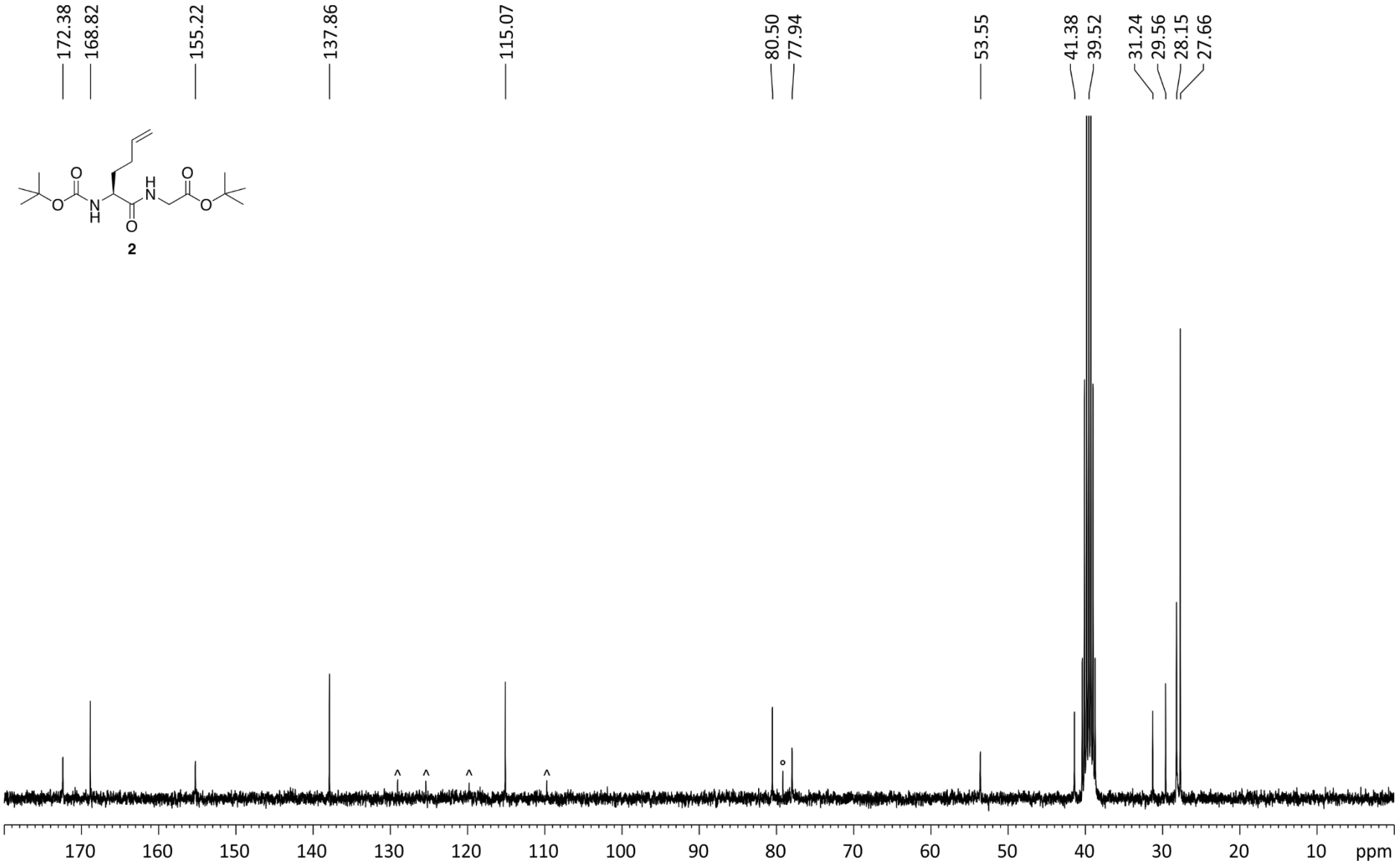

Figure S32: ^{13}C-NMR spectrum of Boc-Hag-Gly-O^{t}Bu **2** (75 MHz, 300 K, DMSO-d_6). ° Signal of $CHCl_3$. ^ Signals of HOBt.

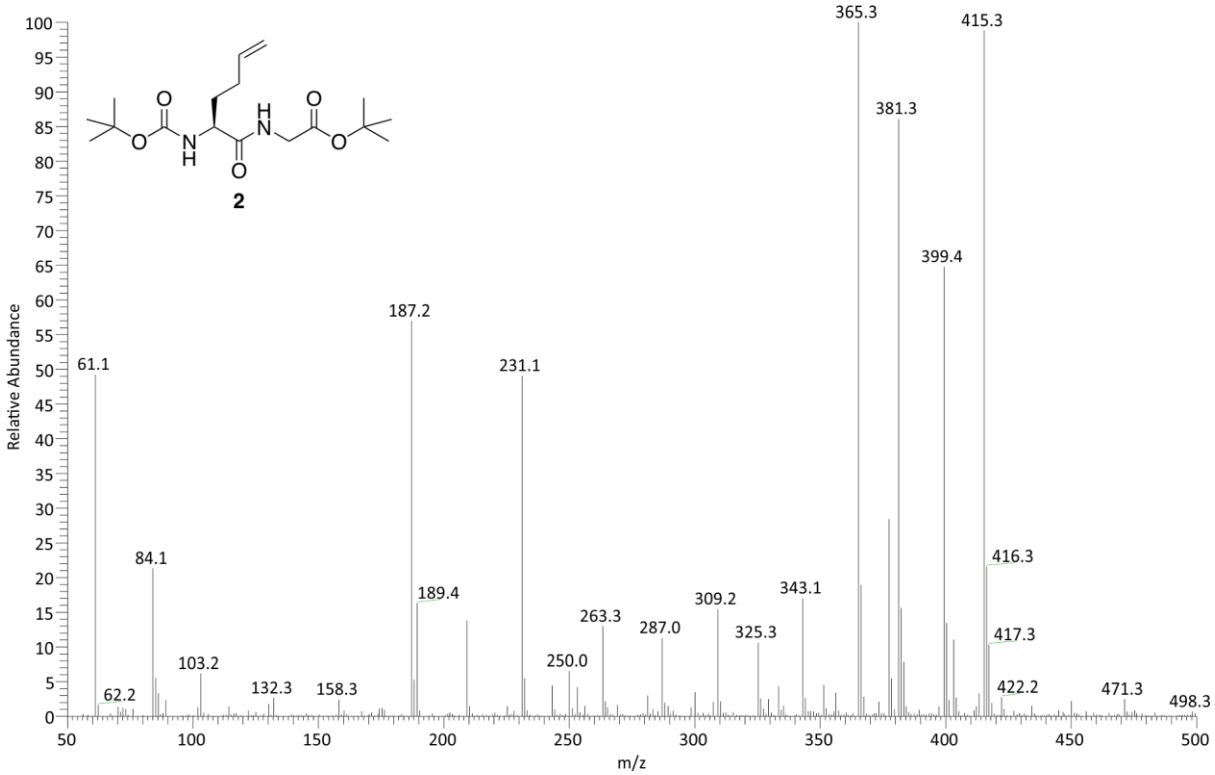

Figure S33: ESI+ mass spectrum with charge pattern m/z of Boc-Hag-Gly-O^{t}Bu **2**.

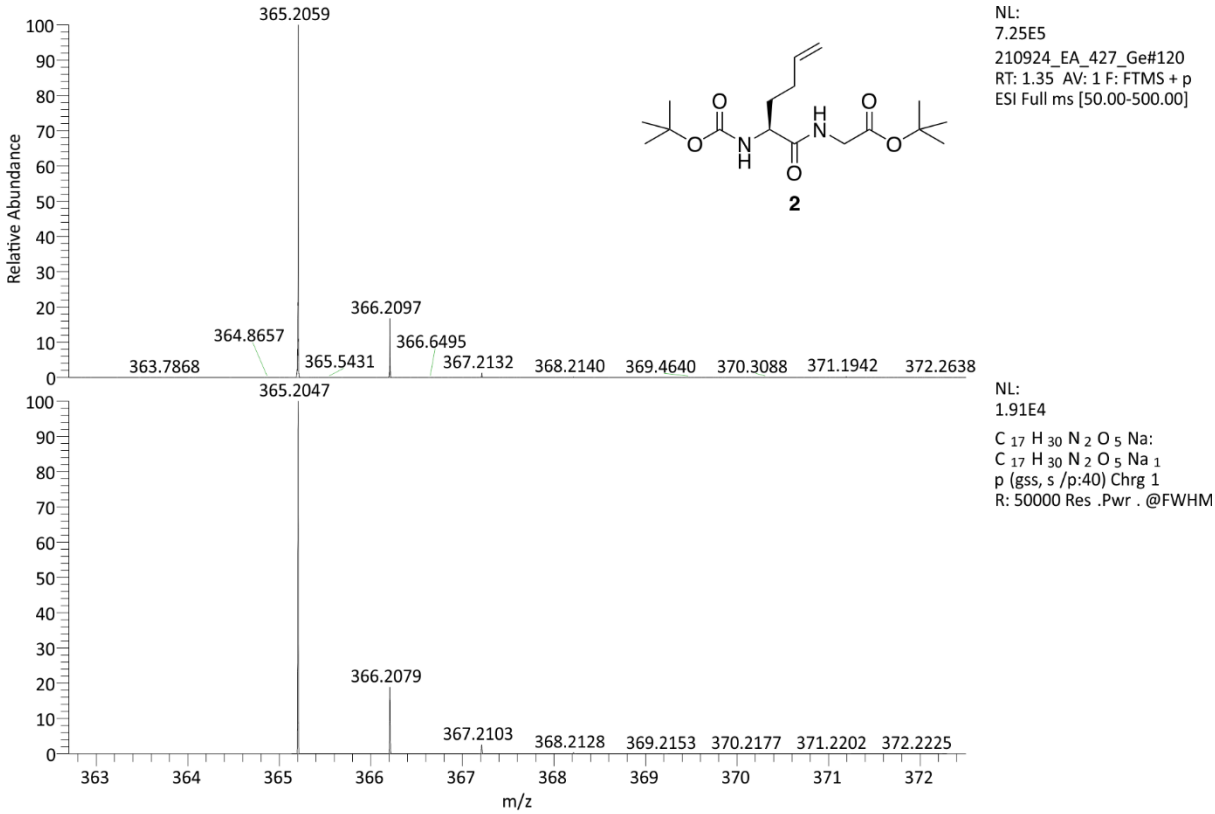

Figure S34: High resolution mass spectrum with isotope pattern of Boc-Hag-Gly-O^{t}Bu **2**.

***tert*-Butyl-((2*S*)-2-((*tert*-butoxycarbonyl)amino)-4-(oxiran-2-yl)butanoyl)glycinate (Boc-Enl-Gly-O^{t}Bu, 3)**

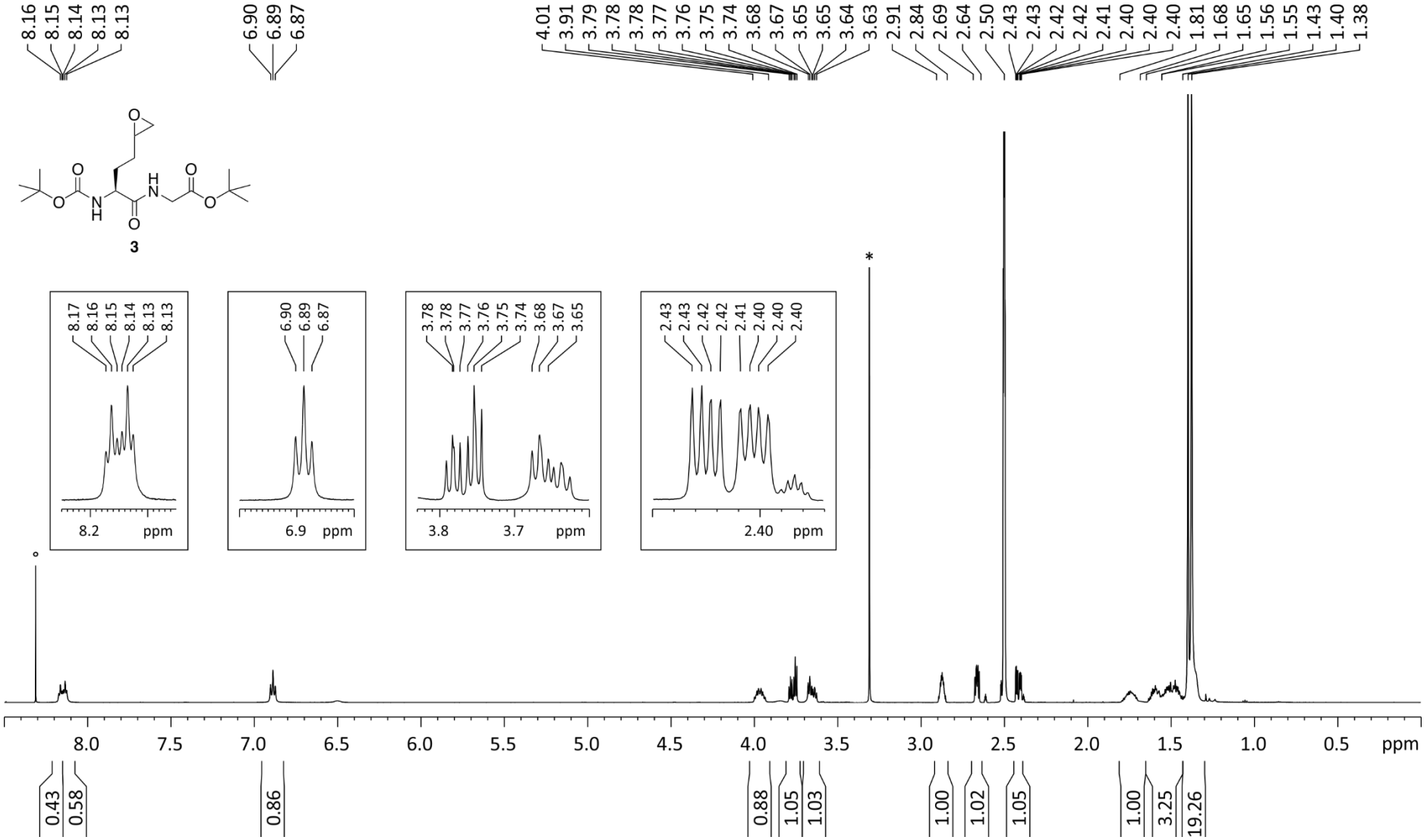

Figure S35: ^{1}H-NMR spectrum of Boc-Enl-Gly-O^{t}Bu **3** (600 MHz, 300 K, DMSO-d_6). * Signal of H_2O. ° Signal of $CHCl_3$.

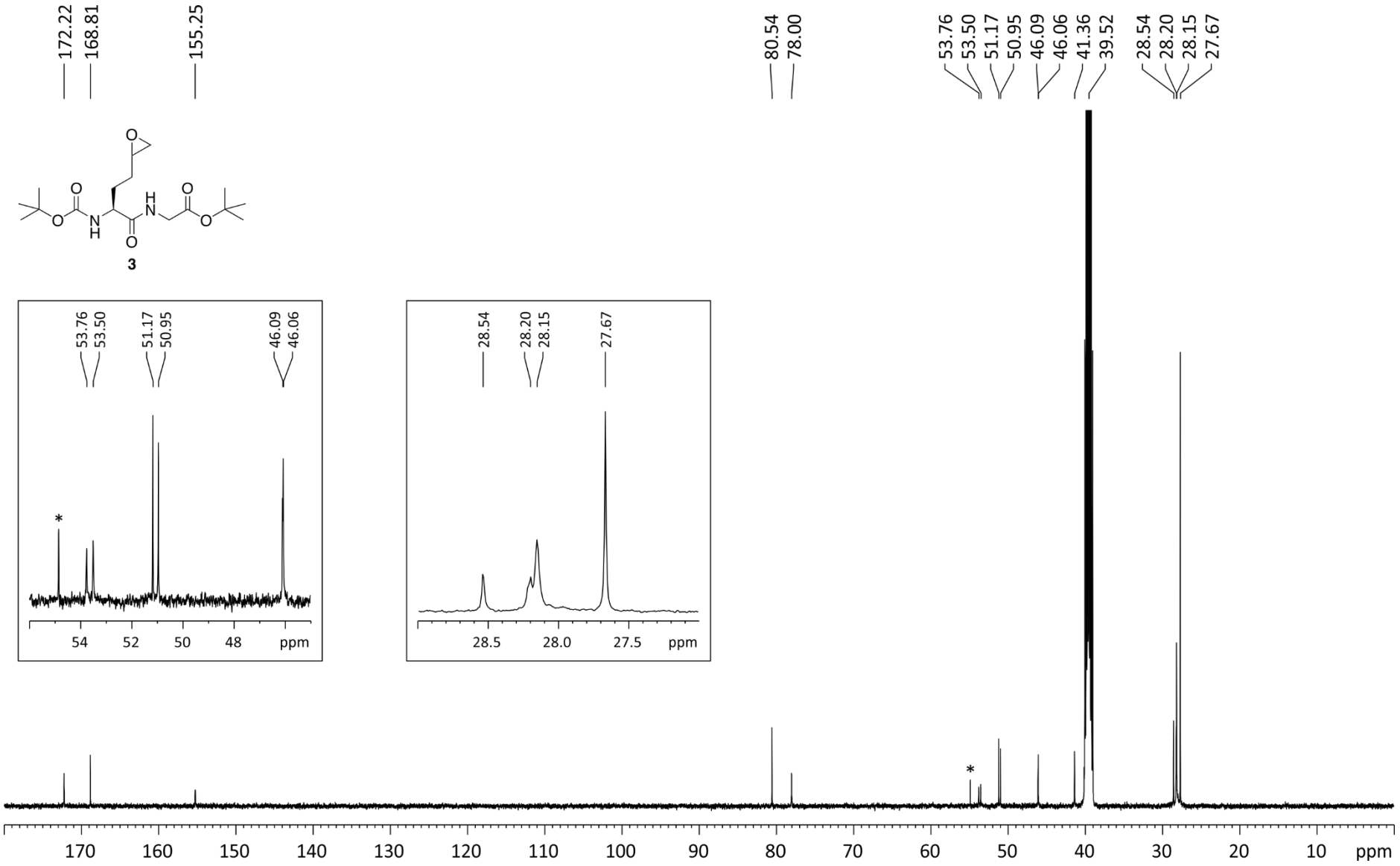

Figure S36: ^{13}C-NMR spectrum of Boc-Enl-Gly-O^{t}Bu **3** (125 MHz, 300 K, DMSO-d_6). * Signal of CH_2Cl_2.

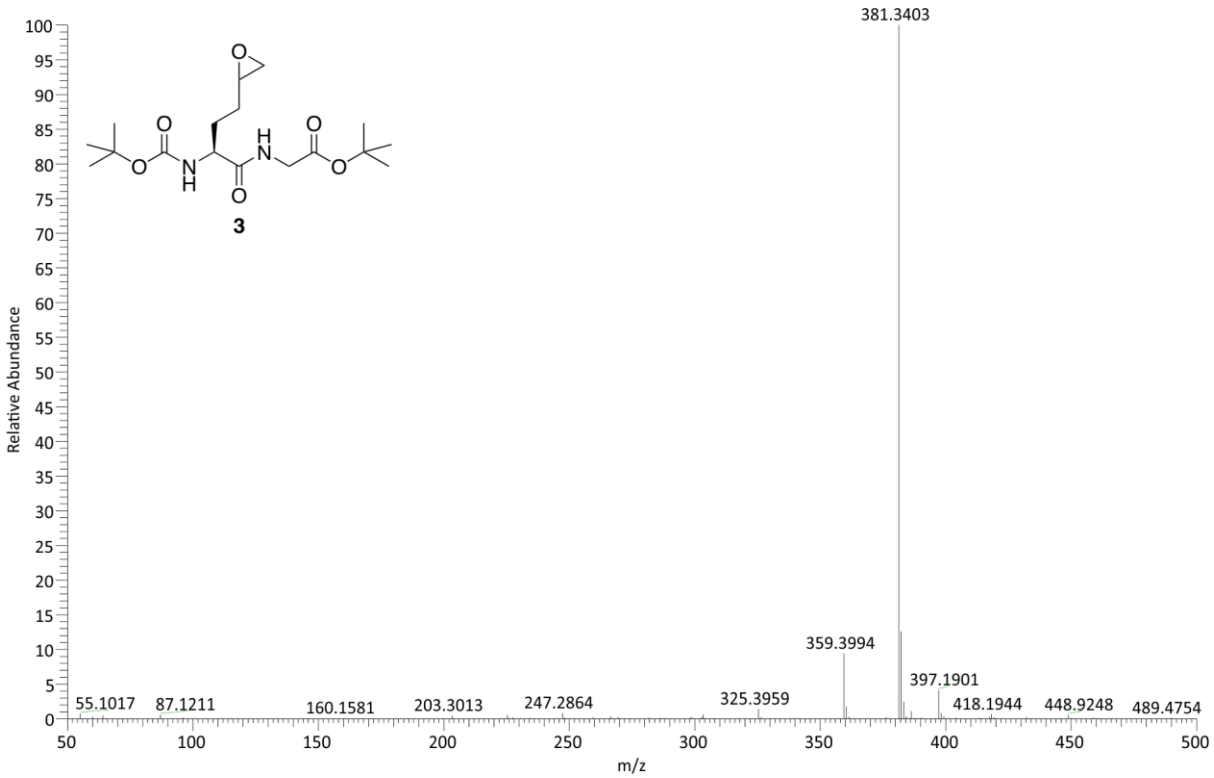

Figure S37: ESI+ mass spectrum with charge pattern m/z of Boc-Enl-Gly-O^{t}Bu **3**.

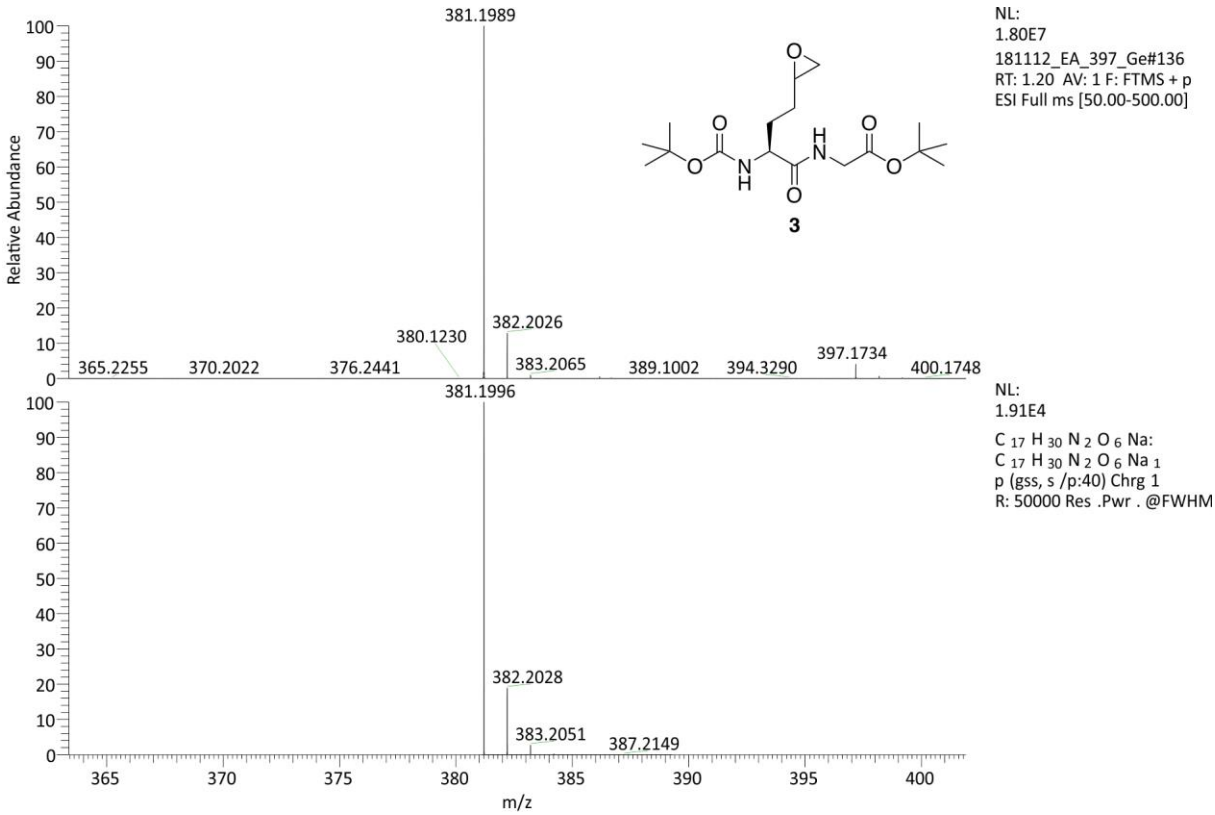

Figure S38: High resolution mass spectrum with isotope pattern of Boc-Enl-Gly-O^{t}Bu **3**.

((2*S*)-2-Amino)-6-((trimethylammonium)trifluoroacetate)-5-hydroxyhexanoyl)glycine hydrotrifluoroacetate (H_2N-Hyl$(Me)_3$-Gly-OH · TFA, 4)

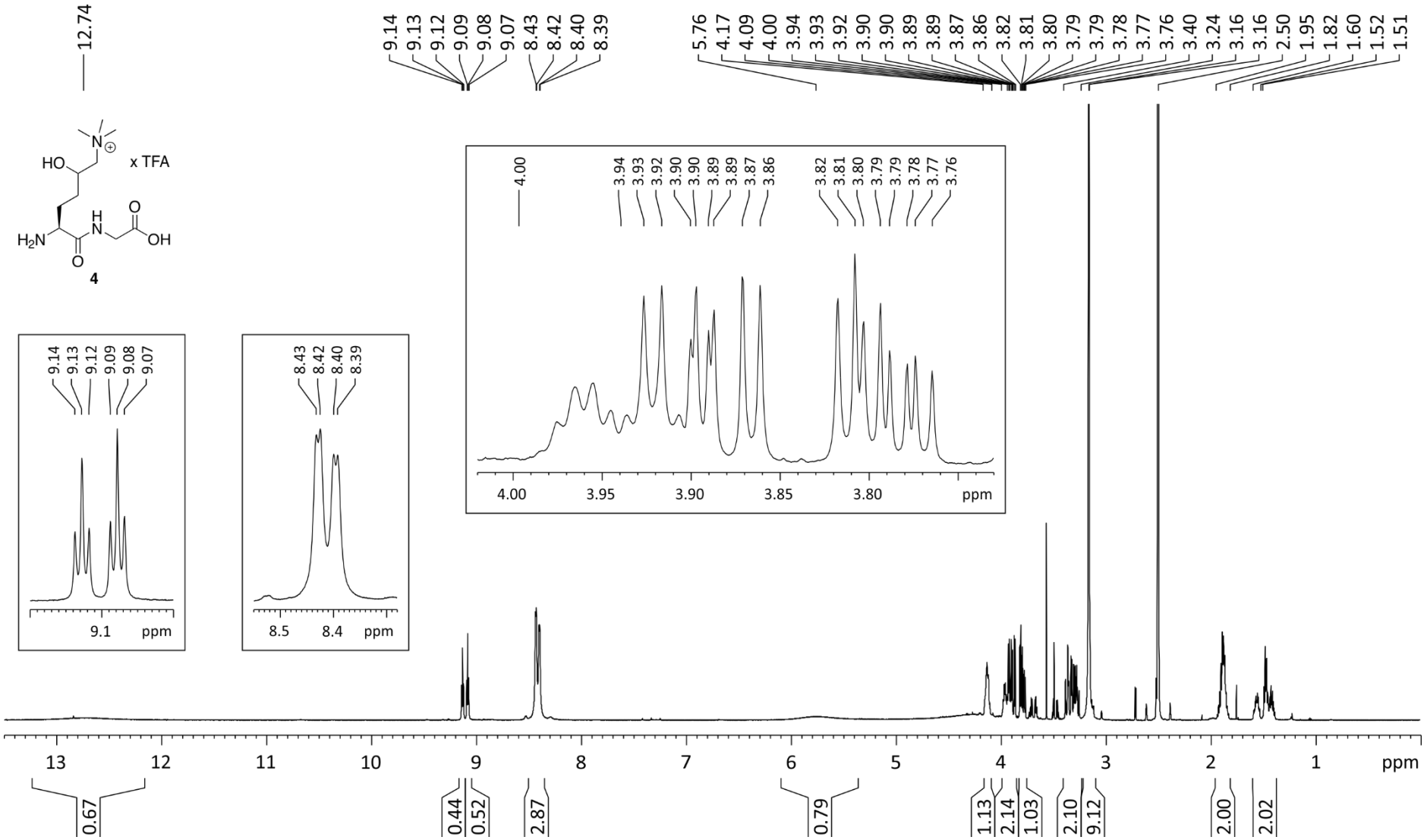

Figure S39: ^{1}H-NMR spectrum of H_2N-Hyl$(Me)_3$-Gly-OH · TFA **4** (600 MHz, 300 K, DMSO-d_6).

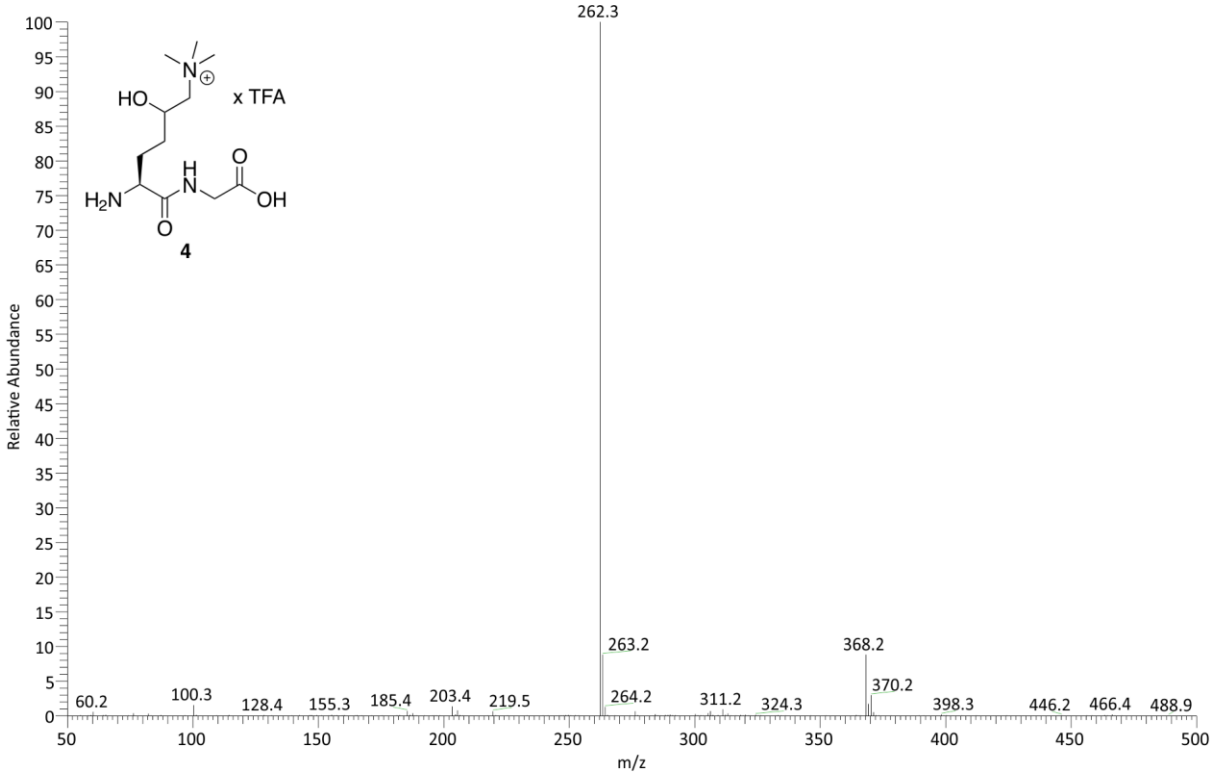

Figure S40: ESI+ mass spectrum with charge pattern m/z of H_2N-Hyl(Me)$_3$-Gly-OH · TFA **4**.

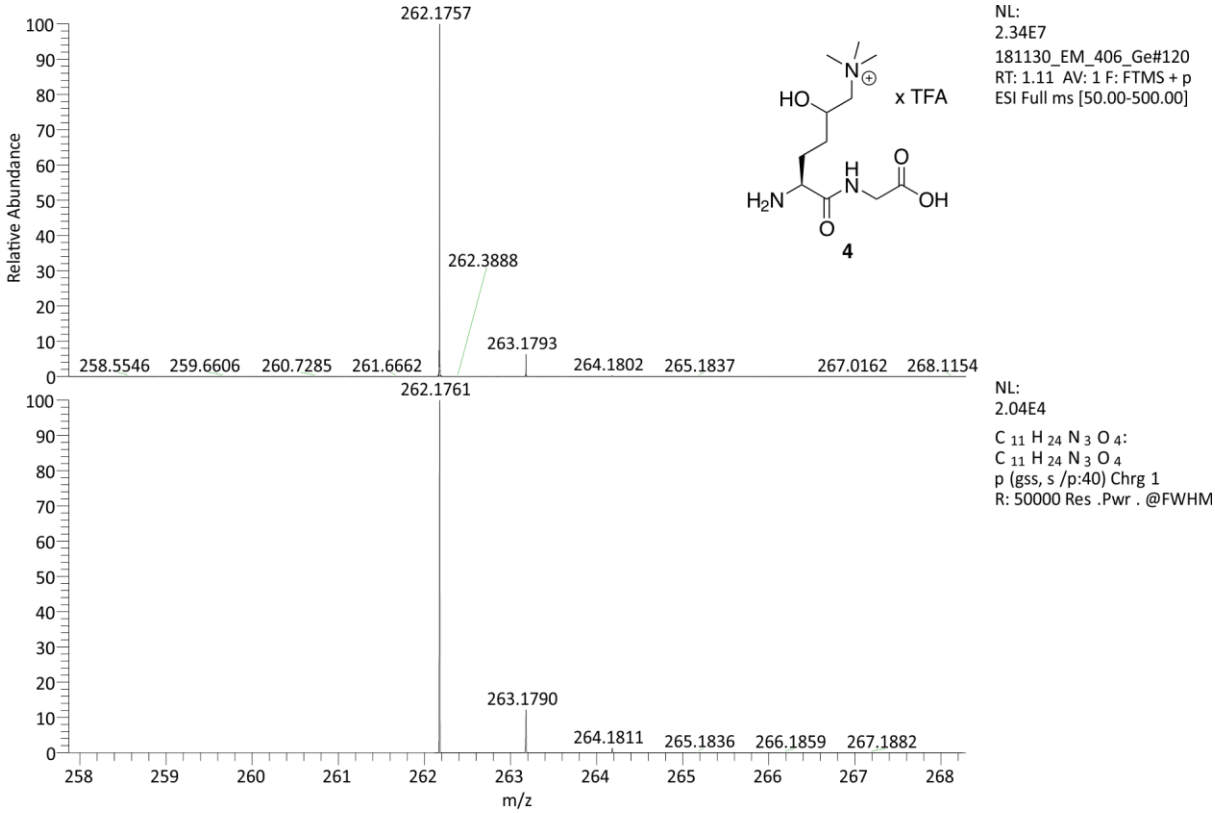

Figure S41: High resolution mass spectrum with isotope pattern of H_2N-Hyl(Me)$_3$-Gly-OH · TFA **4**.

((2*S*)-2-((Fluorenylmethyloxycarbonyl)amino)-6-((trimethylammonium)trifluoroacetate)-5-hydroxyhexanoyl)glycine hydrotrifluoroacetate (Fmoc-Hyl(Me)$_3$-Gly-OH · TFA, 5)

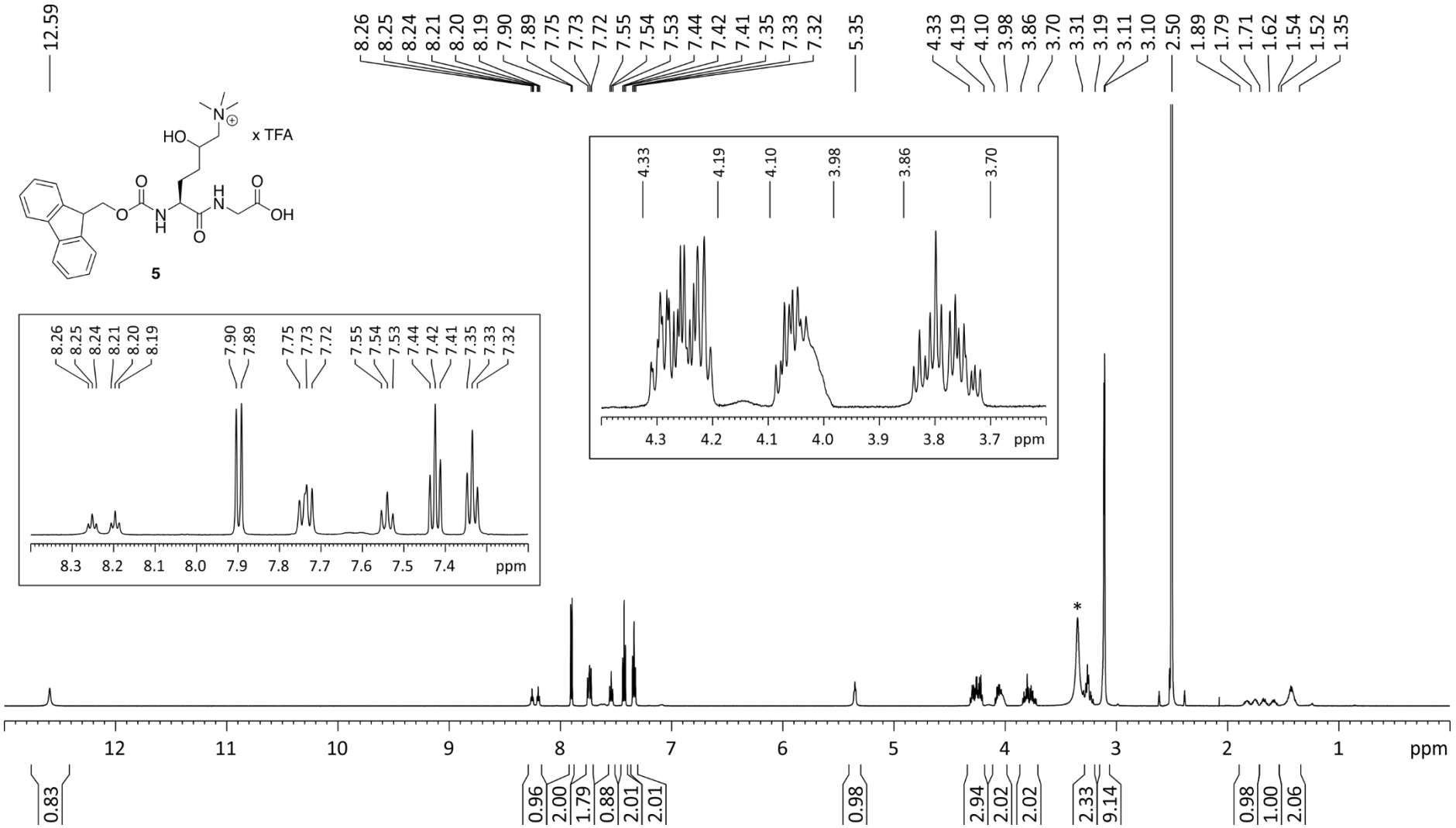

Figure S42: ^{1}H-NMR spectrum of Fmoc-Hyl(Me)$_3$-Gly-OH · TFA **5** (600 MHz, 300 K, DMSO-d_6). * Signal of H_2O.

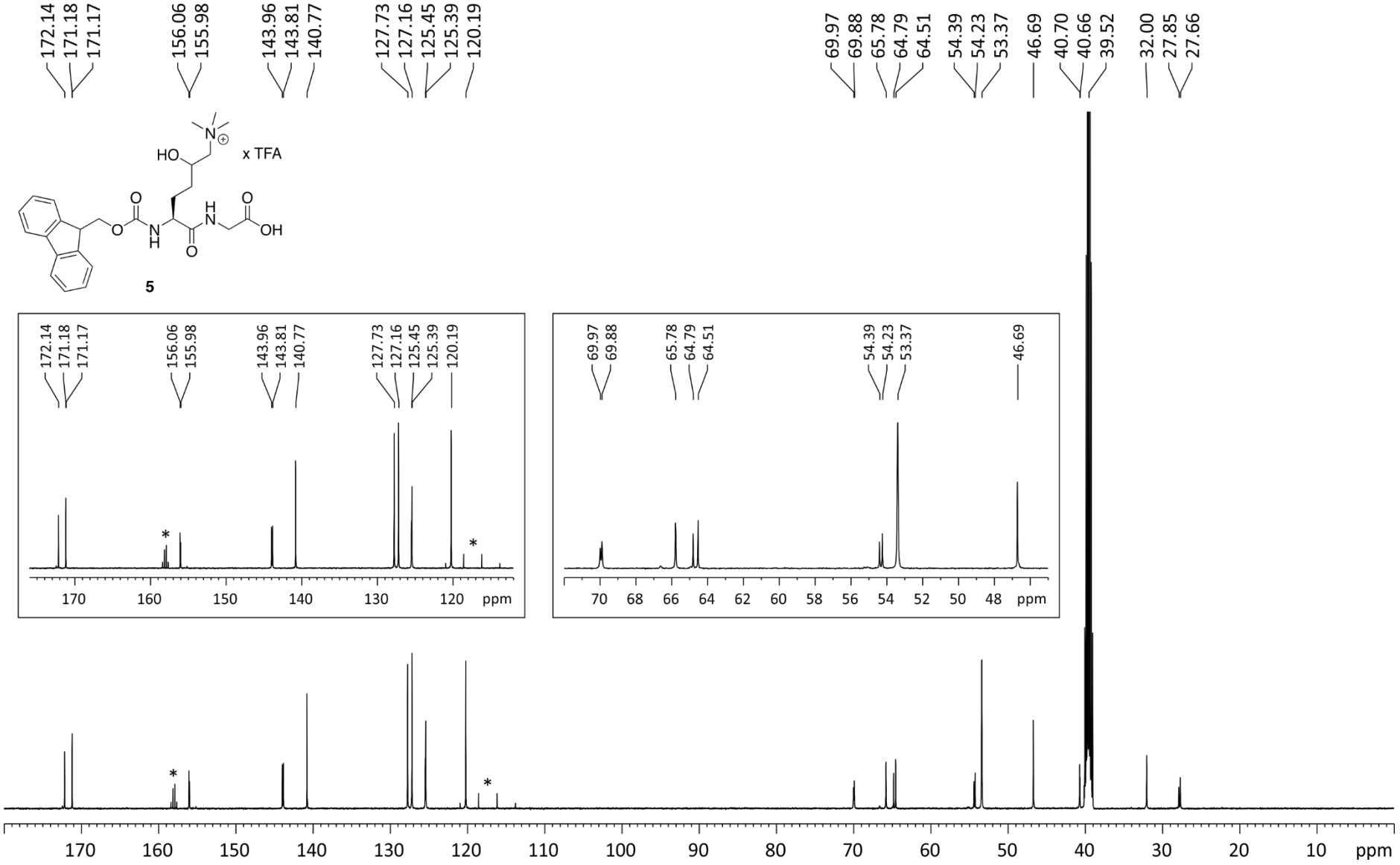

Figure S43: ^{13}C-NMR spectrum of Fmoc-Hyl(Me)$_3$-Gly-OH · TFA **5** (125 MHz, 300 K, DMSO-d_6). * Signals of TFA.

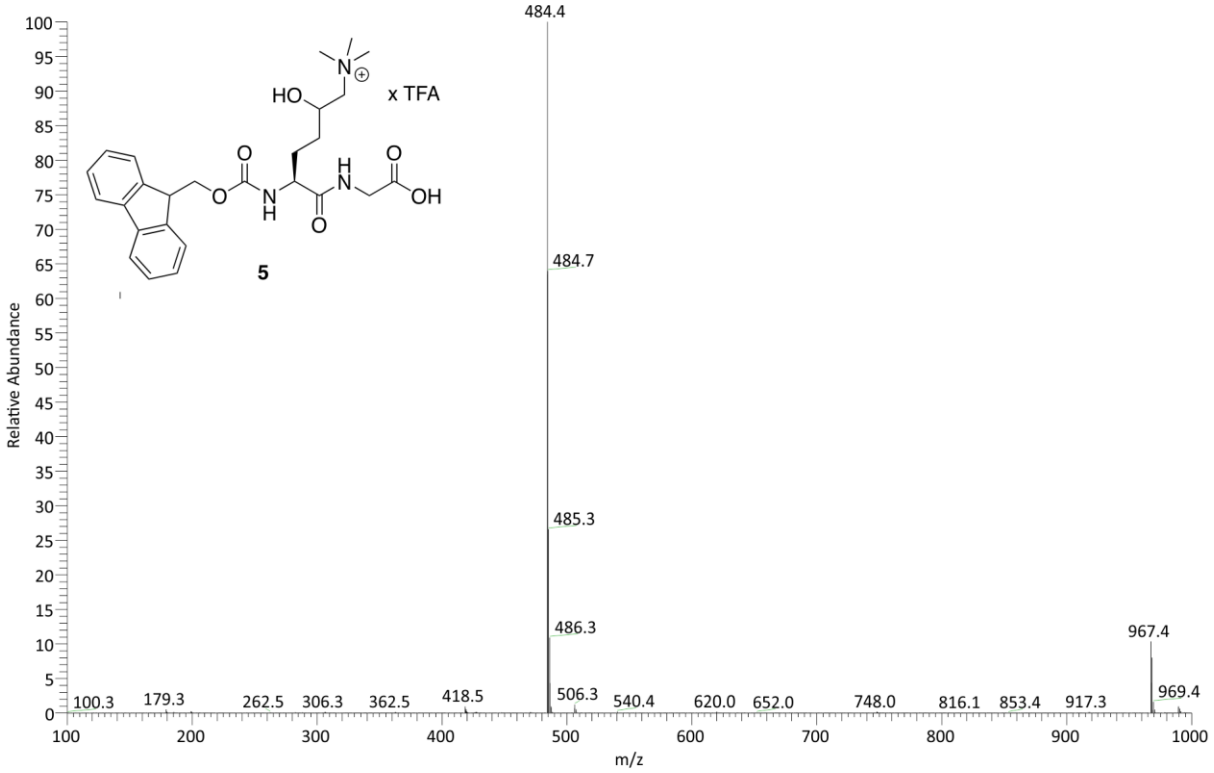

Figure S44: ESI+ mass spectrum with charge pattern m/z of Fmoc-Hyl(Me)$_3$-Gly-OH · TFA **5**.

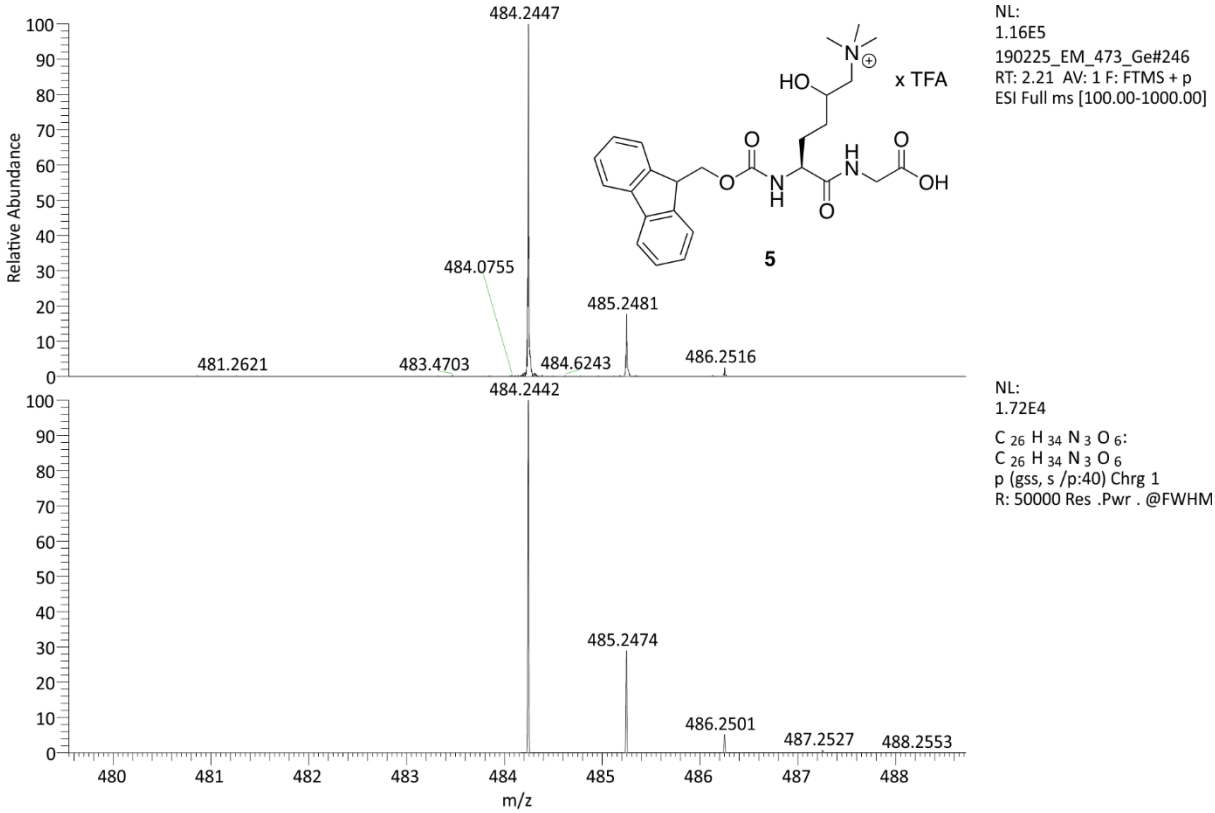

Figure S45: High resolution mass spectrum with isotope pattern of Fmoc-Hyl(Me)$_3$-Gly-OH · TFA **5**.

3-(*tert*-Butyldimethylsilyloxy)propylamine (S4)

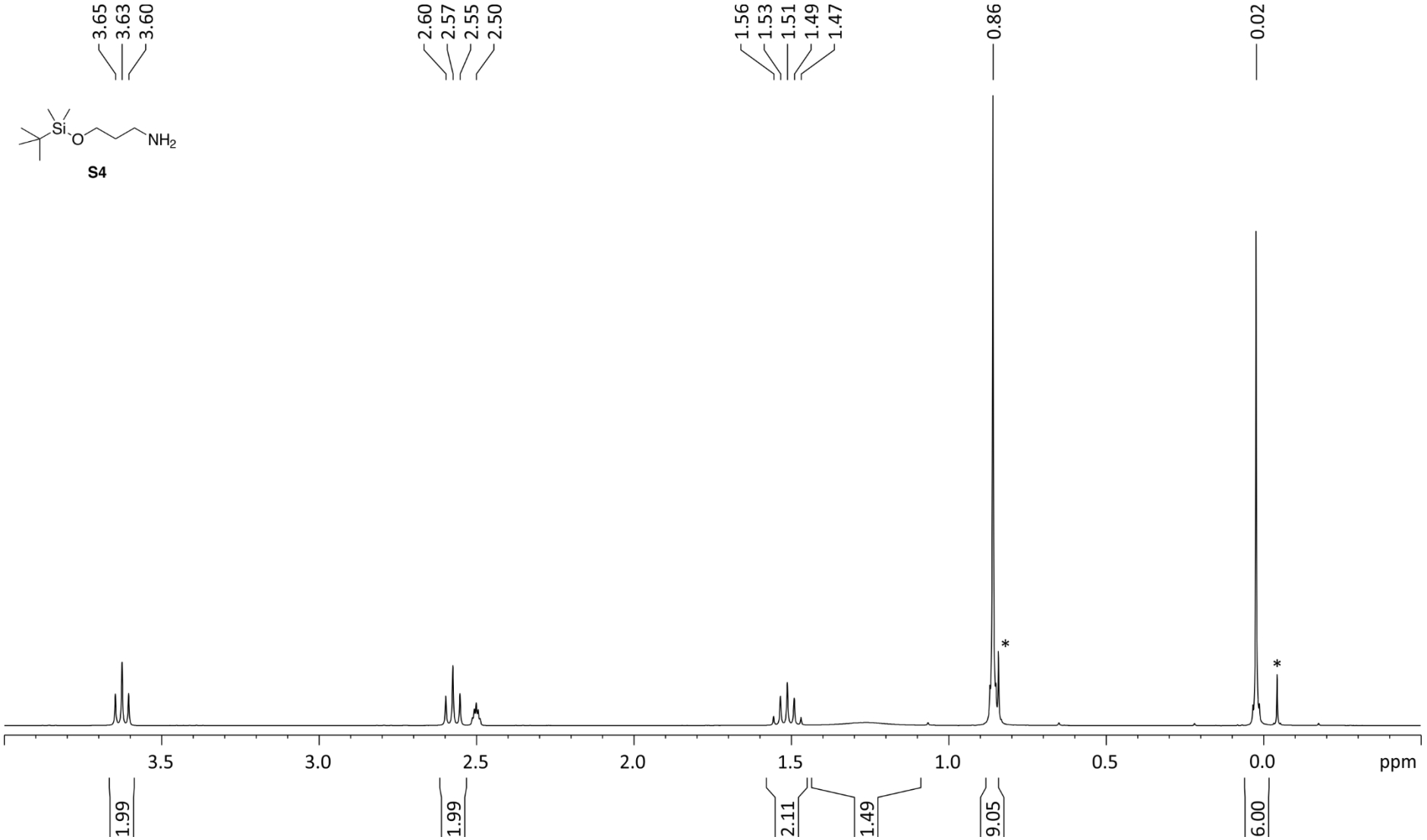

Figure S46: ^{1}H-NMR spectrum of 3-(*tert*-butyldimethylsilyloxy)propylamine **S4** (300 MHz, 300 K, DMSO-d_6). * Signals of TBDMS-OH.

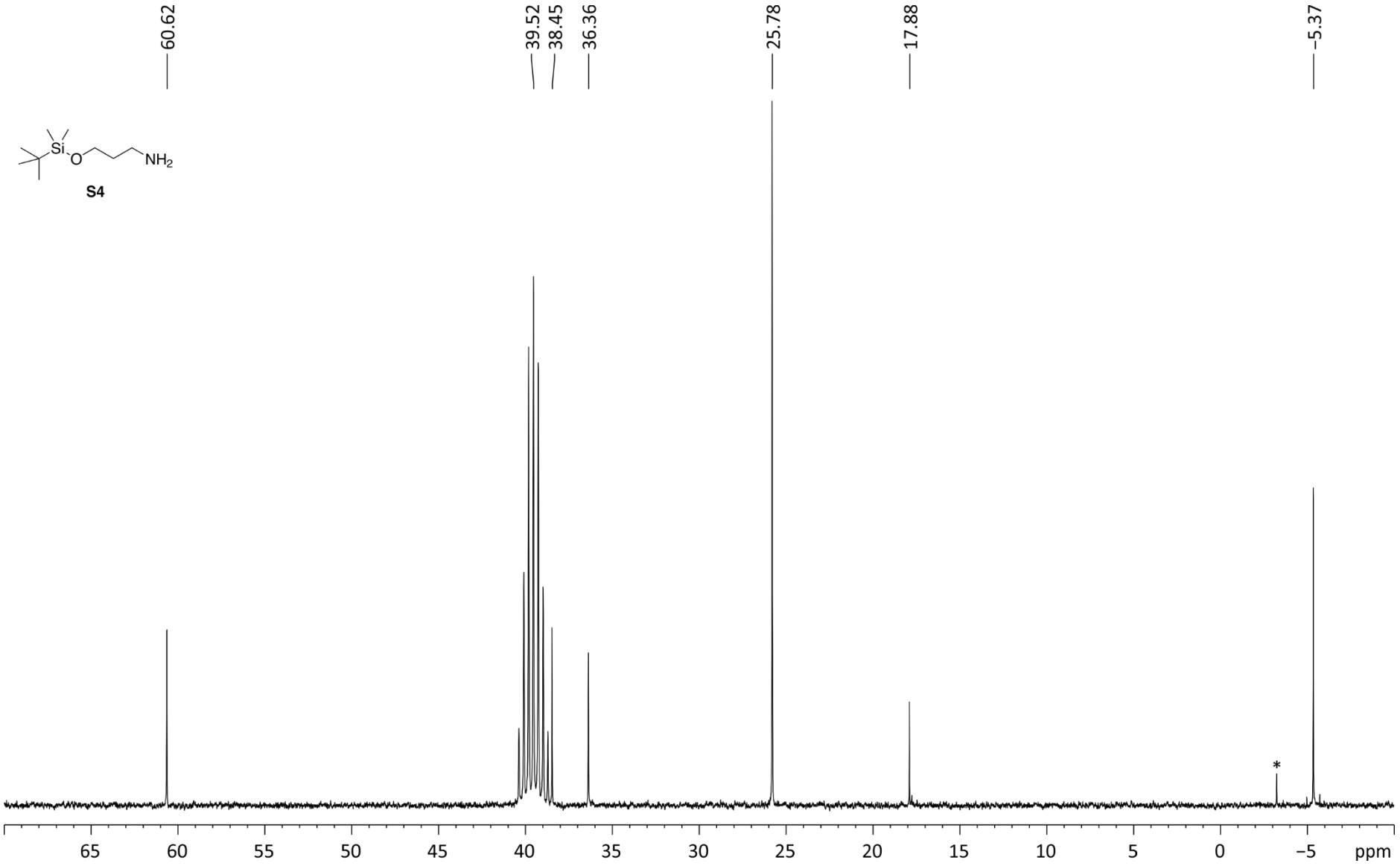

Figure S47: ^{13}C-NMR spectrum of 3-(*tert*-butyldimethylsilyloxy)propylamine **S4** (75 MHz, 300 K, DMSO-d_6). * Signal of TBDMS-OH.

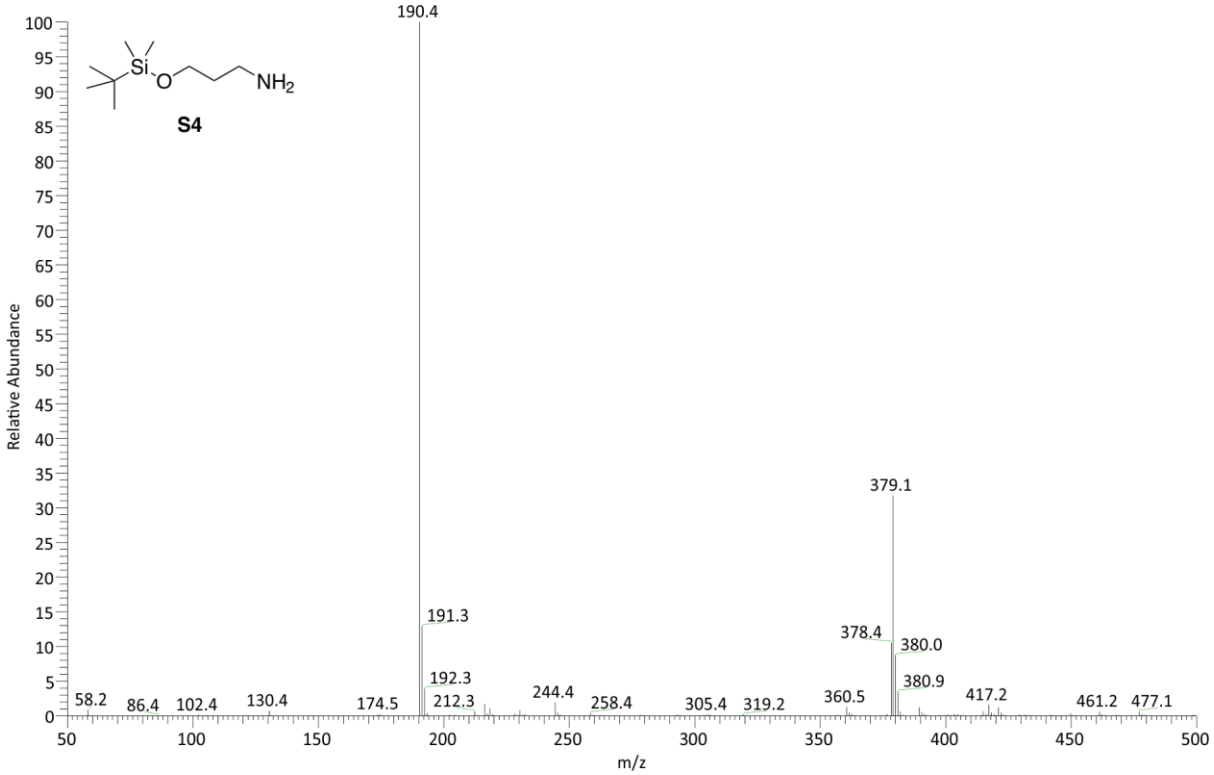

Figure S48: ESI+ mass spectrum with charge pattern m/z of 3-(*tert*-butyldimethylsilyloxy)propyl-amine **S4**.

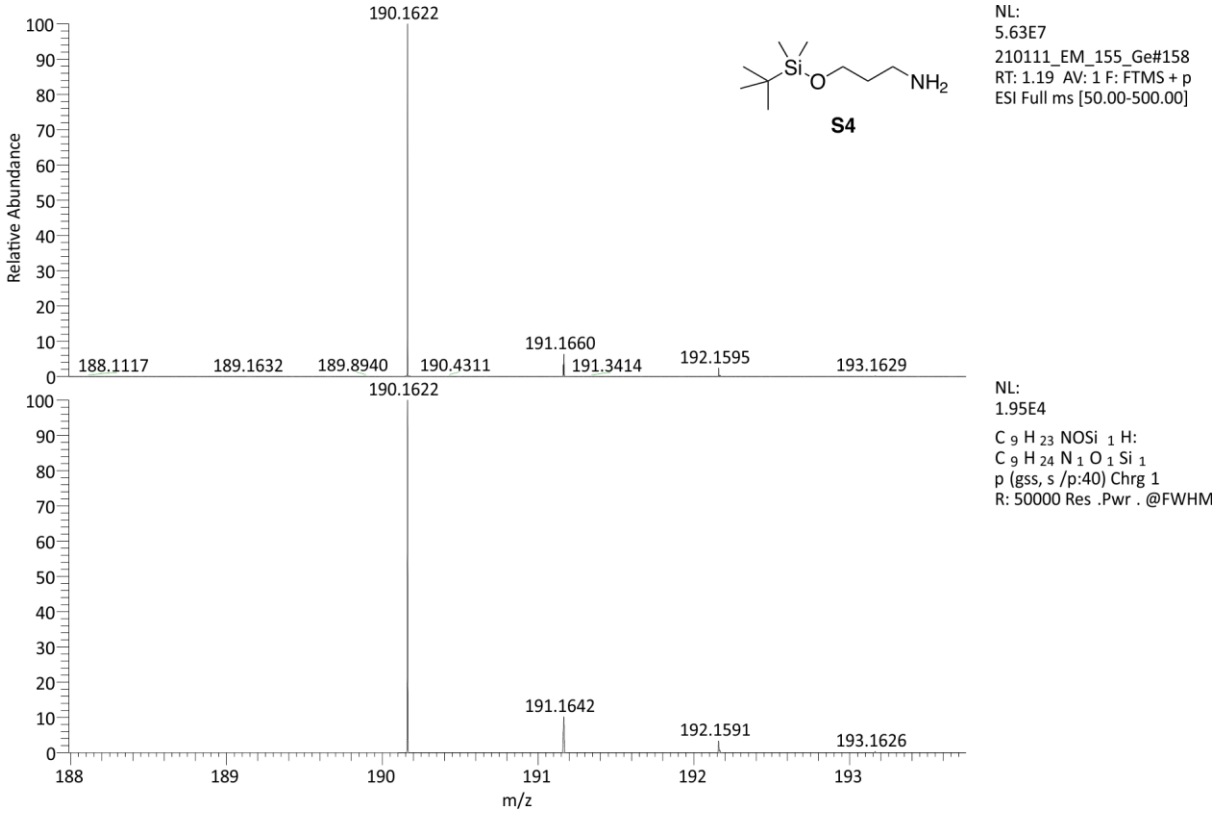

Figure S49: High resolution mass spectrum with isotope pattern of 3-(*tert*-butyldimethylsilyloxy) propylamine **S4**.

_N_-(3-(_tert_-butyldimethylsilyloxy)propyl)-2-nitrobenzenesulfonamide (S5)

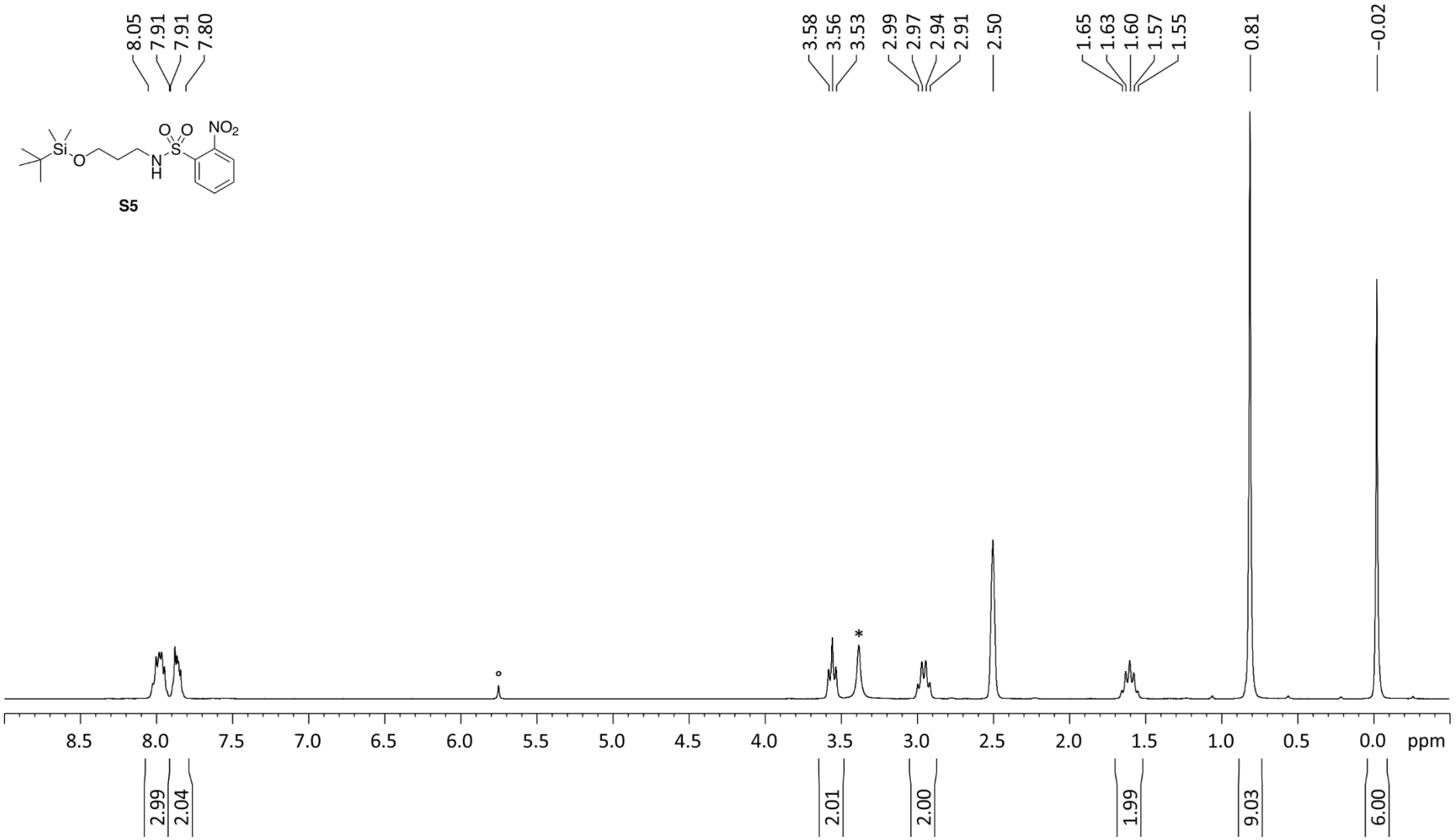

Figure S50: ^{1}H-NMR spectrum of *N*-(3-(*tert*-butyldimethylsilyloxy)propyl)-2-nitrobenzenesulfon-amide **S5** (250 MHz, 300 K, DMSO-d_6). * Signal of H_2O. ° Signal of CH_2Cl_2.

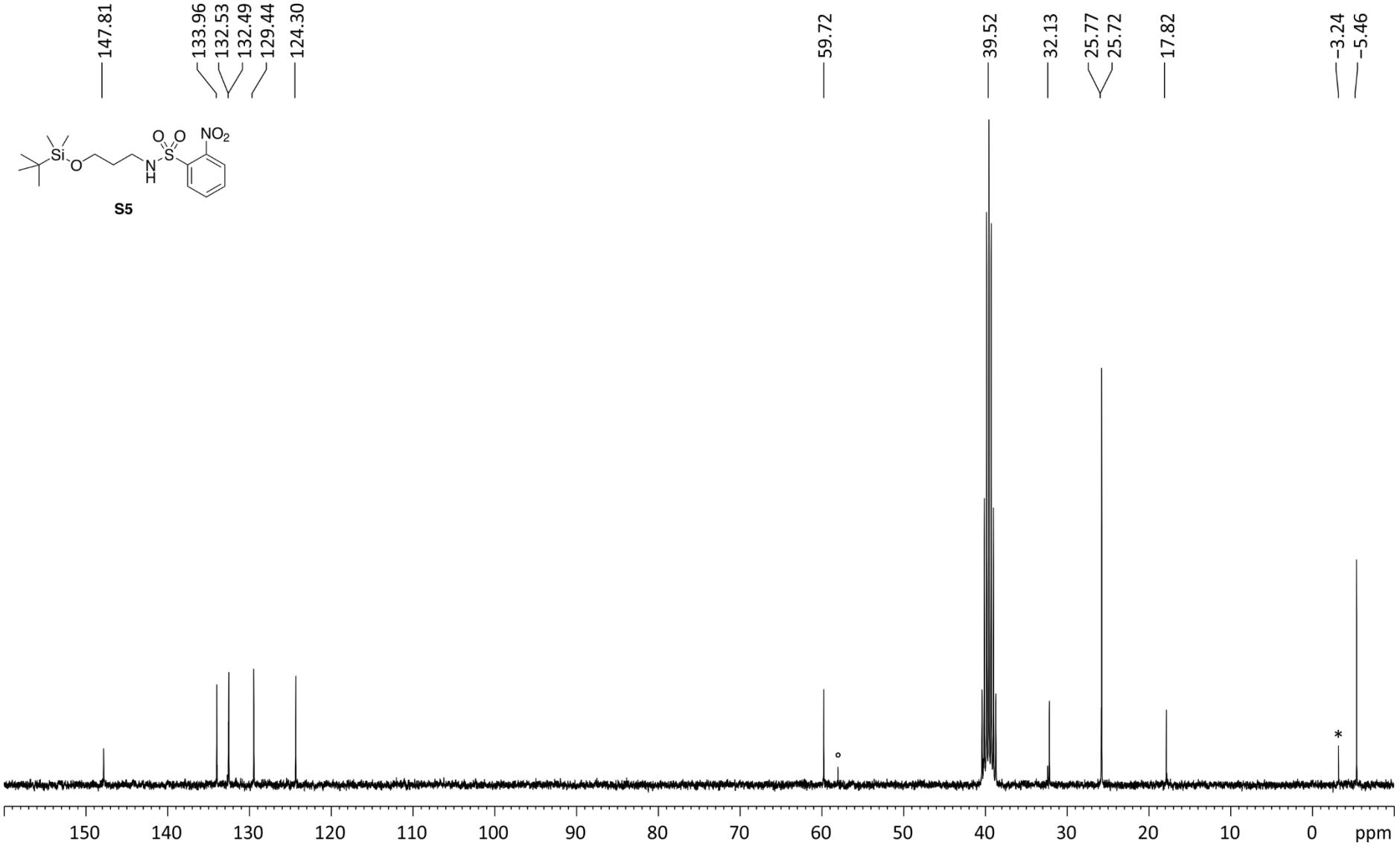

Figure S51: ^{13}C-NMR spectrum of *N*-(3-(*tert*-butyldimethylsilyloxy)propyl)-2-nitrobenzenesulfon-amide **S5** (75 MHz, 300 K, DMSO-d_6). ° Signal of CH_2Cl_2. * Signal of TBDMS-OH

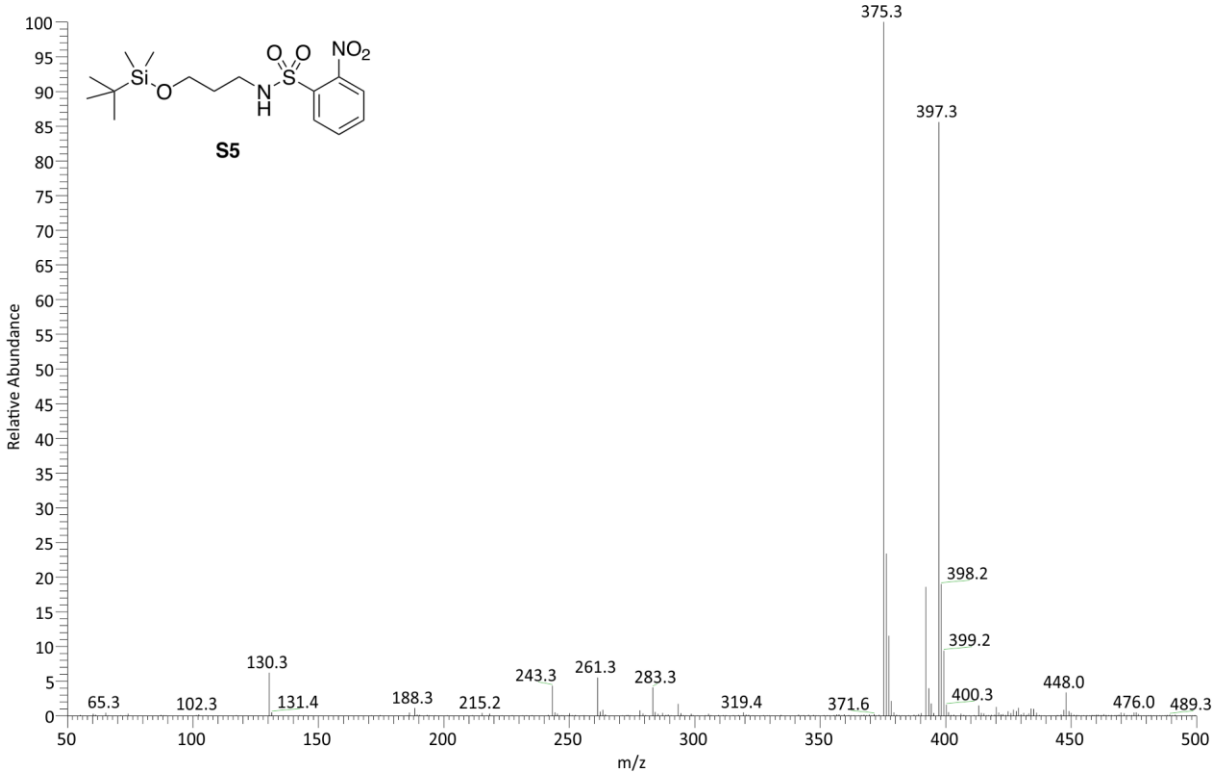

Figure S53: ESI+ mass spectrum with charge pattern m/z of *N*-(3-(*tert*-butyldimethylsilyloxy) propyl)-2-nitrobenzenesulfonamide **S5**.

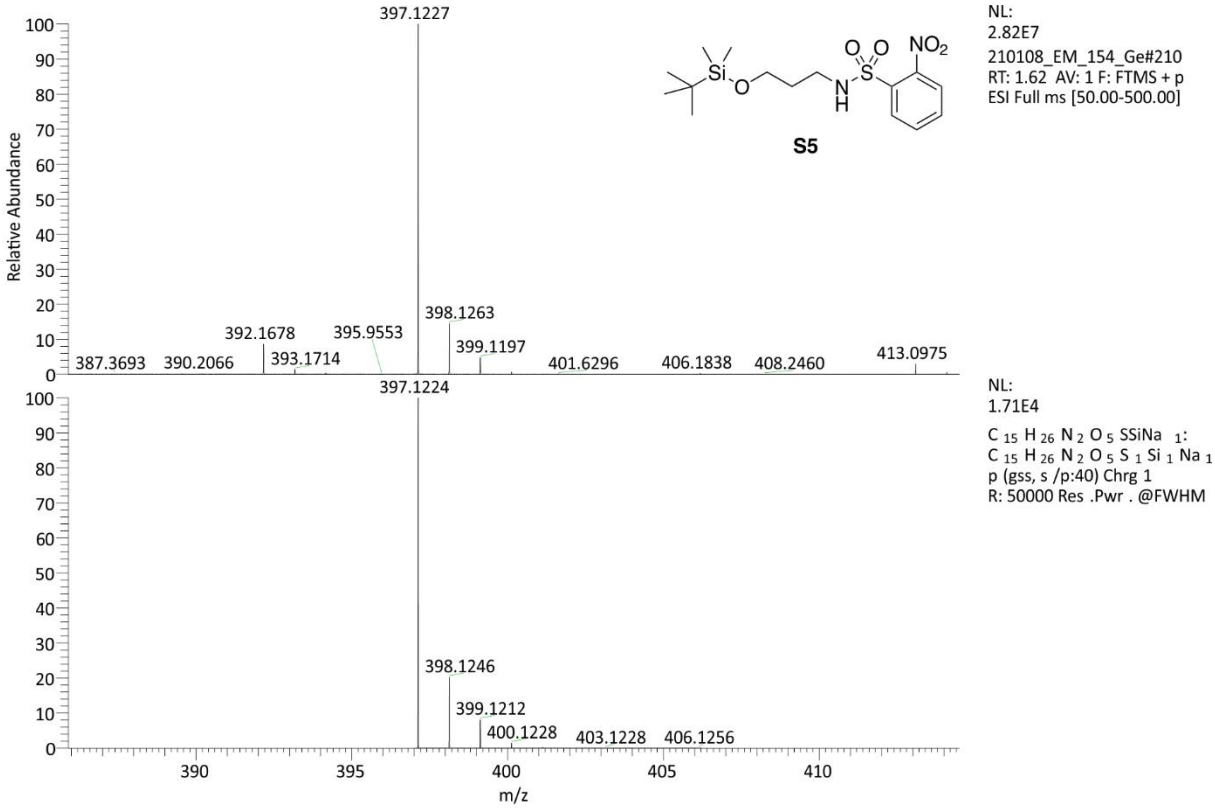

Figure S54: High resolution mass spectrum with isotope pattern of *N*-(3-(*tert*-butyldimethyl-silyloxy)propyl)-2-nitrobenzenesulfonamide **S5**.

***N*-(3-(*tert*-butyldimethylsilyloxy)propyl)-*N*-(3-(dimethylamino)propyl)-2-nitrobenzenesulfonamide (S6)**

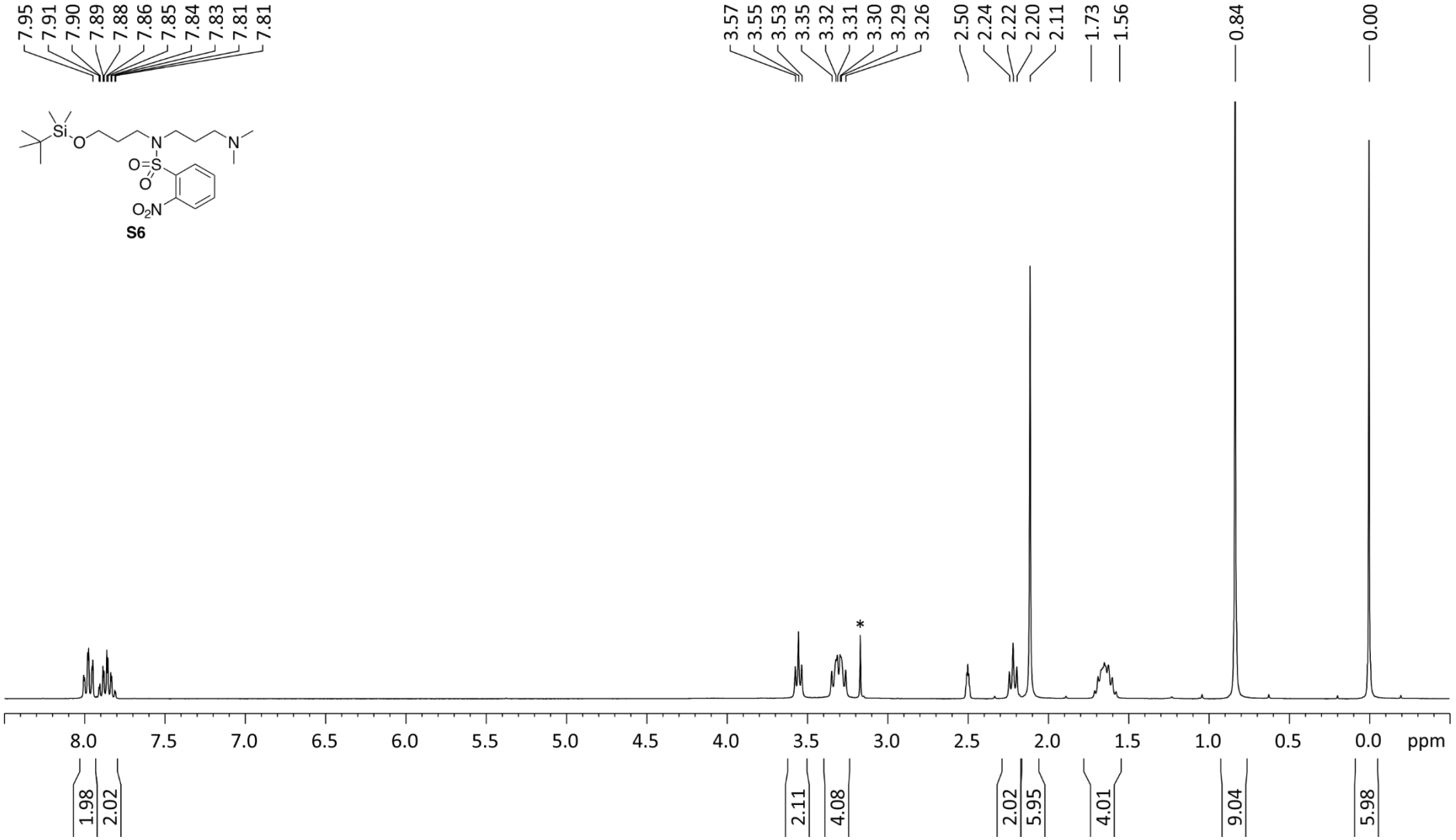

Figure S55: ^{1}H-NMR spectrum of *N*-(3-(*tert*-butyldimethylsilyloxy)propyl)-*N*-(3-(dimethylamino)propyl)-2-nitrobenzenesulfonamide **S6** (300 MHz, 300 K, DMSO-d_6). * Signal of H_2O.

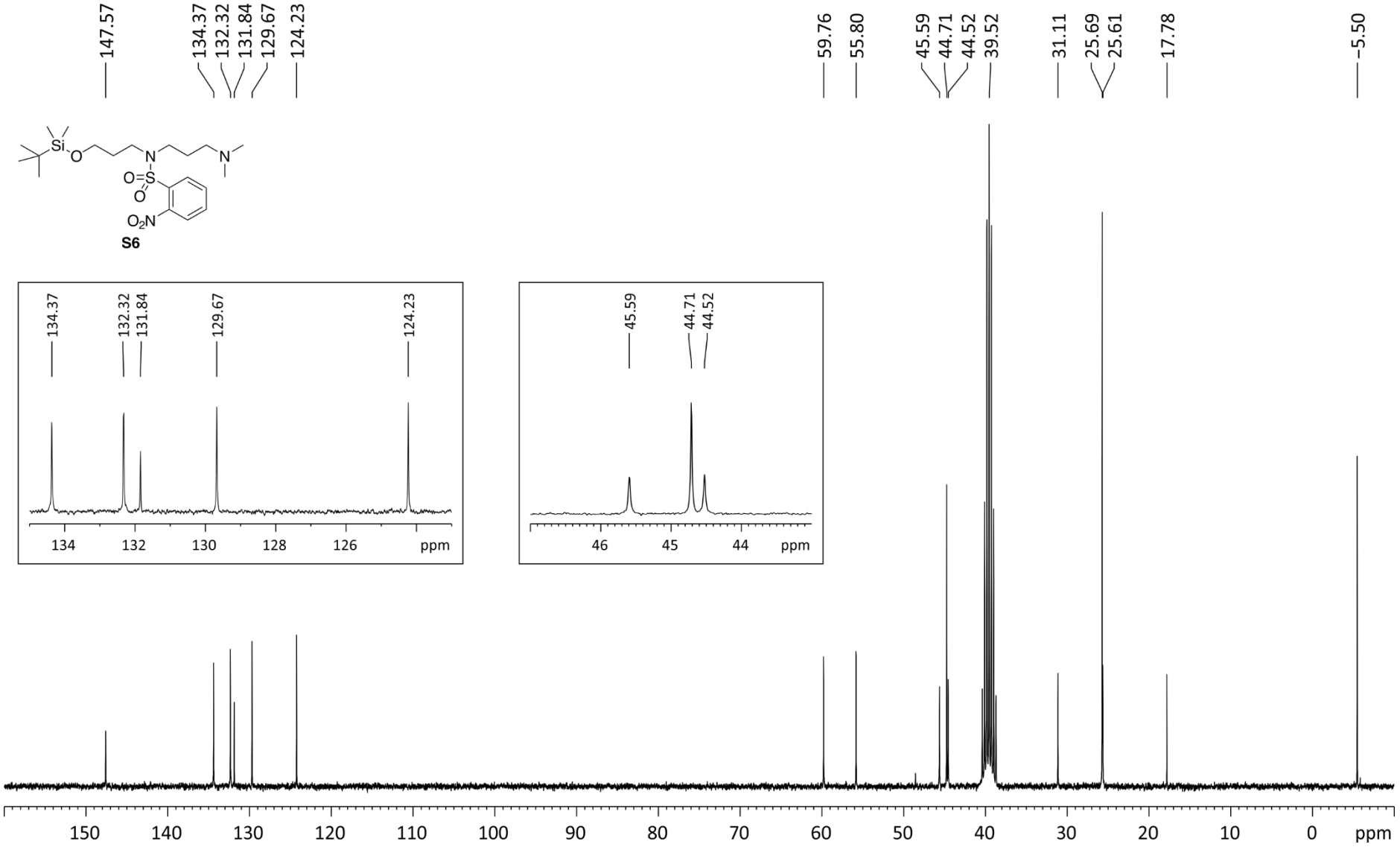

Figure S56: ^{13}C-NMR spectrum of *N*-(3-(*tert*-butyldimethylsilyloxy)propyl)-*N*-(3-(dimethylamino)propyl)-2-nitrobenzenesulfonamide **S6** (75 MHz, 300 K, DMSO-d_6).

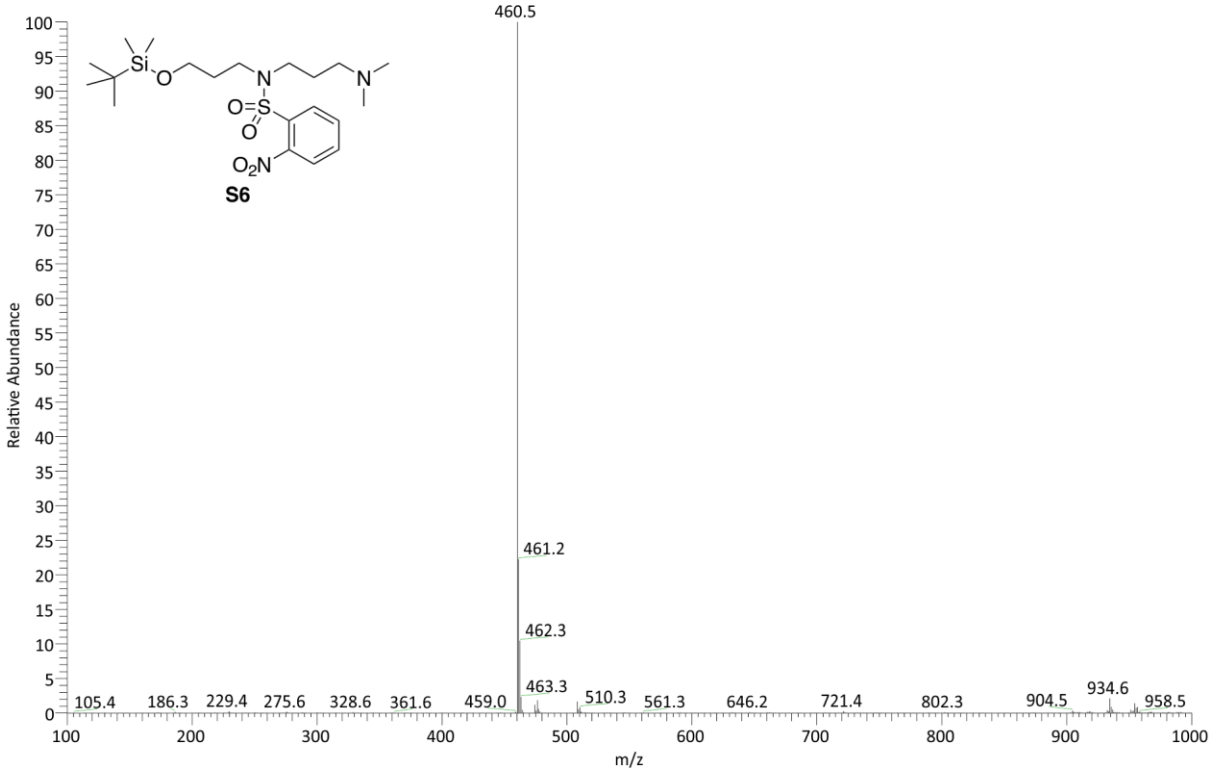

Figure S57: ESI+ mass spectrum with charge pattern m/z of *N*-(3-(*tert*-butyldimethylsilyloxy) propyl)-*N*-(3-(dimethylamino)propyl)-2-nitrobenzenesulfonamide **S6**.

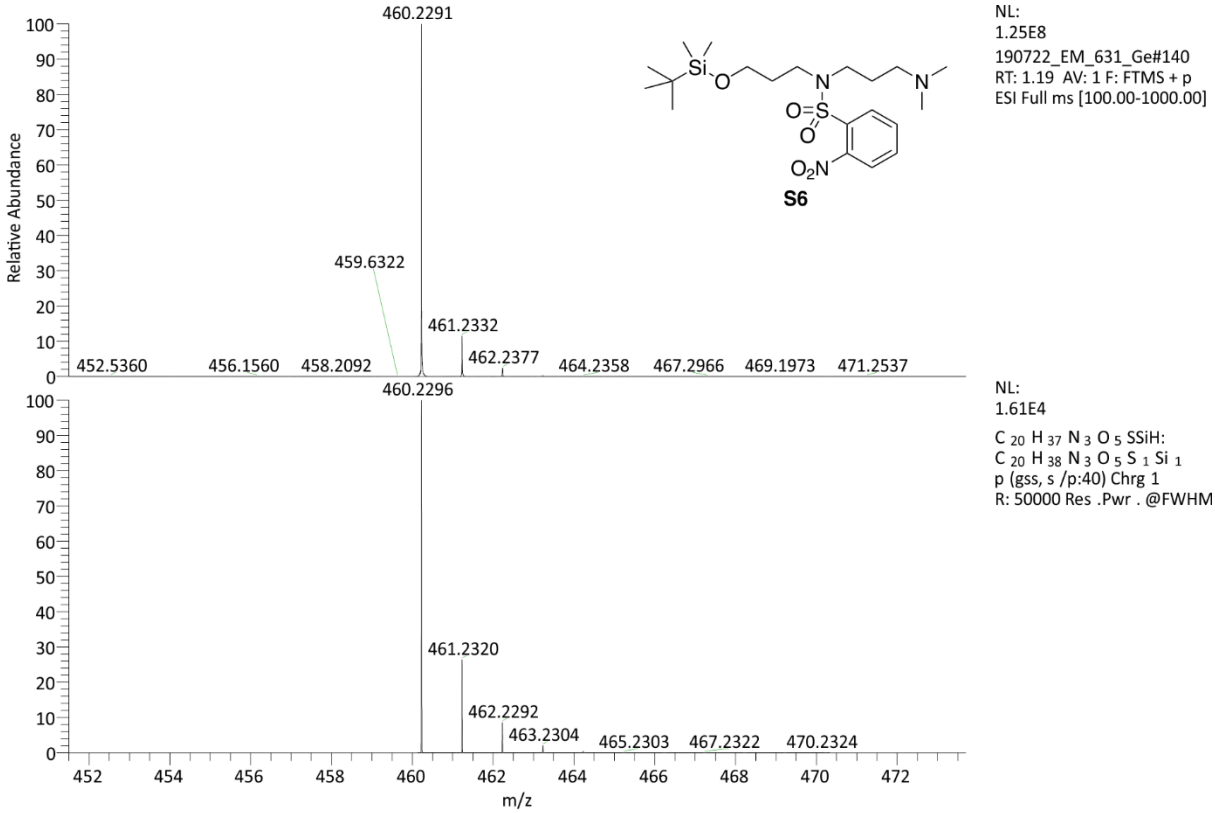

Figure S58: High resolution mass spectrum with isotope pattern of *N*-(3-(*tert*-butyldimethyl-silyloxy)propyl)-*N*-(3-(dimethylamino)propyl)-2-nitrobenzenesulfonamide **S6**.

_N_-(3-(dimethylamino)propyl)-_N_-(3-hydroxypropyl)-2-nitrobenzenesulfonamide (6)

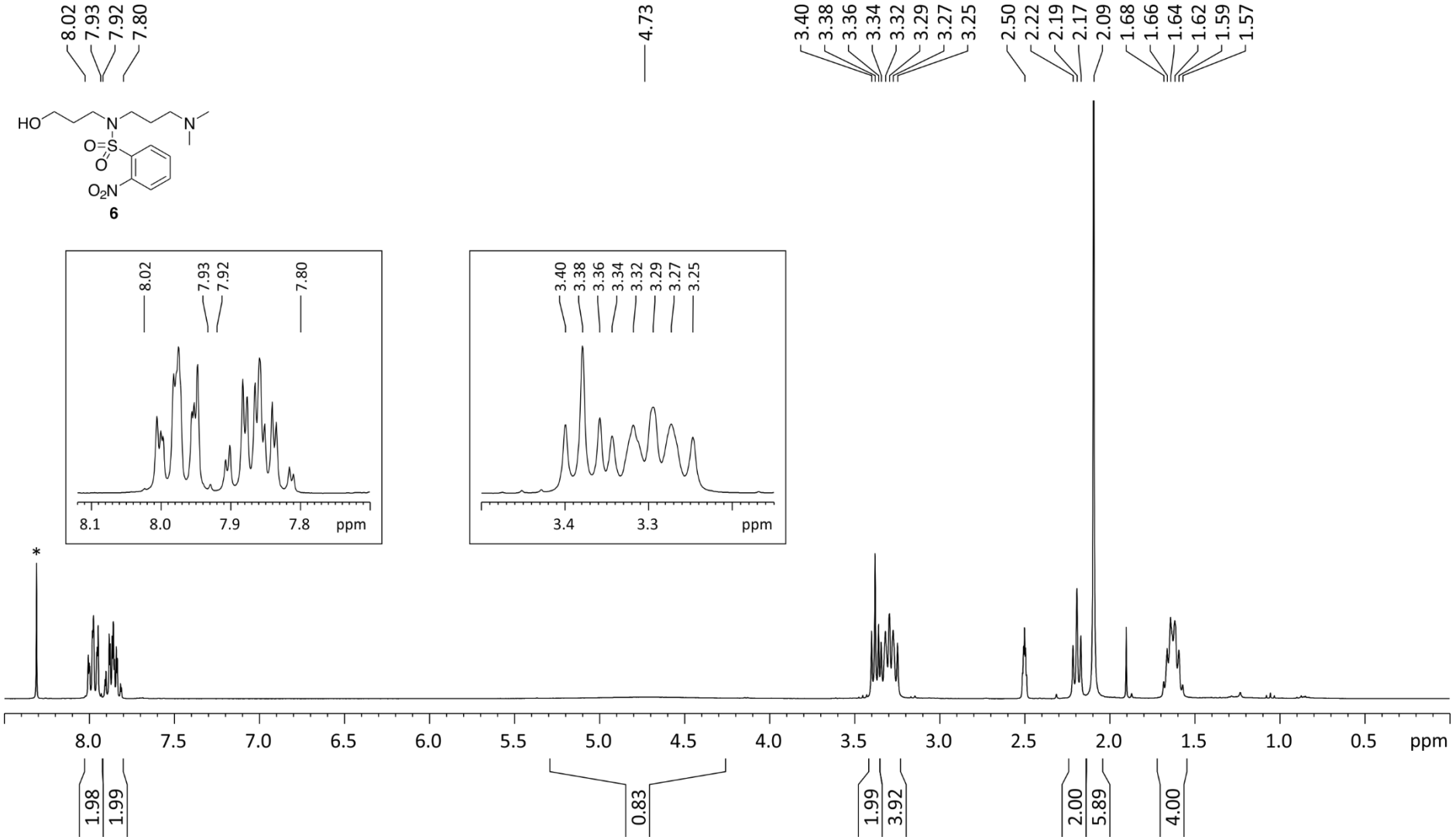

Figure S59: ^{1}H-NMR spectrum of *N*-(3-(dimethylamino)propyl)-*N*-(3-hydroxypropyl)-2-nitrobenzenesulfonamide **6** (300 MHz, 300 K, DMSO-d_6). * Signal of $CHCl_3$.

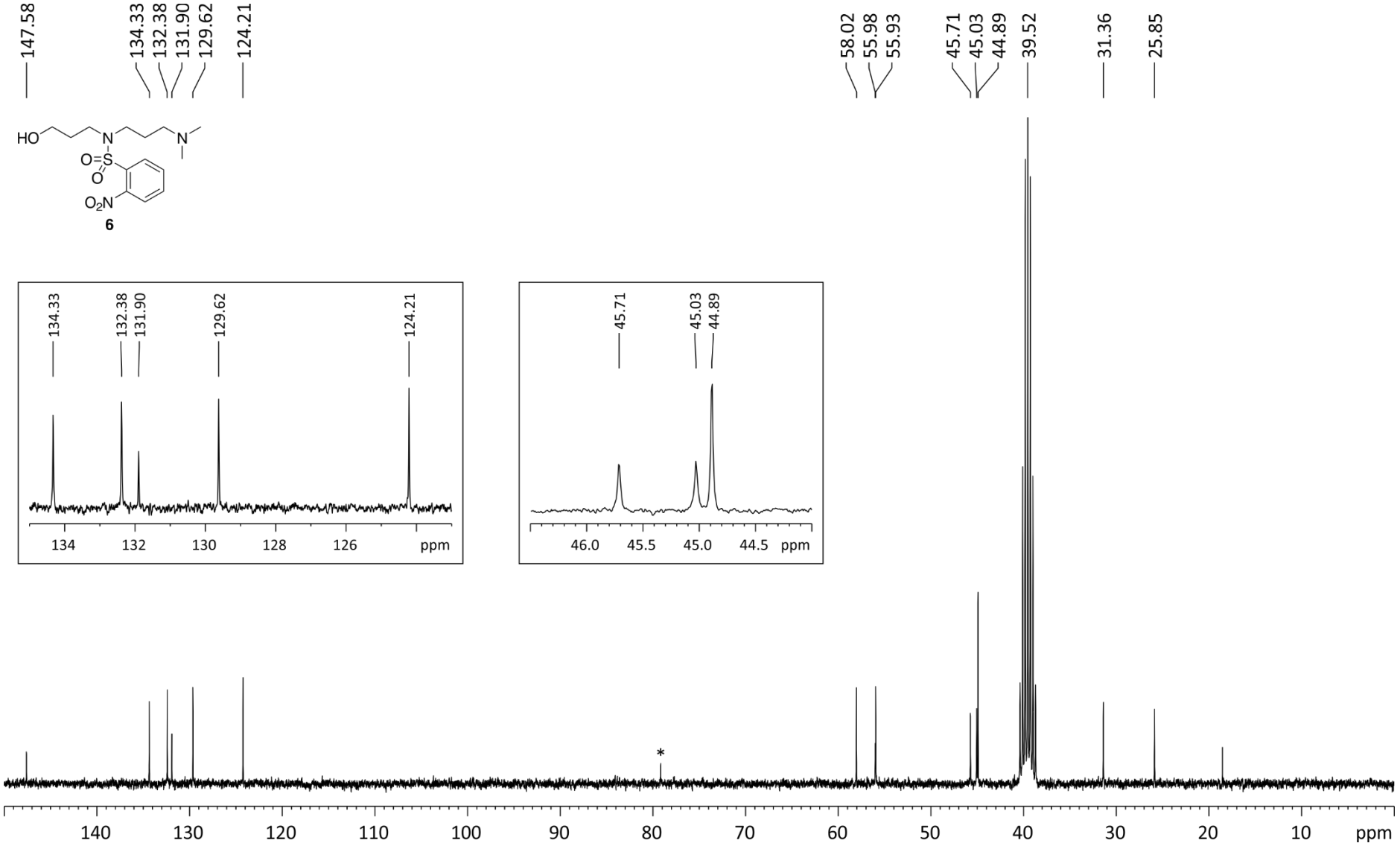

Figure S60: ^{13}C-NMR spectrum of *N*-(3-(dimethylamino)propyl)-*N*-(3-hydroxypropyl)-2-nitrobenzenesulfonamide **6** (75 MHz, 300 K, DMSO-d_6). * Signal of $CHCl_3$.

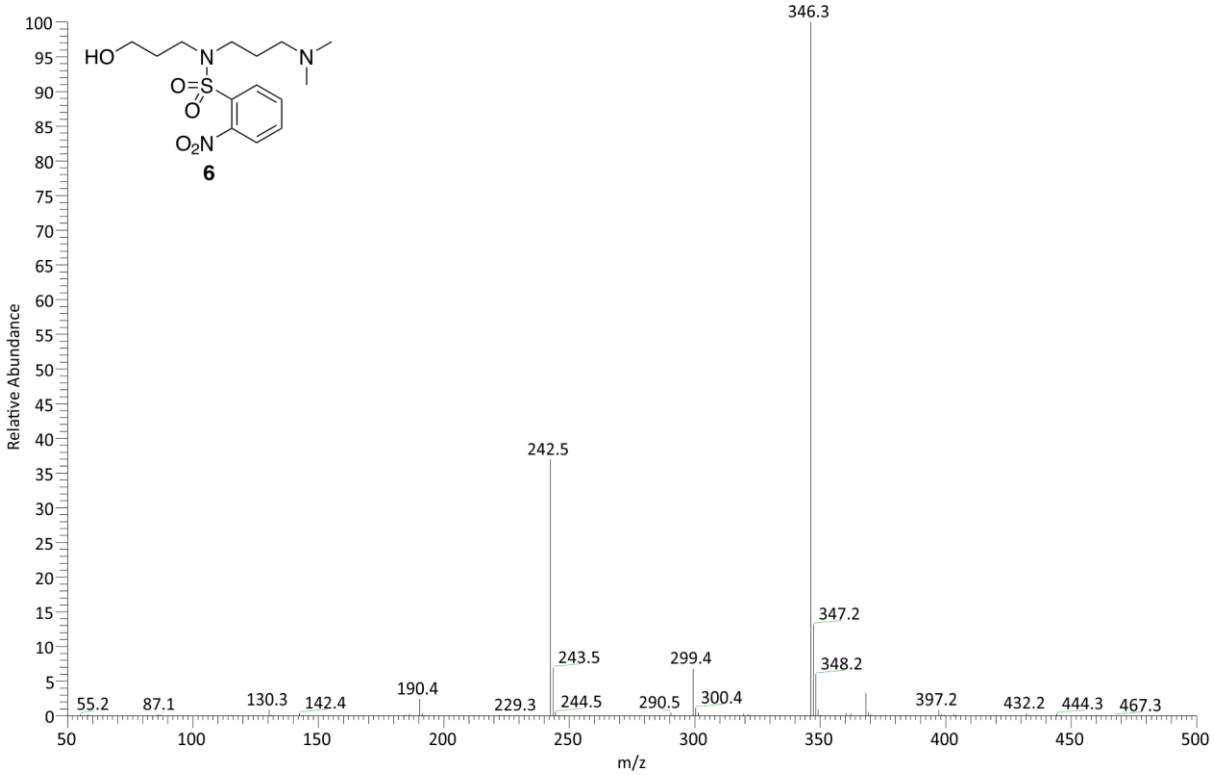

Figure S61: ESI+ mass spectrum with charge pattern m/z of *N*-(3-(dimethylamino)propyl)-*N*-(3-hydroxypropyl)-2-nitrobenzenesulfonamide **6**.

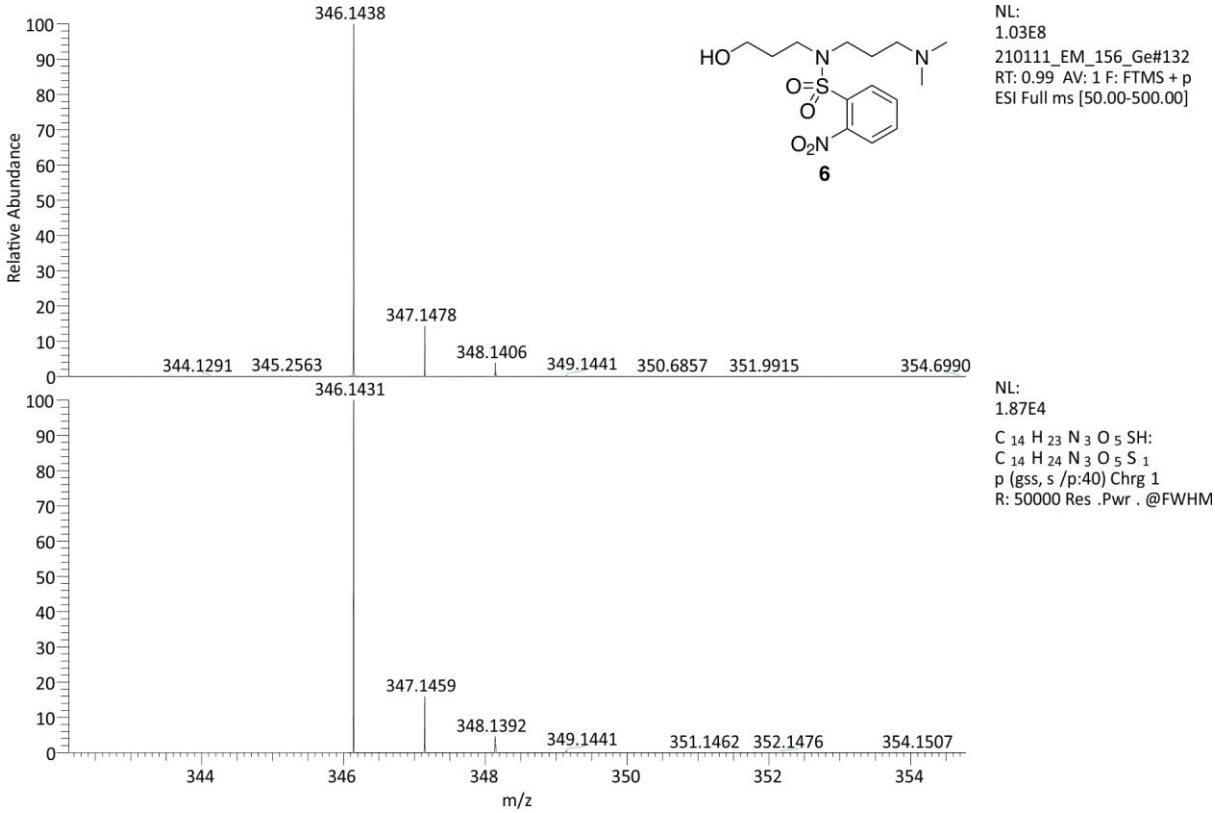

Figure S62: High resolution mass spectrum with isotope pattern of *N*-(3-(dimethylamino)propyl)-*N*-(3-hydroxypropyl)-2-nitrobenzenesulfonamide **6**.

***tert*-Butyl-(2*S*)-2-[(*tert*-butoxycarbonyl)amino]-6-[(benzyloxycarbonyl)amino]hexanoate (Boc-Lys(Cbz)-O^{t}Bu, S7)**

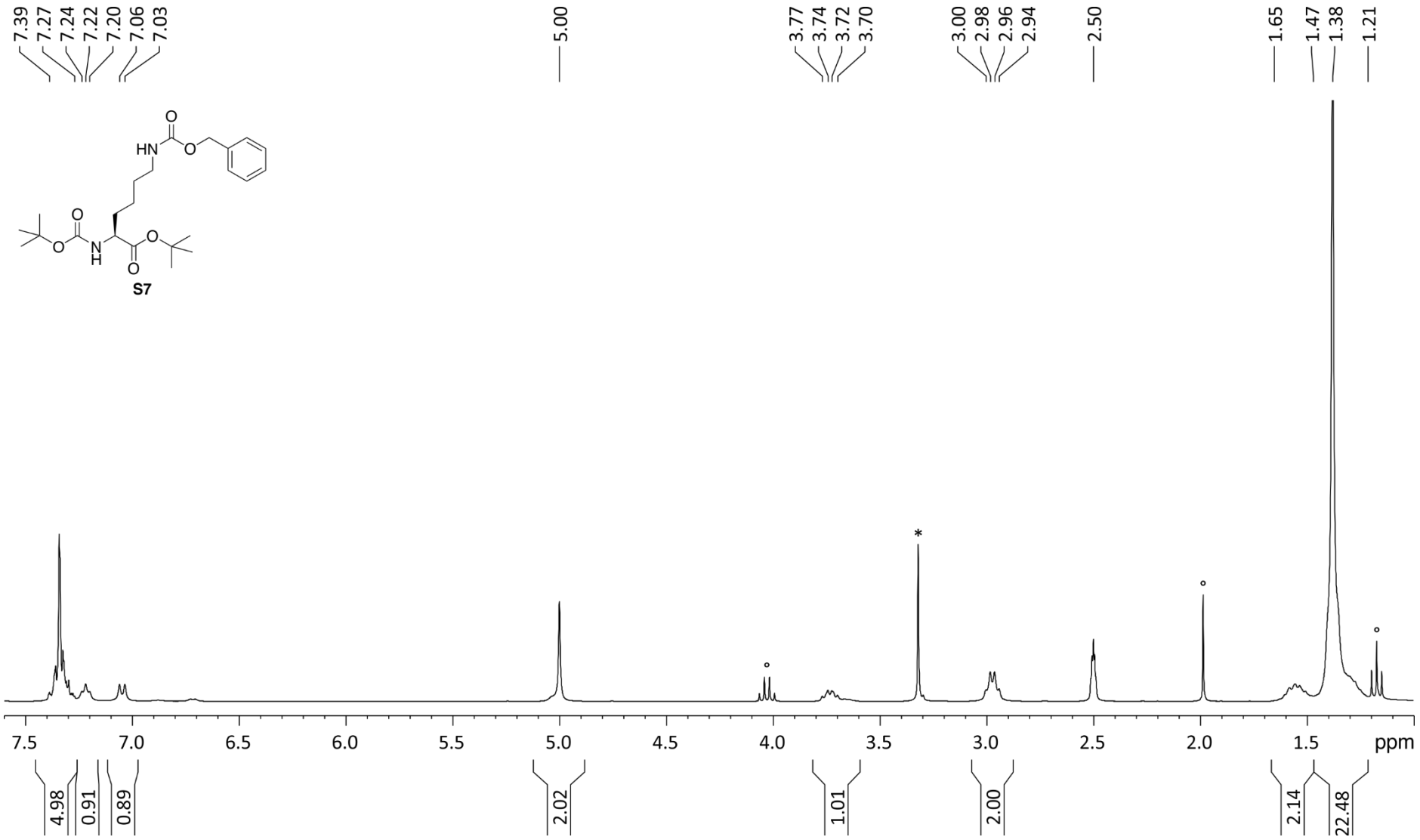

Figure S63: ^{1}H-NMR spectrum of Boc-Lys(Cbz)-O^{t}Bu **S7** (300 MHz, 300 K, DMSO-d_6). * Signal of H_2O. ° Signals of EtOAc.

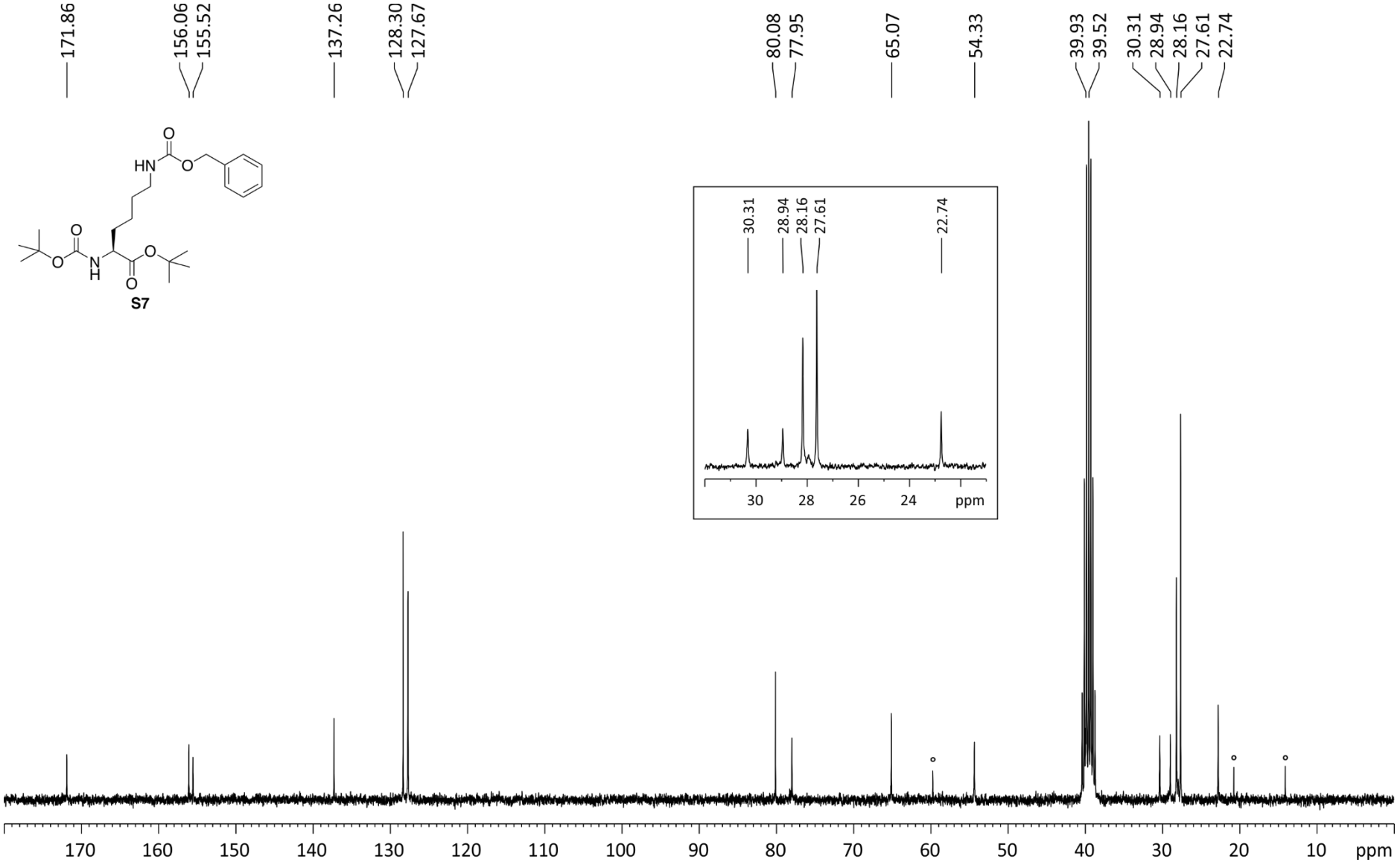

Figure S64: ^{13}C-NMR spectrum of Boc-Lys(Cbz)-O^{t}Bu **S7** (75 MHz, 300 K, DMSO-d_6). ° Solvent signals of EtOAc.

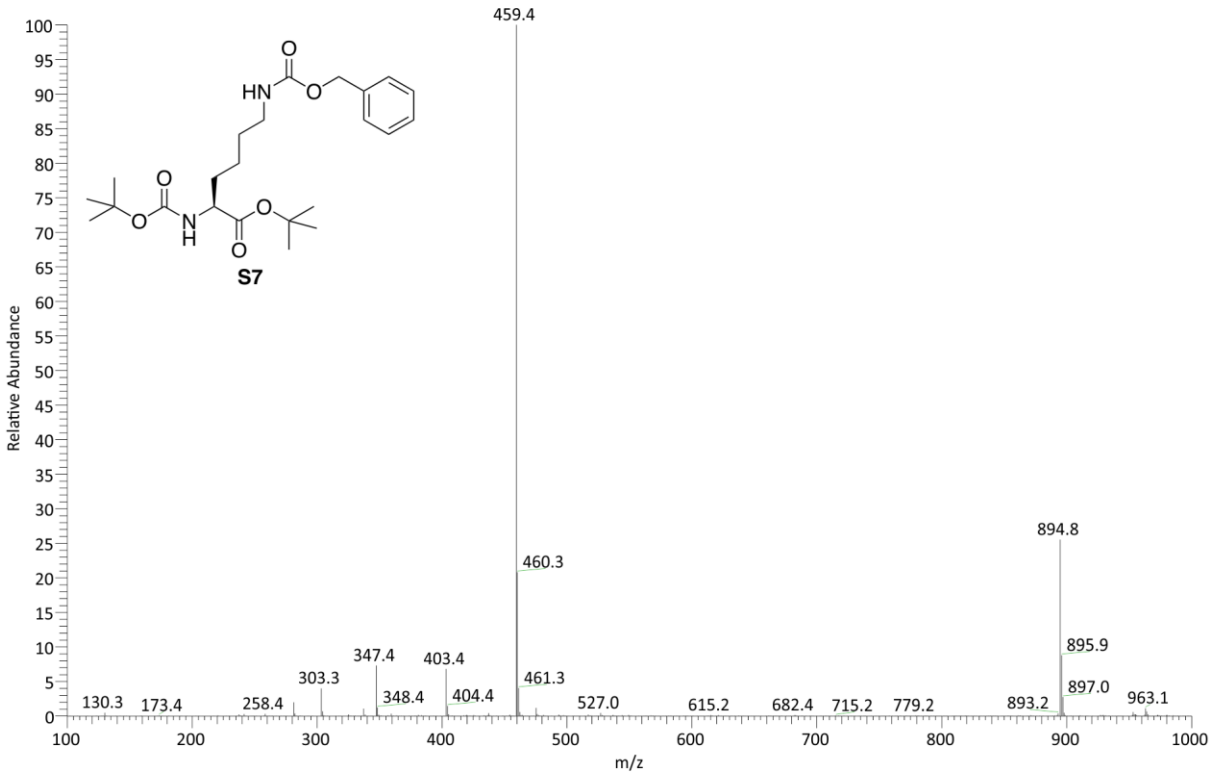

Figure S65: ESI+ mass spectrum with charge pattern m/z of Boc-Lys(Cbz)-O^{t}Bu **S7**.

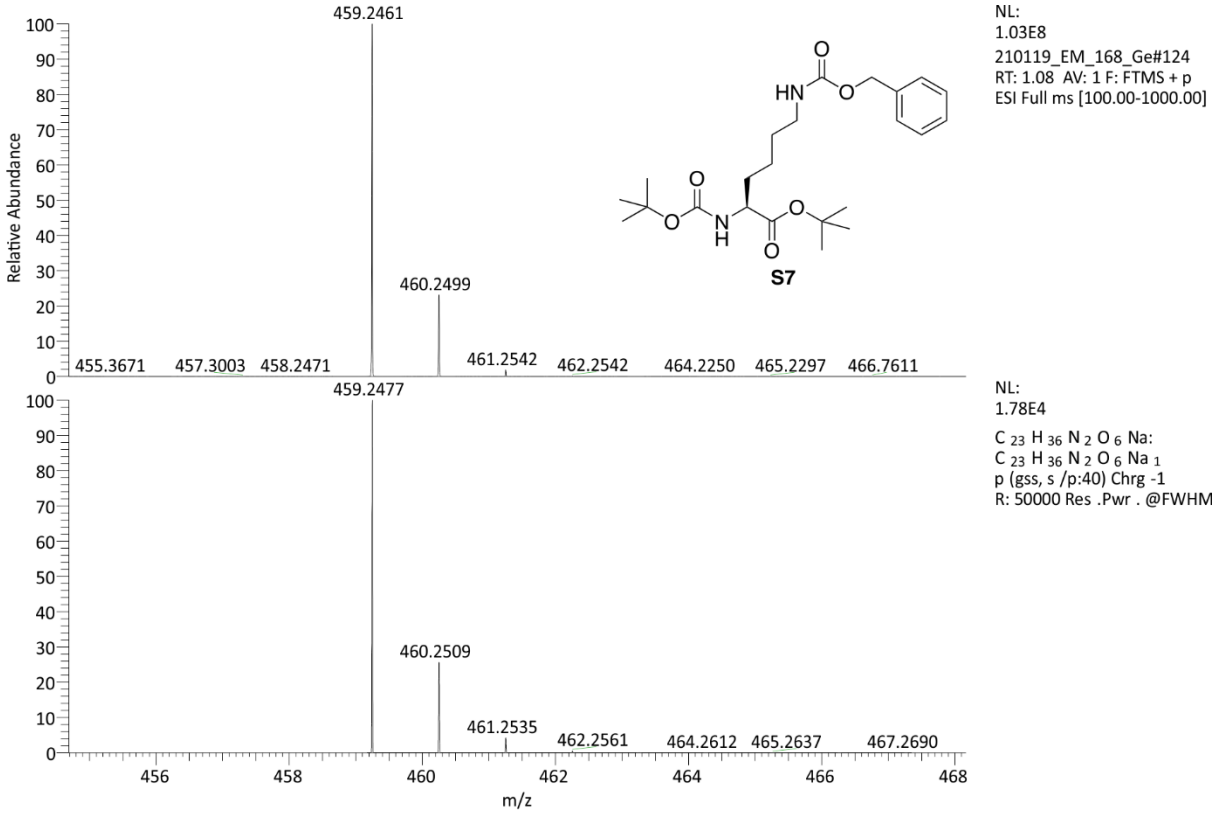

Figure S66: High resolution mass spectrum with isotope pattern of Boc-Lys(Cbz)-O^{t}Bu **S7**.

***tert*-Butyl-(2*S*)-2-[(*tert*-butoxycarbonyl)amino]-6-amino-hexanoate hydrochloride (Boc-Lys-O^{t}Bu · HCl, S8)**

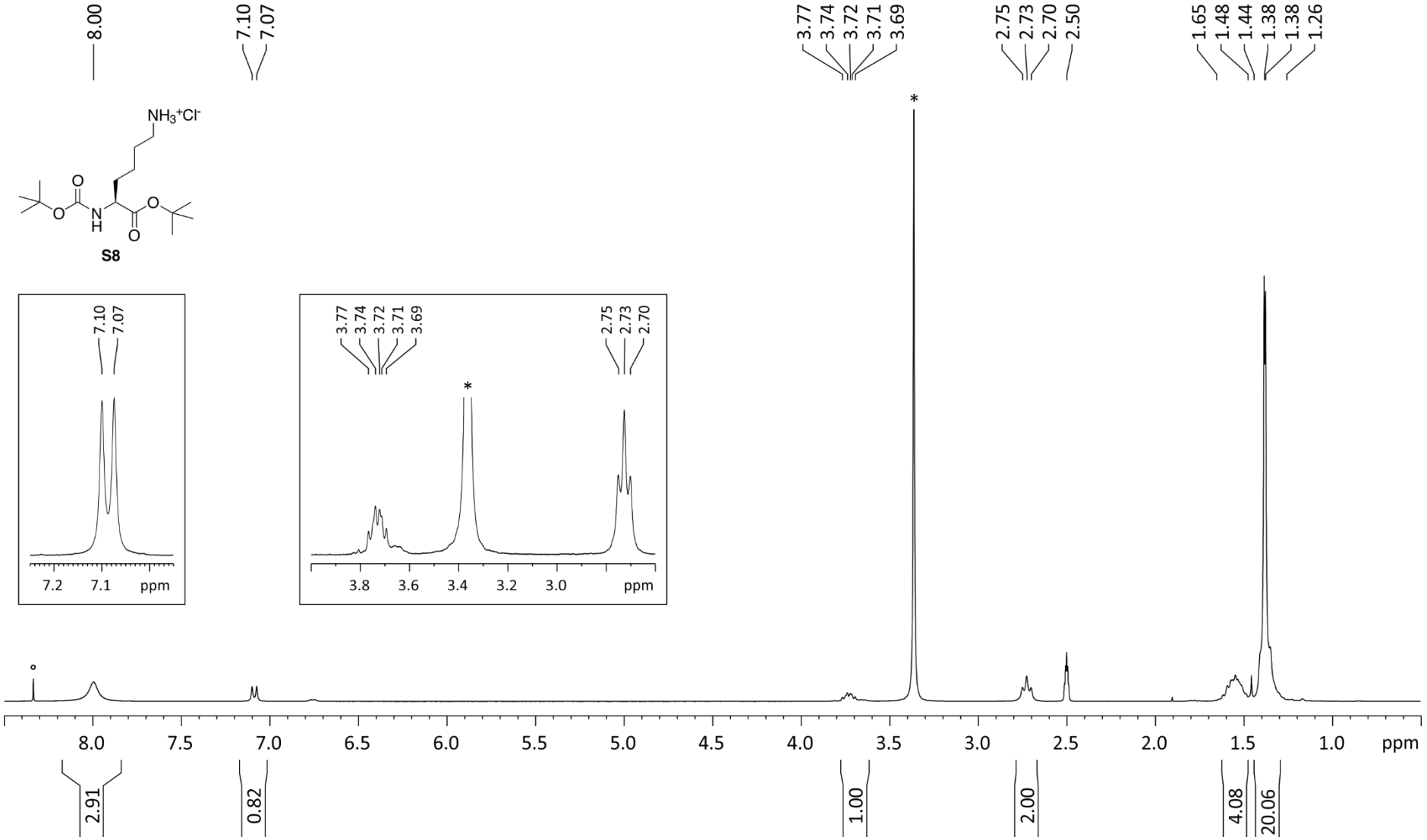

Figure S67: ^{1}H-NMR spectrum of Boc-Lys-O^{t}Bu · HCl **S8** (300 MHz, 300 K, DMSO-d_6). * Signal of H_2O. ° Signal of $CHCl_3$.

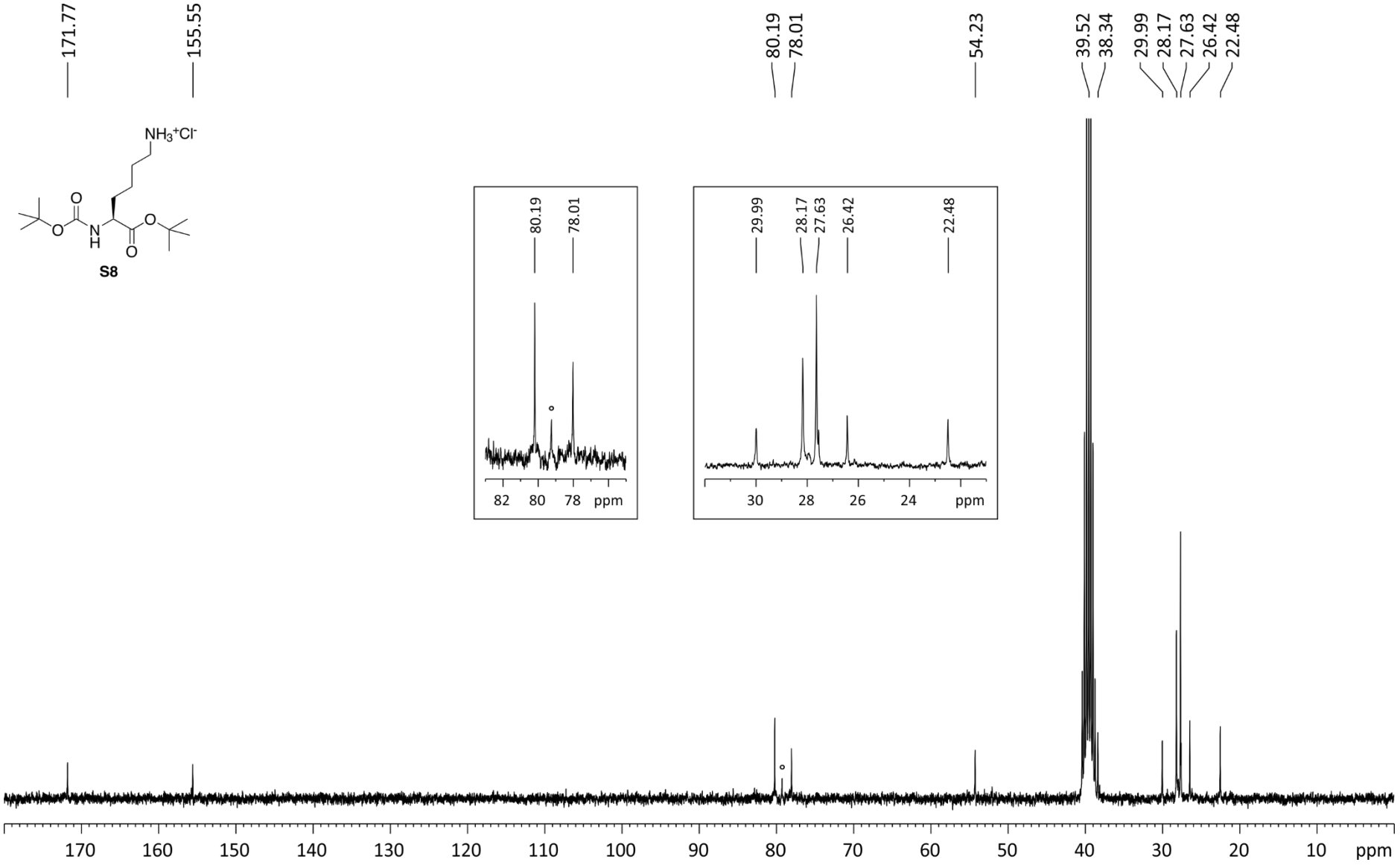

Figure S68: ^{13}C-NMR spectrum of Boc-Lys-O^{t}Bu · HCl **S8** (75 MHz, 300 K, DMSO-d_6). ° Signal of $CHCl_3$.

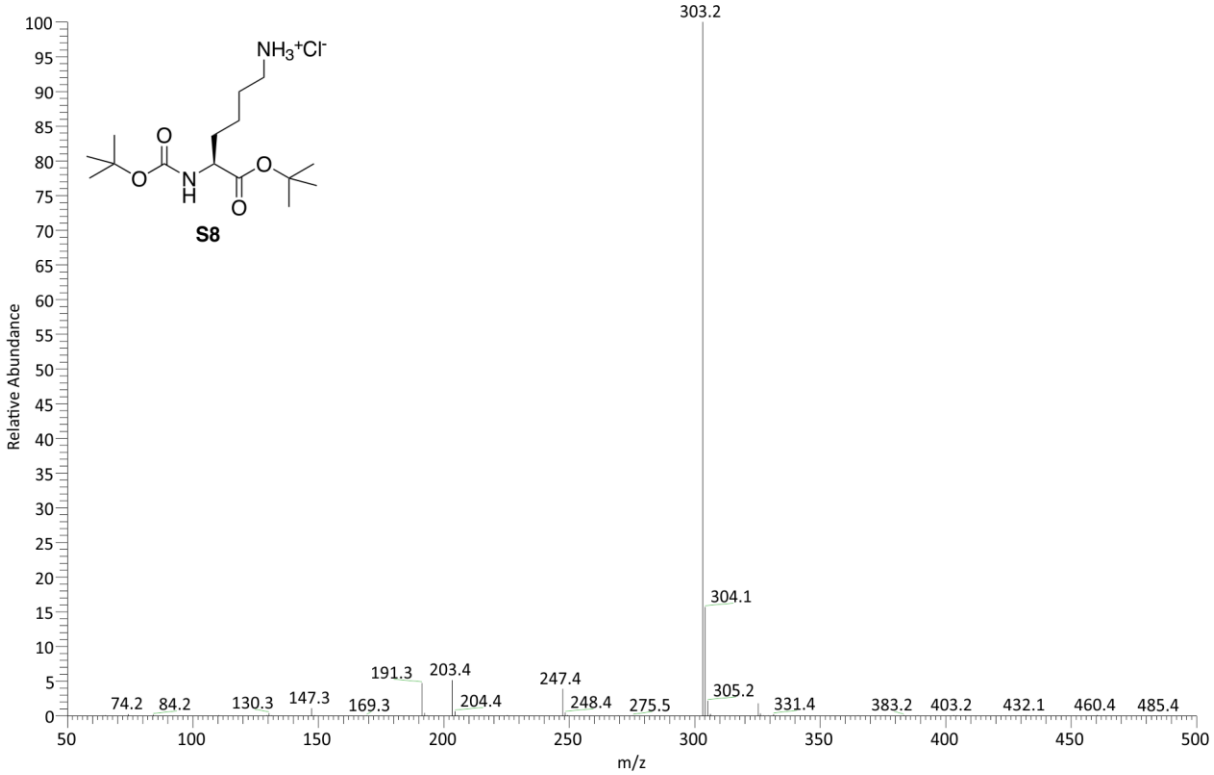

Figure S69: ESI+ mass spectrum with charge pattern m/z of Boc-Lys-O^{t}Bu · HCl **S8**.

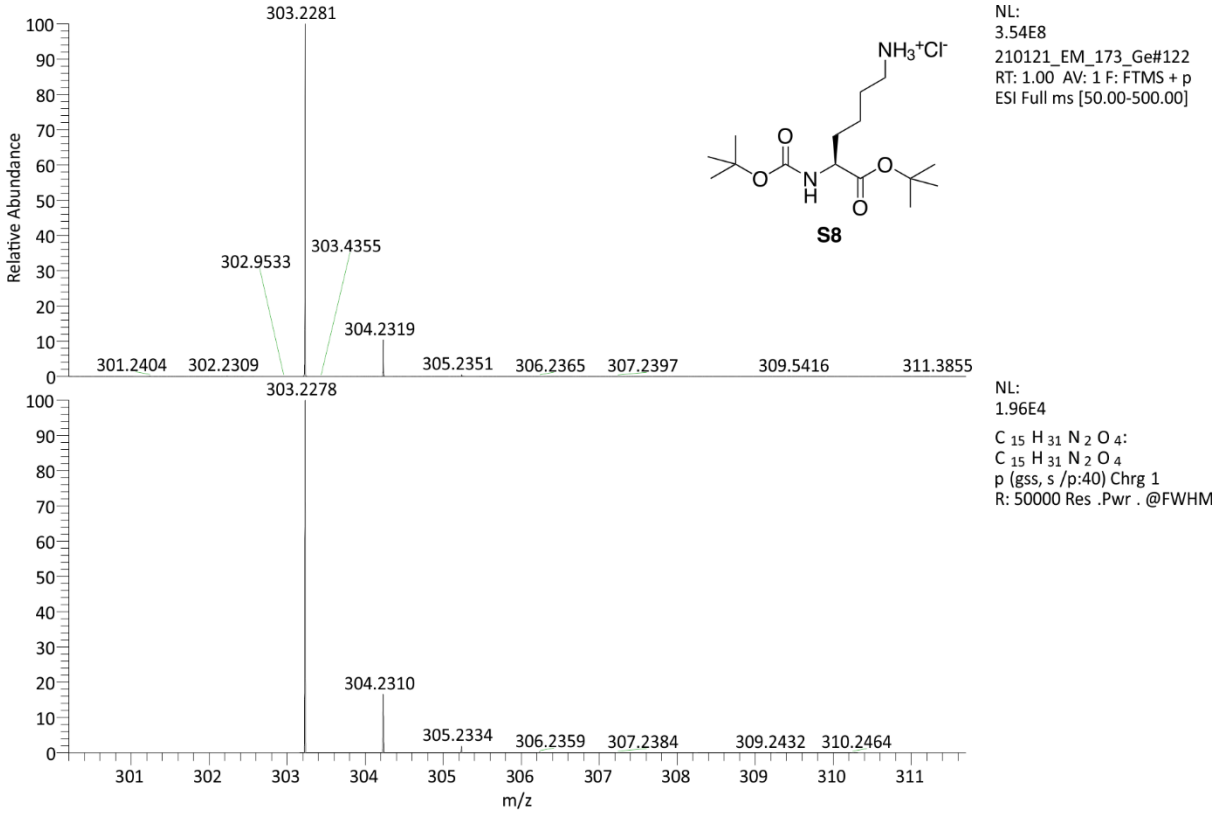

Figure S70: High resolution mass spectrum with isotope pattern of Boc-Lys-O^{t}Bu · HCl **S8**.

tert-Butyl-(2*S*)-2-[(_tert_-butoxycarbonyl)amino]-6-[(2-nitrobenzenesulfonyl)amino]hexanoate (Boc-Lys(Ns)-O^{t}Bu, 7)

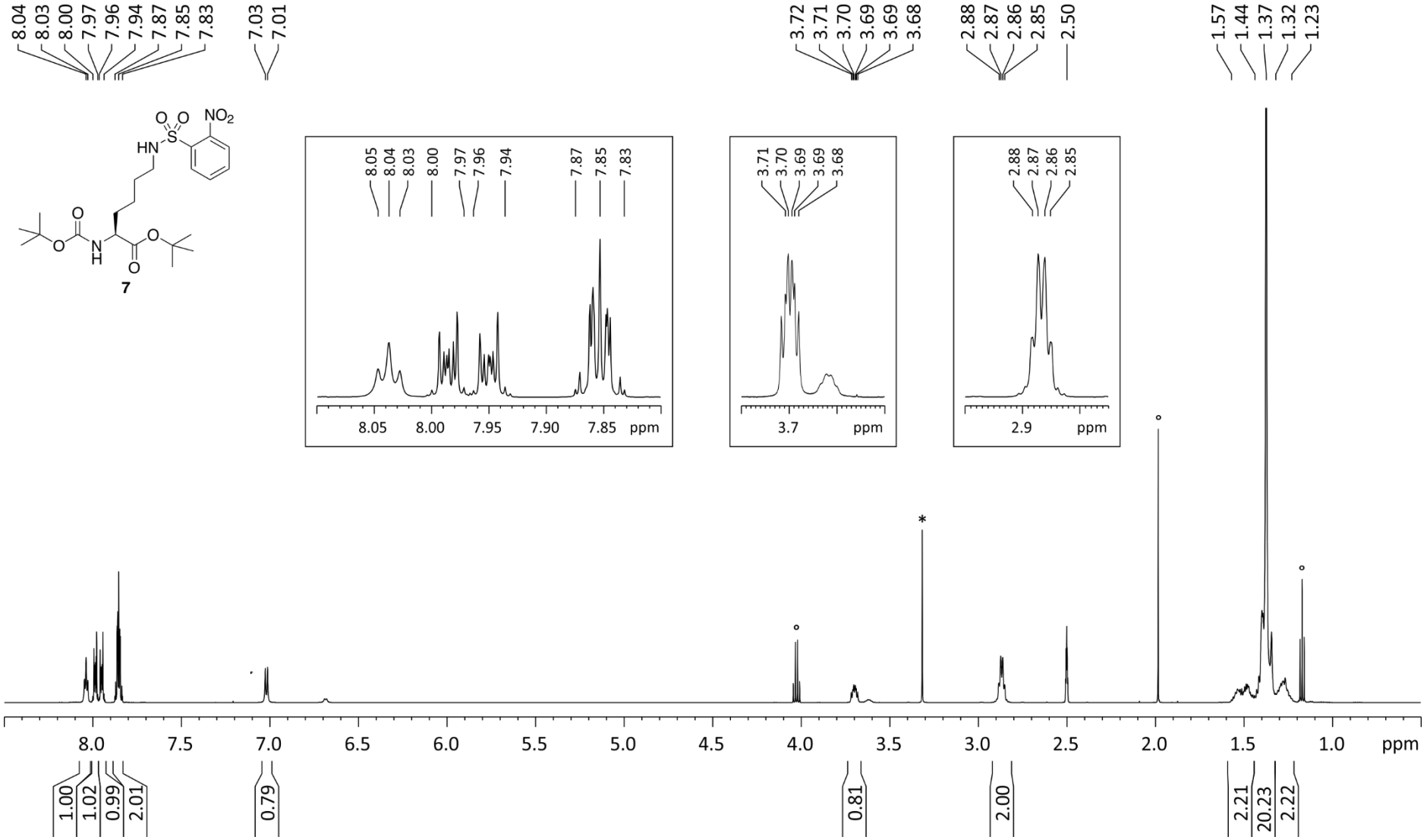

Figure S71: ^{1}H-NMR spectrum of Boc-Lys(Ns)-O^{t}Bu **7** (600 MHz, 300 K, DMSO-d_6). * Signal of H_2O. ° Signals of EtOAc.

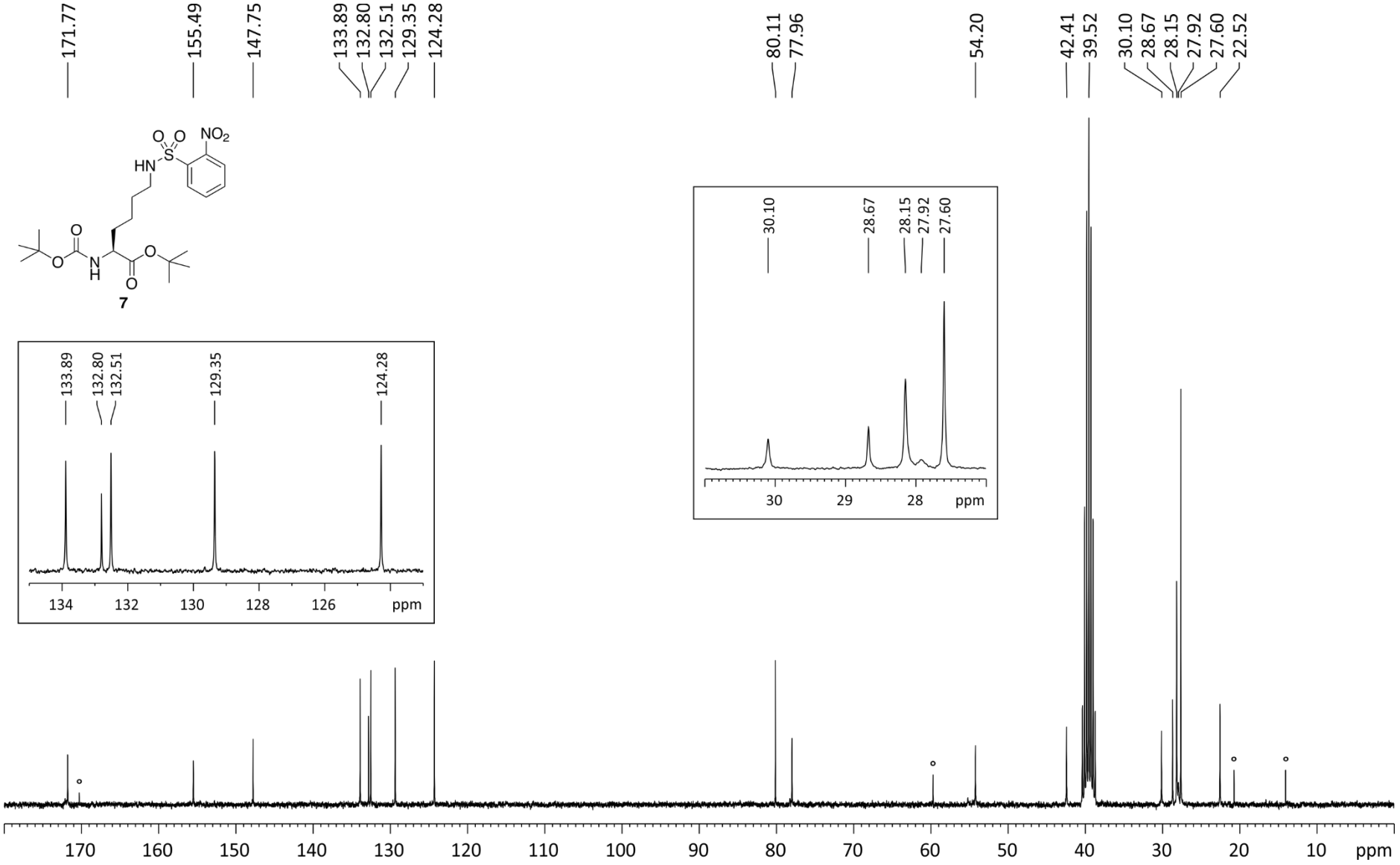

Figure S72: ^{13}C-NMR spectrum of Boc-Lys(Ns)-O^{t}Bu **7** (75 MHz, 300 K, DMSO-d_6). ° Signals of EtOAc.

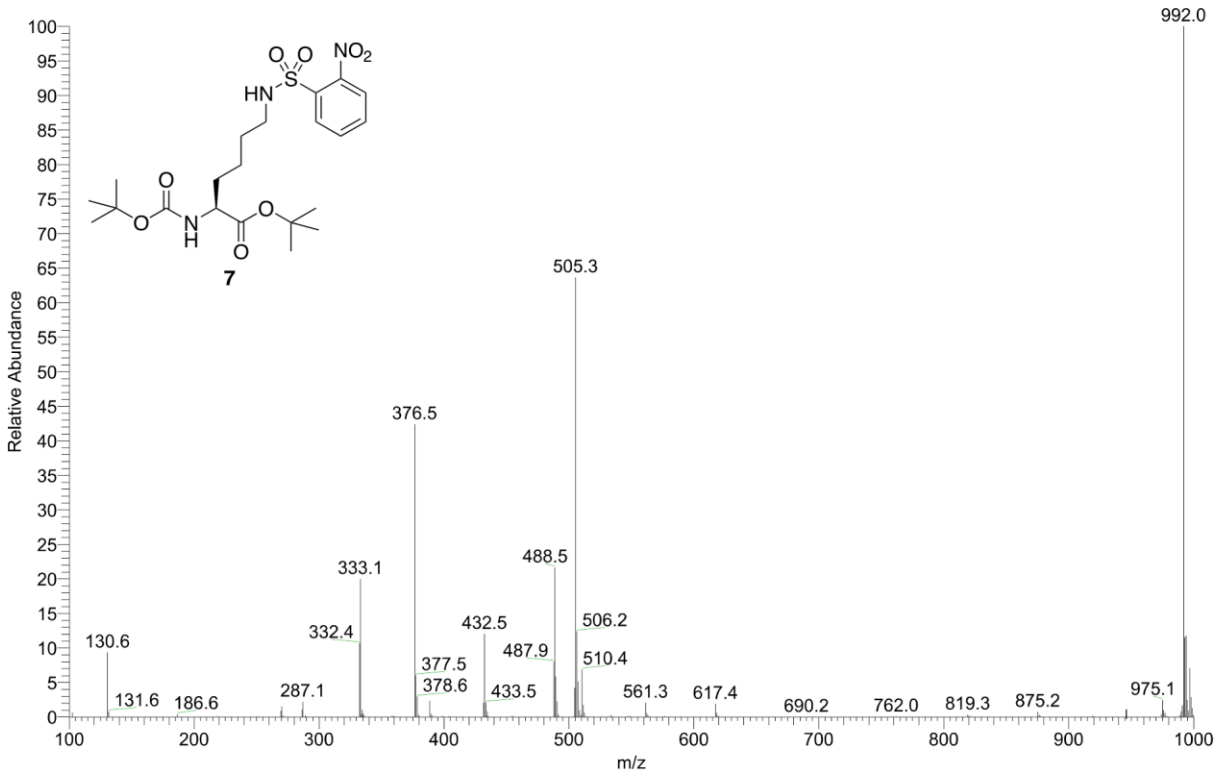

Figure S73: ESI+ mass spectrum with charge pattern m/z of Boc-Lys(Ns)-O^{t}Bu **7**.

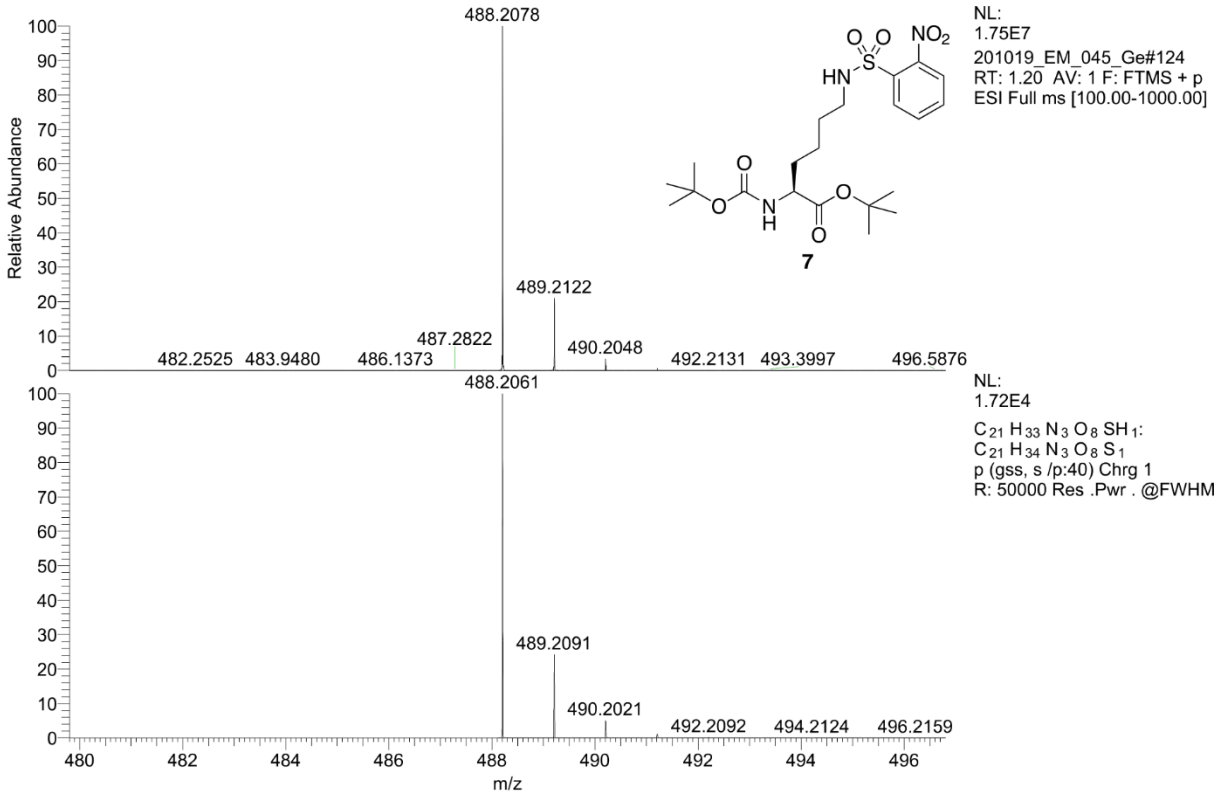

Figure S74: High resolution mass spectrum with isotope pattern of Boc-Lys(Ns)-O^{t}Bu **7**.

***tert*-Butyl-(2*S*)-2-[(*tert*-butoxycarbonyl)amino]-6-{3-[(3-dimethylaminopropyl)-(2-nitrobenzene-sulfonyl)amino]propyl}-6-(2-nitrobenzenesulfonyl)amino] hexanoate (Boc-Kdp(Me)$_2$(Ns)$_2$-O^{t}Bu, 8)**

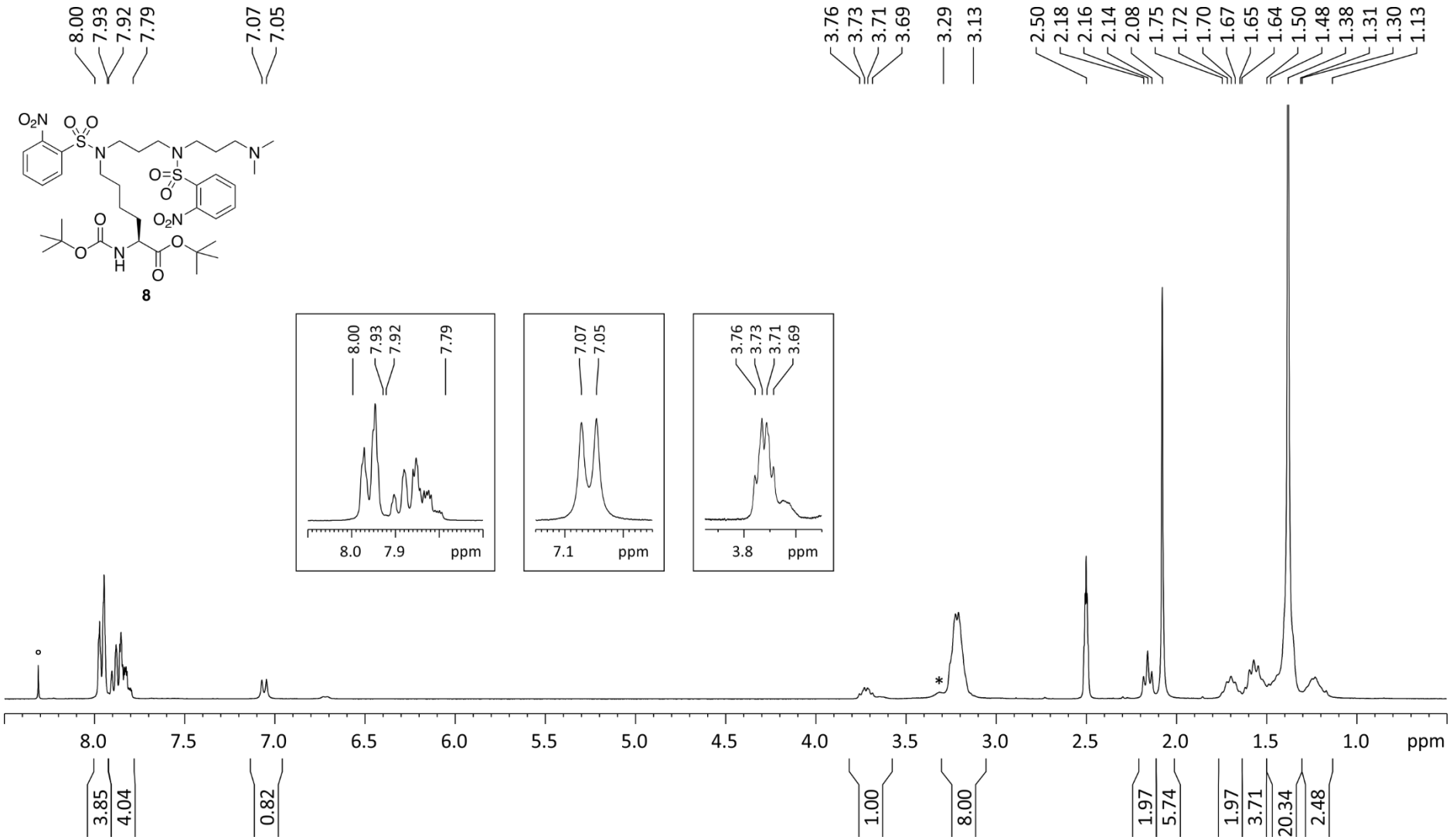

Figure S75: ^{1}H-NMR spectrum of Boc-Kdp(Me)$_3$(Ns)$_2$-O^{t}Bu **8** (300 MHz, 300 K, DMSO-d_6). * Signal of H_2O. ° Signal of $CHCl_3$.

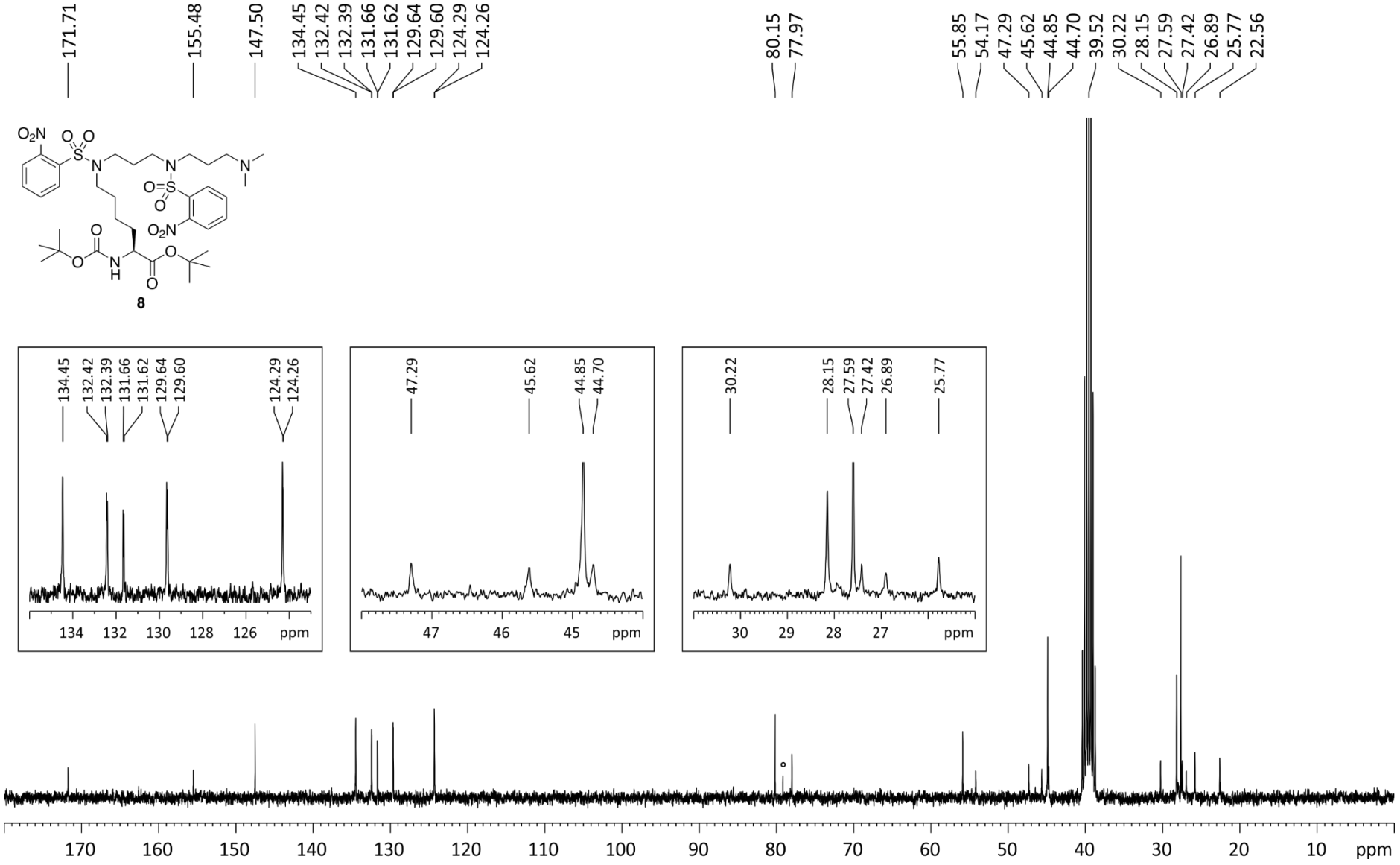

Figure S76: ^{13}C-NMR spectrum of Boc-Kdp(Me)$_3$(Ns)$_2$-O^{t}Bu **8** (75 MHz, 300 K, DMSO-d_6). ° Signal of $CHCl_3$.

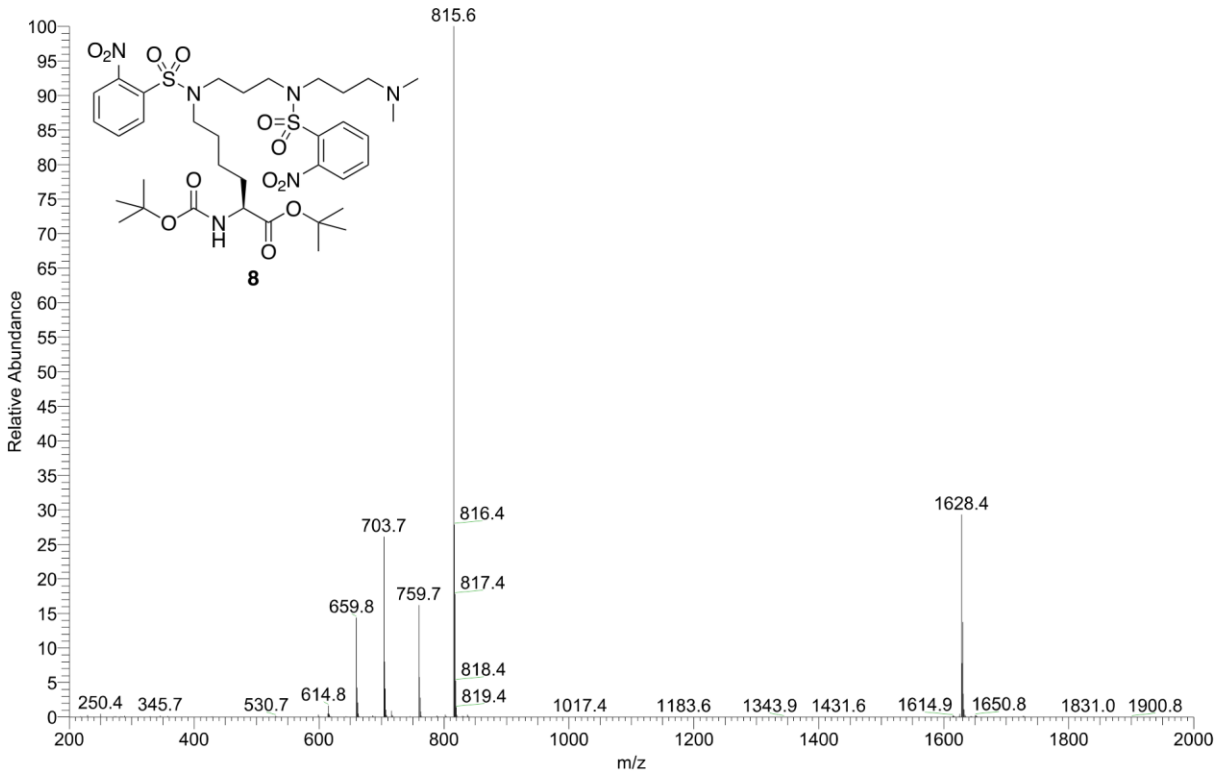

Figure S77: ESI+ mass spectrum with charge pattern m/z of Boc-Kdp(Me)$_3$(Ns)$_2$-O^{t}Bu **8**.

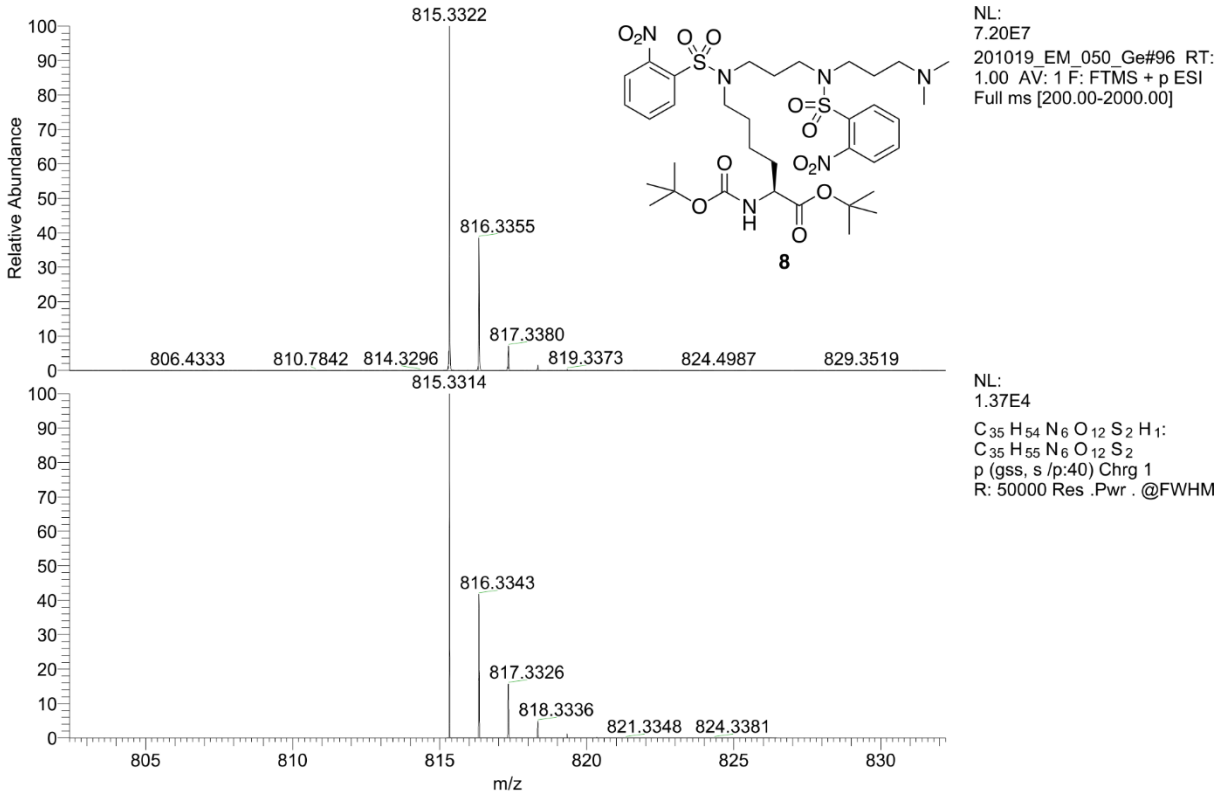

Figure S78: High resolution mass spectrum with isotope pattern of Boc-Kdp(Me)$_3$(Ns)$_2$-O^{t}Bu **8**.

(2S)-2-Amino-6-{3-[(3-dimethylaminopropyl)-(2-nitrobenzenesulfonyl)amino]propyl}-6-(2-nitrobenzenesulfonyl)amino]hexanoic acid hydrotrifluoroacetat (H_2N-Kdp$(Me)_2(Ns)_2$-OH · TFA, 9)

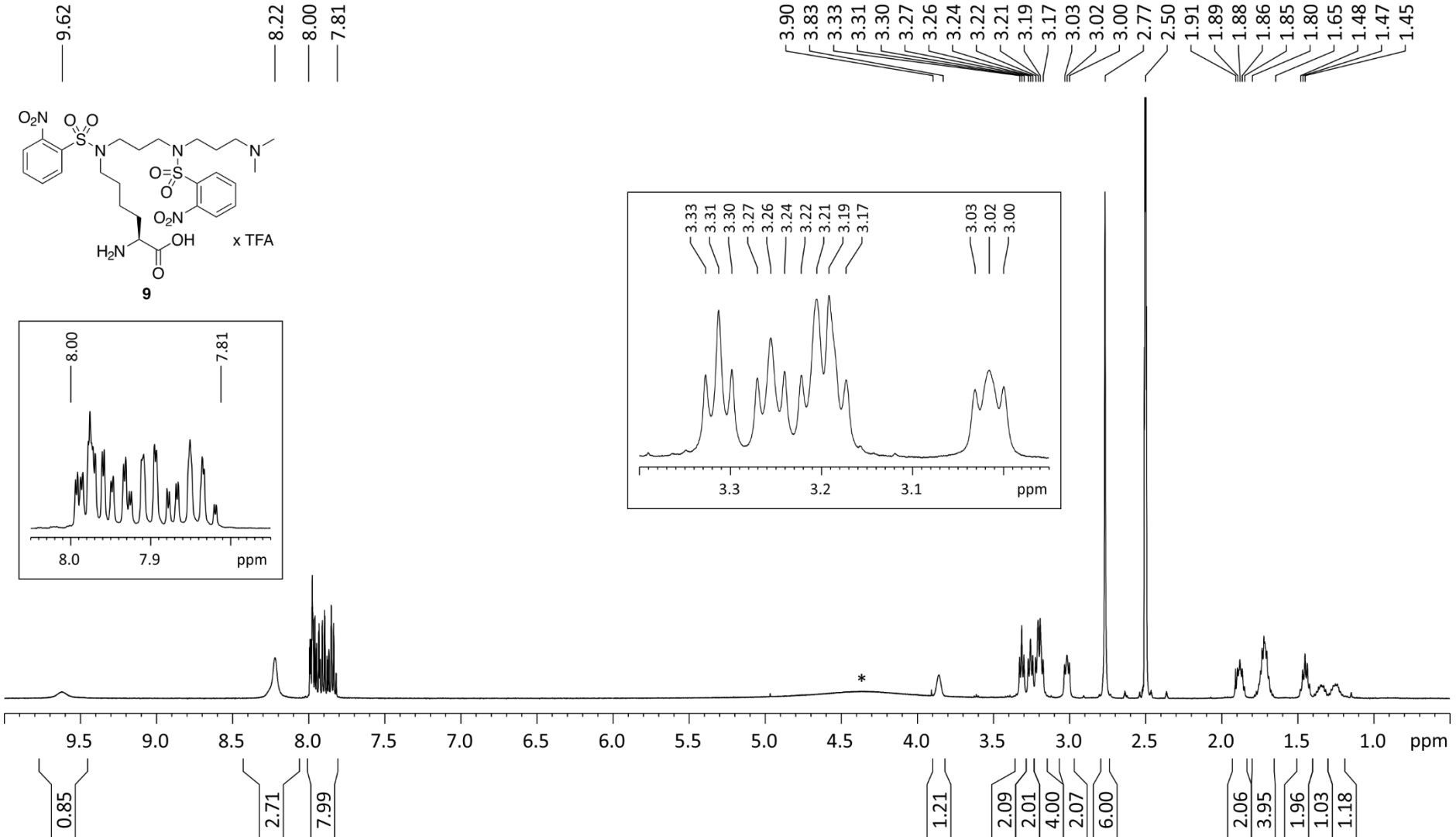

Figure S79: ^{1}H-NMR spectrum of H_2N-Kdp$(Me)_3(Ns)_2$-OH · TFA **9** (500 MHz, 300 K, DMSO-d_6). * Signal of H_2O.

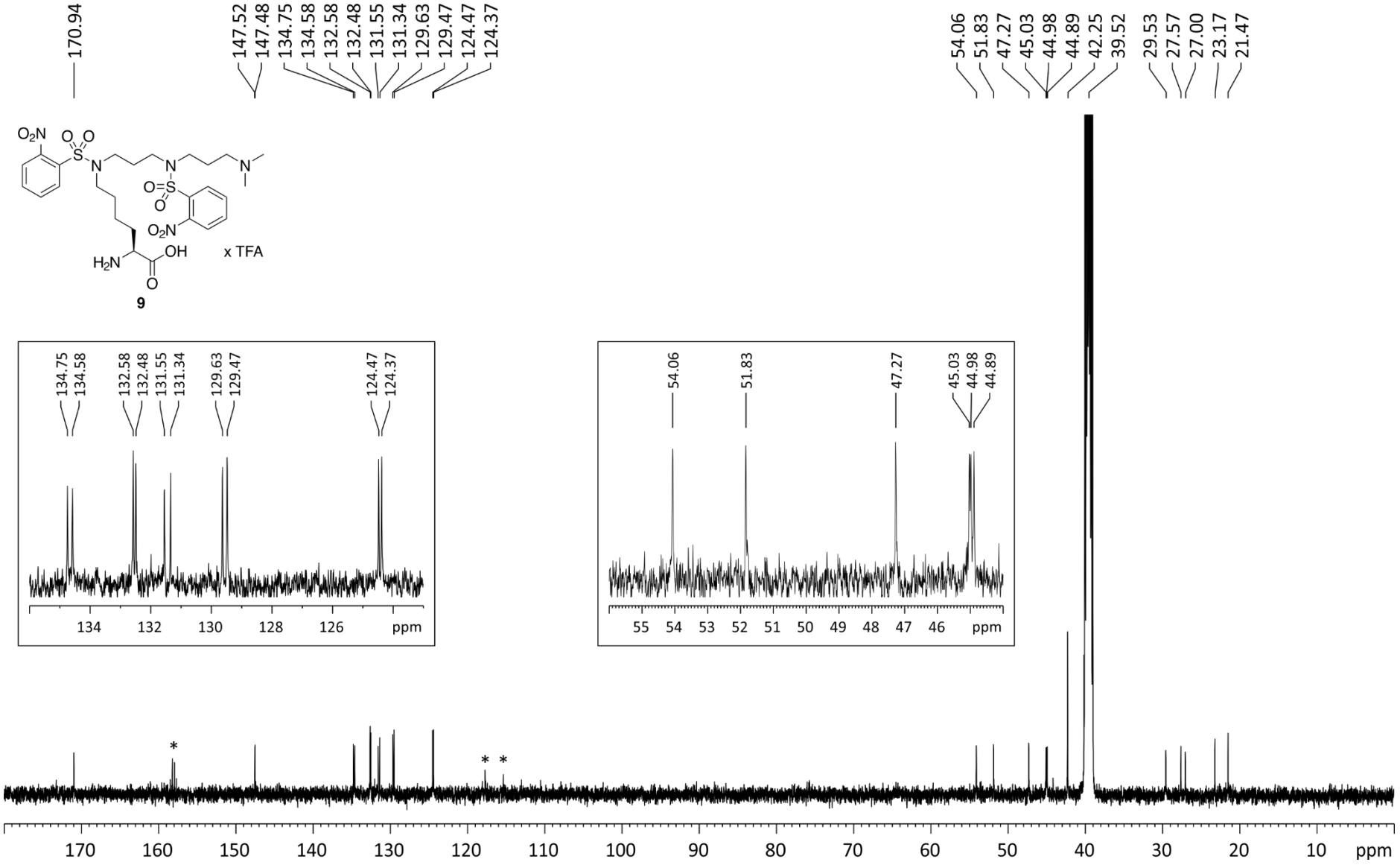

Figure S80: ^{13}C-NMR spectrum of H_2N-Kdp(Me)$_3$(Ns)$_2$-OH · TFA **9** (125 MHz, 300 K, DMSO-d_6). * Signals of TFA.

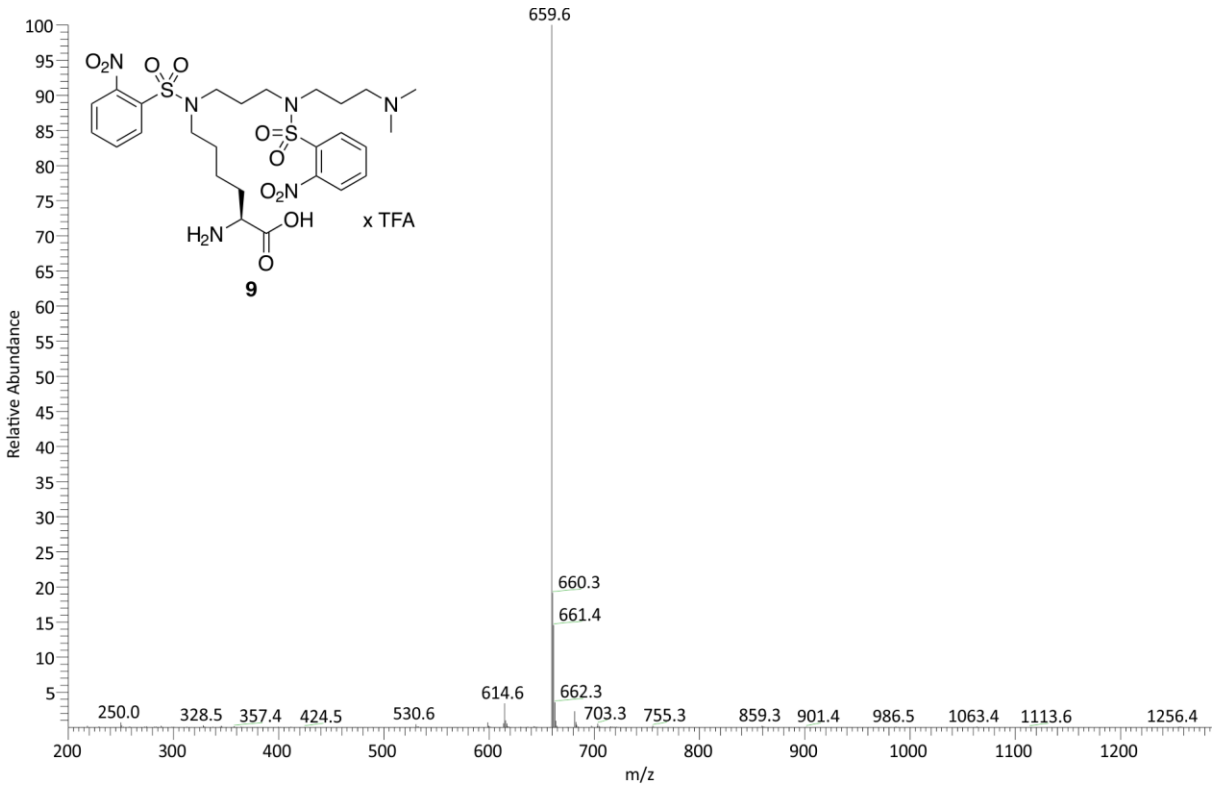

Figure S81: ESI+ mass spectrum with charge pattern m/z of H_2N-Kdp$(Me)_3(Ns)_2$-OH · TFA **9**.

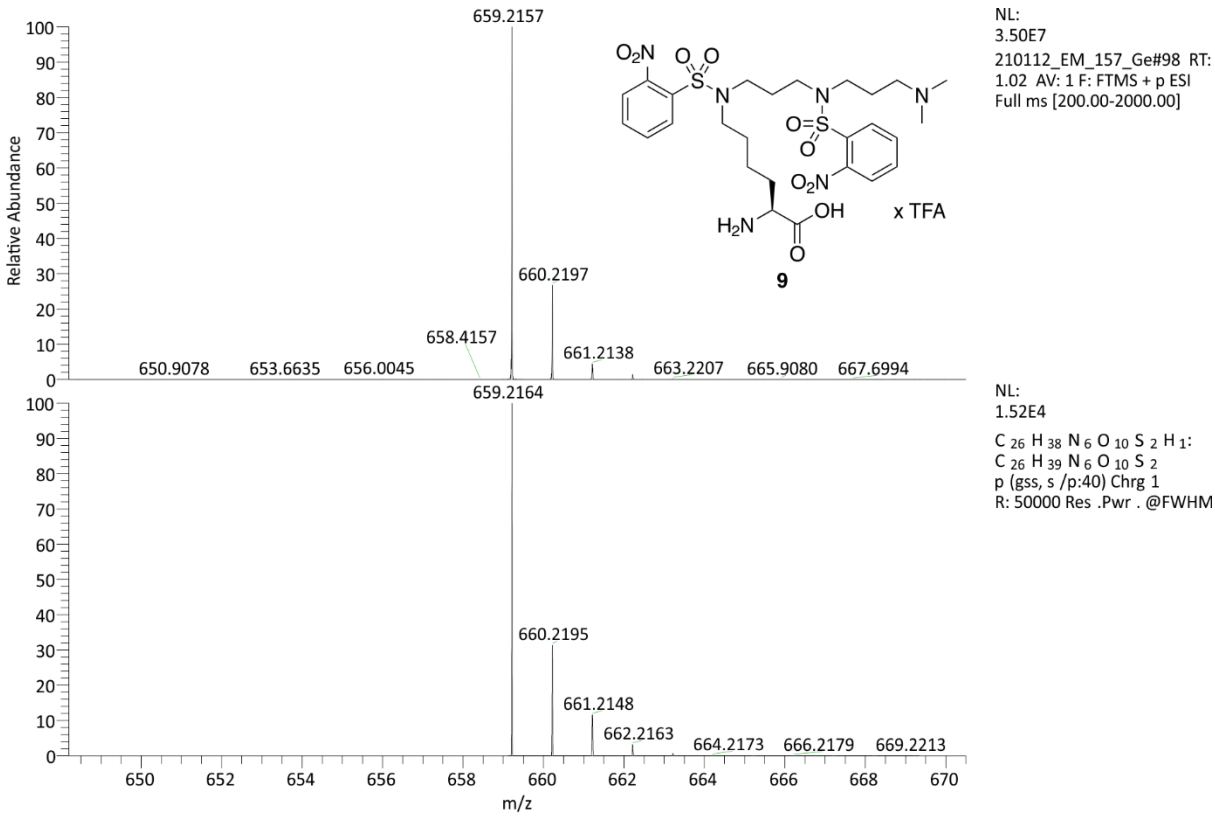

Figure S82: High resolution mass spectrum with isotope pattern of H_2N-Kdp$(Me)_3(Ns)_2$-OH · TFA **9**.

(2*S*)-2-[(Fluorenylmethyloxycarbonyl)amino]-6-{3-[(3-dimethylaminopropyl)-(2-nitrobenzenesulfonyl)amino]propyl}-6-(2-nitrobenzenesulfonyl)amino] hexanoic acid hydrotrifluoroacetate (Fmoc-Kdp(Me)$_2$(Ns)$_2$-OH · TFA, 10)

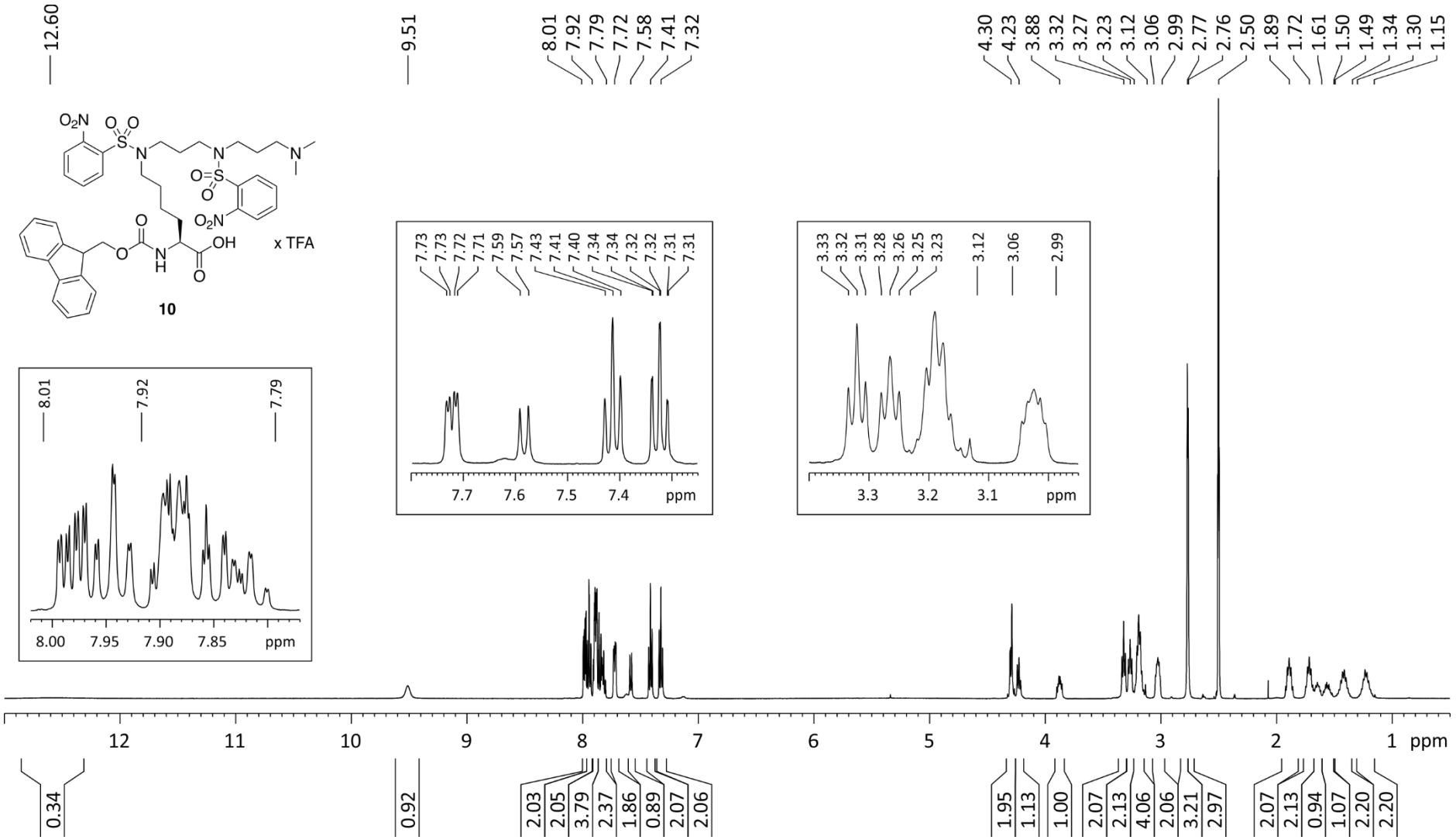

Figure S83: ^{1}H-NMR spectrum of Fmoc-Kdp(Me)$_2$(Ns)$_2$-OH · TFA **10** (500 MHz, 300 K, DMSO-d_6).

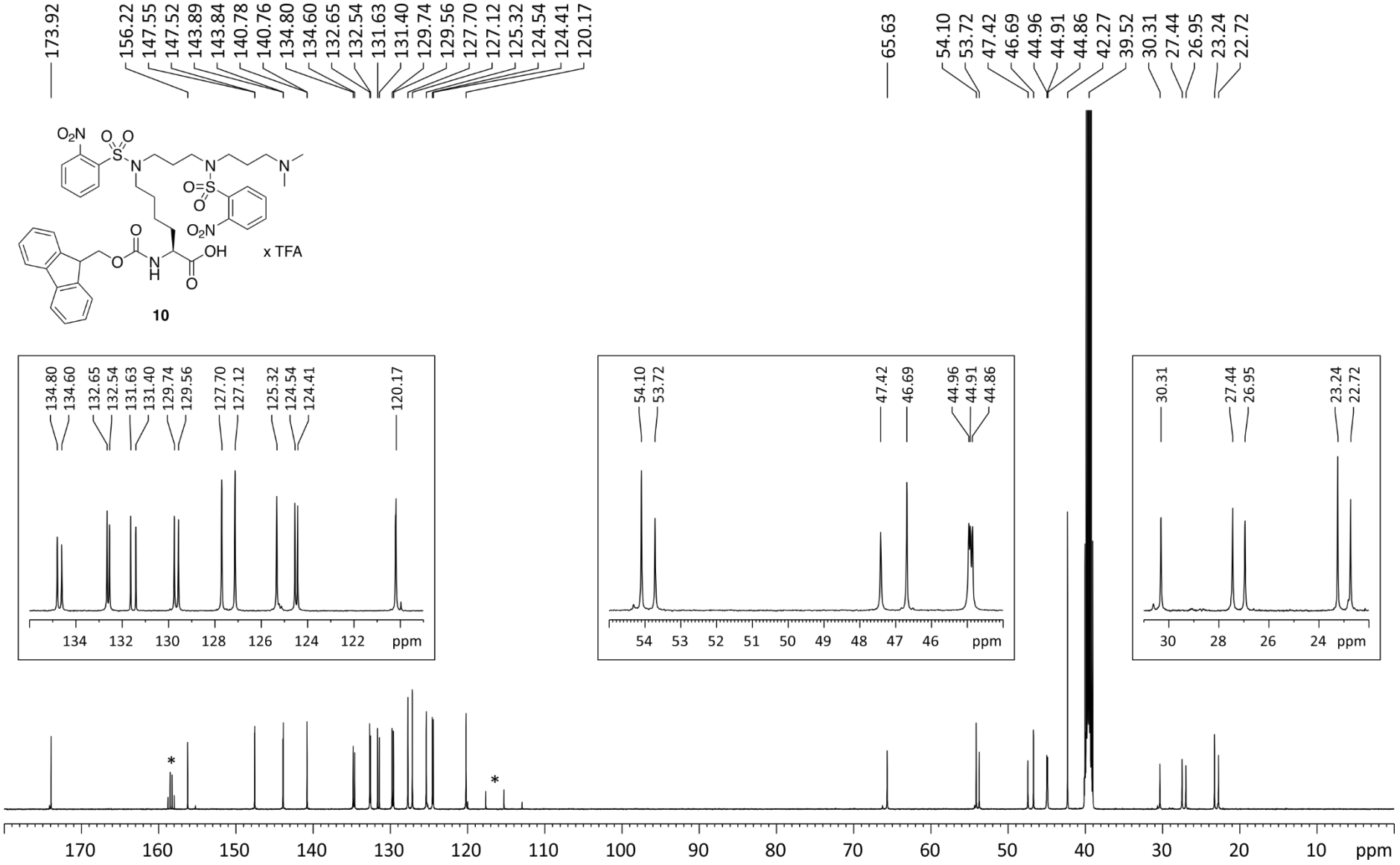

Figure S84: ^{13}C-NMR spectrum of Fmoc-Kdp(Me)$_2$(Ns)$_2$-OH · TFA **10** (125 MHz, 300 K, DMSO-d_6). * Signals of TFA.

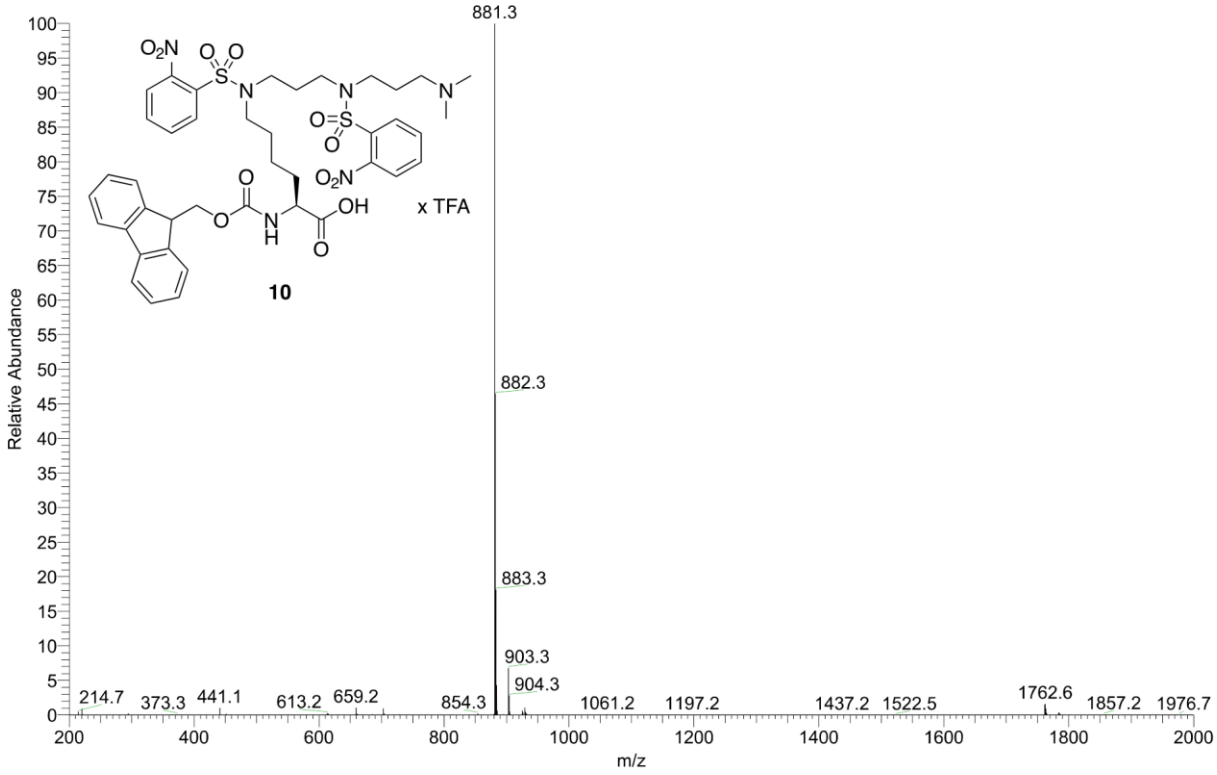

Figure S85: ESI+ mass spectrum with charge pattern m/z of Fmoc-Kdp(Me)$_2$(Ns)$_2$-OH · TFA **10**.

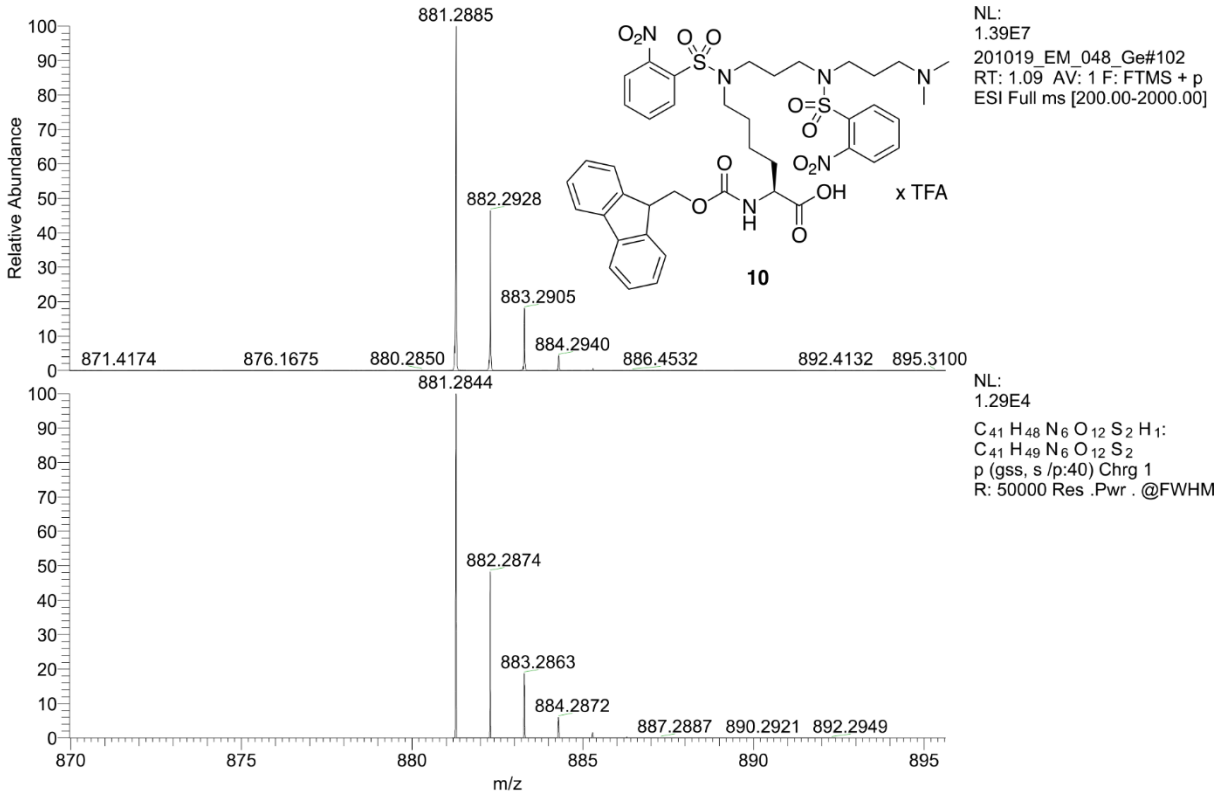

Figure S86: High resolution mass spectrum with isotope pattern of Fmoc-Kdp(Me)$_2$(Ns)$_2$-OH · TFA **10**.

***tert*-Butyl-(2*S*)-2-[(Fluorenylmethyloxycarbonyl)amino]-6-{3-[(3-dimethylaminopropyl)-(2-nitrobenzenesulfonyl)amino]propyl}-6-(2-nitrobenzene-sulfonyl)-L-lysyl-L-alaninate hydrotrifluoroacetate (Fmoc-Kdp(Me)$_2$(Ns)$_2$-Ala-O^{t}Bu · TFA, S9)**

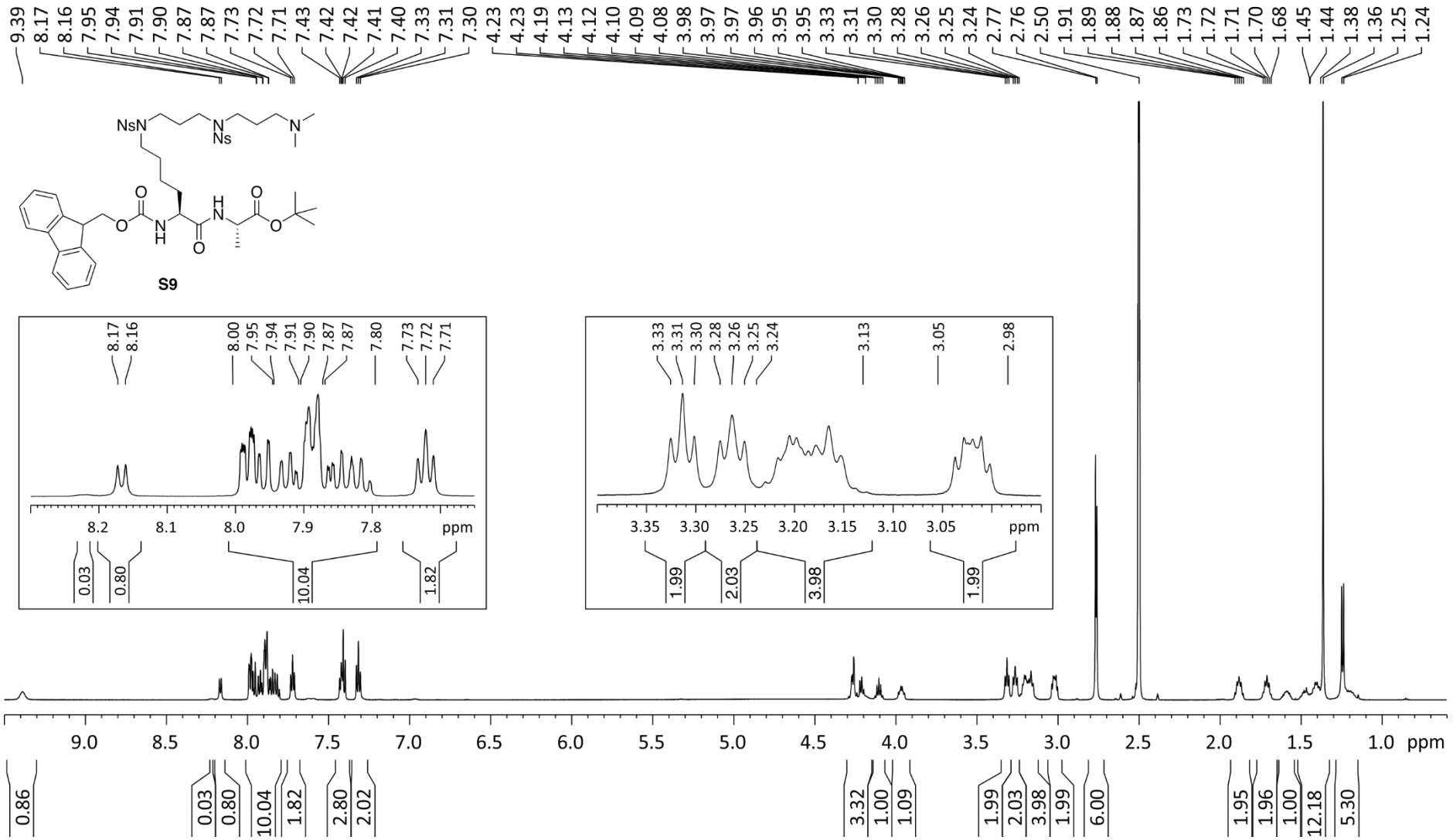

Figure S87: ^{1}H-NMR spectrum of Fmoc-Kdp(Me)$_2$(Ns)$_2$-Ala-O^{t}Bu · TFA **S9** (600 MHz, 300 K, DMSO-d_6).

***O*-(*tert*-Butyldimethylsilyl)-L-serine (H_2N-Ser(TBS)-OH, S10)**

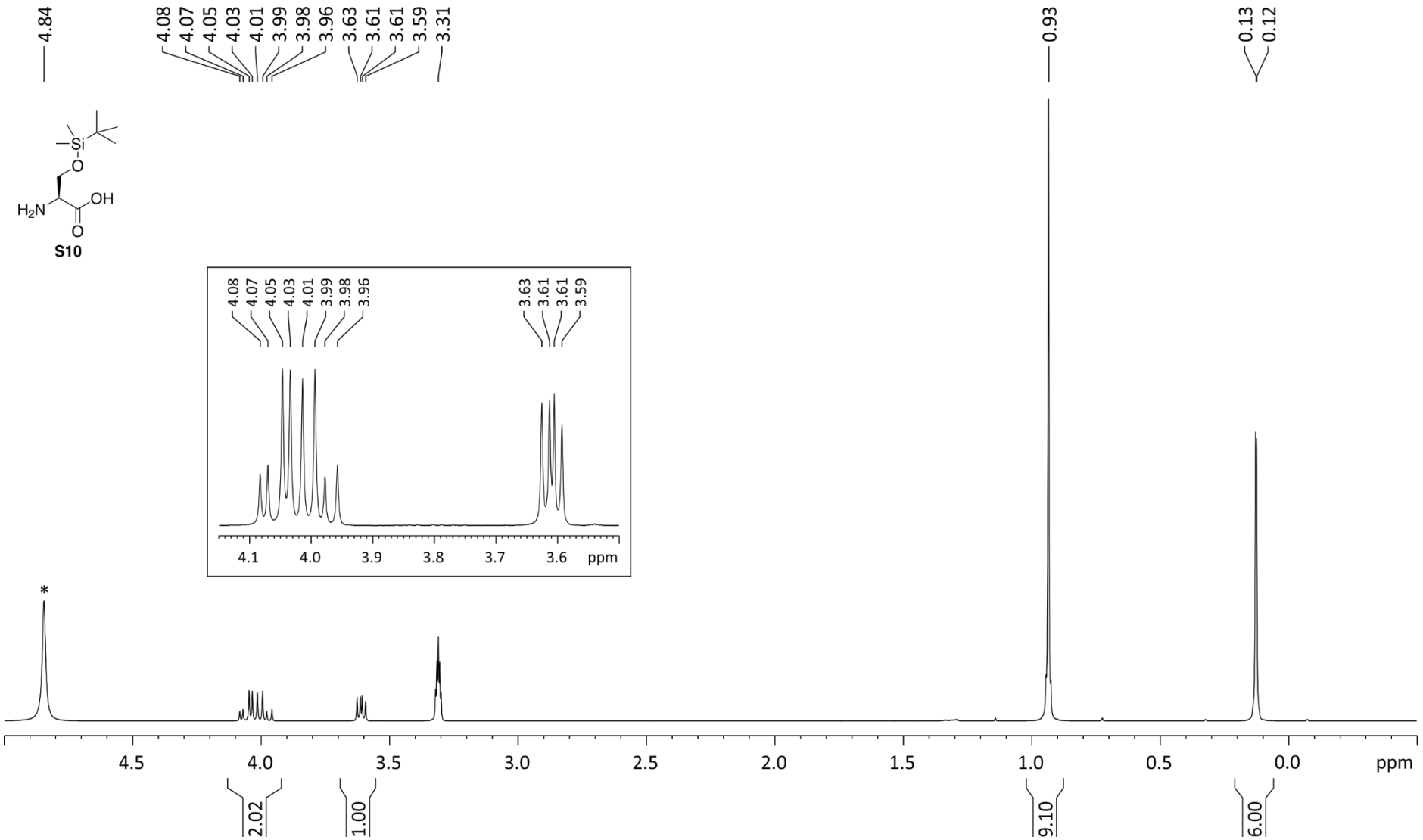

Figure S88: ^{1}H-NMR spectrum of H_2N-Ser(TBS)-OH **S10** (300 MHz, 300 K, CD_3OD). * Signal of H_2O.

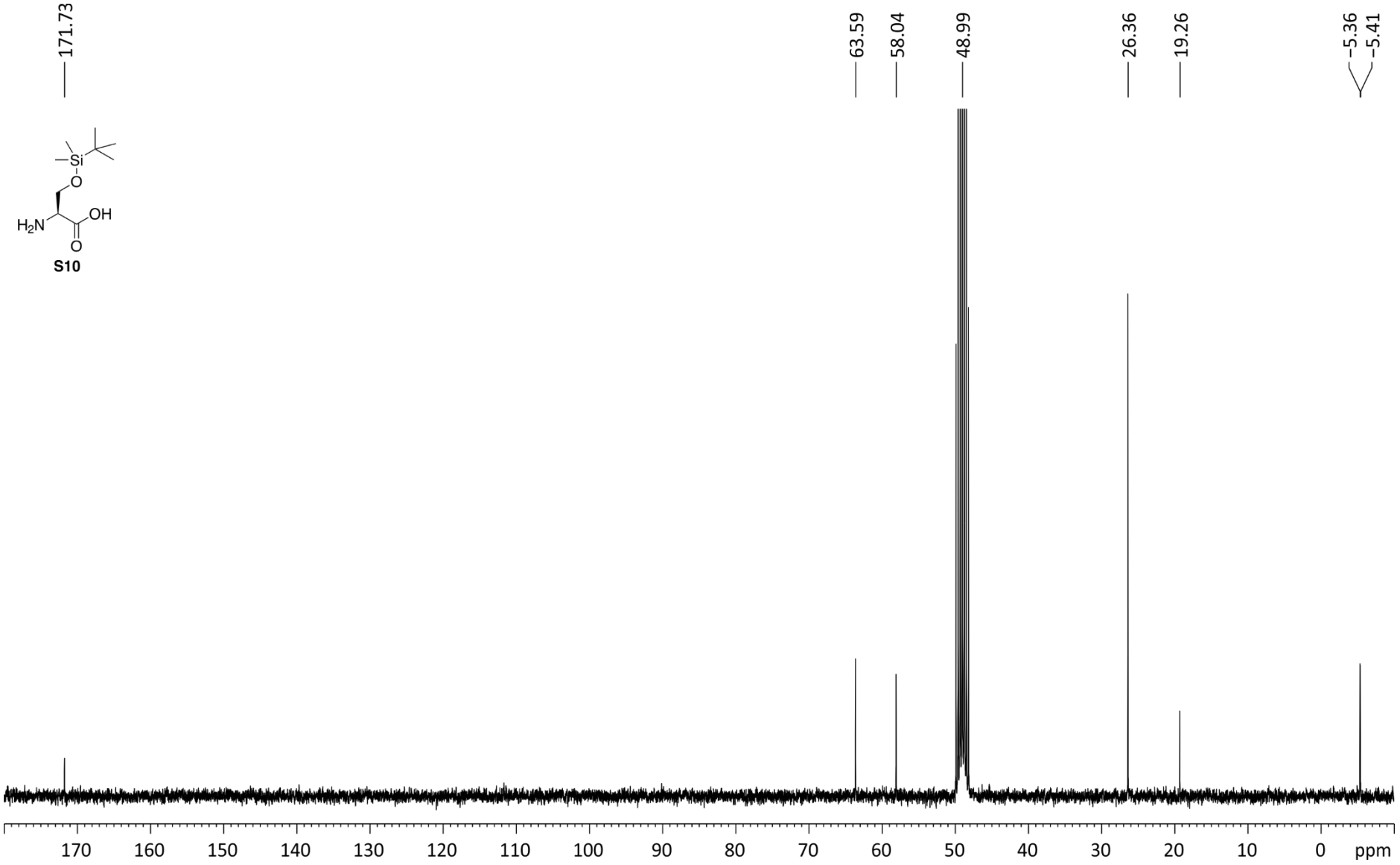

Figure S89: ^{13}C-NMR spectrum of H_2N-Ser(TBS)-OH **S10** (75 MHz, 300 K, CD_3OD).

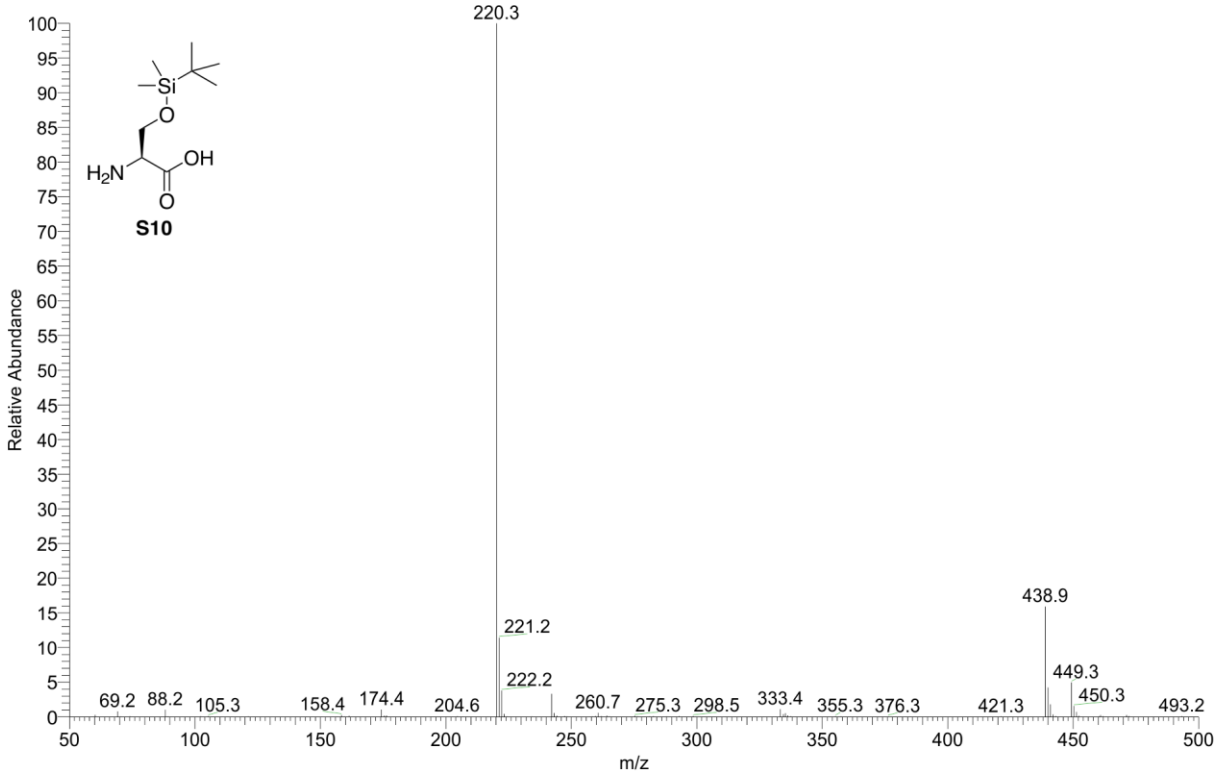

Figure S90: ESI+ mass spectrum with charge pattern m/z of H_2N-Ser(TBS)-OH **S10**.

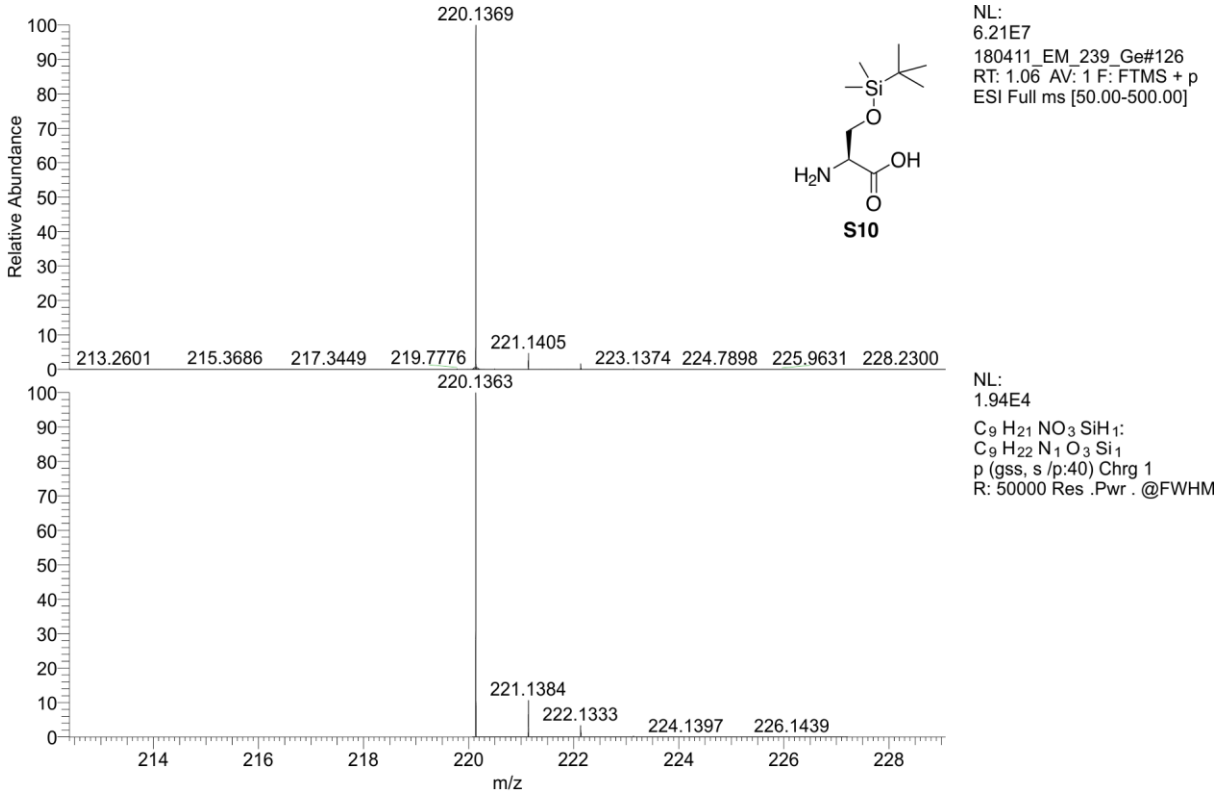

Figure S91: High resolution mass spectrum with isotope pattern of H_2N-Ser(TBS)-OH **S10**.

_N_-(Fluorenylmethyloxycarbonyl)-_O_-(_tert_-butyldimethylsilyl)-L-serine (Fmoc-Ser(TBS)-OH, S11)

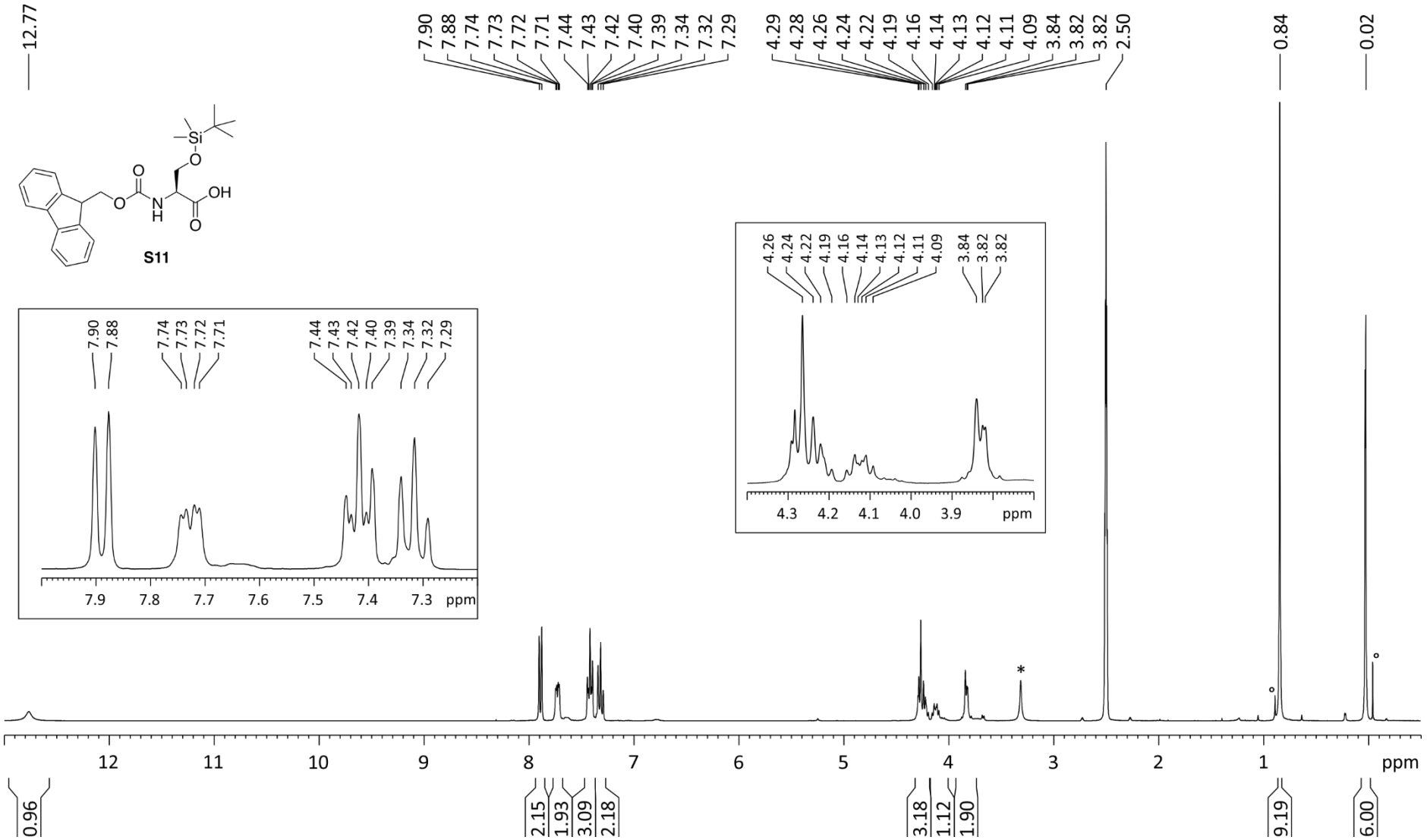

Figure S92: ^{1}H-NMR spectrum of Fmoc-Ser(TBS)-OH **S11** (300 MHz, 300 K, DMSO-d_6). * Signal of H_2O. ° Signals of TBDMS-OH.

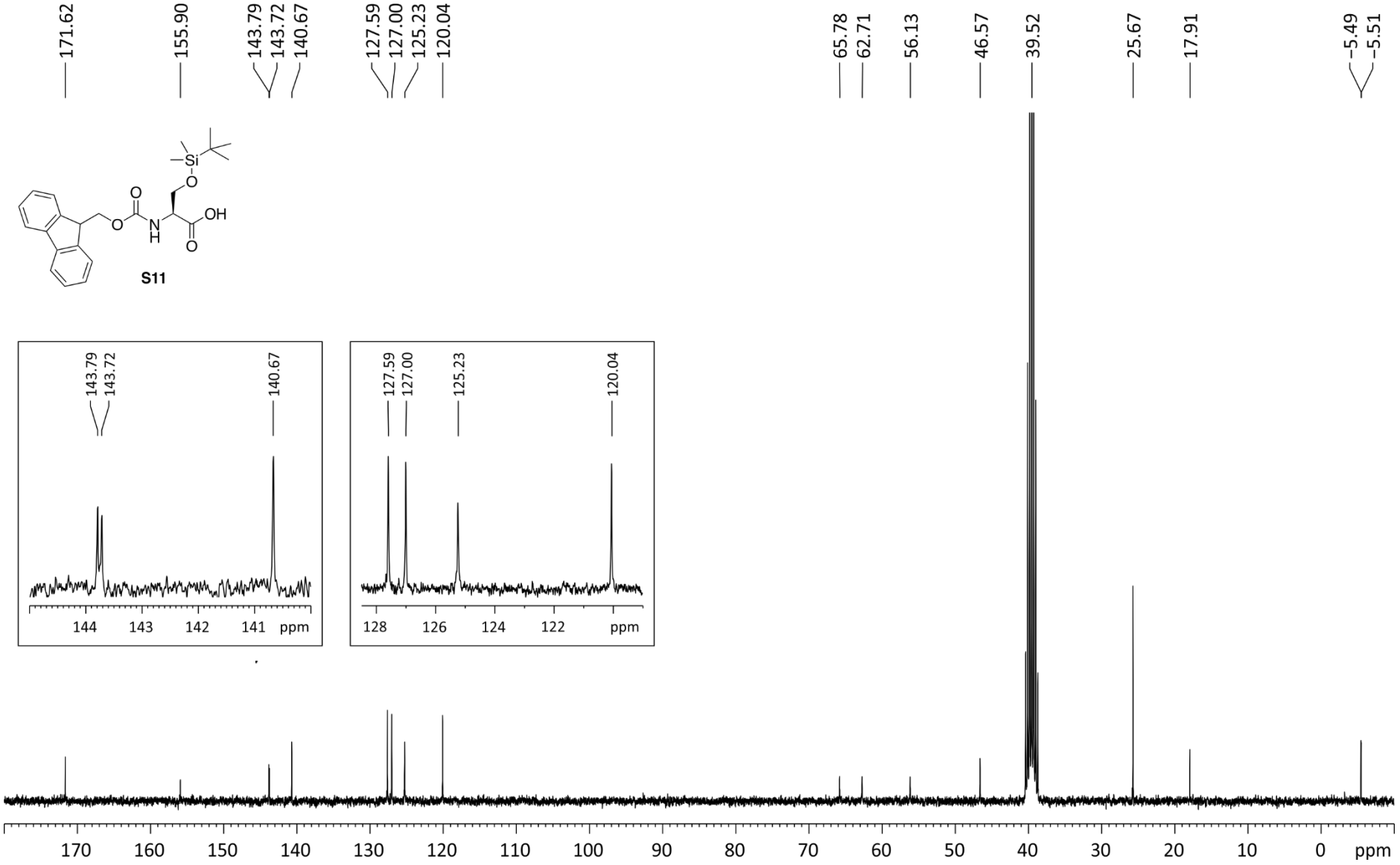

Figure S93: ^{13}C-NMR spectrum of Fmoc-Ser(TBS)-OH **S11** (75 MHz, 300 K, DMSO-d_6).

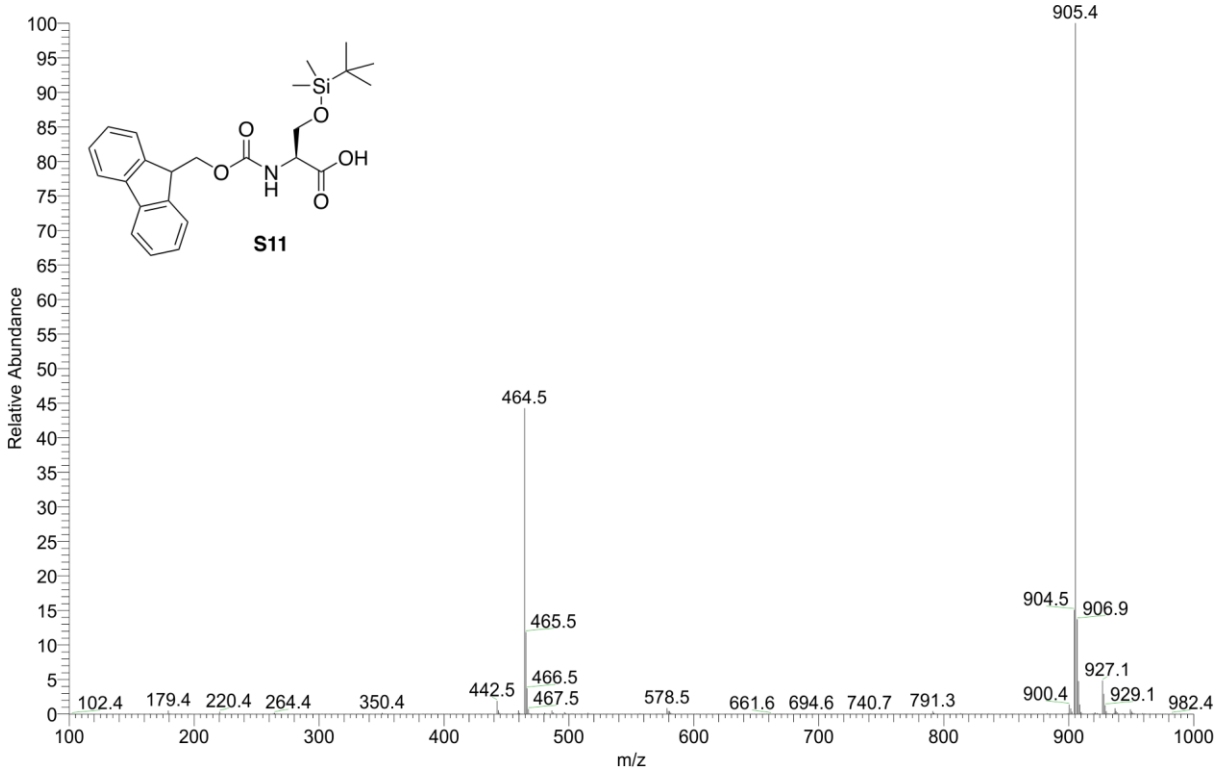

Figure S94: ESI+ mass spectrum with charge pattern m/z of Fmoc-Ser(TBS)-OH **S11**.

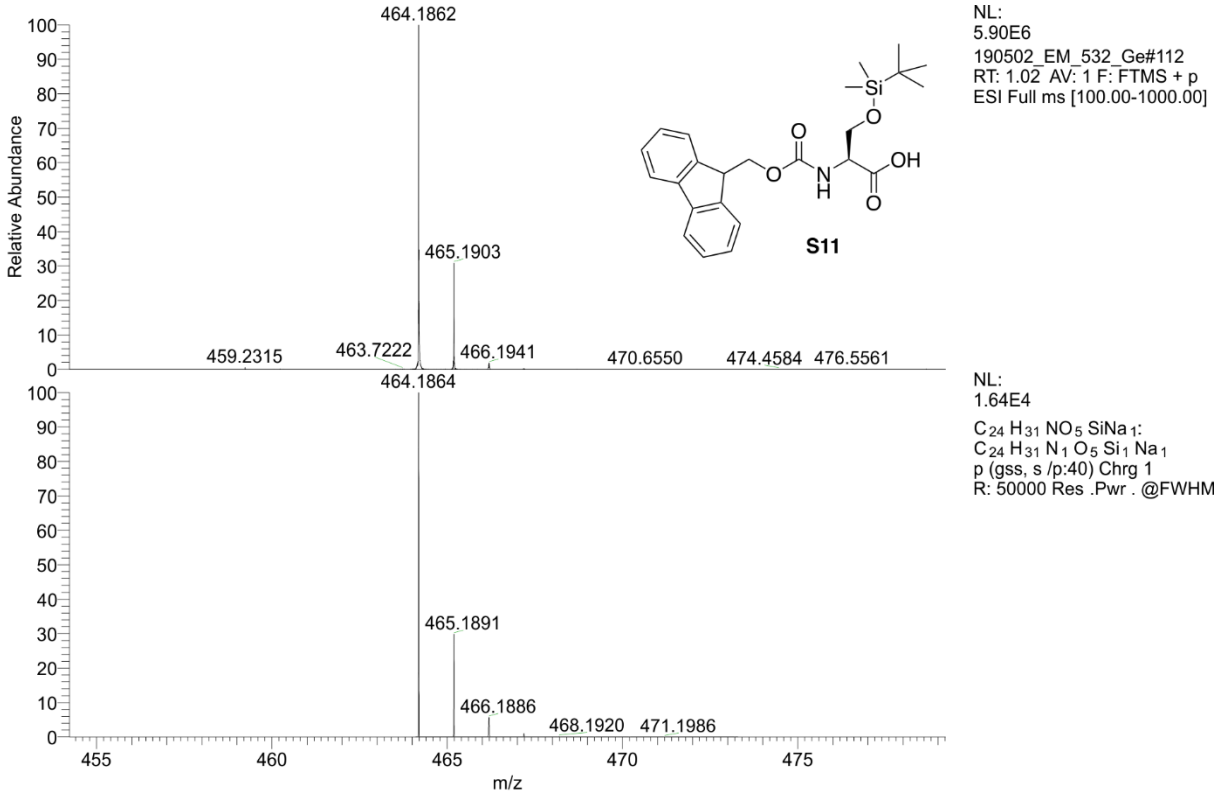

Figure S95: High resolution mass spectrum with isotope pattern of Fmoc-Ser(TBS)-OH **S11**.

***N*-(*tert*-Butoxycarbonyl)-*O*-(*tert*-butyldimethylsilyl)-L-serine (Boc-Ser(TBS)-OH, S12)**

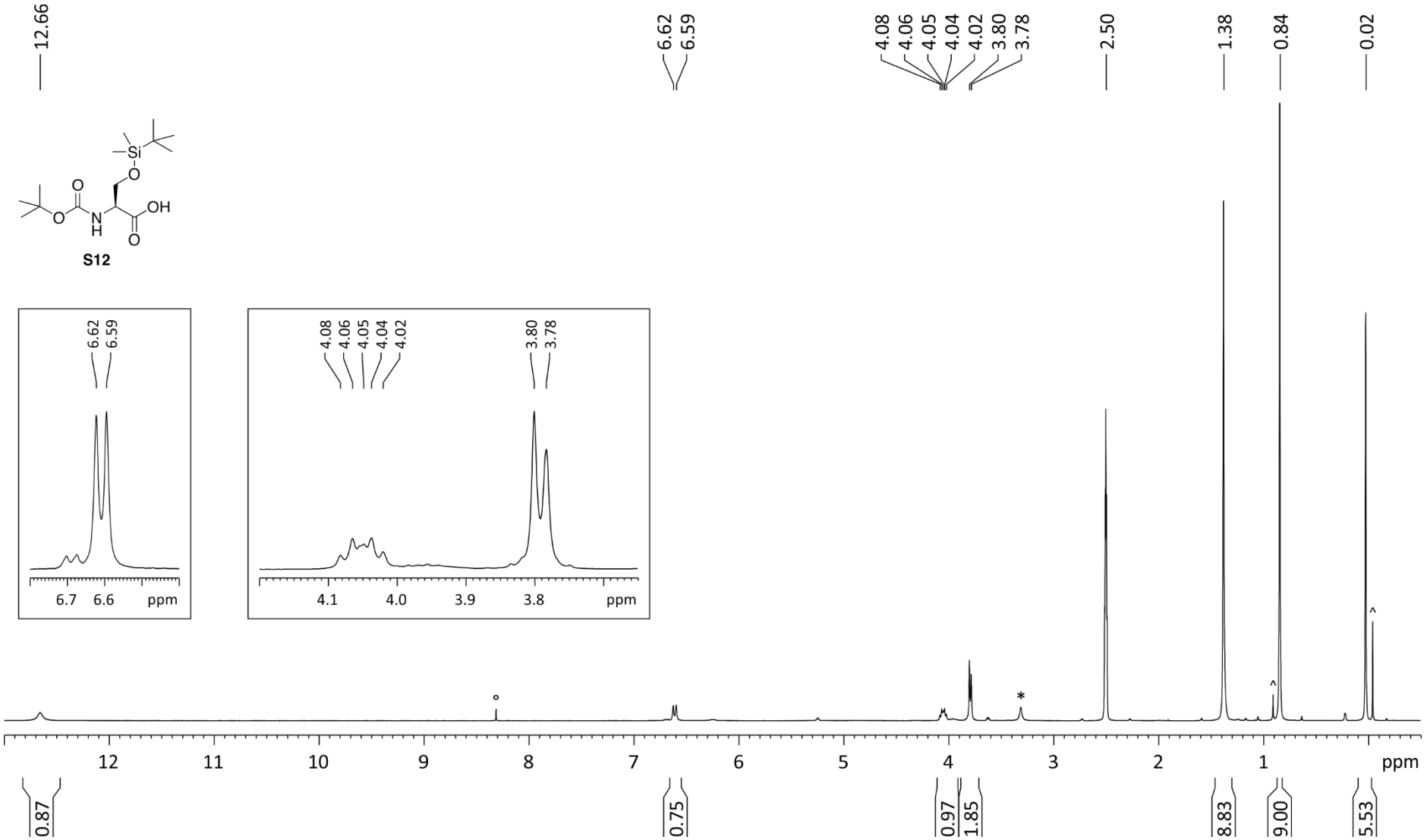

Figure S96: ^{1}H-NMR spectrum of Boc-Ser(TBS)-OH **S12** (300 MHz, 300 K, DMSO-d_6). * Signal of H_2O. ° Signal of $CHCl_3$. ^ Signal of TBDMS-OH.

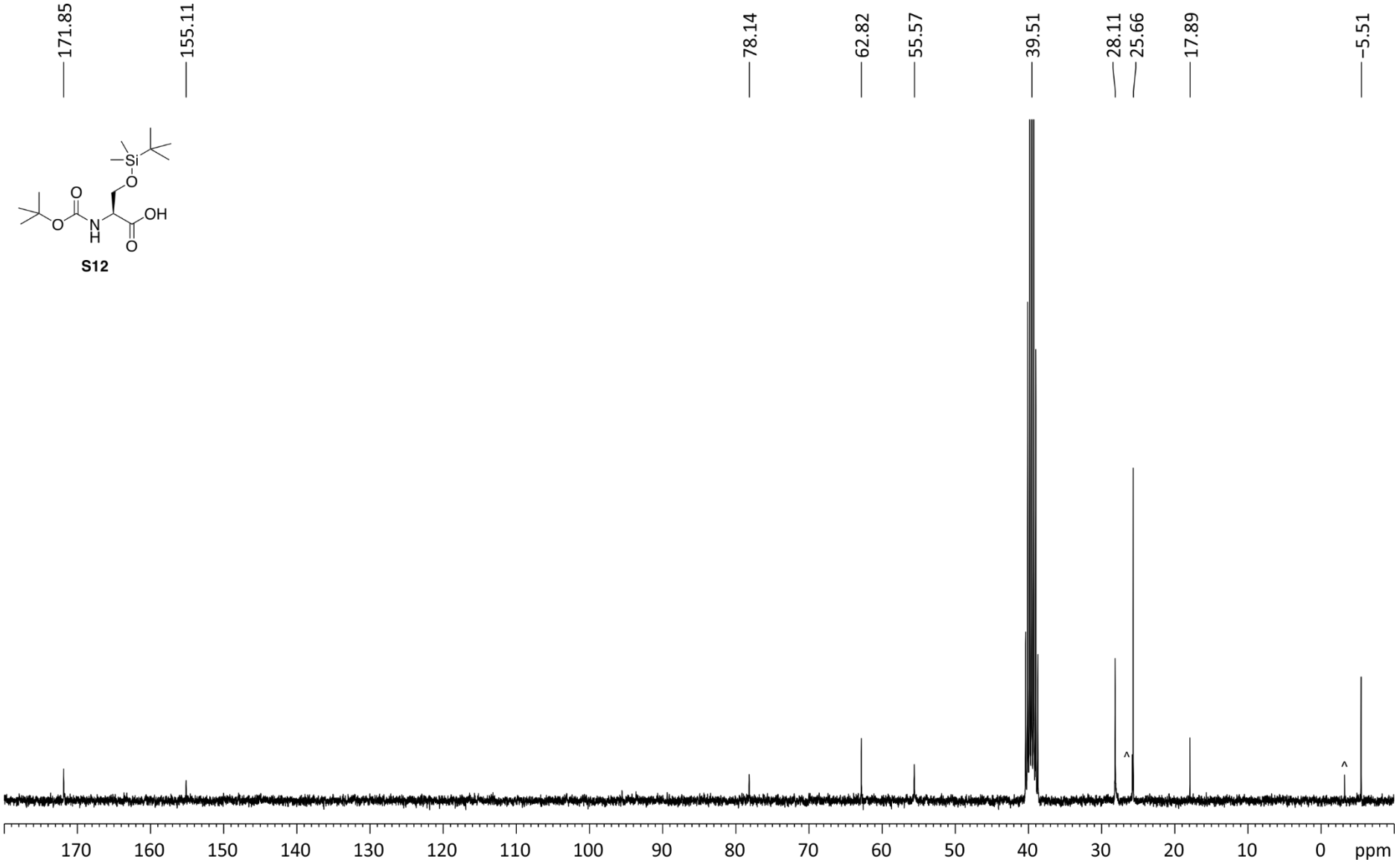

Figure S97: ^{13}C-NMR spectrum of Boc-Ser(TBS)-OH **S12** (75 MHz, 300 K, DMSO-d_6). ^ Signal of TBDMS-OH.

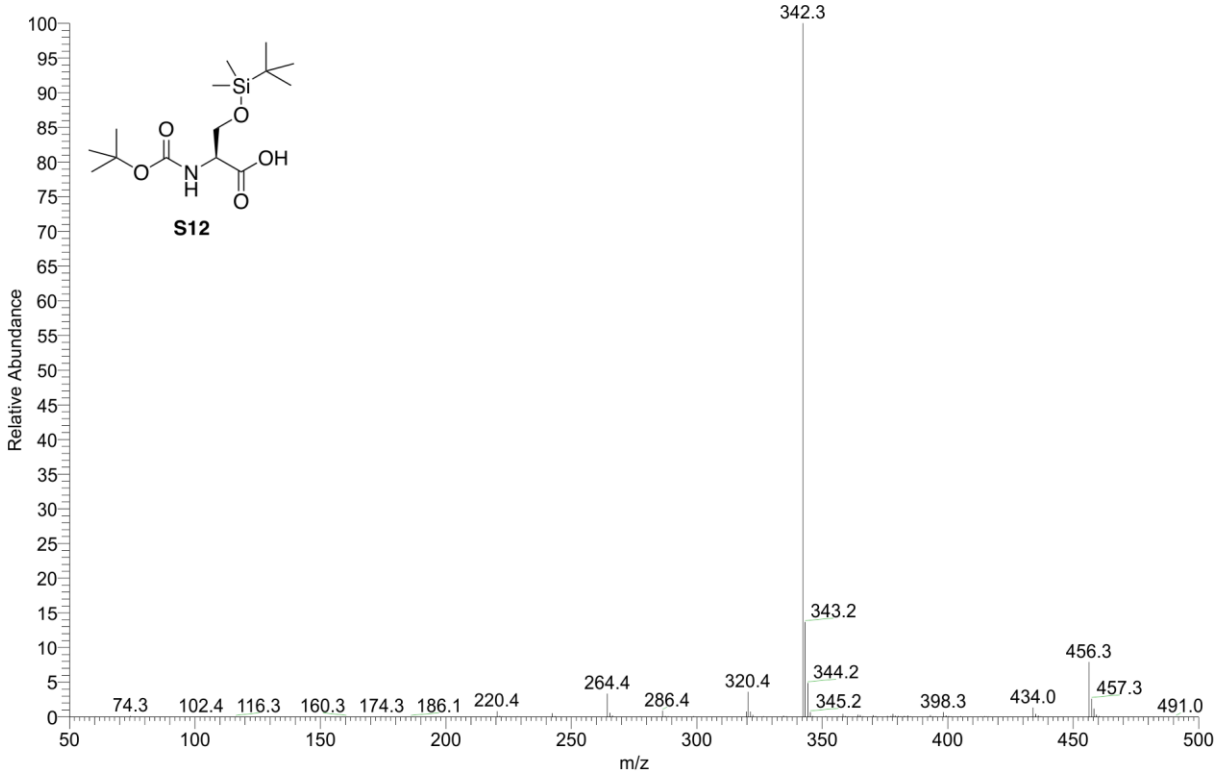

Figure S98: ESI+ mass spectrum with charge pattern m/z of Boc-Ser(TBS)-OH **S12**.

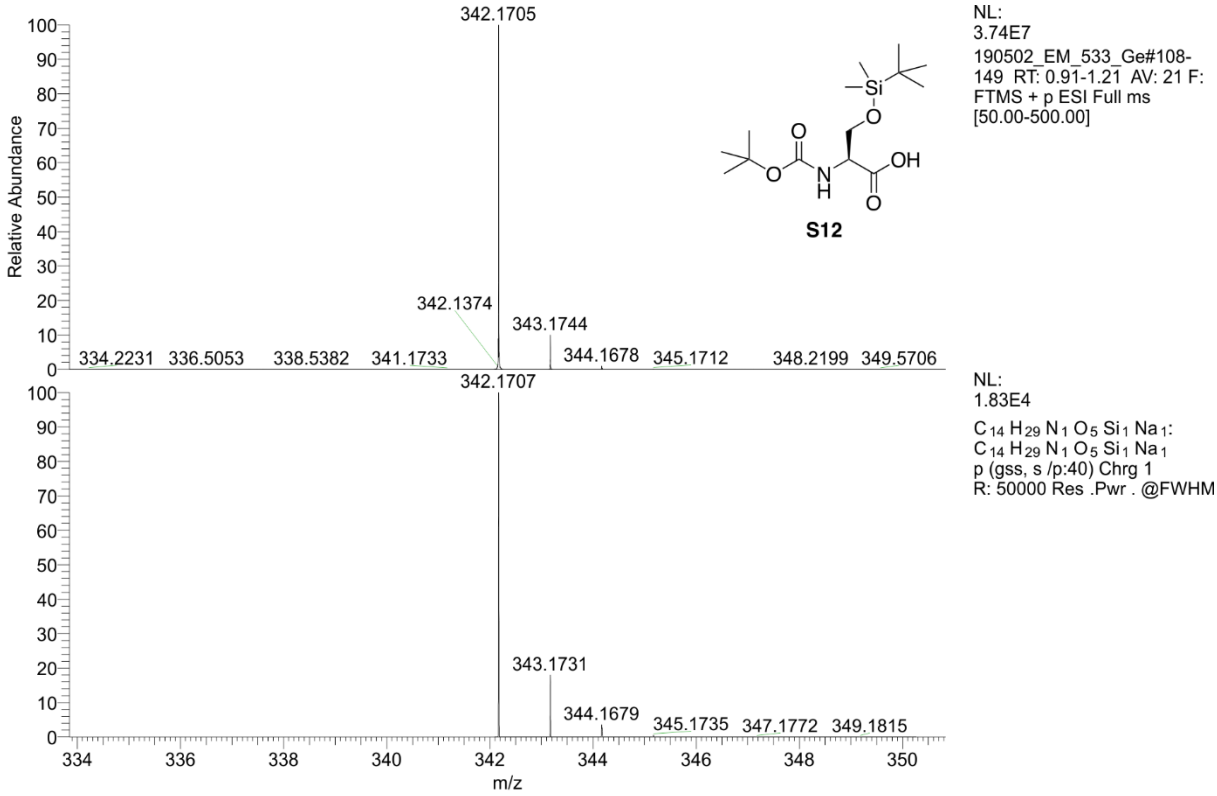

Figure S99: High resolution mass spectrum with isotope pattern of Boc-Ser(TBS)-OH **S12**.

Long-chain polyamines (LCPAa, S13a) and (LCPAb, S13b)

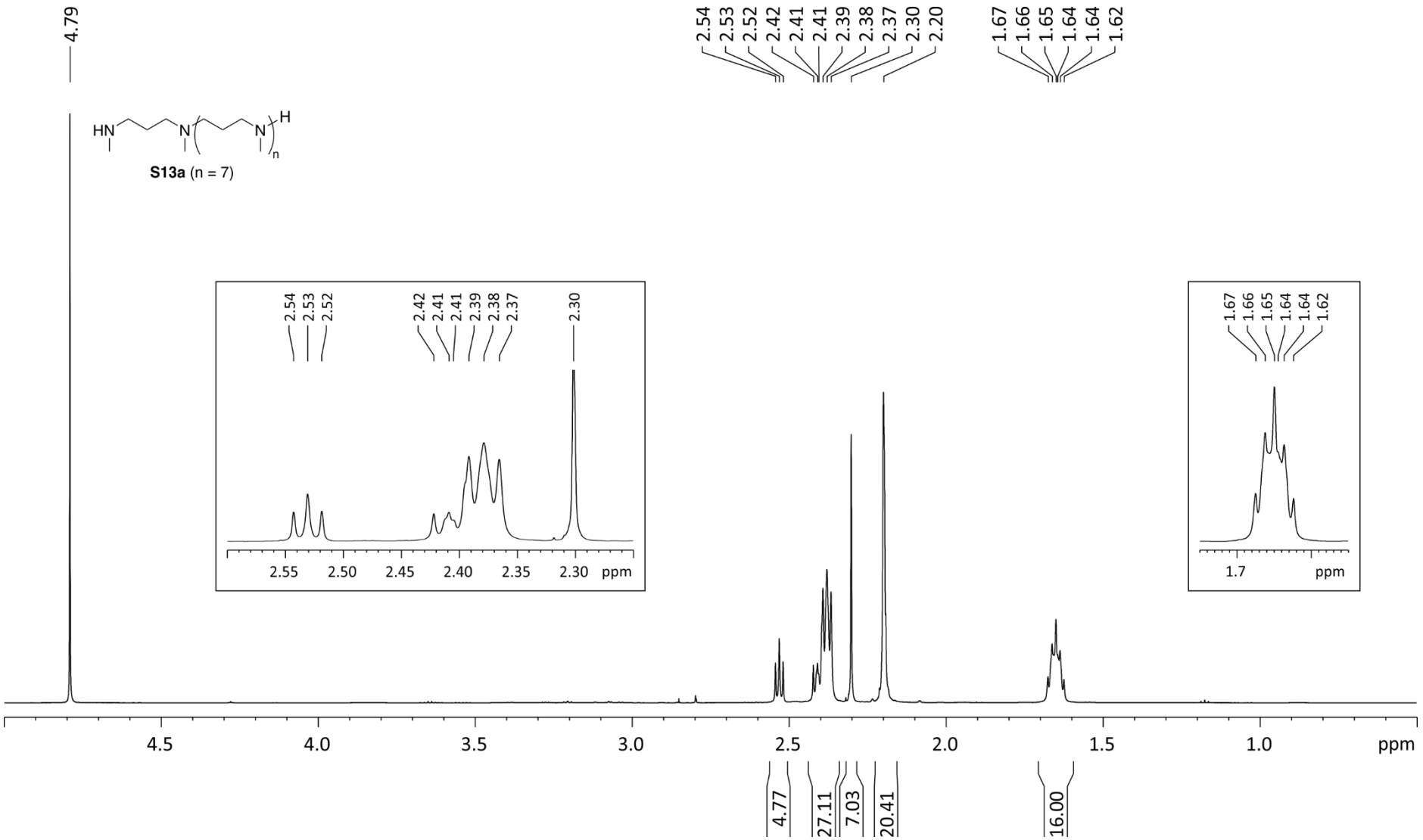

Figure S100: ^{1}H-NMR spectrum of LCPAa **S13a** (600 MHz, 300 K, D_2O).

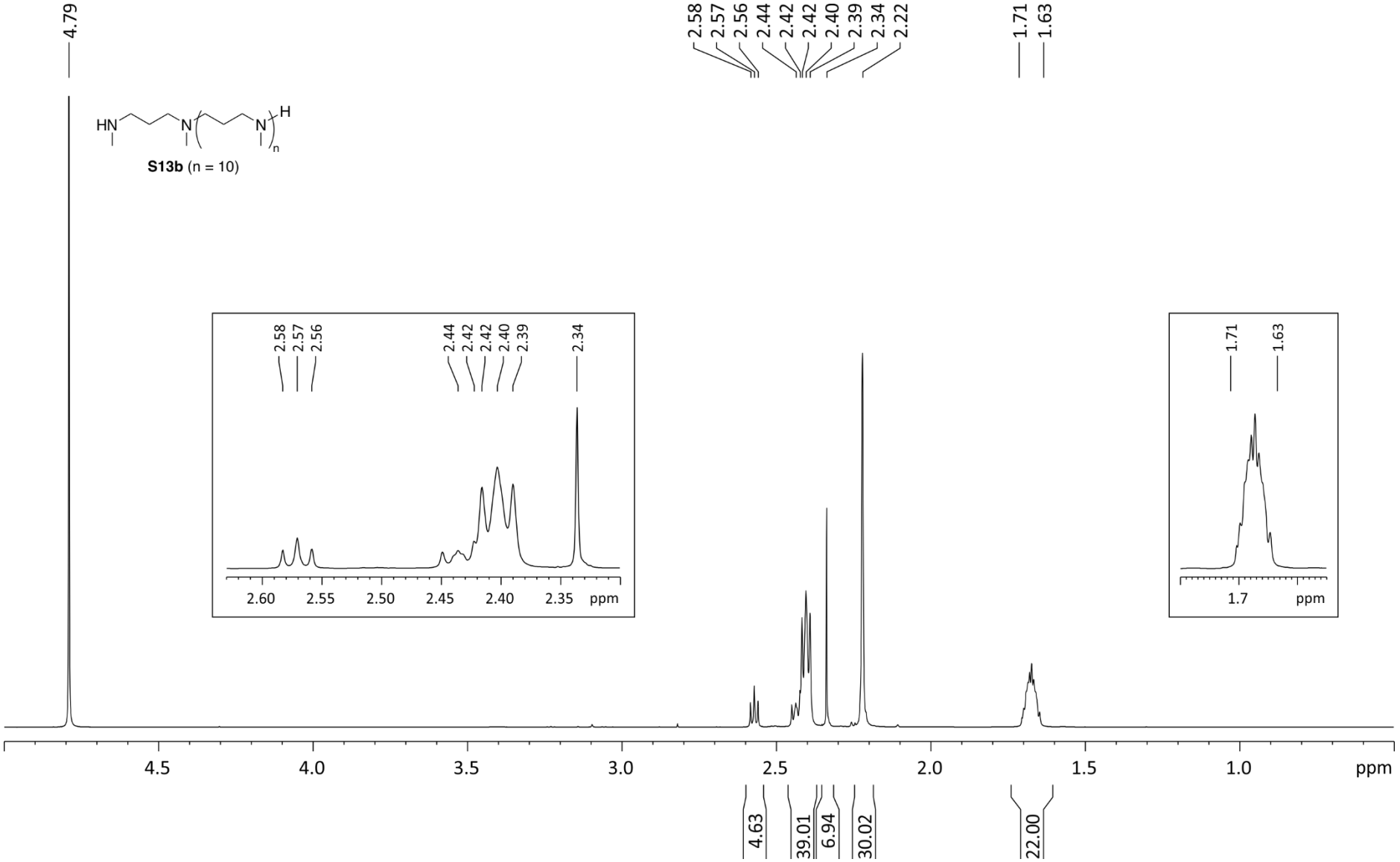

Figure S101: ^{1}H-NMR spectrum of LCPAa **S13b** (600 MHz, 300 K, D_2O).

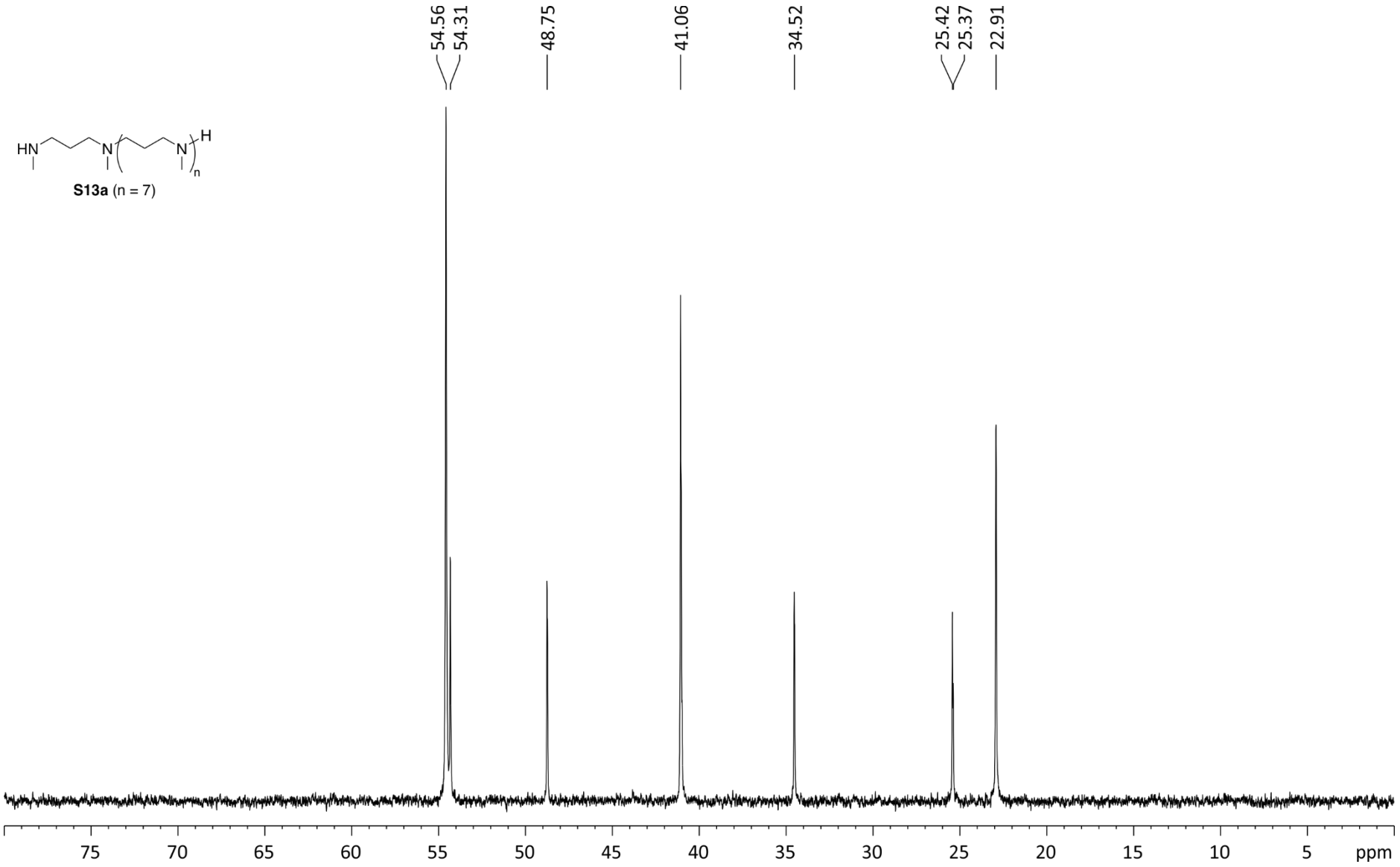

Figure S102: ^{13}C-NMR spectrum of LCPAa **S13b** (75 MHz, 300 K, D_2O).

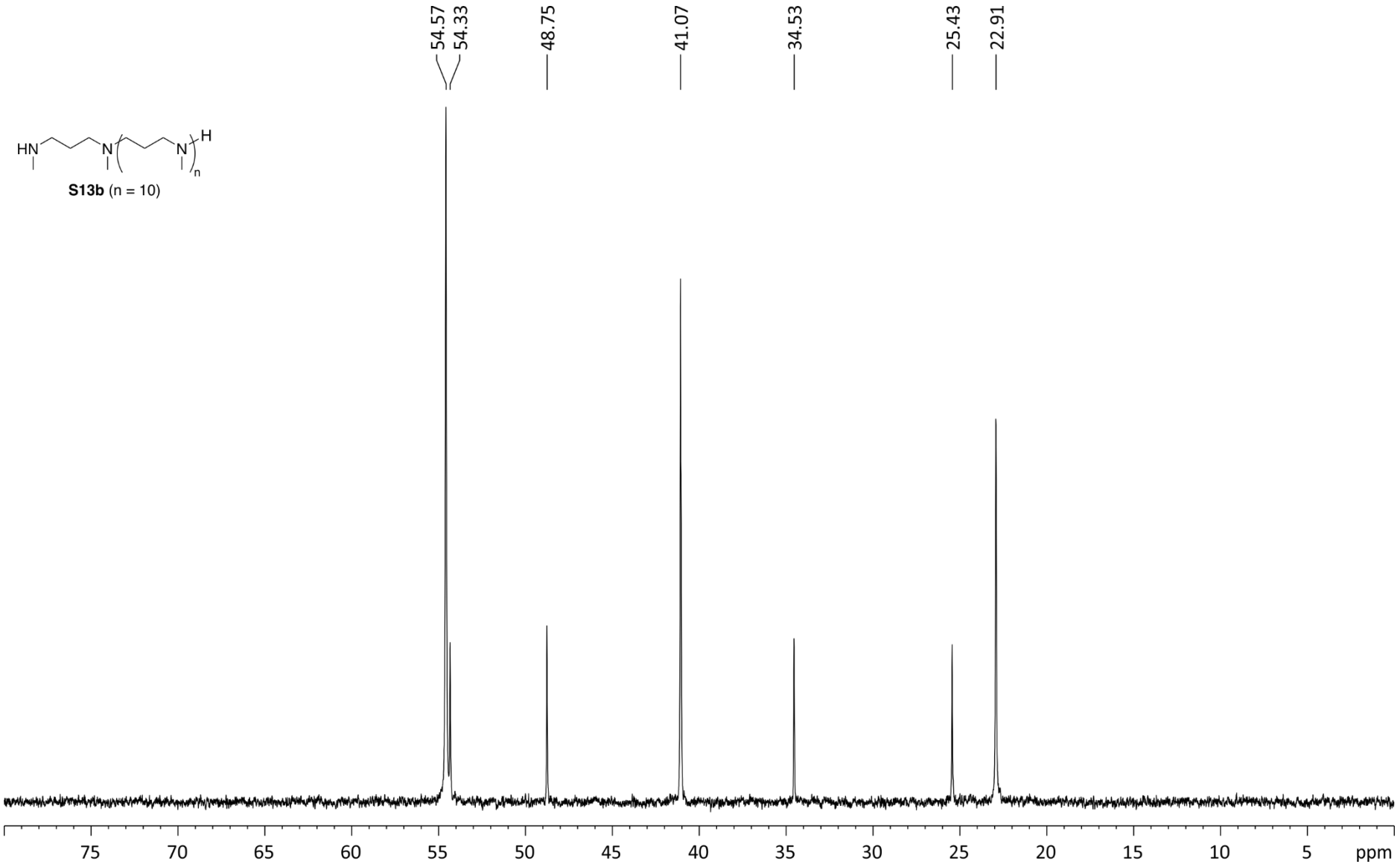

Figure S103: ^{13}C-NMR spectrum of LCPAa **S13a** (75 MHz, 300 K, D_2O).

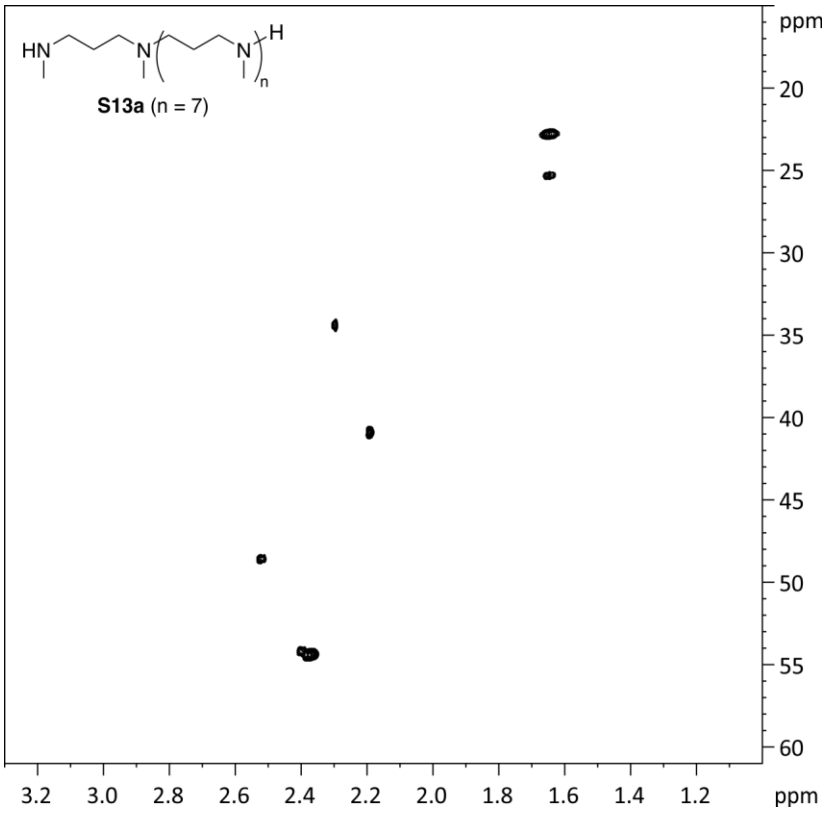

Figure S104: ^{1}H-^{13}C HSQC spectrum of LCPAa **S13a** (600 MHz, 300 K, D_2O).

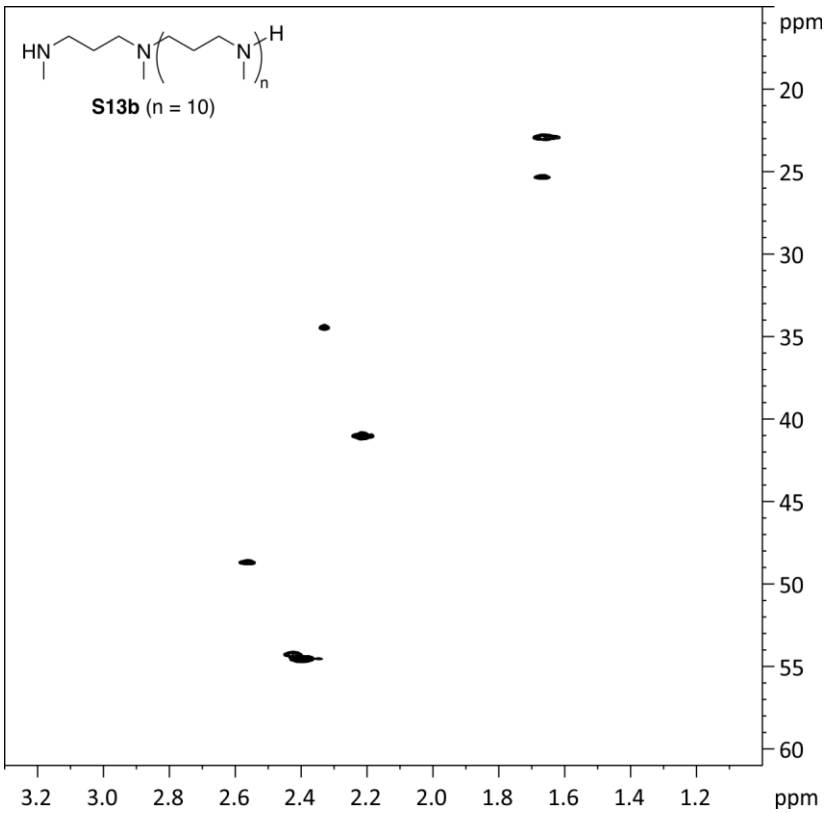

Figure S105: ^{1}H-^{13}C HSQC spectrum of LCPAa **S13b** (600 MHz, 300 K, D_2O).

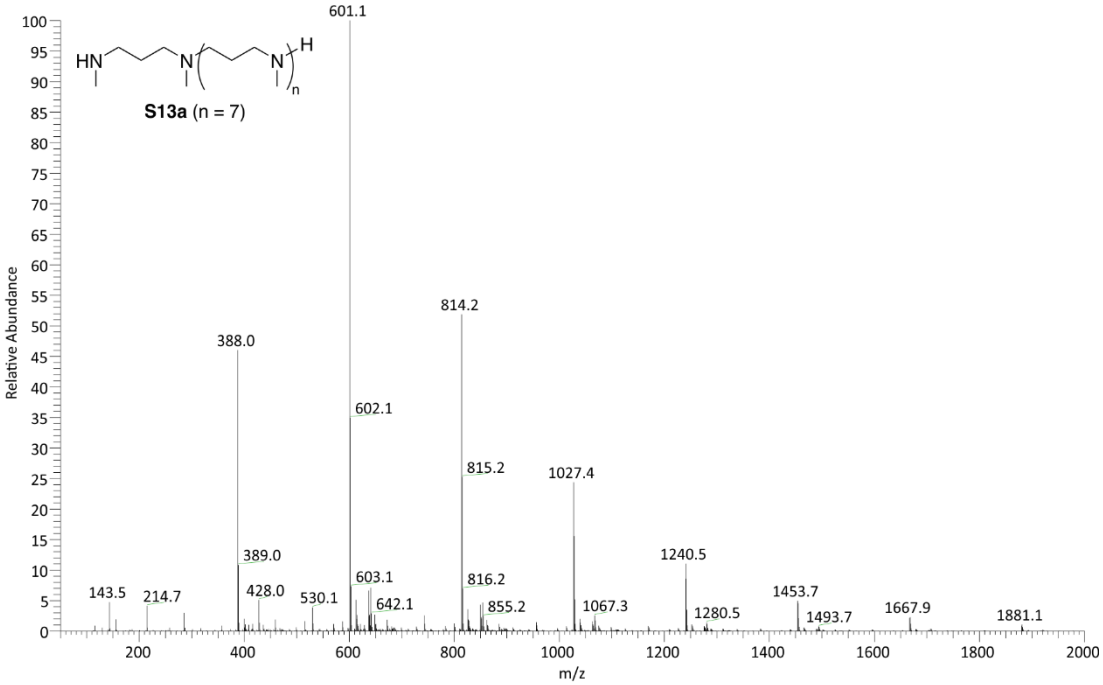

Figure S106: ESI+ mass spectrum with charge pattern m/z of LCPAa **S13a**. Distribution of chain length of LCPAa **S13a** mixture describes an approximate Gaussian function with n = 7 (601.1 m/z), n = 10 (814.2 m/z), n = 13 (1027.4 m/z), n = 16 (1240.5 m/z), n = 19 (1453.7 m/z), n = 22 (1667.9 m/z) and n = 25 (1881.1 m/z).

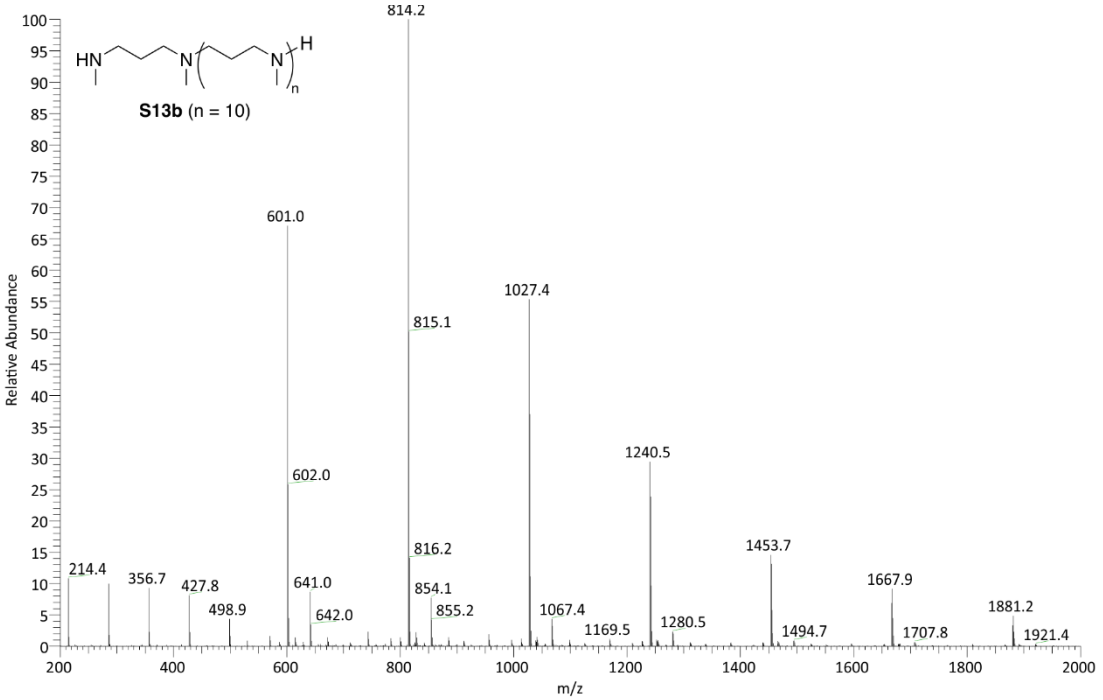

Figure S107: ESI+ mass spectrum with charge pattern m/z of LCPAa **S13b**. Distribution of chain length of LCPAa **S13b** mixture describes an approximate Gaussian function with n = 7 (601.1 m/z), n = 10 (814.2 m/z), n = 13 (1027.4 m/z), n = 16 (1240.5 m/z), n = 19 (1453.7 m/z), n = 22 (1667.9 m/z) and n = 25 (1881.1 m/z).

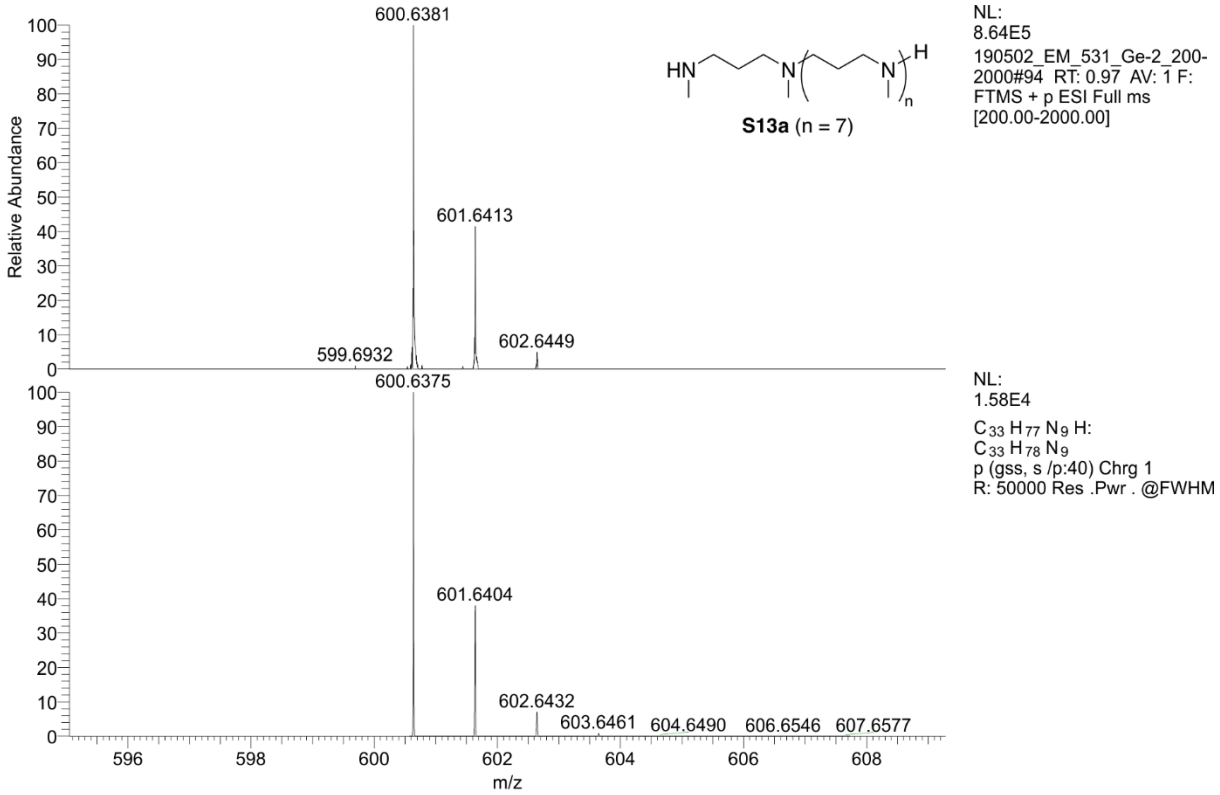

Figure S108: High resolution mass spectrum with isotope pattern of LCPAa **S13a** with a chain length of 9 nitrogen.

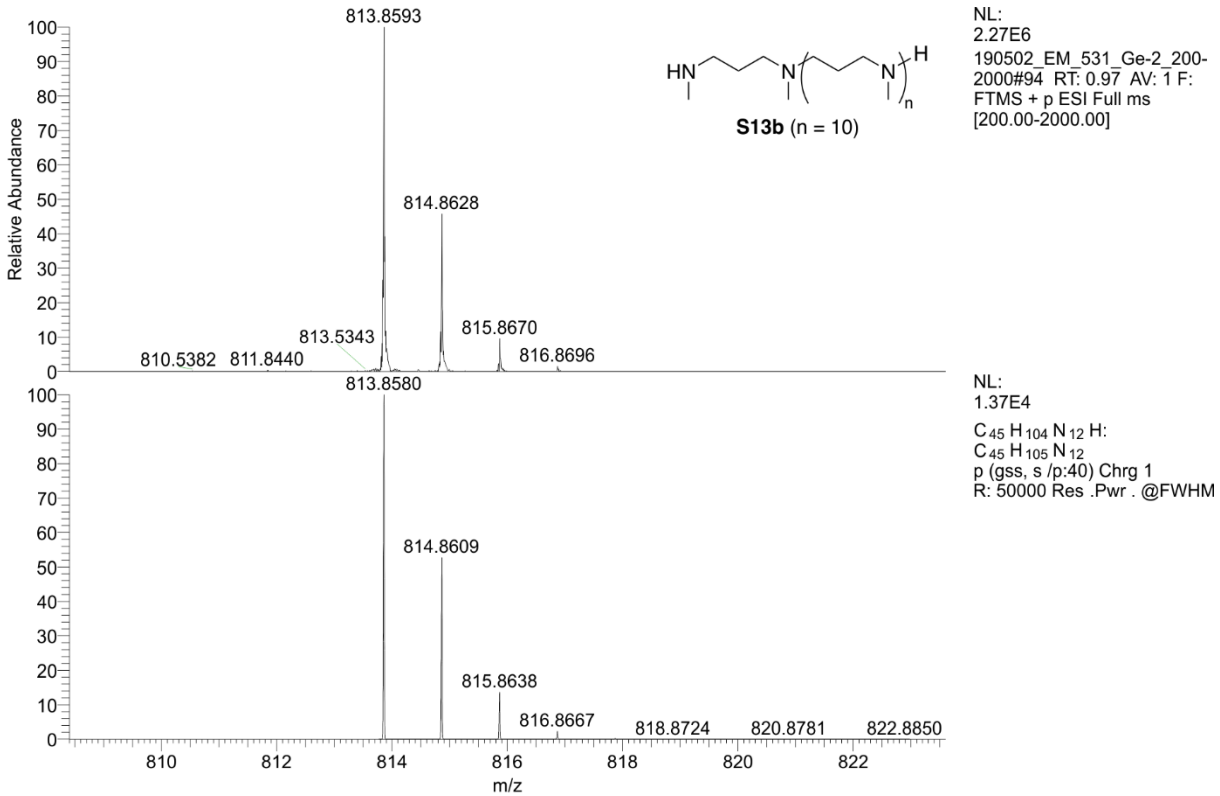

Figure S109: High resolution mass spectrum with isotope pattern of LCPAb **S13b** with a chain length of 12 nitrogen.

Ser-pSer-Lys-Lys-Ser-Gly-pSer-Tyr-Ser-Gly-pSer-Lys-Gly-Ser-Lys (p3-Sil01, S14)

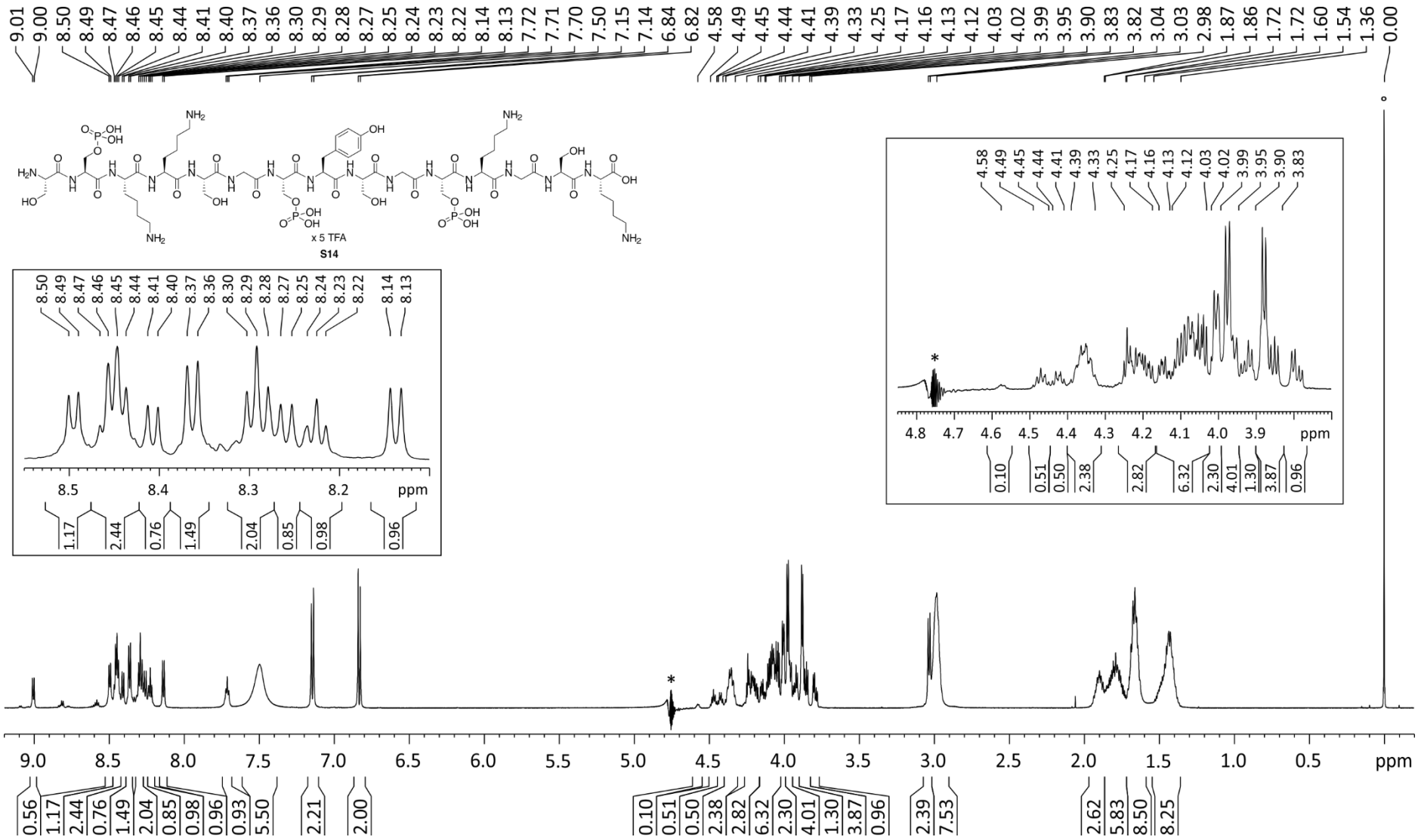

Figure S110: ^{1}H-NMR spectrum of p3-Sil01 **S14** (600 MHz, 300 K, H_2O/D_2O (9:1), pH 3.0). * Signal of H_2O. ° Signal of the internal standard TSP-d_4.

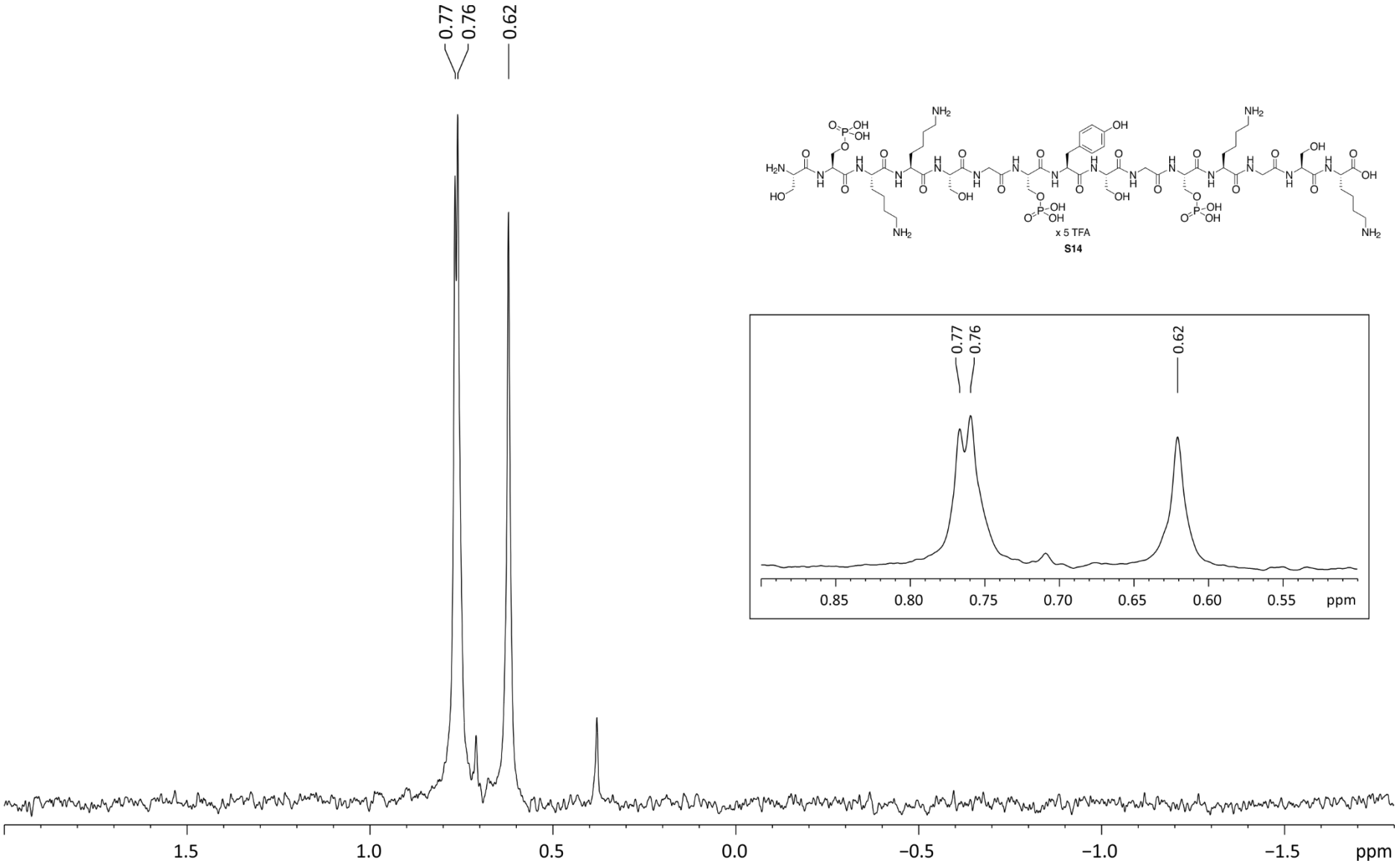

Figure S111: $^{31}P\{^{1}H\}$-NMR spectrum of p3-Sil01 **S14** (202 MHz, 300 K, H_2O/D_2O (9:1), pH 3.0).

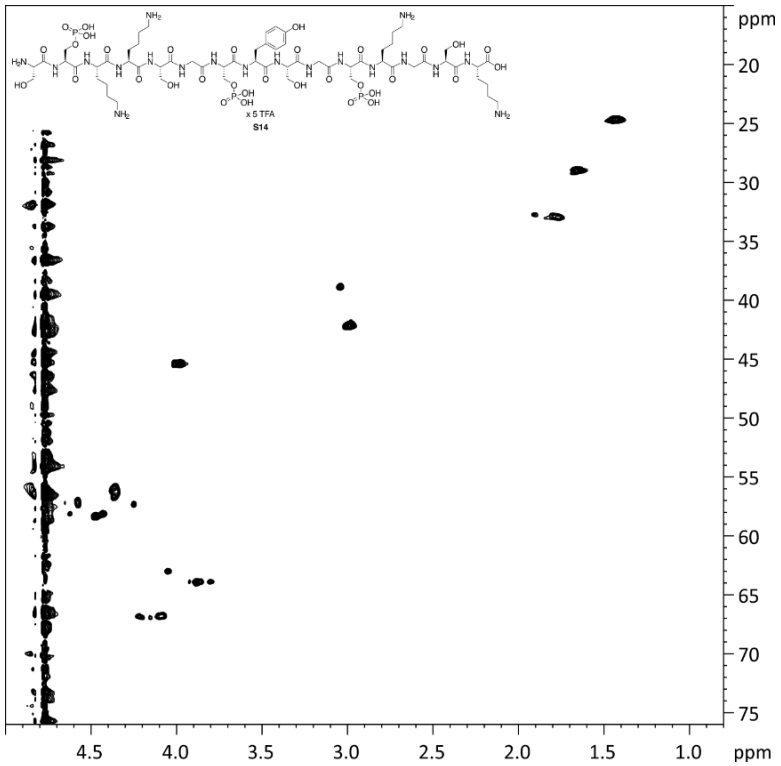

Figure S112: ^{1}H-^{13}C HSQC spectrum of p3-Sil01 **S14** (600 MHz, 300 K, H_2O/D_2O (9:1), pH 3.0).

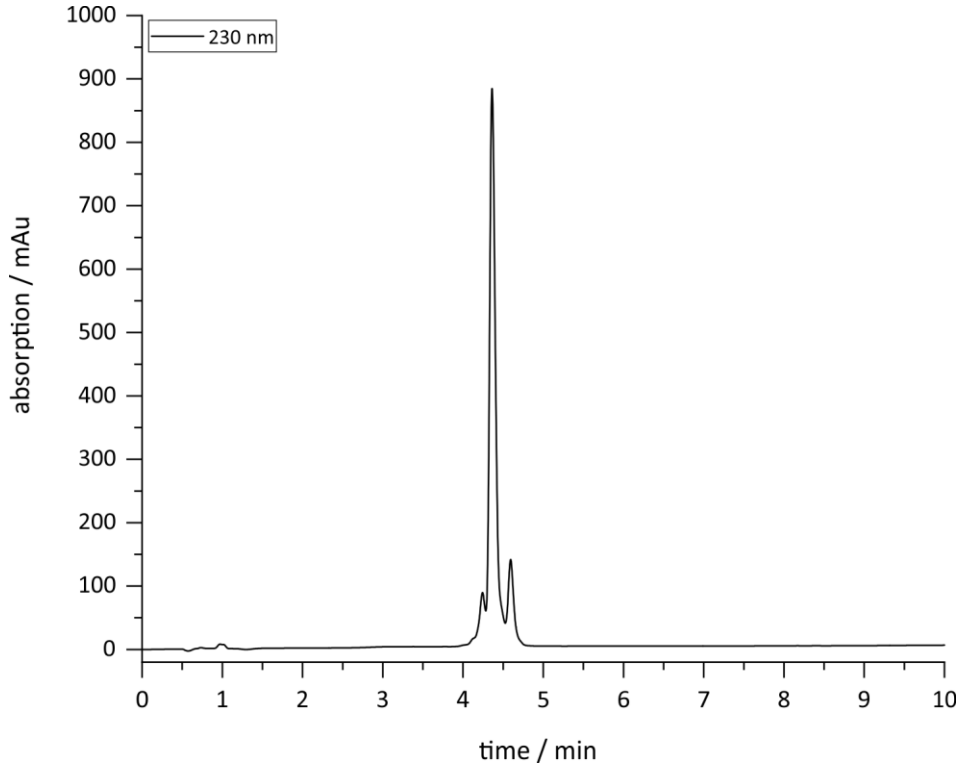

Figure S113: Chromatogram of p3-Sil01 **S14**. t_R = 4.360 min, purity ≥ 85%, (0% → 30% MeCN + 0.085% TFA in H_2O + 0.1% TFA, 10 min, 28 °C, 0.45 mL/min, 230 nm, ACE Ultracore 2.5 SuperC18, 150 mm x 2.1 mm).

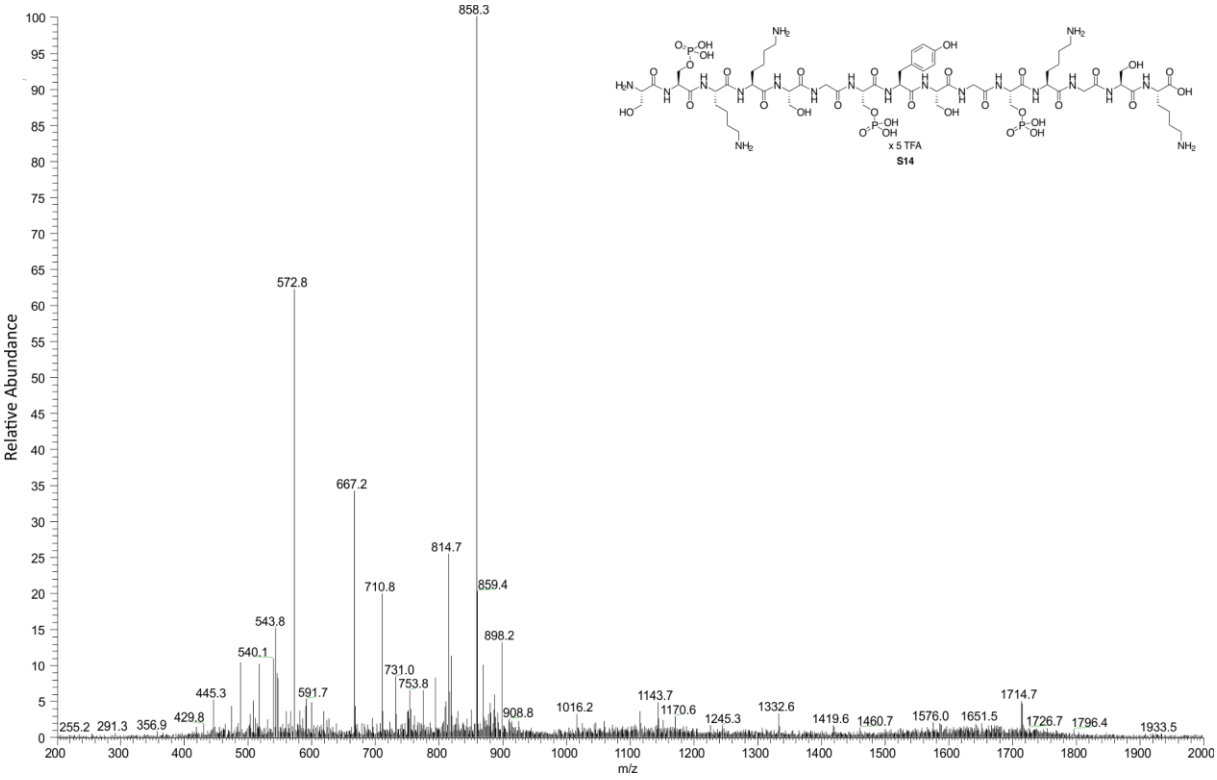

Figure S114: ESI+ mass spectrum with charge pattern m/z of p3-Sil01 **S14** with z = 1 (1714.7 m/z), z = 2 (858.3 m/z) and z = 3 (572.8 m/z).

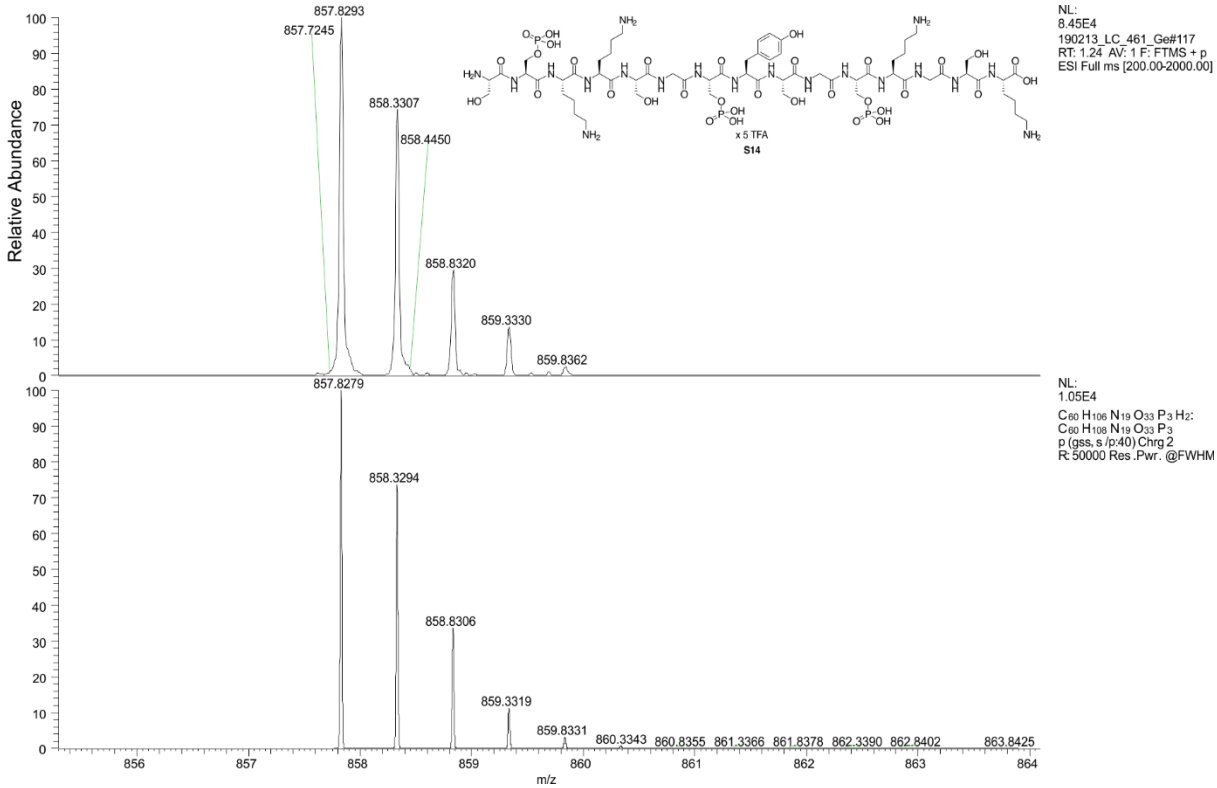

Figure S115: High resolution mass spectrum with isotope pattern of p3-Sil01 **S14**.

pSer-pSer-Lys-Lys-pSer-Gly-pSer-Tyr-pSer-Gly-pSer-Lys-Gly-pSer-Lys (p7-Sil01, S15)

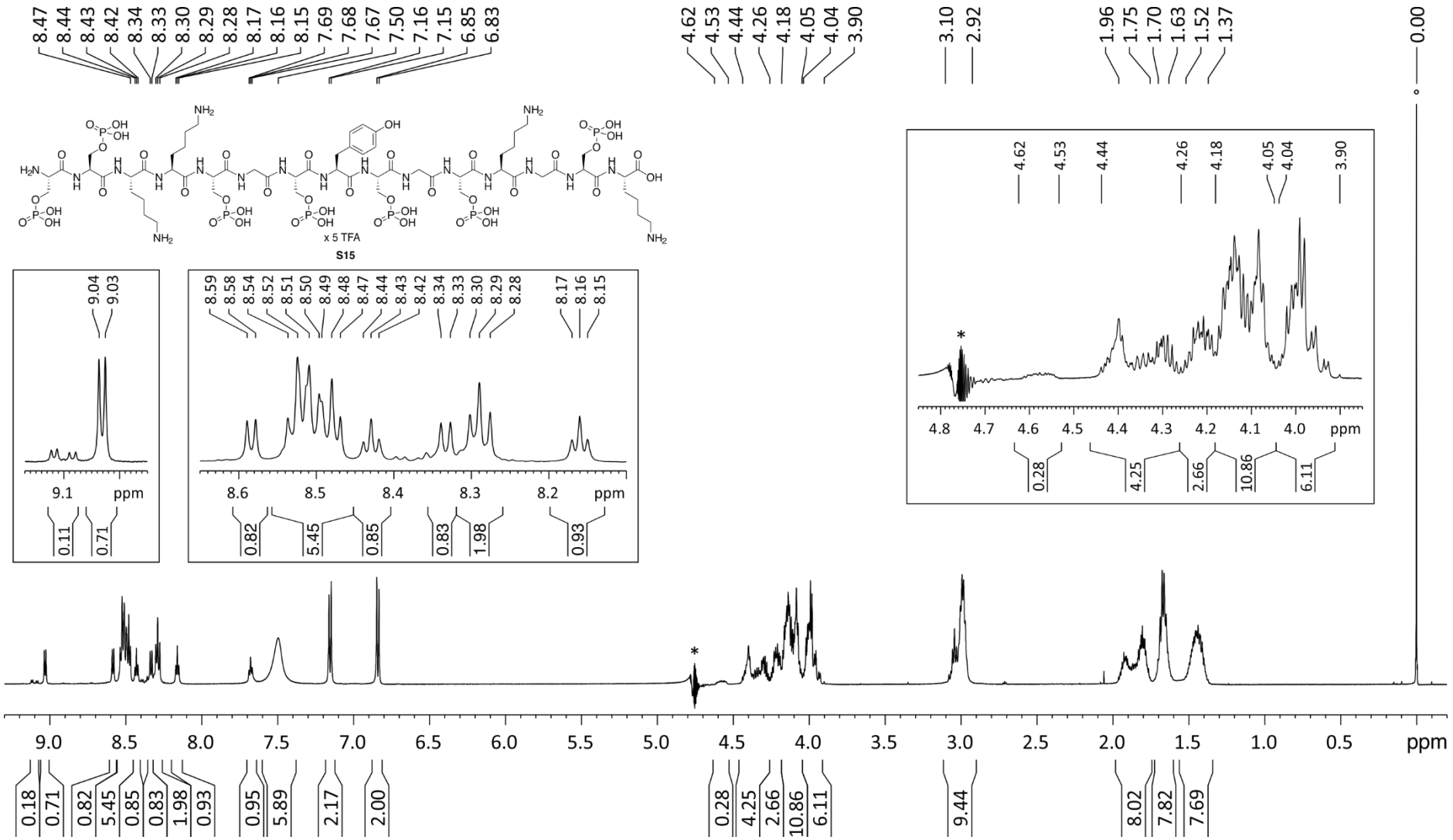

Figure S116: ^{1}H-NMR spectrum of p7-Sil01 **S15** (600 MHz, 300 K, H_2O/D_2O (9:1), pH 3.0). The integral ratios result in an NMR purity of ≥ 85 %.* Signal of H_2O. ° Signal of the internal standard TSP-d_4.

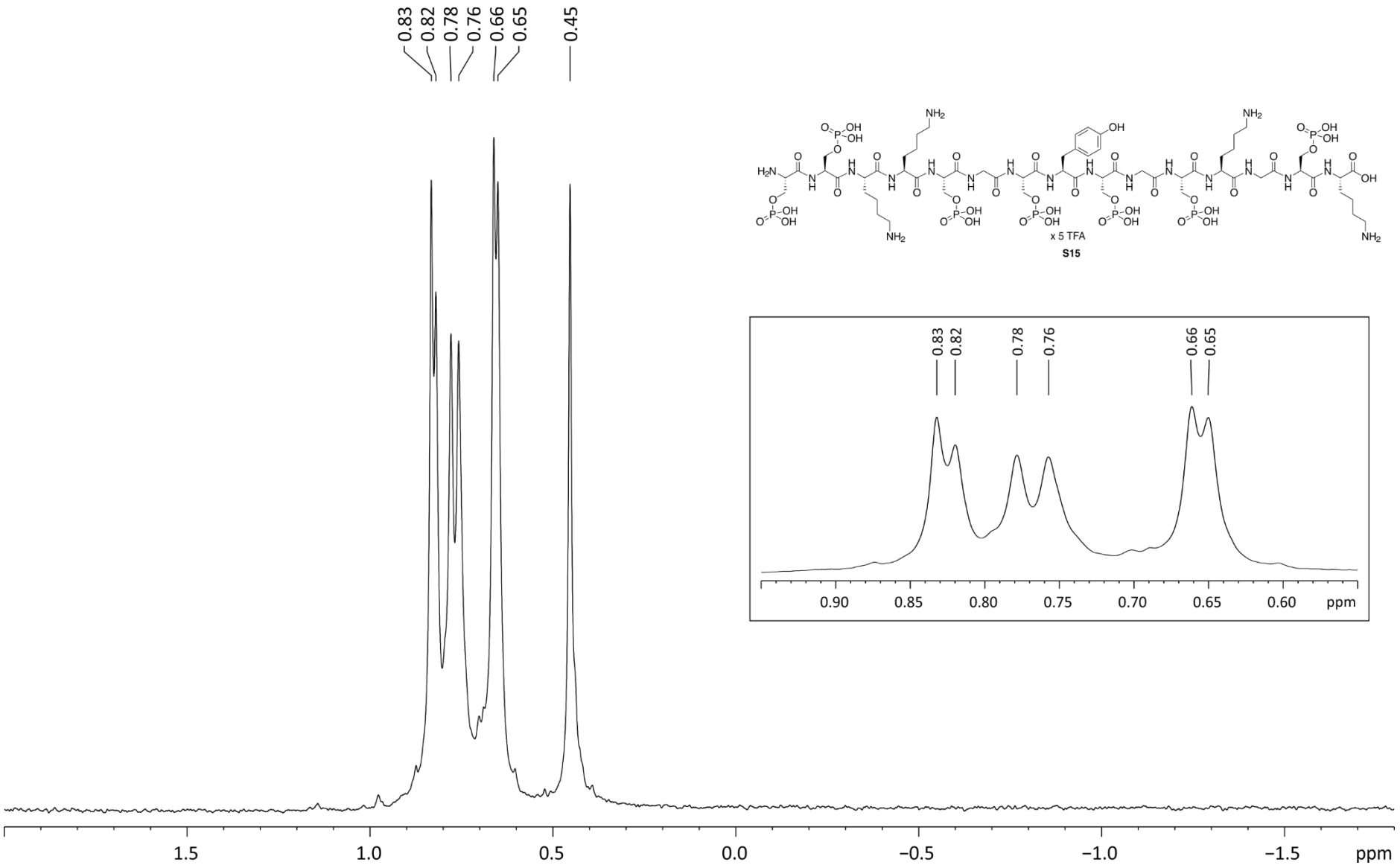

Figure S117: $^{31}P\{^{1}H\}$-NMR spectrum of p7-Sil01 **S15** (202 MHz, 300 K, H_2O/D_2O (9:1), pH 3.0).

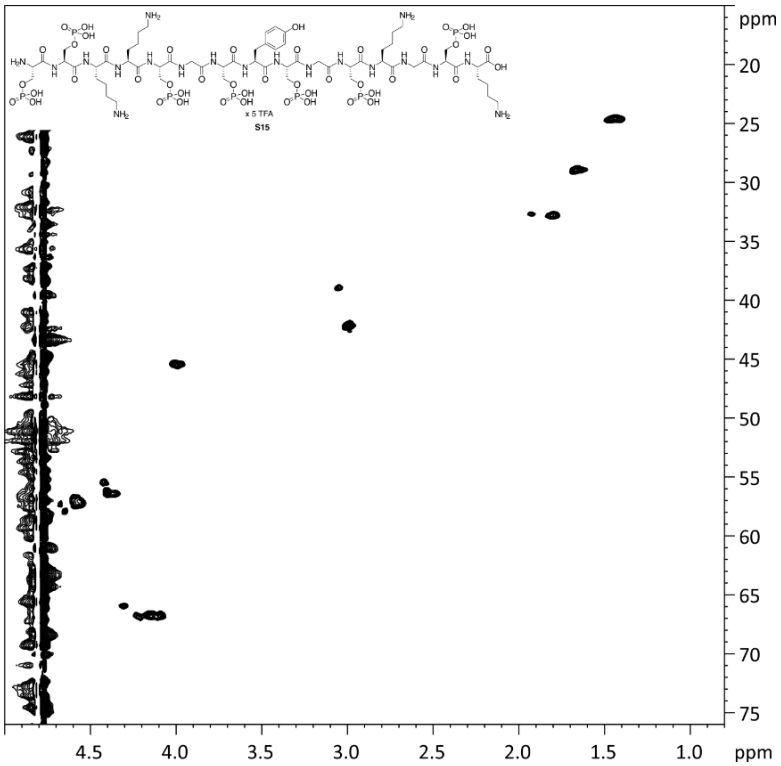

Figure S118: ^{1}H-^{13}C HSQC spectrum of p7-Sil01 **S15** (600 MHz, 300 K, H_2O/D_2O (9:1), pH 3.0).

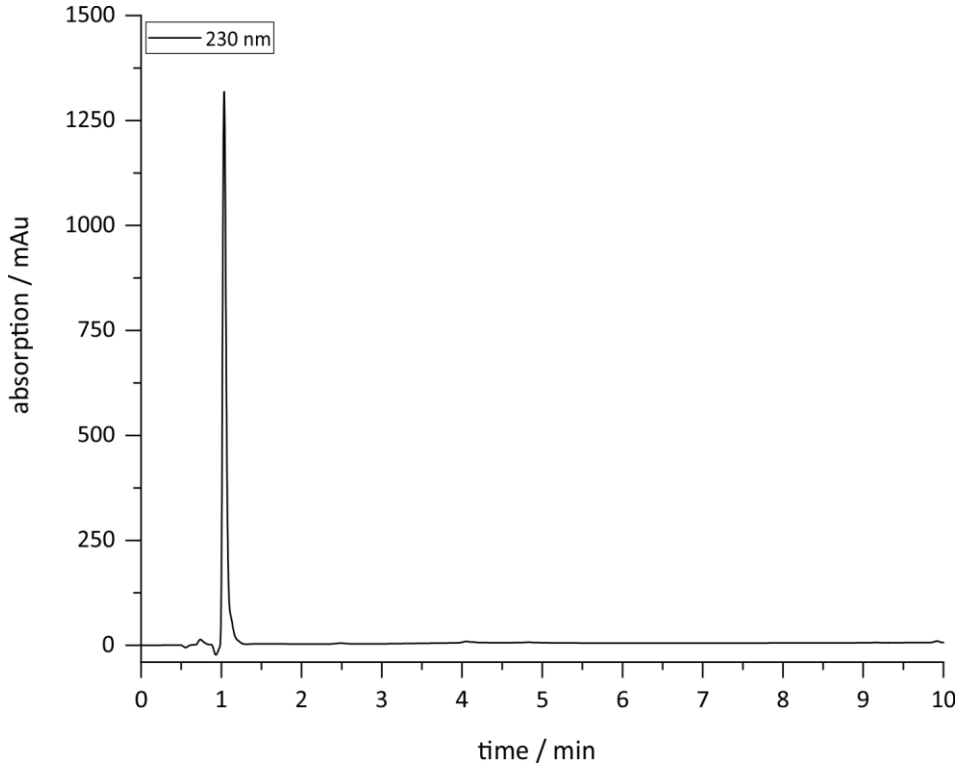

Figure S119: Chromatogram of p7-Sil01 **S15**. t_R = 1.037 min, (1% → 30% MeCN + 0.085% TFA in H_2O + 0.1% TFA, 10 min, 28 °C, 0.45 mL/min, 230 nm, ACE Ultracore 2.5 SuperC18, 150 mm x 2.1 mm).

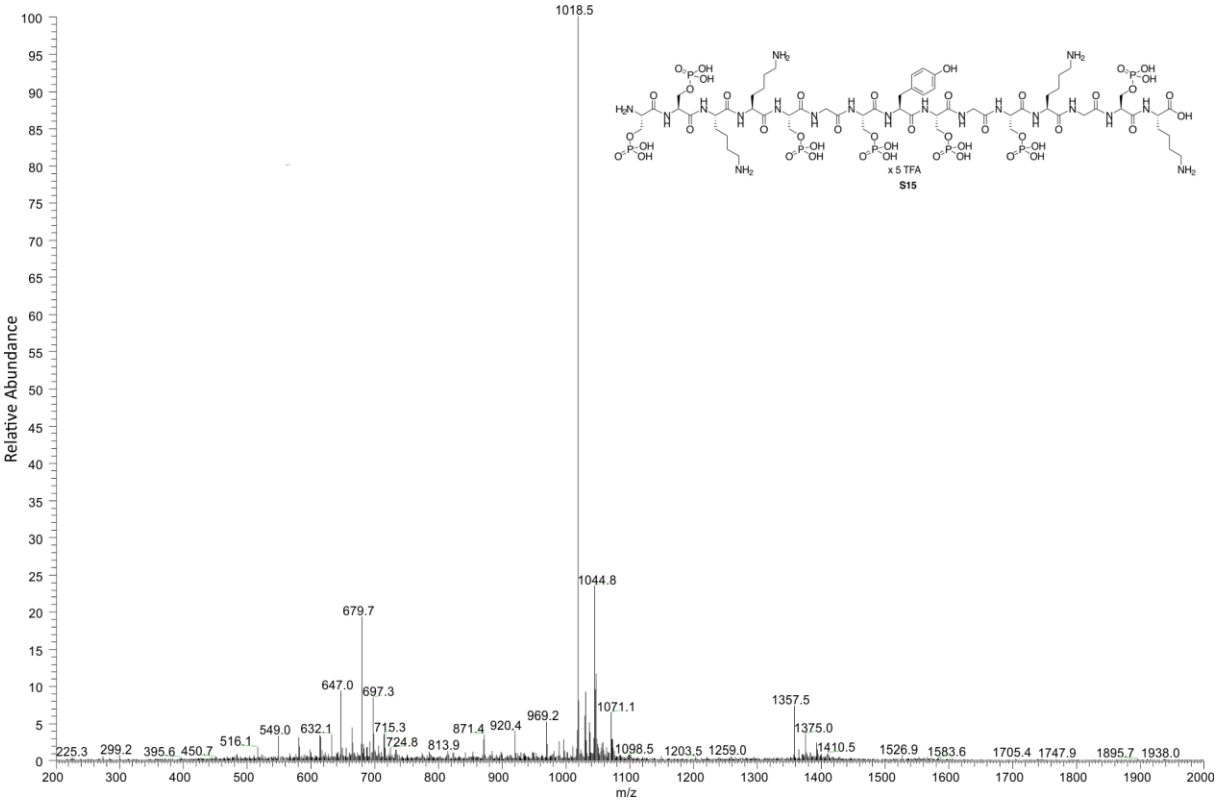

Figure S120: ESI+ mass spectrum with charge pattern m/z of p7-Sil01 **S15** with z = 2 (1018.6 m/z), and z = 3 (679.7 m/z).

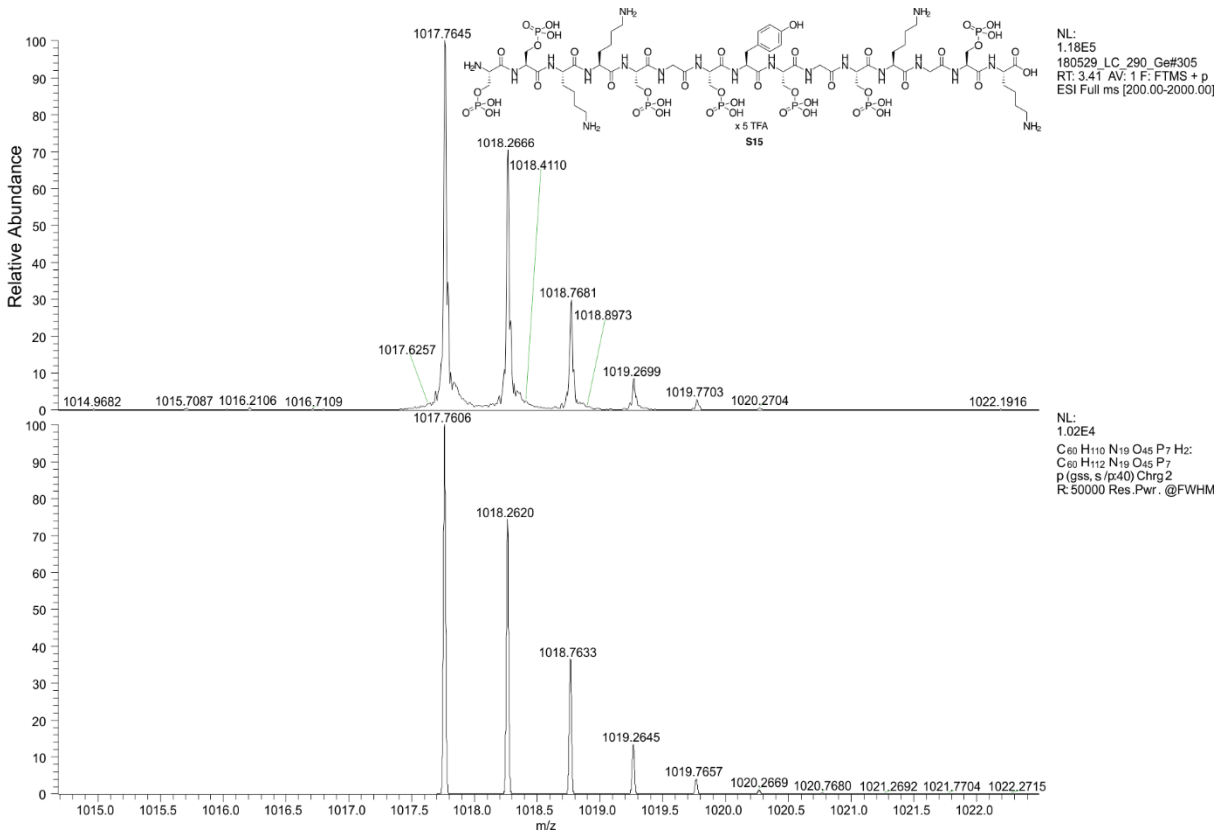

Figure S121: High resolution mass spectrum with isotope pattern of p7-Sil01 **S15**.

pSer-pSer-Kdp(NH)$_2$(Me)$_2$-Lys(Me)$_2$-pSer-Gly-pSer-Tyr-pSer-Gly-pSer-pHyl(Me)$_3$-Gly-pSer-Kdp(NH)$_2$(Me)$_2$ (*syn*Sil-1A$_1$, S16)

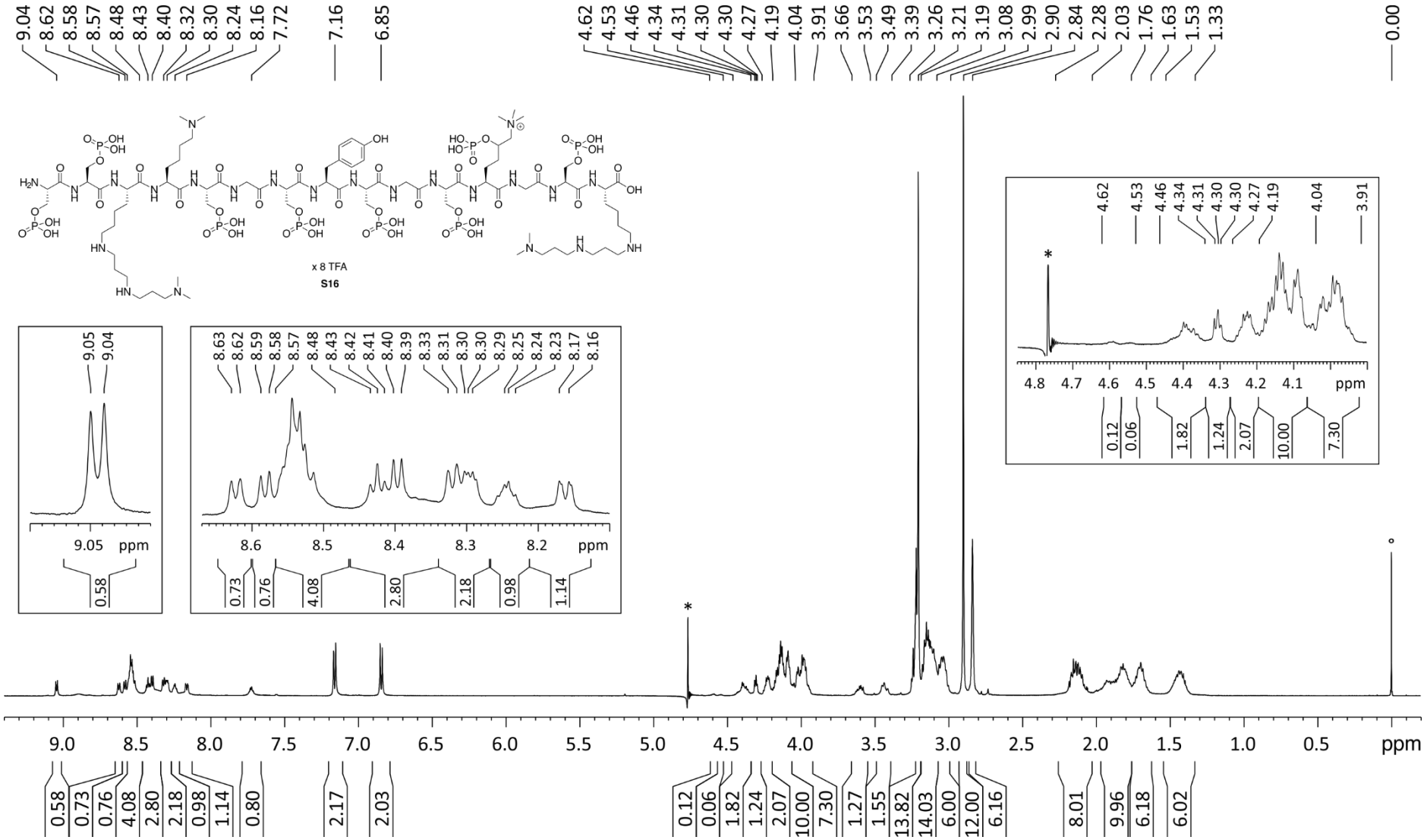

Figure S122: ^{1}H-NMR spectrum of *syn*Sil-1A$_1$ **S16** (600 MHz, 300 K, H_2O/D_2O (9:1), pH 3.0). * Signal of H_2O. ° Signal of the internal standard TSP-d_4.

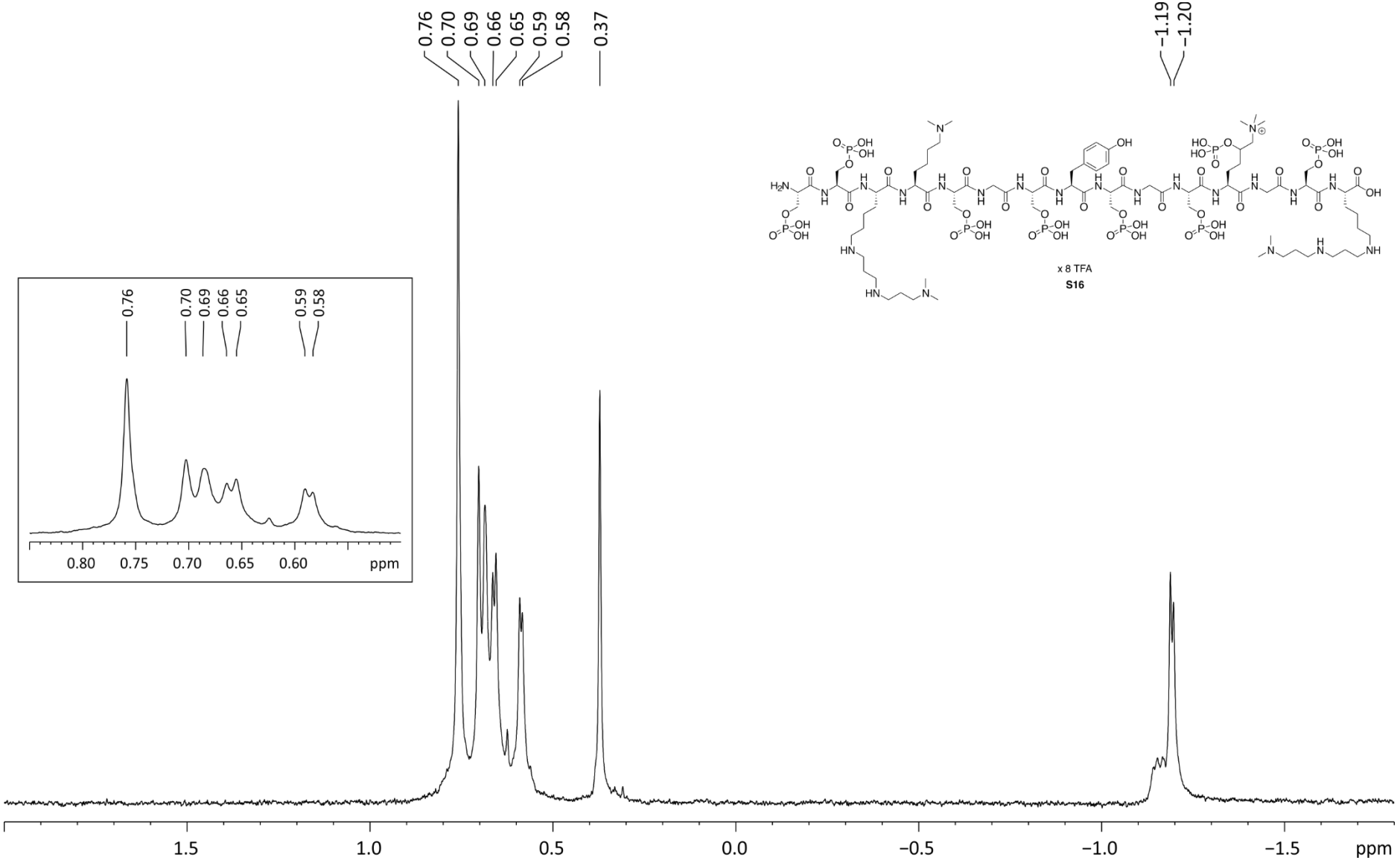

Figure S123: $^{31}P\{^{1}H\}$-NMR spectrum of *syn*Sil-1A$_1$ **S16** (202 MHz, 300 K, H_2O/D_2O (9:1), pH 3.0).

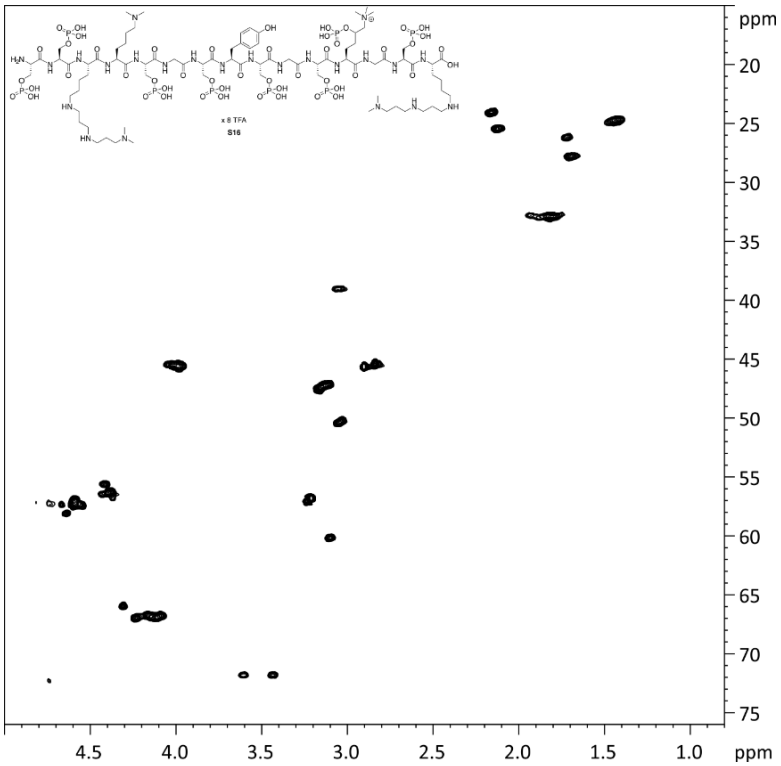

Figure S124: ^{1}H-^{13}C HSQC spectrum of *syn*Sil-1A$_1$ **S16** (600 MHz, 300 K, H_2O/D_2O (9:1), pH 3.0).

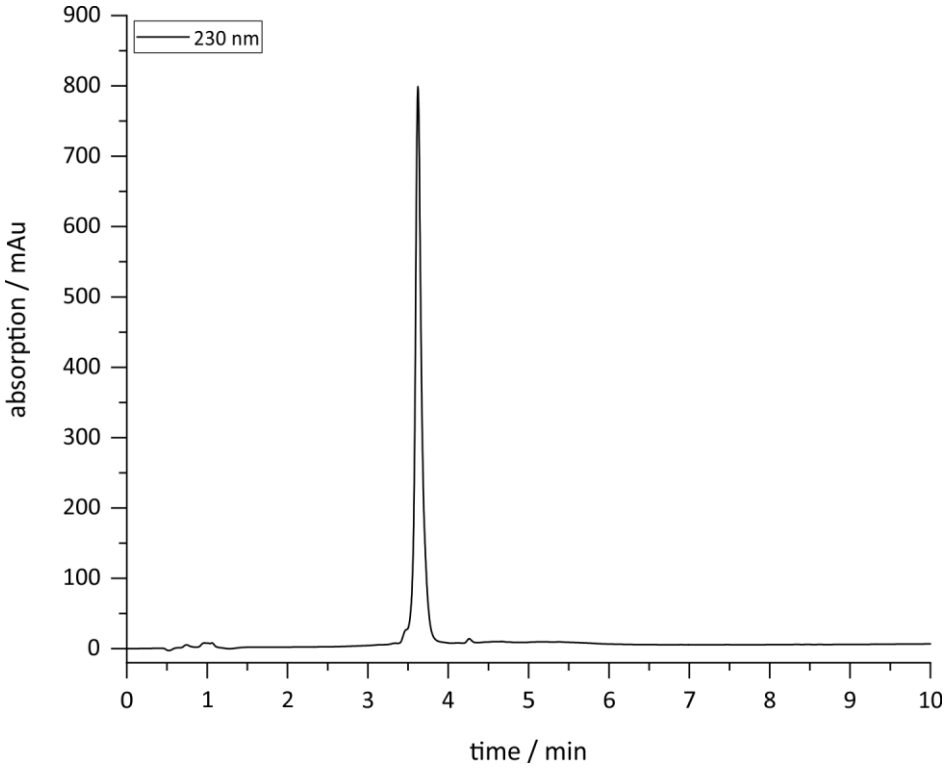

Figure S125: Chromatogram of *syn*Sil-1A$_1$ **S16**. t_R = 3.623 min, purity ≥ 98%, (0% → 30% MeCN + 0.085% TFA in H_2O + 0.1% TFA, 10 min, 28 °C, 0.45 mL/min, 230 nm, ACE Ultracore 2.5 SuperC18, 150 mm x 2.1 mm).

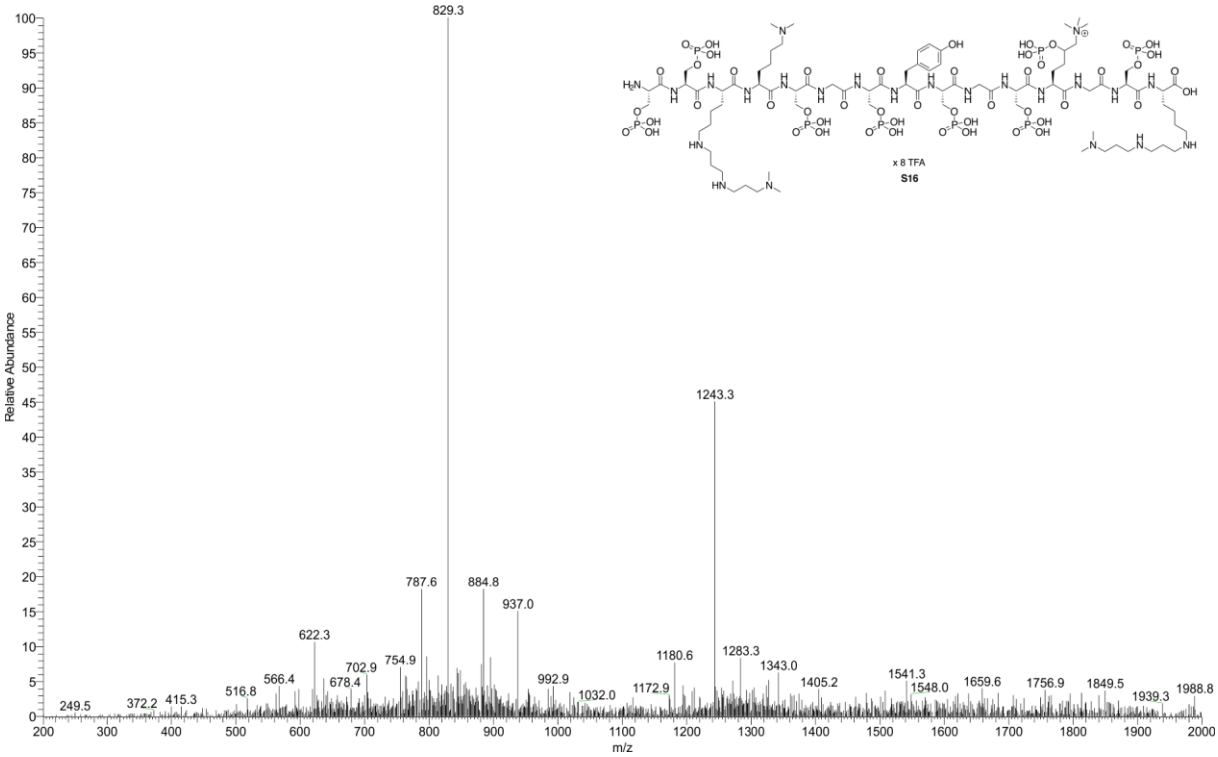

Figure S126: ESI+ mass spectrum with charge pattern m/z of *syn*Sil-1A$_1$ **S16** with z = 2 (1243.3 m/z), z = 3 (829.3 m/z),and z = 4 (622.3 m/z).

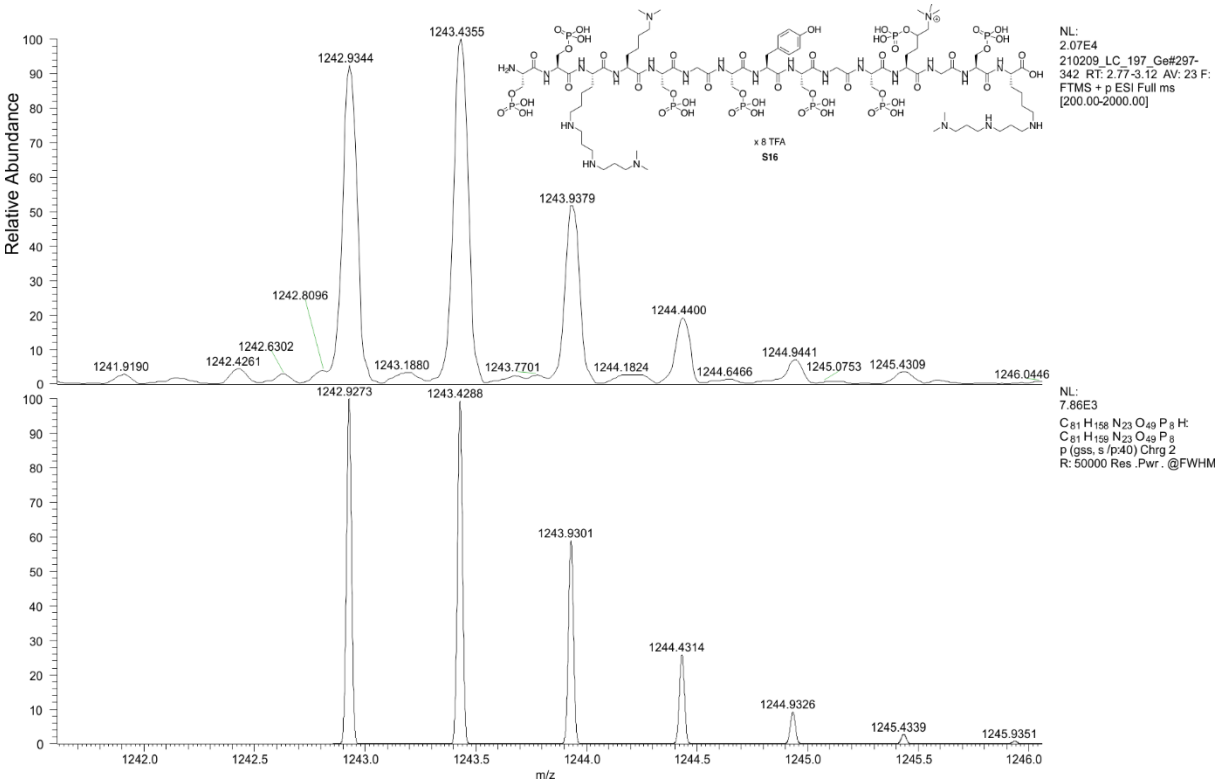

Figure S127: High resolution mass spectrum with isotope pattern of *syn*Sil-1A$_1$ **S16**.

Supplementary Information References

1 P. Danner, M. Morkunas and M. E. Maier, *Org. Lett.*, 2013, **15**, 2474.

2 A. Padwa, P. Rashatasakhon, A. D. Ozdemir and J. Willis, *J. Org. Chem.*, 2005, **70**, 519.

3 V. V. Annenkov, S. N. Zelinskiy, E. N. Danilovtseva and C. C. Perry, *Arkivoc*, 2009, **13**, 116.

4 E. Kaiser, R. L. Colescott, C. D. Bossinger and P. I. Cook, *Anal. Biochem.*, 1970, **34**, 595.

5 W. S. Hancock and J. E. Battersby, *Anal. Biochem.*, 1976, **71**, 260.

6 T. Vojkovsky, *Pept. Res.*, 1995, **8**, 236.

7 N. Kröger, S. Lorenz, E. Brunner and M. Sumper, *Science*, 2002, **298**, 584.

8 F. Daus, E. Pfeifer, K. Seipp, N. Hampp and A. Geyer, *Org. Biomol. Chem.*, 2020, **18**, 700.

9 R. K. Iler, *The chemistry of silica. Solubility, polymerization, colloid and surface properties, and biochemistry*, Wiley, New York, NY, 1979.

10 R. Wieneke, A. Bernecker, R. Riedel, M. Sumper, C. Steinem and A. Geyer, *Org. Biomol. Chem.*, 2011, **9**, 5482.

11 A. Krezel and W. Bal, *J. Inorg. Biochem.*, 2004, **98**, 161.

12 a) C. S. Johnson, *Prog. Nucl. Magn. Reson. Spectrosc.*, 1999, **34**, 203; b) W. S. Price, K. Hayamizu, H. Ide and Y. Arata, *J. Magn. Reson.*, 1999, **139**, 205.

13 Database of Macromolecular Movements, http://molmovdb.org/, (accessed 27 October 2021).

14 a) A. G. Palmer, J. Cavanagh, P. E. Wright and M. Rance, *J. Magn. Reson.*, 1991, **93**, 151; b) L. Kay, P. Keifer and T. Saarinen, *J. Am. Chem. Soc.*, 1992, **114**, 10663; c) J. Schleucher, M. Schwendinger, M. Sattler, P. Schmidt, O. Schedletzky, S. J. Glaser, O. W. Sørensen and C. Griesinger, *J. Biomol. NMR*, 1994, **4**, 301.